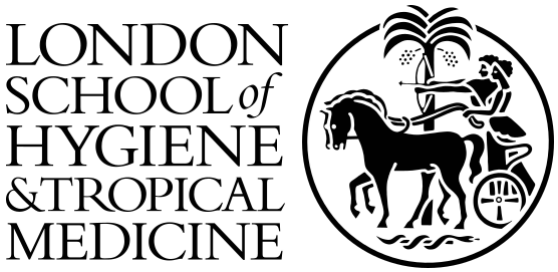

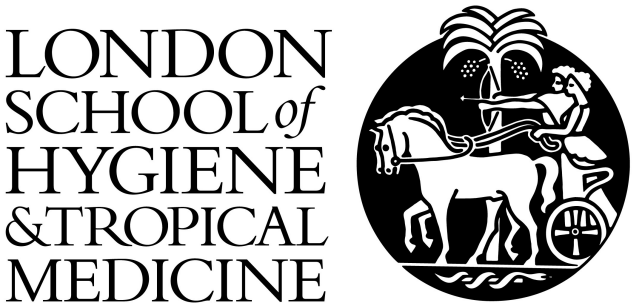

Natural killer cell responses to *Plasmodium falciparum*-infected red blood cells

Asia-Sophia Wolf

Thesis submitted in accordance with the requirements
for the degreee of Doctor of Philosophy

University of London

August 2016

Department of Immunology and Infection
Faculty of Infectious and Tropical Diseases

London School of Hygiene & Tropical Medicine

Funded by the Thorpe Legacy PhD Studentship

I, Asia-Sophia Wolf, confirm that the work presented in this thesis is my own. Where information has been derived from other sources, I confirm that this has been indicated in the thesis.

Abstract

NK cells are known to respond *in vitro* to *P. falciparum*-infected red blood cells (iRBCs), although responses are highly heterogeneous between donors. Although their role during malaria infection is not fully understood, they may play a role in cytokine production during early infection, and furthermore may interact with and kill iRBCs. The work described in this thesis examines the role of NK cell receptors in determining the functional outcomes of NK cell activation by iRBCs, focusing on NK cell responses to exogenous cytokines and the phenotypic and functional profiles of NK cells from malaria naive (LSHTM) and malaria exposed (Ugandan) subjects.

In a model of early activation of NK cells by accessory cell-derived cytokines, I have shown a key role for IL-18 in mediating NK cell responses during both primary and secondary immune responses as IL-18 synergises with cytokines from the common gamma chain family.

NK cells from LSHTM donors showed low background expression of IFN-γ and CD25, but responded to iRBCs by secretion of IFN-γ, which was potentiated by exogenous IL-15. By contrast, NK cells from Ugandan donors showed higher background CD25 expression and signs of *in vivo/ex vivo* preactivation and enhanced responsiveness to IL-15, but did not make any appreciable response to iRBCs. Potential explanations for these findings are explored and discussed. KIR genotype and KIR expression also varied between LSHTM and Ugandan donors. Specifically, expansions of KIR2DL1+ CD57+ NKG2C+ NK cell populations (possibly driven by human cytomegalovirus (HCMV) infection) were observed in the Ugandan donors. Conversely, percentages of KIR2DL3+ and 2DS4+ NK cells were higher among LSHTM donors, indicating that HLA genotype or allelic KIR polymorphisms may influence KIR expression.

Finally, the formation of NK-iRBC conjugates, which may be a precursor to NK cell-mediated killing of iRBCs, was observed in cells from nearly all donors, but did not correlate with other functional responses. Analysis of KIR expression and NK cell functional responses indicated that donors expressing inhibitory KIR2DL5 had reduced numbers of

conjugates. Further experiments indicated that KIR2DL5 might be specifically upregulated after incubation with iRBCs, and that individuals carrying a normally non-expressed *KIR2DL5* gene may be able to express this gene under certain circumstances. This tentatively suggests a role for KIR2DL5 during NK cell responses to malaria infection, and suggests a possible function for a common but frequently non-expressed gene.

In summary, my work suggests that NK cell responses are strongly influenced by cytokine receptor and KIR expression, which in turn depend on NK cell maturation status. KIR expression patterns may in part explain differential NK responses to iRBCs between LSHTM and Ugandan donors. I also propose a possible role for KIR2DL5 in malaria infection, and a reason for the low expression of this gene in African populations.

Acknowledgements

First of all I would like to thank my supervisor, Eleanor Riley, for allowing me to do a PhD in her group and for guiding me in the right direction whilst putting up with some of my truly bizarre lab presentations and/or thought processes. I have learnt so much from you and my time here, and I feel acutely how much I have learnt and yet how little I know, which is clearly the reason to keep doing science.

I am also extremely grateful to Chrissy Roberts for talking to me about KIRs, and for his advice and help with the KIR genotyping and 2DL5 work in this thesis. Thank you (I think) for getting me interested in KIRs, for the work and life advice, and for making me talk to people at conferences. I also enjoyed the pictures of dragons.

I would particularly like to thank Martin Goodier and Matt White for their incredible patience and help over the last four years, and for the many conversations about science and other topics, even when it was all too much. Thank you also to Carolyn Nielsen for starting her PhD at the same time, and for being a lab mate and friend. The Biscuit Society will live always in our hearts. OCS forever.

I would like to thank Carolynne Stanley, who has a magical list of blood donors, and Liz King for keeping the LSR II working, sometimes in spite of our collective best efforts to run it into the ground. Thank you both for being incredibly helpful and patient. I am also very grateful to Isaac Ssewanyana and Prasanna Jagannathan for the Ugandan PBMCs, and to Hollie Burrell-Saward for her help with my attempts at confocal microscopy. I would also like to thank Sam Sherratt for the ImageStream pictures, and to apologise for bringing KIR2DL5 into his life (the best KIR). The Hafalla group have also been fantastic, and I'm glad we had lab meetings together (although I realise they may be less glad).

Although they are not really my lab group, I would like to thank the Baker group and everyone in the malaria lab for being lovely people and answering all my questions about life, the universe and everything. I would especially like to thank Eloise Walker for teaching me everything I know about parasite culturing, and for running lab 312 like a well-oiled

machine.

Lastly, I would like thank Justin and my family, who have always taken an interest in the welfare of my parasites and have been the best support anyone could ask for. I very sincerely dedicate this thesis to you.

Contents

List of Figures

List of Tables

Abbreviations

ACT	Artemisin-based combination therapy
ADCC	Antibody dependent cell-mediated cytotoxicity
AMA-1	Apical membrane antigen 1
ANOVA	Analysis of variance
BfA	Brefeldin A
CNV	Copy number variation
DAPI	4',6-diamidino-2-phenylindole
DC	Dendritic cell
ddPCR	Droplet digital PCR
EDTA	Ethylenediaminetetraacetic acid
ER	Endoplasmic reticulum
EtBr	Ethidium bromide
FAM	Fluorescein
FCS	Foetal calf serum
HCC	High concentration cytokine (IL-12/IL-18)
HCMV	Human cytomegalovirus
HCV	Hepatitis C virus
HEX	Hexachlorofluorescein
HIV	Human immunodeficiency virus
HLA	Human leukocyte antigen
ICAM-1	Intercellular Adhesion Molecule 1
IFN-γ	Interferon gamma
Ig	Immunoglobulin
IL	Interleukin
iRBC	Infected red blood cell
ITAM	Immunoreceptor tyrosine-based activation motif
ITIM	Immunoreceptor tyrosine-based inhibition motif
ITNs	Insecticide treated bed nets

KIR	Killer immunoglobulin-like receptor
KLR	Killer lectin-like receptor
LCC	Low concentration cytokine (IL-12/IL-18)
LFA-1	Lymphocyte function-associated antigen 1
MCMV	Murine cytomegalovirus
MFI	Mean fluorescence intensity
MHC	Major histocompatibility complex
MSP	Merozoite surface protein
NCR	Natural cytotoxicity receptor
NK cell	Natural killer cell
NO	Nitric oxide
PAMP	Pathogen associated molecular pattern
PBMC	Peripheral blood mononucleocyte
PBS	Phosphate buffered saline
PCR	Polymerase chain reaction
pDC	Plasmacytoid DC
PfEMP1	*P. falciparum* erythrocyte membrane protein 1
PfRH5	*P. falciparum* reticulocyte binding-like homologue
PRR	Pattern recognition receptor
ROS	Reactive oxygen species
SLE	Systemic lupus erythematosus
SNP	Single nucleotide polymorphism
TAP	Transporter associated with antigen processing
TBE	Tris/borate/EDTA
TFGβ	Transforming growth factor beta
TLR	Toll-like receptor
TNFα	Tumor necrosis factor alpha
TRAIL	TNF-related apoptosis-inducing ligand
TRAP	Thrombospondin-related adhesion protein
uRBC	Uninfected red blood cell

1 Introduction

1.1 Natural killer cells

Natural killer (NK) cells are large, granular lymphocytes that are traditionally considered part of the innate immune system and comprise 5-20% of peripheral blood mononucleocytes (PBMCs). NK cells have classically been described as being capable of activation without prior exposure to antigen, and recognise cells expressing abnormal patterns of surface molecules [1], although it is now understood that they undergo a complex process of education and licencing to allow their activation and function [2]. During infection, the two main functions of NK cells are cytokine production and cytotoxic killing. These functions can be triggered by three distinct but complementary activation pathways: cytokine activation, antibody dependent cell-mediated cytotoxicity (ADCC), and activation by missing 'self' molecules. NK cells interact with potential target cells via a variety of cell surface receptors, including the killer immunoglobulin (Ig)-like receptor (KIR) family that interacts with major histocompatibility complex (MHC) molecules (reviewed in [3]), killer lectin-like receptors (KLRs) such as NKG2A and NKG2C that interact with human leukocyte antigen (HLA)-E, and natural cytotoxicity receptors (NCRs) such as NKp30 and NKp46. The outcome of these interactions can be direct lysis of the target cell by the NK cell, which creates an important role for NK cells in killing infected or transformed cells.

1.1.1 NK cell phenotypic markers and maturation

NK cells are defined as CD56+ CD3- lymphocytes in humans and have traditionally been divided into subsets of CD56 bright and CD56 dim, with functions of cytokine production and cytotoxicity respectively. A more nuanced marker of maturity is CD57 expression, where CD56 bright and CD56 dim CD57- cells produce the majority of NK-derived cytokines and CD56 dim CD57+ cells are optimised for efficient killing of multiple target cells [4, 5]. NK cell expression of CD57 is considered a marker of terminal differentiation, indicating a reduced capacity for cytokine production [6] and proliferation [7, 8] but enhanced cytotoxic functions (reviewed in [5]) compared to less mature CD56 bright NK cells. The pathway of functional NK cell maturation is thought to move from less mature, cytokine producing CD56 bright CD57- (referred to in this thesis as CD56 brights) to CD56dim CD57- (CD57-), through NK cells with intermediate CD57 expression (CD57int), and finally to mature, terminally differentiated CD56 dim CD57+ (CD57+) cells [6, 9]. Expression of NK cell receptors varies between these subsets, with a broad classification of CD56 bright NK cells as NKG2A+ NKG2C- KIR-, and CD57+ NK cells as NKG2A- NKG2C+ KIR+. The proportion of CD57+ NK cells naturally increases with age [10] but it is not clear if this is a result of ageing per se, because of cumulative infections throughout life which drive NK cell maturation, or both. Human cytomegalovirus (HCMV) is a common herpesvirus thought to drive NK cell differentiation and the accumulation of NKG2C+ CD57+ NK cells [11, 12], and there is strong evidence that NK cell differentiation and acquistion of both KIRs and NKG2C is accelerated after HCMV infection [11, 13–15]. Although these mature NK cell populations are thought to be important for control of HCMV infection, CD56 bright and CD56 dim CD57- NK cells are more responsive to cytokine stimulation, particularly by the interleukins (IL)-12 and 18, and the reduction of these NK cell subsets has been linked to poorer responses to vaccination [6, 16, 17].

1.1.2 NK cells are early producers of inflammatory cytokines

NK cells are thought to be important producers of inflammatory cytokines during early infection prior to activation of adaptive T cell responses [18–21], of which the most important is interferon gamma (IFN-γ). *In vitro*, NK cells are capable of producing IFN-γ after activation by exogenous cytokines, in particular IL-12 and IL-18 [22–24]. However, during infection, cytokines are produced at different time points and from diverse cellular sources; these drive specific NK activation pathways that can be finely controlled to be effective during infection but limit pathology caused by uncontrolled activation. During infection with two classic Th1-type pathogens, *Salmonella enterica* and *Plasmodium falciparum*, NK cells require activating signals from three distinct sources: a priming or pre-activation signal of either IL-2 or IL-15 from T cells or dendritic cells (DCs) respectively, IL-12 and IL-18 from macrophages, and direct contact with macrophages [25, 26] (Figure 1.1).

Both *in vivo* and *in vitro* studies on humans and *in vivo* mouse models have indicated an important role for all of IL-12, IL-18, IL-2 and IL-15 in the development and proper functioning of the immune system, and of NK cells in particular (reviewed in [27–29]). Macrophages are thought to be the primary source of IL-12 and IL-18 during bacterial or protozoan infection, due to pathogen recognition by macrophages via pattern recognition receptors (PRR) such as toll-like receptors (TLRs) (reviewed in [30, 31]). IL-12 and IL-18 are well established by *in vitro* models to stimulate release of IFN-γ by NK cells [22, 32, 33]. However, there is also an increasingly clear role for DC-derived IL-15 in 'priming' NK cells prior to activation, which is proposed to lower the threshold for activation so that NK cells can respond more quickly and strongly to activating stimuli [34–36]. Priming is thought to be particularly relevant during primary infection, when NK cells are early responders and adaptive (T and B cell) immune responses have yet to develop. During secondary immune responses to previously encountered antigens, T cells produce IL-2, which enhances NK cell activation and synergises with IL-12 and IL-18 to drive IFN-γ production [19, 37, 38]. The roles of IL-15 and IL-2 are therefore thought to be similar, but are an example of the temporal separation in cytokine production during innate and adaptive responses which

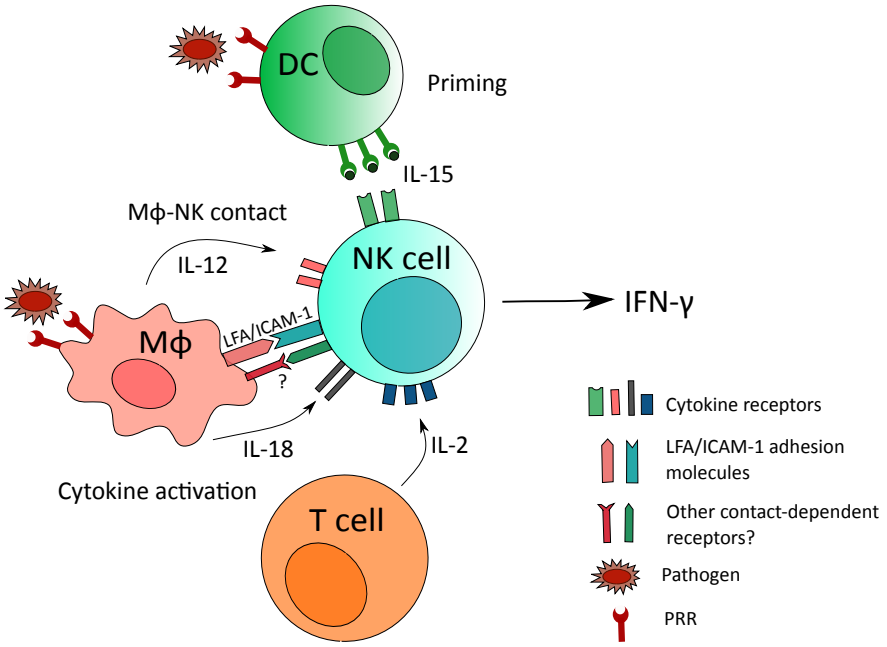

Figure 1.1: Cytokine driven NK cell activation. To drive cytokine production by NK cells (primarily IFN-γ), NK cells require three types of signals. Circulating macrophages (Mφ) recognise pathogen via pattern recognition receptors (PRR) and secrete IL-12 and IL-18 to activate NK cells. In a primary infection, dendritic cells (DC) recognise pathogen via PRR and prime NK cells via trans-presentation of IL-15, or during a secondary infection, antigen-specific memory T cells produce IL-2 to enhance NK cell responses. NK cells also require direct contact with macrophages, mediated by adhesion molecules such as ICAM-1 and LFA-1.

allows fine control of immune activation [39–41]. Further introduction of these cytokines and their roles in NK cell activation can be found in Chapter 3.

Direct contact with macrophages has been shown in several *in vitro* infection models to play an important role in human NK cell activation [25, 26, 42]. This interaction is thought to be primarily mediated via the adhesion molecules ICAM-1 and LFA-1, and in the absence of this contact NK cells have reduced levels of IFN-γ production [26, 43, 44]. There is also some evidence that ICAM-1 may be upregulated by IL-12 and IL-18 to enhance NK cell-macrophage interactions [45, 46]. During viral infections, DC-NK cell contact is also considered essential for strong upregulation of anti-viral responses (reviewed in [47]), and

may present activating cytokines including IL-12 and IL-15 directly to NK cells from the dendritic cell surface [34, 48, 49], as well as express ligands for the activating KLR, NKG2D, to induce NK cell activation [47].

1.1.3 Cytotoxic responses and killing by NK cells

The classical function of NK cells is their ability to kill transformed or infected target cells through the release of pre-formed lytic granules. Upon activation by a compromised target cell, an NK cell can form an immune synapse with the cell, mediated by a ring of adhesion molecules shepherded by filamentous actin reorganisation to maintain close contact with the target. Lytic granules stored within the NK cell are transported to the site of the synapse and release perforin, a pore-forming molecule, to penetrate the target cell membrane, followed by serine proteases such as granzyme which induce apoptosis (reviewed in [50]). Activated NK cells can also express ligands such as Fas ligand (FasL) and TNF-related apoptotic inducing ligand (TRAIL) that bind the death receptors Fas and TRAIL receptor (TRAIL-R) on the target cell surface, causing downstream intracellular signalling and death via caspase activation (reviewed in [51]). There are thought to be three main mechanisms for triggering this cytotoxicity that work both independently and in combination (Figure 1.2).

Firstly, cytotoxic NK cell responses can be driven by cytokines including the type I interferons, IFN-α and IFN-β, which are predominantly produced and recognised by plasmacytoid DCs (pDCs) during viral infection. pDCs are activated by viral pathogen associated molecular patterns (PAMPs), which are recognised by TLRs and produce type I interferons (reviewed in [52, 53]), which may drive further pDC activation in a positive feedback loop [35]. DCs (both myeloid and plasmacytoid) also transpresent IL-15 to NK cells [48], and the combination of IL-15 and IFN-α/β is thought to drive both cytotoxic responses and IFN-γ production by NK cells [35, 47, 48, 54].

The second mechanism for cytotoxicity is antibody dependent cell-mediated cytotoxicity (ADCC). ADCC was originally described as a mechanism for targeted killing of influenza-

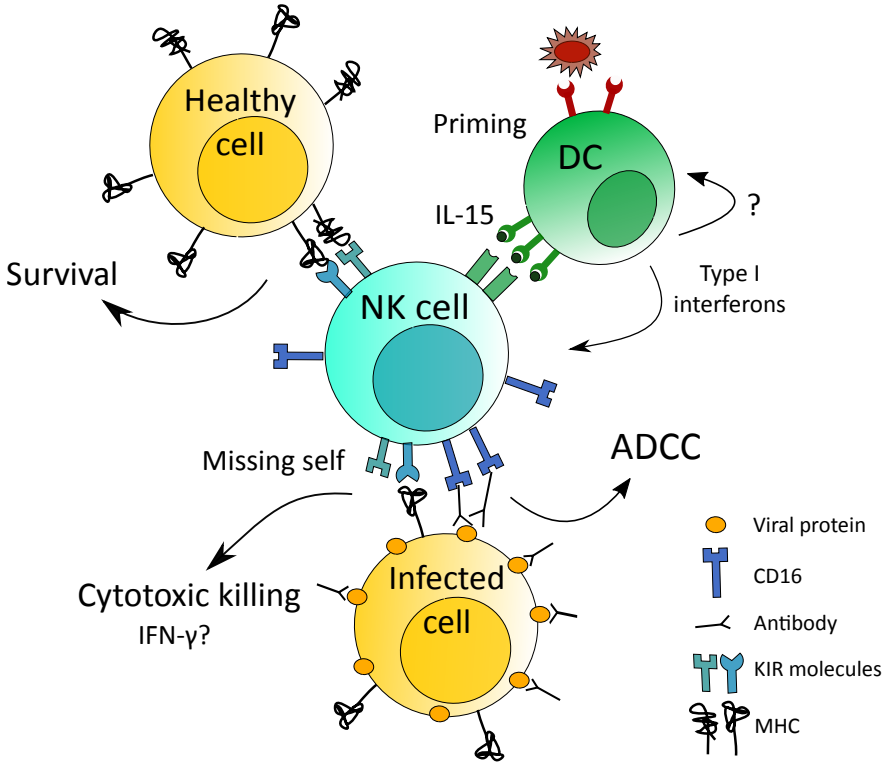

Figure 1.2: Mechanisms of NK cell cytotoxicity. The three mechanisms for cytotoxicity are represented in this schematic. DCs are activated by pathogen to produce type I interferons and present IL-15 to NK cells. CD16 on the NK cell surface crosslinks antibody bound to viral proteins on an infected target cell, driving ADCC. Inhibitory KIR receptors are bound by self-MHC molecules on healthy cells, leading to survival of the uninfected cell, but loss of MHC on the infected cell leads to detection of missing-self by the NK cell and killing of the target.

infected cells [55], and is thought to be important for the killing of infected cells in a non-MHC restricted manner [56] and for disposal of antibody-bound pathogens. Mature CD57+ NK cells express the Fc receptor FcγRIIIa, also known as CD16, which binds the invariant Fc portion of B cell-derived IgG antibodies bound to target antigens. Binding of multiple Fc portions cross-links CD16 on the NK cell and triggers NK cell cytotoxicity against the antibody-bound target cell or immune complex via ADCC [57]. This therefore provides a clear role for NK cells during specific adaptive immune responses via interaction with antigen-specific IgG molecules [58]. CD16 ligation is also thought to induce cytokine

production by NK cells, including IFN-γ upregulation [38, 59].

Lastly, NK cells can detect both activating ligands, such as viral proteins or host stress markers, and the absence of MHC class I molecule expression on the surface of target cells. For example, NCRs and KLRs such as NKp30, NKp46 and NKG2D can recognise a tumour cell marker (B7-H6), haemagglutinins, and the stress markers MICA and MICB respectively, which provide activating signals to the NK cell and induce anti-tumour and anti-viral cytotoxic responses (reviewed in [60, 61]). Conversely, infected cells can down-regulate cellular expression of MHC class I to evade detection by CD8 T cells, but this leaves them vulnerable to killing by NK cells. MHC class I molecules interact with KIRs on NK cells to provide inhibitory signals, preventing activation. If MHC expression is lost or downregulated, NK cells lack KIR-mediated inhibitory signals and will become cytotoxic towards the target cell, which is known as the 'missing-self hypothesis' [1, 62], or if MHC expression is altered but not totally lost, the altered-self hypothesis [63] (Figure 1.3).

The missing-self hypothesis is a key tenet of cellular immunology. Cytotoxic CD8 T cells are capable of detecting antigens presented by MHC class I molecules as part of the adaptive immune system, and efficiently kill cells presenting non-self antigens as a marker of infection or cellular mutation. However, various pathogens have evolved evasion mechanisms to this form of immune surveillance by inducing downregulation of surface MHC class I molecules, thus preventing antigen presentation to T cells. In turn, NK cells are capable of detecting a loss of MHC expression that indicates an infection or harmful mutation within the cell and triggers cytotoxic killing. Healthy cells, therefore, expressing normal levels of MHC class I and few or no activating ligands, will not activate NK cells; likewise, the few somatic cells that do not express either MHC or activating ligands (primarily red blood cells and neurons) are thought to be ignored by NK cells [62]. Cells that have lost or reduced MHC class I expression, such as cells infected with human immunodeficiency virus (HIV) or HCMV [64], will be targeted by NK cells, as will cells with normal MHC class I expression but increased expression of activating ligands such as the previously mentioned stress or tumour cell markers.

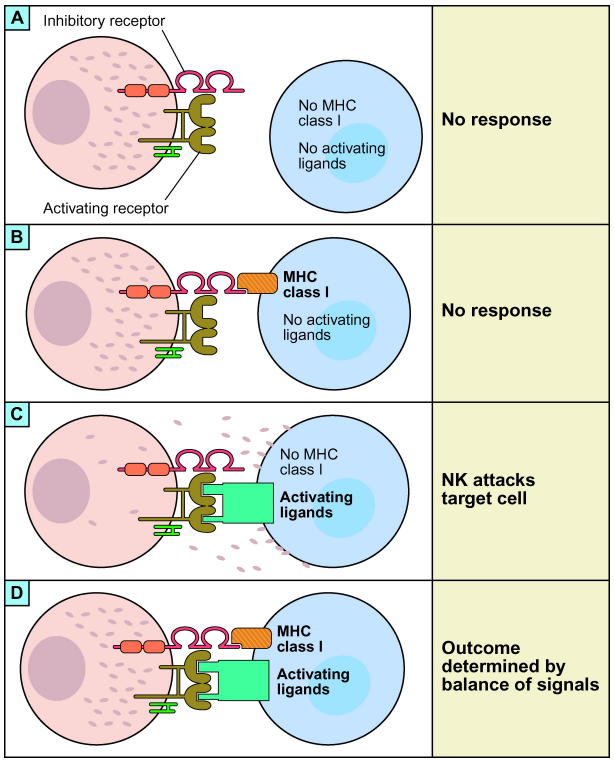

Figure 1.3: Interactions of an NK cell with a target cell and possible outcomes based on receptor expression. This schematic proposes four possible outcomes from interaction between an NK cell and a target cell. Certain somatic cells do not express either inhibitory (MHC) or activating ligands, leaving them presumably unnoticed by NK cells (A). Healthy cells expressing normal levels of MHC class I molecules without activating stress/infection ligands bind NK cell KIR and survive (B). Infected or transformed target cells that have lost MHC expression and upregulate stress or pathogen ligands are killed by NK cells (C). Target cells expressing MHC but also upregulating activating ligands will bind both inhibitory and activating NK cell receptors, and the net signal determines whether cytotoxic killing occurs (D). Figure from L. Lanier, 2005, *Annual Reviews* [62].

1.1.4 NK cell surface receptors

NK cells express multiple germline encoded receptors that regulate NK cell responses and are capable of detecting a wide range of antigens, although they do not undergo recombination or hypermutation as do T and B cell receptors. Broadly, these functional receptors can be divided into three categories: NCRs, KLRs, and KIRs.

1.1.4.1 Natural cytotoxicity receptors (NCRs)

Natural cytotoxicity receptors are a group of activating receptors consisting of NKp30, NKp44 and NKp46, which can signal independently or synergistically [65]. These three receptors are functionally similar but structurally and sequentially distinct, and they bind a variety of pathogen-derived ligands, including haemagglutinin from influenza and poxviruses, and cancer-associated markers, such as B7-H6 and BAG6 which are expressed on the surface of tumour cells [66]. Detection of these ligands is crucial for NK-mediated cytotoxicity, and reduction of NCR expression is associated with resistance of leukaemia cells to NK cytotoxicity and with decreased killing of tumour cells *in vitro* (reviewed in [60, 66]).

1.1.4.2 Killer lectin-like receptors (KLRs)

Killer lectin-like receptors include the NKG2 family, which consists of both inhibitory and activating receptors. NKG2A, C and E are glycoproteins that form heterodimers with the common invariant subunit CD94; CD94 is thought to mediate expression of the dimer on the NK cell surface while NKG2 mediates signal transduction [67]. CD94/NKG2A/C/E heterodimers recognise the non-classical MHC class I molecule HLA-E [68, 69]. Unlike the classical MHC molecules, HLA-E has a restricted ability to bind peptides, and preferentially binds TAP-dependent signal peptides derived from other MHC class I molecules [70]. TAP is a transporter protein that mediates peptide binding to MHC class I molecules, and can be downregulated during infection as an evasion mechanism to avoid presentation of non-self antigens to T cells [71]. TAP-dependent HLA-E expression therefore acts as a signal that proper antigen processing and presentation to classical MHC molecules (HLA-A, HLA-B and HLA-C) is occurring within the cell, and if HLA-E expression is downregulated as a result of TAP and/or classical MHC antigen processing loss, an inhibitory signal will not be transduced via NKG2A, leading to NK cell killing [67]. By contrast, NKG2C binding of HLA-E induces an activating signal [68]. This is balanced by co-expression of inhibitory KIRs on the NK cell [14], restraining cytotoxic responses if MHC class I

molecules are properly expressed on the target cell, or by NKG2A coexpression, which binds HLA-E with greater affinity than NKG2C [72]. Additionally, some viruses have developed mechanisms for maintaining HLA-E expression on a target cell while suppressing classical HLA presentation. For example, during HCMV infection, the glycoprotein UL40 specifically upregulates HLA-E expression [73], which would normally protect the infected cell from lysis via NKG2A; however, NKG2C-mediated activation is thought to target cells with high HLA-E expression, which may be one reason for the expansion of NKG2C+ NK cells seen in HCMV+ individuals [74]. The role of NKG2A and NKG2C in NK cell function is described in further detail in Chapter 5, Section 5.1.2. NKG2D is an activating receptor that does not dimerise with CD94 or recognise HLA-E, but instead binds ligands that are generally not expressed on healthy cells, such as stress-induced MICA and MICB found on tumour cells and the ULBP family (reviewed in [61, 75]).

1.1.4.3 Killer immunoglobulin-like receptors (KIR)

Killer Ig-like receptors are a family of transmembrane glycoproteins that regulate NK cell activation. KIRs can be either activating or inhibitory based on their intracellular signalling pathways, but are most commonly thought of as inhibitory receptors due to their role in detecting polymorphic MHC class I molecules on the surface of somatic cells. KIR-MHC interactions form the basis of the missing-self hypothesis, as previously described. Inhibitory KIRs expressed on mature NK cells bind MHC class I molecules, transmitting an inhibitory signal and preventing NK cell activation. Lack of, or downregulation of, MHC leads to loss of KIR-mediated inhibition, allowing NK cell killing via this missed signal. In humans, KIRs recognise the classical MHC class I molecules HLA-A, HLA-B and HLA-C, as well as certain non-classical MHC. KIR2DL4 is thought to recognise HLA-G [76], which is important during pregnancy (reviewed in [77]), and heparan sulfate, which is widely expressed on epithelial cells [78], but the evidence for interaction between these molecules and 2DL4 is unclear. Ligands for several other KIRs, in particular KIR2DL5 and the activating KIRs, are unknown, although classical MHC class I molecules that bind inhibitory long-tailed KIRs are hypothesised to also bind the activating short homologues

with a lower affinity (see Table 1.1), which has so far only been shown for KIR2DL1/S1 [79], and suggested for 3DL1/S1 [80, 81]. The KIR family is found in both human and non-human primates, and shares functional similarities with the lectin receptor Ly49 family found in mice, although these two families are structurally and evolutionarily distinct [2, 82].

Signal type	KIR	Ligand	No. alleles	General references
Inhibitory	2DL1	HLA-C2	26	[3, 83]
	2DL2	HLA-C1, HLA-C2	15	[83, 84]
	2DL3	HLA-C1	11	[3]
	2DL5A	unknown	10	[85, 86]
	2DL5B	unknown	21	[87]
	3DL1	HLA-Bw4, some HLA-A	59	[88, 89]
	3DL2	HLA-A*03, *11	25	[3]
	3DL3	unknown	56	[90]
Activating	2DL4	HLA-G, heparan sulfate?	27	[76, 78]
	2DS1	HLA-C2	15	[79]
	2DS2	possibly HLA-C1	20	[91]
	2DS3	possibly HLA-C1	12	[90, 92]
	2DS4	HLA-C, HLA-A*11	30	[93, 94]
	2DS5	unknown	14	[95]
	3DS1	HLA-Bw4?	16	[80]

Table 1.1: A summary of the KIR molecules and their known ligands. HLA classes (A, B, C) show significant overlap as ligands for different KIRs, but have different binding affinities for KIRs and may selectively interact with specific alleles of both KIR and MHC molecules. The number of known KIR alleles (based on Campbell and Purdy, 2011 [96]) is indicated, along with a reference for useful background information on that KIR.

KIRs are classified by their number of extracellular Ig-like domains (two or three, denoted 2D or 3D), and the length of the cytoplasmic domain that mediates signalling (long or short). Long cytoplasmic tails contain immunoreceptor tyrosine-based inhibitory motifs

(ITIM) that mediate inhibitory signalling, whereas short cytoplasmic tails lack these ITIMs and instead associate with transmembrane adapter proteins such as DNAX activation protein of 12 kDa (DAP12) carrying activating ITAMs ([97], reviewed in [96]) (Figure 1.4). One exception is KIR2DL4, which is an activating KIR with one intracellular ITIM motif that also interacts with an FcεRI adaptor protein [76].

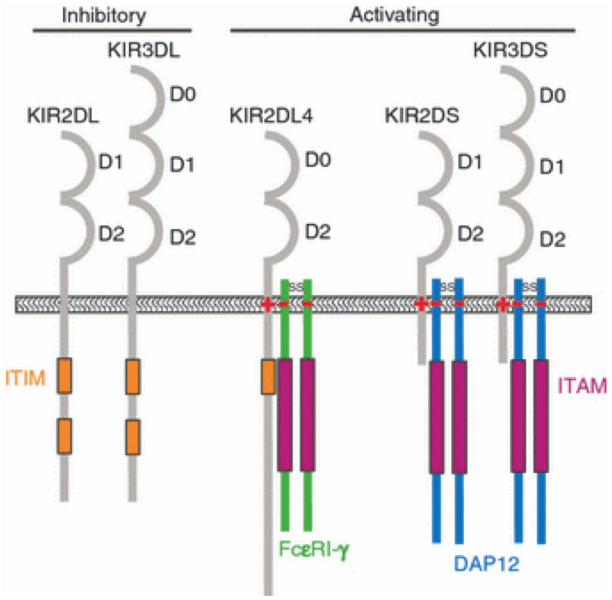

Figure 1.4: The structural arrangement of KIR molecules: KIRs have two or three extracellular domains that bind MHC or other ligands, and then have either long (2DL/3DL) cytoplasmic tails containing ITIM motifs, or short (2DS/3DS) tails which bind adaptor molecules (DAP12 or DAP10) containing ITAM motifs. 2DL4 is an exception as it has a long cytoplasmic tail but also binds the adaptor protein FcεRI-γ, which conveys activating function. Figure from KS Campbell and AK Purdy, 2011, *Immunology* [96].

The KIR locus is found on chromosome region 19q13.4, and encodes 17 known KIR genes. *KIR3DL3* and *KIR3DP1* (a pseudogene) delineate the centromeric region of this locus, and *KIR2DL4* and *KIR3DL2* the telomeric region, between which lies the point of reciprocal recombination that is a focal point for reassortment of the centromeric and telomeric regions and the generation of new haplotypes [3] (Figure 1.5). KIR genes are highly polymorphic and show high levels of allelic diversity, which can lead to some dissent regarding the exact number of KIR genes, mainly based on whether *KIR2DL2* and *2DL3*, and *KIR3DL1* and *3DS1*, are separate genes or alleles [98]. For the purposes of this thesis, they will

be considered separate genes. A further complication is the inconsistent distinction of *KIR2DL5A* and *KIR2DL5B*, which are exclusively found on the telomeric and centromeric regions of the KIR locus respectively and are variably considered as being two highly homologous genes or as alleles of one gene, *KIR2DL5* [99].

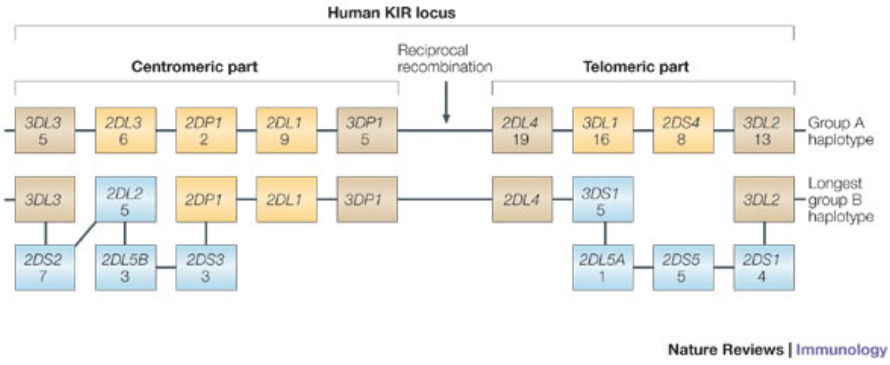

Figure 1.5: KIR genes on the A and B haplotypes can vary widely, but are almost always bracketed between the framework genes KIR3DL3 and KIR3DL2. The division into the centromeric and telomeric parts, creating the point of reciprocal recombination between the genes KIR3DP1 and KIR2DL4, allows for frequent recombination to create haplotype diversity. Figure from P. Parham, 2005, *Nat. Rev. Immunol.* [3].

KIR genes are commonly grouped into two haplotypes, A and B, comprising a combination of KIR genes commonly inherited together. A haplotypes consist of the KIRs *3DL3, 2DL3, 2DP1, 2DL1, 3DP1, 2DL4, 3DL1, 2DS4* and *3DL2*, and can contain some or all of these genes, which are predominantly inhibitory. B haplotypes include any of the other KIR genes (*KIR2DL2, KIR2DL5*, all short KIRs other than *KIR2DS4*) and can also contain A haplotype genes (reviewed in [3, 100]), and so carriage of a B haplotype tends to increase the number of activating KIRs present in an individual. Inhibitory KIRs are important for 'licensing' NK cells and permitting cytotoxic function (described further in Section 1.1.5), and so an AA haplotype may be protective during viral infection [83]; however, apart from their role in immunity, NK cells have an important role in remodelling the spiral arteries carrying blood to the placenta during pregnancy, and it has been suggested that a combination of maternal KIR2DL1-expressing uterine NK cells and foetal HLA-C2-expressing trophoblasts in the absence of the activating receptor KIR2DS1, especially when

the mother herself is HLA-C1 homozygous, may lead to over-inhibition of NK cells and insufficient blood flow to the placenta, thus seriously increasing the risk of pre-eclampsia and stillbirth (reviewed in [77]). Activating B haplotype genes can reduce this risk, but conversely increase the risk of having a large baby due to overly deep placental invasion and increased blood supply; obstructed labour carries its own risks to both mother and child during birth [77]. Therefore A and B haplotypes can both be advantageous and disadvantageous, and are thought to have evolved under selective pressure from reproduction as well as through their potential benefits in pathogen resistance [83].

An important factor in KIR diversity within a population is therefore presence or absence of each KIR gene: as mentioned, the point of reciprocal recombination allows switching of centromeric and telomeric regions between haplotypes, creating, for example, new combinations of centromeric A and telomeric B KIR genes or vice versa. Similarly, high sequence homology between KIR genes, and between the intergenic regions separating them, facilitates non-reciprocal recombination that allows deletion, duplication or recombination of individual KIR genes, creating new combinations of genes on the centromeric or telomeric regions [3], although this predominantly occurs within B haplotypes which show much greater variety than A haplotypes [101]. Variety in the A haplotype comes predominantly from allelic diversity rather than gene content [83], and allelic variation in individual KIR genes is high, as illustrated in Table 1.1, due to single nucleotide polymorphisms (SNPs) which generate alleles with different binding affinities for KIR ligands. Allelic diversity also affects expression levels of KIRs on the NK cell surface due to polymorphisms in the gene promoter regions [102], or by creating stop codons leading to truncated proteins [103].

KIRs are unusual in that individual genes are transcribed independently from others on the gene cluster [104]. Each KIR gene is thought to contain multiple transcriptional promoters which determine expression, and the level of activity of these bidirectional promoters (producing both sense and antisense mRNA transcripts) determines the percentage of NK cells on which that KIR is expressed [105]. Promoter regions are also subject to SNPs at transcription factor binding sites, and these polymorphisms predict promoter functional

activity [104]. Diversity is therefore created by apparently stochastic expression of KIRs on the NK cell surface [104]. However, it is possible that KIR expression is selected for based on expression of self-MHC ligands [106], or that temporal expression patterns determine the level of KIR expression within the total NK cell population [84].

HLA molecules corresponding to MHC class I (known as HLA-A, -B and -C) are the key ligands for KIRs, and play an important role in 'licensing' or 'educating' NK cells. HLA molecules are found on the surface of nearly all somatic cells, and are composed of an MHC class I heavy chain and a light β2-microglobulin chain, and were previously best characterised for presenting intracellular peptides to T cells and interacting with the T cell receptor (TCR) via the Vα and Vβ TCR domains. However, HLA molecules also interact with KIRs in a similar conformation to the TCR by binding the D1 and D2 KIR domains to the α1 and α2 domains of HLA. The footprint of KIR/HLA binding is distinct from TCR/HLA binding, but overlaps and thus prevents simultaneous binding of both a T cell and an NK cell to the same HLA molecule [107].

HLA-C is the only KIR ligand found in all individuals and has two forms, which differ by an amino acid residue at position 80 [108]. HLA-C1 carries an asparagine residue (Asn80), and HLA-C2 carries a lysine residue (Lys80), which determines which KIR each form can bind [107]: KIR2DL1 binds HLA-C2 with high affinity, KIR2DL3 binds HLA-C1 with weaker affinity, and KIR2DL2 binds both HLA-C1 and -C2 [96, 109]. Although other HLA molecules, particularly HLA-Bw4, are thought to be important in KIR-HLA interactions and disease association [88, 110], both forms of HLA-C are conserved in all human populations and are considered to be important for both NK cell responsiveness to infectious diseases and for reproduction and pregnancy ([108]; reviewed in [77, 83]). The HLA locus is found on chromosome 6p21 and assorts independently of KIR genes, so there is no guarantee that a somatic cell will express the 'correct' self-ligand for an NK cell expressing an inhibitory KIR; killing of healthy cells through this mismatch is prevented by NK cell licensing, as described in the next section.

1.1.5 NK cell licensing by self-MHC

The theory of NK cell education or licensing proposes that NK cells expressing KIR molecules are required to interact with self-MHC molecules in order to confer functional activity on the NK cell, and that in the absence of this interaction NK cells are unlicensed and hyporesponsive in the missing-self state (reviewed in [111]). NK cell education therefore provides a mechanism for NK cell tolerance seen in individuals who lack appropriate MHC class I expression ('KIR-ligand mismatch'), who would otherwise be expected to suffer from severe NK cell-derived autoimmunity [112]. MHC-licensed NK cells, unlike unlicensed cells, are capable of cytotoxic responses *in vitro* to MHC-deficient cells and tumour cells (reviewed in [113]), although it is not clear to what extent licensing affects cytokine production by NK cells. Although there are multiple proposed models for how licensing occurs (reviewed in [113]), it seems likely that this is a 'tuneable' model of activation that can change based on environmental factors and may essentially regulate the threshold at which NK cells become activated. Licensing is thought to be mediated predominantly via inhibitory receptors, and in particular the inhibitory KIRs 2DL1, 2DL2 and 2DL3 due to their binding to HLA-C molecules. The traditional concept of licensing as it was first proposed suggested that all NK cells should express 'at least one' inhibitory receptor, whether the KLR NKG2A or a KIR, depending on the maturation stage of the NK cell, in order to provide self-tolerance [114]. This is likely to be an oversimplification of how NK cells avoid autoimmunity, not least because unlicensed populations of NK cells have been detected in peripheral blood in most if not all individuals (reviewed in [111]), although it is possible that some of these cells may also express NKG2A. However, it is unclear whether KIR repertoires are generated stochastically on the NK cell surface, so that expression is essentially random and NK cells expressing KIR that recognise self-MHC become licensed [115], or whether KIR expression is acquired in a 'ligand-instructed' model which modifies KIR expression patterns based on which HLA molecules are expressed, so that an NK cell will sequentially express KIRs until one binds MHC and potentially compete for expression [84] (described further in Chapter 5). The binding affinity of KIRs to MHC may also differ

based on allelic variation, so that the 'strength' of education is proportional to the NK cell functional capacity, and expression of multiple inhibitory KIRs may lead to increased NK cell responsiveness [116].

The role of activating KIRs in licensing is unclear, but it is has been proposed that recognition of an MHC ligand by an activating KIR (so far only shown for 2DS1 and HLA-C2) can modulate the NK cell activation threshold to create a hyporesponsive NK cell population, roughly analogous to negative T cell selection without the death of the NK cell (reviewed in [117]). This was observed in *KIR2DS1*+ individuals homozygous for HLA-C2 who carried 2DS1+ 2DL1- NK cell subsets that 'tuned down' recognition of target cells while maintaining the capacity to produce cytokines [118], and suggests that both inhibitory and activating KIRs play an important role in NK cell licensing. Additionally, preactivation of NK cells with inflammatory cytokines appeared to lessen the difference in NK cell activity between licensed and unlicensed cells [2], and therefore it has been proposed that unlicensed cells (or cells with a 'high' activation threshold) are hyporesponsive during normal conditions but are capable of becoming fully active during infection in the presence of multiple activating stimuli, such as both cytokine stimulation and contact dependent signals. Further support for this hypothesis are data showing that in a mouse model, unlicensed populations were important in controlling murine cytomegalovirus (MCMV) infection [119]. How this might be reconciled with expansions of KIR2DL1 or 2DL3+ NK cells during HCMV infection is unclear [13] (described further in Chapter 5), and may represent alternative immune responses to counter immune evasion by the virus.

1.2 Malaria

Malaria is a mosquito-borne protozoal disease most commonly characterised by fever, fatigue and headache, which can progress to severe anaemia, cerebral malaria, acute respiratory distress and death. It is estimated that 3.2 billion people are at risk of malaria [120], and in 2015 there were an estimated 214 million cases of malaria and 438,000 deaths worldwide; of these deaths, 70% were in children under five years old [121]. The burden of

malaria falls most heavily on south Asia and sub-Saharan Africa. Eighty percent of cases and 90% of deaths occurred in Africa, and the Democratic Republic of the Congo and Nigeria together accounted for an estimated 35% of global malaria deaths.

The cost of malaria treatment in sub-Saharan Africa is estimated by the WHO to be nearly $300 million per year, without taking into account other healthcare interventions or lost workdays due to illness [121]. Additionally, even where mortality rates are low, morbidity due to malaria is high as long term health effects can include neurological impairment and epilepsy. The burden of malaria in both physical and socioeconomic terms is therefore high, and limits the ability of a country to increase its financial and healthcare prospects in the absence of effective disease control.

Although malaria is still a major global problem, progress has been made in recent years due to the widespread use of insecticide-treated bed nets (ITNs), indoor residual spraying of insecticides, and improved diagnosis and treatment [121]. However, parasite resistance to artemisinin-based combination therapy (ACT) drugs has been detected at multiple sites around Cambodia and southeast Asia [122, 123], though this has not yet spread to Africa [124, 125]. It is widely accepted that sustainable malaria control would be facilitated by the advent of a highly effective malaria vaccine.

1.2.1 Biology and transmission

Malaria is caused by protozoan parasites of the genus *Plasmodium*. The main *Plasmodium* species capable of causing disease in humans are *P. falciparum, P. knowlesi, P. malariae, P. ovale and P. vivax*; of these, *P. falciparum* is widespread in Africa and the most frequent cause of complications and mortality, whereas *P. vivax* is the predominant strain in south and southeast Asia. *P. knowlesi* is an emerging zoonosis that is prevalent in macaques and has entered the human population in southeast Asia, accounting for the majority of malaria cases in Malaysia [126].

The *Plasmodium* life cycle requires two hosts, mammalian and mosquito. A female *Anophe-*

les mosquito becomes infected when she takes a blood meal from an infected host. In the mosquito gut, the parasite reproduces sexually, generating genetic diversity, and daughter sporozoites invade the mosquito salivary glands. During the next blood meal, sporozoites enter the mammalian bloodstream and migrate to the liver to replicate asexually where they develop into exo-erythrocytic schizonts before rupturing and releasing merozoites into the blood to invade red blood cells [127]. Within red blood cells, parasites mature from rings into trophozoites and then schizonts, which subsequently rupture and release around twenty merozoites into the bloodstream that go on to invade new erythrocytes. This cycle of rupture and invasion of red blood cells is thought to be responsible for the symptoms and immunopathology of malaria [121]. Some ring-stage parasites will develop into male and female gametocytes, which will be picked up by another mosquito to continue the cycle.

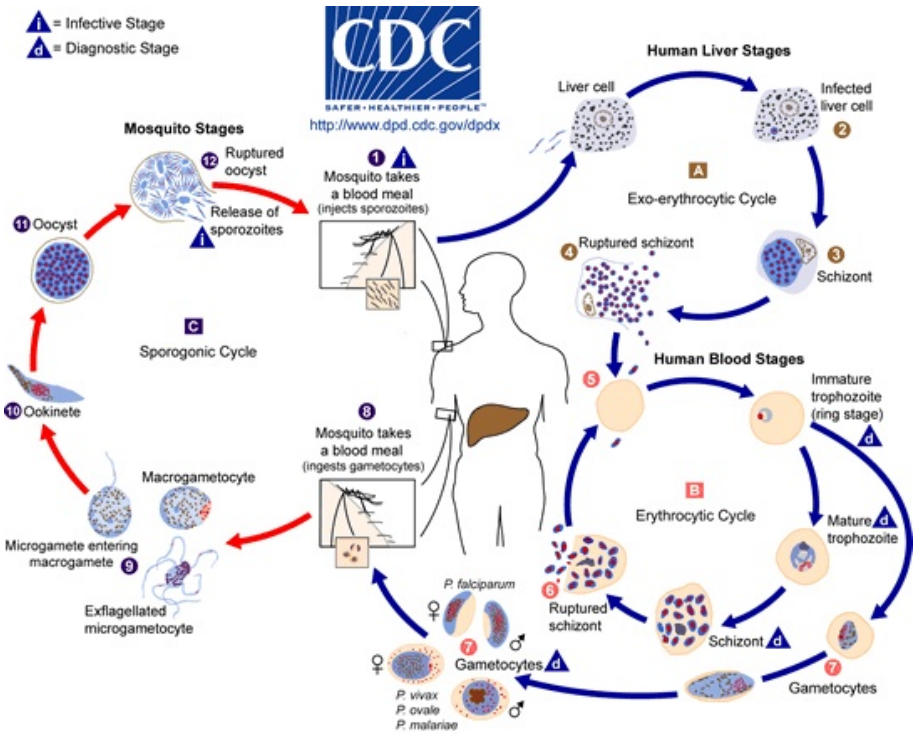

Figure 1.6: The lifecycle of *Plasmodium* in the human and mosquito host. Symptoms and pathology occur only during the human blood stages. Diagram from the Centers for Disease Control [127].

1.2.2 Clinical disease

Clinical malaria in humans is usually characterised by fever, fatigue, vomiting and headaches. Severe malaria is most common in children under five, and mortality is high. The most serious complications include cerebral malaria, severe anaemia, and acute respiratory distress due to metabolic acidosis. Cerebral malaria is the most serious neurological complication of malaria and involves impaired consciousness, coma, seizures, blindness and, if untreated, death. This is thought to be due to sequestration of parasites in blood vessels within the brain combined with an excessive inflammatory immune response [128]. Onset of clinical symptoms of malaria is usually between 7 and 11 days after infection with *P. falciparum* once the parasites reach the erythrocytic stage. Unlike vivax malaria, falciparum malaria does not have a hypnozoite stage where parasites are dormant in the liver and so relapses are not seen after parasite clearance; however, reinfection due to re-exposure or recrudescence of a sub-clinical infection is common.

In areas of high transmission, clinical immunity to malaria develops over time, reducing the mortality and morbidity of disease so that most infections in adults are asymptomatic. However, complete immunity to *P. falciparum* is rarely achieved. The incidence of severe malaria in high-transmission settings appears to peak within the first few years of life (reviewed in [129]), which accounts for the fact that the majority of malaria deaths are in children under five [121]. Uncomplicated clinical malaria is still prevalent in children up to around ten years old, after which infections are frequent but asymptomatic [129, 130], where parasites are detectable in the blood by microscopy or PCR but no symptoms are present. However, parasitaemia is still detectable in all age groups up to 60 years old [129], showing that naturally acquired sterile immunity is essentially non-existent. These profiles of severe and mild disease occur in older age groups in lower-transmission regions [130, 131], and so as malaria control measures become more successful at reducing malaria incidence and transmission, episodes of clinical malaria are likely to become less concentrated in children and spread across all age groups [132]. There is also evidence that cerebral malaria may be more likely in areas with low transmission compared to high or moderate transmission

areas [131]; this may be because severe malaria takes the form of cerebral malaria in older children and adults, who bear the disease burden in low transmission settings, whereas young children are more likely to suffer from severe malarial anaemia, which has a lower case fatality rate [133].

In many countries, treatment for *P. falciparum* is ACT, which combines artemisinin-based compounds with a second anti-malarial drug with a longer half-life, such as piperaquine [122], amodiaquine, or lumefantrine [134]. Resistance to chloroquine is still widespread in many Asian and African countries, although there is some evidence that resistance has decreased since chloroquine use was discontinued [135, 136]. Resistance to ACTs, detected in southeast Asia, is linked to mutations in the *P. falciparum kelch13* gene, and is characterised by slow clearance of parasites during treatment [123, 137, 138]. These mutations have not yet been widely observed in Africa, but there is one report of *kelch* mutations associated with resistance in Senegal [139], and molecular and clinical surveillance is ongoing in multiple regions.

1.2.3 Immune responses to malaria

As the malaria parasite undergoes several life cycle stages and presents different antigens at each stage, both humoral and cellular immune mechanisms are required to control and eliminate infection. In mouse models, early production of the pro-inflammatory cytokine IFN-γ was found to be essential for control of parasitaemia and in its absence mice swiftly succumbed to infection ([140]; reviewed in [141]). The main sources of IFN-γ are CD4 T cells and NK cells, where CD4 T cells are essential for activating and driving immune responses, including antibody and CD8 T cell responses, throughout the course of infection. Mice depleted of B cells and CD8 T cells were unable to control mid stage and chronic infections and also died [141]. NK cells are important early producers of IFN-γ in humans *in vitro* [18] and may act against liver stage and intra-erythrocytic parasites [141, 142]. IFN-γ is thought to act primarily by activating macrophages to phagocytose merozoites and parasitised erythrocytes in both an opsonization-dependent [143] and opsonization-independent

manner [140], and by inducing macrophages to produce parasiticidal free radicals such as nitric oxide (NO) and superoxide, which combine to form short-lived but highly damaging peroxynitrite capable of efficiently killing infected erythrocytes [144].

In humans, antibody responses to the erythrocytic parasite stage are important for clinical immunity (reviewed in [145]) and have been shown to be protective via passive antibody transfer [146]. Antibodies can directly impede merozoite invasion of red blood cells by blocking merozoite binding sites [147] and enhancing complement-mediated lysis of merozoites and extracellular gametocytes [148]. Opsonization to enhance anti-malarial neutrophil [149, 150] and macrophage activity [151] is also thought to be a key function of erythrocytic-stage antibodies. Antibodies may also target variant surface antigens on infected red blood cells (iRBCs) to enhance iRBC killing and prevent sequestration to endothelial cells (reviewed in [152]). The breadth of antibody responses has been found to both increase with age [153] and to be inversely proportional to clinical episodes of malaria, indicating that antibodies to multiple parasite antigens may synergise and confer protection [154] and strongly contribute to the decreased incidence of clinical disease in individuals with multiple exposures to malaria [153]. However, it is still unclear how many episodes of malaria are required to generate a long-lasting antibody repertoire or how long the antibody response lasts (reviewed in [145, 152]). Antibodies against pre-erythrocytic parasites (i.e. sporozoites and liver-stage parasites) do not appear to be highly effective during natural infections due to the very short time that sporozoites are free in the bloodstream, but are likely to be beneficial in older adults with a wide range of antibodies (reviewed in [155]); however, anti-sporozoite antibodies are of considerable interest for vaccine development because of their potential to eliminate parasites before an infection is established.

Cellular responses to malaria are wide ranging, but feature CD4 and CD8 T cells, NK cells, $\gamma\delta$ T cells, macrophages, neutrophils and dendritic cells. CD4 T cells are thought to be key producers of multiple cytokines, which control parasitaemia (IFN-γ) and regulate the inflammatory immune response (IL-10), and activate other cellular responses such as antibody production by B cells, CD8 T cell proliferation and survival, and phagocytosis

by macrophages. There are several subsets of CD4 T cells producing different cytokines that are often classified as Th1, Th2, Th17, follicular T helper (Tfh), and T regulatory (Treg) cells, all of which are thought to be involved in the malaria response. However these populations also appear to be highly plastic and capable of changing function and subset (reviewed in [156]).

A strong pro-inflammatory cytokine response against malaria has been shown to be beneficial in mouse models [140], and failure to respond swiftly to infection is often associated with poorer outcomes. However, uncontrolled inflammatory responses have also been associated with immunopathology, including progression to cerebral malaria [157, 158]. Both IFN-γ and tumour necrosis factor (TNFα) have been implicated in these studies [159, 160], and data suggest that an imbalance between pro- and anti-inflammatory cytokines may lead to severe malaria. Conversely, a lack of IFN-γ in mouse models is invariably fatal as mice succumb to overwhelming parasitaemia [161–163]. IL-10 has been shown to be a key regulator of the immune response to malaria [162], and populations of IFN-γ+ IL-10+ Th1 CD4 cells have been found in both mice [164, 165] and humans [166]. Production of multiple cytokines throughout infection to both activate and regulate the inflammatory response may therefore be the main function of the classic 'Th1' T cells (reviewed in [167]); however, in human children, having a population of IFN-γ+ IL-10+ T cells was protective against immunopathology causing severe malaria, but at the cost of chronic infection and failure to clear parasites [168]. Greater IL-10 production and lower levels of TNFα are therefore suggested to herald a shift towards asymptomatic infections, but potentially prevent the development of sterile immunity ([168]; reviewed in [169]).

Th17 cells appear to be activated during malaria infection, but as yet have no clearly defined role ([165]; reviewed in [170]). B cell activation was traditionally thought to be driven by IL-4 from Th2 cells, but more recent studies have suggested that Tfh cells residing in the germinal centres and producing IL-21 and IL-4 may play a more important role in antibody production (reviewed in [171]). Tfh cells were also found to be important for maintaining germinal centres and controlling B cell differentiation into long-lived plasma cells and memory B cells [172]. The role of Treg cells in human studies is unclear (reviewed

in [169]). Experimentally infected individuals with high proportions of Tregs in peripheral blood had higher parasitaemia than other subjects [173], and people with naturally low frequencies of Tregs appeared to be resistant to malaria [174]. However, the role of Tregs appears to vary at different times during the inflammatory response (interfering with parasite control vs. resolution and preventing pathology) and may depend on the genetic background of the individual.

CD8 T cells do not have a clear role during blood stage infections, but have been shown to kill infected hepatocytes in a contact-dependent manner in attenuated sporozoite vaccine models using mouse and non-human primate models [175, 176]. The role of IFN-γ in this killing is unclear, with evidence both for [177] and against it [175, 178], and the traditional model of killing via granzyme release onto infected cells may predominate here. However, IFN-γ is used as a functional readout for CD8 activation during vaccine target studies [179, 180], and CD8 T cells are a source of IFN-γ. CD4 T cells have been shown to be important for the development of CD8 effector and memory populations ([181]; reviewed in [170]), and as the hepatocyte stage represents a population bottleneck for the parasite, killing by CD8 T cells after priming with irradiated sporozoites was shown to prevent blood stage infections in rhesus monkeys [176]. Dendritic cells are also thought to prime CD8 T cells against sporozoite antigens, and may therefore contribute to the formation of memory responses for future infections (reviewed in [182]).

The role of NK cells during malaria infection is still being determined. There is clear evidence from *in vitro* studies that NK cells produce IFN-γ in response to blood stage parasites [18, 26, 183], and some studies with mouse models suggest that NK cell depletion leads to increased parasitaemia and that NK cells may be required for strong IFN-γ responses [34, 184]. The current proposed role therefore suggests that NK cells primarily produce cytokines, and may be most important within the first 18 hours of infection, after which T cells begin to take over cytokine production [37]. However, there is also some evidence from humanised mouse models [142] that NK cells can directly kill iRBCs. Evidence concerning the role of NK cells during malaria infection is described in greater detail in Chapter 4.

Some mouse models have indicated that inital parasitaemia is mainly controlled by macrophages [185] rather than with IFN-γ from NK or CD8 T cells, but this differs between mouse models and has not been established in humans. However, phagocytosis of infected cells and free merozoites is an important clearance mechansim to reduce parasitaemia [186], and DCs and macrophages activated by both IL-12 and IFN-γ from CD4 T cells and NK cells are important for parasite clearance throughout infection. Overexpression of IL-10 early in infection may therefore be detrimental because it supresses macrophage activity and allows parasitaemia to increase [165]. Opsonization of infected iRBCs and merozoites by antibodies also enhances parasite clearance by macrophages [151].

1.2.4 Vaccine development and potential targets

Immunisation with attenuated or irradiated whole sporozoites has been shown to generate sterile immunity in humans [187, 188], and vaccines targeting sporozoite antigens such as circumsporozoite protein (CSP) show promise [189, 190]. This includes the RTS,S/AS01 vaccine, which uses the CSP antigen and so far has shown modest protection against severe malaria and reduced the number of malarial episodes in young children [189, 191]. However, anti-CSP antibody titres must be maintained at very high levels to confer protection, and even with a fourth booster vaccination of RTS,S at 18 months, efficacy against clinical disease was not predicted to significantly outlast the duration of the study (32 months) [192]. Research is therefore ongoing to determine both new immunogenic targets and better vaccine delivery methods, including viral vectored vaccines (reviewed in [190]). Vaccines aimed at liver stage parasite antigens, such as thrombospondin-related adhesion protein (TRAP), are designed to induce CD8 T cell responses (reviewed in [193]), and have had some success in clinical trials [194], but have not yet progressed to larger scale trials; screening for other antibody targets is ongoing [180]. The need for a wide variety of immune effectors has complicated attempts to target malaria blood stage antigens with a vaccine, as it is still unclear which antibodies are most effective during infection [195]. Target antigens for vaccines include merozoite surface protein (MSP)-1, -2 and -3, *P. falciparum*

reticulocyte binding-like homologue 5 (PfRH5), and apical membrane antigen 1 (AMA-1), but variability in these proteins between parasite strains and species has so far foiled attempts to produce a blood stage malaria vaccine [196–198] (reviewed in [195]).

1.3 NK cells and malaria

Although T and B cell responses are indisputably crucial during malaria infection, there is increasing evidence that NK cells also play an important role in killing malaria parasites and controlling infection. The role of NK cells is primarily thought to be IFN-γ production, both to kill infected hepatocytes during the pre-erythrocytic stage [199] and to activate macrophages during blood stage infections [42]. *In vitro* studies have indicated that NK cells are capable of responding to iRBCs within six hours [18], and so are important early responders prior to T cell activation [37] (described further in Chapter 4).

Activation of NK cells by iRBCs *in vitro* requires the presence of IL-2, IL-12, and IL-18 [37, 183], direct contact with macrophages via ICAM-1-LFA-1 [26, 43], and direct contact with iRBCs [183], which drive strong IFN-γ, CD69, CD25 and CD107a responses [200]. As described previously, NK cells require both accessory cell contact and cytokine stimulation in order to become activated, but the requirement for direct contact with iRBCs is less well understood. Studies have found that NK cells have significantly lower IFN-γ responses to lysed schizonts compared to whole iRBCs [18, 201], suggesting that NK cells are capable of interacting with iRBCs directly in order to become activated. There is also evidence that NK cells form conjugates with iRBCs for short periods of time [42, 183] and that an immune synapse between the two may form [200], although the receptors and ligands that might mediate this interaction are unknown. These interactions are described further in Chapter 5.

NK cell responses to iRBC are highly heterogeneous between donors, but the differences between individuals causing this are unknown [183]. There is some evidence that KIR genotype may affect NK cell response to blood stage parasites and that an AB KIR hap-

lotype may confer a heterozygote advantage compared to an AA or BB haplotype [202]; however, the receptors mediating this have not been identified. There is also little data available on NK cell responses in semi-immune populations exposed to endemic malaria, and how NK cell responses might change during secondary infection. It may also be that NK cells have a reduced role in cytokine production if memory T cells are swiftly activated, but may take on other functions in parasite clearance later in the course of infection. There are therefore many questions that have yet to be answered with regard to the role of NK cells in malaria, some of which I have attempted to address in this thesis.

1.4 Aims and objectives

The role of NK cells during infection is a field of study that has come to increasing prominence of late, and is of particular interest with regard to how NK cells might affect acquired immune responses, including during vaccination. However, there are a great number of more basic questions about NK cell biology that have yet to be answered, especially as one of the key mediators of NK cell responsiveness, the KIR family, is still only partially understood. In this thesis my research objectives focused on four related aspects of NK cells, which were as follows:

1) To investigate the basic activation requirements of NK cells in order to understand how NK cells might become activated very early in infection when only low concentrations of cytokines are available (Chapter 3).

2) To examine the heterogeneity in functional NK cell responses to *P. falciparum*-infected red blood cells in both a malaria naive population from LSHTM and a malaria exposed population from Uganda (Chapter 4).

3) To examine the phenotypic profiles of NK cells within these two groups of individuals, with a focus on their KIR and NKG2C genotype and phenotype, and how this might affect their responsiveness to *in vitro* stimulation with malaria parasites (Chapter 5).

4) To investigate the role of a particular KIR, *KIR2DL5*, whose expression appeared to be related to NK cell responsiveness to malaria-infected red blood cells, and shows distinct patterns of gene carriage and expression in different populations (Chapter 6).

2 | Materials and methods

2.1 Study subjects

2.1.1 Malaria naive donors

Up to 50ml of venous blood was collected in sterile tubes with sodium heparin (2 I.U. per ml of blood) as an anti-coagulant from healthy volunteers within LSHTM through an anonymised blood donation system. Ethical approval was given by the LSHTM Ethics Committee, application #5520, and informed consent was obtained from all donors. Donors are summarised in Table 2.1 by age at time of blood collection, nationality, and history of malaria. 70% of donors were female. Donors with a known or possible history of malaria were excluded from analyses involving NK cell functional responses to malaria parasites. Donor nationality has been grouped (by country or continent, to preserve anonymity) into the following categories: UK, Europe, North America, Central America, Africa, Asia and Oceania.

2.1.2 Malaria exposed donors

Malaria exposed donors (n= 53) were recruited from two sites in Uganda, Nagongera and Walukuba, with different malaria transmission rates as part of the PRISM cohort at the Infectious Diseases Research Collaboration. Ethical approval was obtained from the Makerere University School of Medicine Research and Ethics Committee (REC REF 2011-203), Uganda National Council for Science and Technology (HS 1074), the LSHTM ethics

Age	Age/years	Nationality	No. donors	History of malaria	No. donors
Mean	36.7	UK	29	No	46
Median	33	Europe	9	Yes	3
Range	23-61	N. America	6	Unsure	1
		C. America	1		
		Africa	1		
		Asia	1		
		Oceania	3		

Table 2.1: **Summary of LSHTM donors.** Donors from LSHTM (n= 50) summarised by age, nationality and history of malaria infection.

committee (reference # 6012), and the University of California, San Francisco Committee on Human Research (reference 027911).

Donors were stratified by age (children under 5, children between 5 and 11 years, adults over 20 years old) and their history of malaria in the last year was recorded (whether they had had malaria and the number of episodes). Parasitaemia at time of collection was measured by thick blood smears for microscopy. Details of donors are summarised in Table 2.2 by age, location, the number of donors with parasitaemia at time of collection, and the number of donors with a malarial episode in the last year. Data on the number of males and females in this population are not available. PBMCs from these donors were isolated from venous blood and cryopreserved in country before shipment to LSHTM.

Malaria transmission at the study sites was defined as low or high based on the entomological innoculation rate (EIR). Walukuba in Jinja district is a peri-urban area near Lake Victoria with low transmission and an estimated EIR of 3.8 infectious bites per person per year. Nagongera sub-county in Tororo, south-eastern Uganda, is a rural area with high transmission and an estimated EIR of 125.0 infectious bites per person per year. Malaria transmission at both sites is perennial.

Age group	Nagongera (n)	Walukuba (n)	Mean age/years	Range/years	Parasitaemia (n)	Malaria in last 365 days (n)
<5	10	10	3.05	1.47-4.67	3	11
5-11	11	10	7.64	5.04-10.1	7	10
20-70	4	8	41.87	21.2-68.2	0	0
Total	25	28	13.70	1.47-68.2	10	21

Table 2.2: **Summary of Ugandan donors.** Donors are grouped by age (<5 years, 5-11 years, 20-70 years). Columns show the number of donors from Nagongera and Walukuba, the mean age and range of each age group, the number of donors with parasitaemia at the time of collection, and the number of donors with episodes of malaria in the past 365 days.

2.2 PBMC isolation and techniques

Peripheral blood mononucleocytes (PBMCs) were isolated from whole blood by layering 25ml of blood on top of 15ml of Histopaque 1077 (Sigma-Aldrich) and centrifuging at 500g for 25 minutes with the centrifuge brake off. PBMCs form a distinct layer at the interface of plasma and Histopaque, and were transferred to a fresh tube using a disposable 25ml pipette and washed twice with RPMI 1640 (Gibco, Life Technologies), centrifuging at 800g for 10 minutes each time. Live cells were counted using a disposable haemocytometer at a 1:1 dilution with Trypan blue dye, and resuspended in a culture medium of 10% foetal calf serum (FCS) (Gibco, ThermoFisher Scientific) and 2mM L-glutamine in RPMI (Sigma). Antibiotics (penicillin/streptomycin) were not used for any assays involving malaria parasites to prevent parasite stress and to avoid masking any bacterial contamination of parasite cultures, but were used for experiments in Chapter 3 as described in the Methods of that chapter.

2.2.1 Freezing PBMCs

PBMCs suspended in culture medium were cryopreserved at 2×10^7 cells/ml with an equal volume of freezing medium (80% FCS, 20% DMSO (Sigma)) for a final concentration of 1×10^7 cells/ml. Cells were cooled in Mr Frosty Freezing Containers (ThermoFisher Scientific) containing isopropanol to -80°C at a rate of -1°C per minute, and transferred to liquid nitrogen for long term storage.

2.2.2 Defrosting cryopreserved PBMCs

Cryopreserved PBMCs were thawed for use in functional and phenotyping assays by pipetting warmed RPMI onto the frozen cells and transferring the thawed cells into 20ml warm RPMI. Cells were centrifuged at 1800rpm for 10 minutes, washed again with RPMI, and rested for at least 1 hour in culture medium (10% FCS, 2mM L-glutamine in RPMI).

2.2.3 NK cell isolation

NK cells were isolated from PBMCs using a StemCell EasySep kit (StemCell Technologies) according to the manufacturer's instructions. This method uses negative selection to enrich NK cells by binding non-NK cells to magnetic beads and holding them in a magnetic field whilst unbound NK cells remain in the supernatant. PBMCs were resuspended in PBS at 5×10^7 cells/ml in a U-bottomed plate and incubated with EasySep Human NK Cell Enrichment Cocktail at 50µl/ml of cells for 10 minutes at room temperature. Cells were then incubated with 100µl/ml of cells EasySep D Magnetic Particles for 10 minutes, then the plate was placed on a plate magnet ("EasyPlate" EasySep magnet) for 15 minutes. The NK cell enriched medium was then pipetted off into a clean plate and spun down to pellet the cells, which were then counted with a disposable haemocytometer in a 1:1 dilution with Trypan blue and resuspended in 10% FCS culture medium for further use.

2.3 Parasite culture

P. falciparum parasites of strain 3D7 were cultured in 25ml complete culture medium and 2ml packed erythrocytes. Two strains of malaria parasites, 3D7A and a transgenic 3D7HT-GFP line [203], were used in experiments. The GFP-expressing 3D7HT-GFP line is described further in Chapter 5. Culture medium was prepared using RPMI 1640 containing 5% Albumax solution and 1% hypoxanthine (Sigma). Albumax solution for parasite culture was made in house from 10% w/v AlbuMAX powder (Gibco), 4% w/v D-glucose (Sigma) and 0.6% w/v L-glutamine (Sigma) in dH_2O, filtered through a 0.2µm filter (Acrodisc Syringe Filter, PALL), and stored at -20°C. Blood (A+ blood group) was obtained from the National Blood Service, London. To remove leukocytes, which inhibit parasite growth, blood was centrifuged at 2500g for 10 minutes and the plasma and buffy coat pipetted off. Packed erythrocytes were diluted 1:1 with RPMI and kept at 4°C for up to one week.

To keep parasites within cultures synchronous, parasites were periodically treated with sorbitol to kill late stage parasites, leaving only ring-stage parasites alive [204]. Predom-

inantly ring stage cultures were centrifuged at 800g for 2 minutes and the supernatant discarded. Packed blood cells were incubated with 6ml warmed sorbitol (0.05g/ml) for 2 minutes, then centrifuged at 800g for 2 minutes. The supernatant was discarded and the parasites washed twice with warm RPMI to remove any remaining sorbitol, then put back into culture with fresh culture medium and checked the next day.

For counting, glass slides with a thin blood film of parasites were stained in 10% freshly prepared Giemsa stain for 10 minutes and counted at 100× magnification. Giemsa was prepared in a 10ml syringe (BD Plastipack) with a blunt needle at a dilution of 1:10 from the stock solution (Giemsa Improved R66 Solution, VWR Chemicals) and filtered through a 0.2µm filter (PALL) before use. Parasites were maintained at 1-2% iRBCs in 4% hematocrit unless increased parasitaemia was required for experiments, and were kept at 37°C in a 5% CO_2 incubator in a 100ml filter-top flask (Nunc). Culture medium was changed every 1-2 days and fresh blood provided as required. Cultures were tested regularly for *Mycoplasma* contamination with LookOut Mycoplasma QPCR Detection Kit (Sigma-Aldrich).

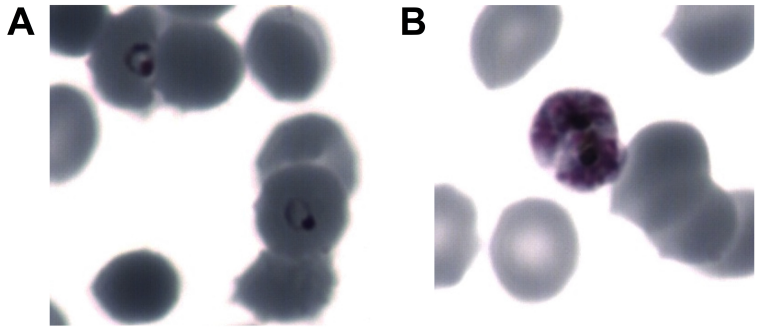

Figure 2.1: **iRBCs in culture.** *P. falciparum* infected red blood cells at the ring stage (A) and mid to late schizont stage (B). Schizont stage parasites have segmented nuclei and a crystal of hemozoin (a haemoglobin waste product) containing iron, visible as a dark spot in the centre of the schizont.

2.3.1 Parasite purification by MACS

At mid-to-late schizont stage, parasites at 5-10% parasitaemia were purified by magnetic-activated cell sorting (MACS) (Miltenyi Biotec) using sterile MACS Cell Separation CS Columns mounted on a VarioMACS separator magnet. MACS CS Columns consist of ferromagnetic fibres with a stop cock at the neck of the column, allowing control of the flow rate through the column. Schizonts form iron-containing hemozoin as a waste product of haemoglobin digestion, which causes late stage iRBCs to be retained in the MACS column by the magnet while allowing uninfected RBCs and early stage iRBCs to flow through. When freed from the magnetic field, schizonts can be eluted from the column.

iRBCs in culture were centrifuged at 800g for 2 minutes and most of the supernatant removed. A MACS column was saturated with warm RPMI, and iRBCs at 30% hematocrit were passed through the column at a rate of around 2 droplets per second. The column was washed with warm RPMI to remove any unbound erythrocytes and non-schizont stage parasites, then removed from the magnetic separator and washed again with warm RPMI to elute the schizont-stage parasites. Schizonts were then centrifuged at 800g for 2 minutes and resuspended in warm culture medium prior to use. This process gave a mid-to-late stage schizont purity of 85-100%, as determined by microscopy. Columns could be throughly flushed with 70% ethanol and stored in 70% ethanol at 4°C for reuse, and used up to three times before purification quality was compromised.

2.4 Assays for PBMC function and phenotype

For functional assays measuring NK cell activation, PBMCs were incubated in 96 well U-bottom plates (Nunc) in culture medium (10% FCS, 2mM L-glutamine in RPMI) with stimuli for 18 hours overnight at 37°C, 5% CO_2, unless otherwise stated. Brefeldin A (BfA) (BD Biosciences) was added to culture at 15 hours to inhibit protein trafficking from the endoplasmic reticulum and allow accumulation of intracellular IFN-γ. Anti-CD107a antibody (BD) was added from the beginning of culture at 2µl per well. PBMCs in culture

medium alone were used as a negative control for each donor, and a high concentration of the cytokines IL-12 and IL-18 (at 5ng/ml and 50ng/ml respectively, both PeproTech) was used as a positive control (referred to as HCC). After 18 hours, the samples were stained with antibodies for flow cytometry. Cells were centrifuged at 800g for 5 minutes, then washed twice with cold FACS buffer (1% FCS, 0.05% sodium azide (Sigma) and 5mM EDTA (Invitrogen) in PBS). Cells were then incubated for 20 minutes at 4°C in the dark with 10µl of the surface antibody master mix before washing with FACS buffer. To fix and permeablise the samples, cells were incubated in 70µl CytoFix/CytoPerm (BD) for 20 minutes at room temperature in the dark. Cells were then washed with Permwash (BD) twice, or until any red blood cells present were no longer visible in the wells (conditions using uninfected red blood cells (uRBCs) as a control for malaria-infected RBCs). Cells were then stained with 10µl intracellular antibodies for 20 minutes at 4°C in the dark. Cells were washed again with Permwash, then resuspended in 220µl FACS buffer and transferred to clean alpha tubes ready for flow cytometry. Antibody staining panels are detailed in the methods section of each results chapter.

For phenotypic analysis of NK cells, PBMCs were incubated with medium alone, uRBCs or MACS-purified schizont stage iRBCs for 2 hours at 37°C, 5% CO_2. After incubation, cells were centrifuged at 500g for 5 minutes, then fixed in 100µl 4% formaldehyde for 15 minutes. Cells were washed twice with FACS buffer and incubated with 10µl surface antibodies for 20 minutes at 4°C in the dark, then washed again and resuspended in FACS buffer for flow cytometry. Some changes in protocol were made between different experiments, which are described in detail in Section 5.2.3, Chapter 5.

2.5 Measuring iRBC-NK cell conjugate formation by FACS

The ability of NK cells to form stable contacts with malaria-infected RBCs has been previously observed in our group and others, as described in Chapter 5. PBMCs were incubated in 96 well U-bottom plates with MACS purified 3D7A iRBCs or 3D7HT-GFP iRBCs for two hours at 37°C, 5% CO_2. Cells were centrifuged at 500g for 5 minutes

and fixed with 4% formaldehyde in PBS for 20 minutes to fix the conjugates. Cells were then washed twice with cold FACS buffer before staining with surface FACS antibodies. Experiments using 3D7A iRBCs were stained for glycophorin A (CD235a) (eBioscience), a surface marker found on all red blood cells, and for CD3- CD56+ NK cells. 3D7HT-GFP iRBCs constitutively express GFP in the cytosol of the malaria parasite, and were stained for NK cell markers only. NK-iRBC conjugates were therefore defined as CD235a+ CD3- CD56+ events or GFP+ CD3- CD56+ events respectively.

2.6 Fluorescence-activated cell sorting (FACS)

Flow cytometry was carried out using a BD LSRII Flow Cytometer. Data were analysed using the Flow Cytometry Analysis Software, FlowJo, v. 7.6.5 (Tree Star, Inc). Prior to sample analysis, fluorescence compensation was carried out using BD CompBead Anti-mouse Ig, κ (BD Biosciences) stained with single antibodies. For the CD3-V500 compensation, unstained cells cultured in medium overnight and fixed in CytoFix/CytoPerm (BD) were used instead of beads. Compensation was calculated by the FACSDiva software (BD) and applied for the duration of the experiment. Fresh compensation beads were prepared for each experiment and compensation calculated each time.

2.7 Confocal microscopy

PBMCs or isolated NK cells were incubated with MACS-purified 3D7HT-GFP schizonts at 37°C for 30-90 minutes in 96 well U-bottomed plates. The cells were centrifuged at 500g for 5 minutes, then fixed in 100µl 1.5% formaldehyde (VWR Chemicals) with 0.1% glutaraldehyde (Sigma) dissolved in PBS for 30 minutes. Fixation was stopped by adding 100µl washing buffer (1x PBS, 0.1% Tween 20). Cells were centrifuged at 500g for 5 minutes and washed again with washing buffer, then blocked with 100µl blocking solution (10% FCS in PBS) for at least 30 minutes at room temperature to reduce non-specific background staining.

After blocking, cells were stained for filamentous actin (F-actin) by incubation with 100µl phalloidin conjugated to AlexaFluor 594 (Molecular Probes, Life Technologies) for 20 minutes at room temperature in the dark. The stock solution of phalloidin (200 units/ml, approximately 6.6µM according to manufacturer's instructions for reconstitution) was diluted 1:40 in PBS and used for staining. Cells were then washed with 100µl washing buffer and centrifuged at 500g for 5 minutes.

To stain DNA with 4',6-diamidino-2-phenylindole (DAPI), cells were incubated with 200µl DAPI (Molecular Probes) diluted to 300nM in PBS for 2-10 minutes at room temperature. Cells were centrifuged and washed twice with washing buffer and once with PBS. Cells were then transferred in residual PBS (maximum volume of 10µl) to coverslips and mixed with a drop of Vectashield Mounting Media (Vector Laboratories) before mounting on slides and sealing with nail polish. Slides were viewed with a Zeiss LSM510 confocal microscope.

2.8 DNA extraction and genotyping

2.8.1 DNA extraction

400µl aliquots of whole blood from each donor were collected and stored at -80°C for DNA extraction. DNA was extracted using the Wizard® Genomic DNA Purification Kit (Promega) according to the manufacturer's instructions (Section 3 of the Wizard Genomic DNA Purification Kit Technical Manual, TM050, Isolating Genomic DNA from Whole Blood (300µl sample)). Briefly, whole blood samples were incubated with Cell Lysis Solution to remove red blood cells, centrifuged, and the supernatant discarded. Pellets were incubated with Nuclei Lysis Solution and Protein Precipitation Solution to penetrate the nuclei of remaining leukocytes and remove cell debris. Supernatants containing DNA were transferred to clean 1.5ml tubes containing isopropanol to precipitate DNA from solution, centrifuged, and DNA pellets washed with 70% ethanol. Supernatants were aspirated off and DNA pellets allowed to air dry, before resuspension in 20µl DNA Rehydration So-

lution. DNA quality and quantity were measured by NanoDrop Spectrophotometer and DNA was stored at 4°C.

2.8.2 Genotyping by PCR

2.8.2.1 KIR genotyping

Samples were typed for KIR genes according to the protocol 3.01 KIR Typing 2 ([205], also published in [206]), designed by Chrissy h. Roberts. Presence or absence of 17 KIR genes (Table 2.3) was detected by sequence-specific primer PCR using the primer sequences in Table B.1, Appendix B. Each gene was detected in a separate PCR reaction, except for KIR3DL3 and 3DX1, which were combined in reaction 13.

Reaction	KIR	Reaction	KIR
1	2DL1	9	2DS4
2	2DL2	10	2DS5
3	2DL3	11	3DS1
4	3DL1	12	2DP1
5	3DL2	13	3DL3/3DX1
6	2DS1	14	2DL4
7	2DS2	15	2DL5
8	2DS3	16	3DP1

Table 2.3: **KIR genotyping PCR reactions.**

PCR mastermix consisted of 85µl 2X HotStarTaq Mastermix (Qiagen) (containing Taq polymerase, buffer and dNTPs), 5.1µl 25mM $MgCl_2$, 32µl nuclease-free dH_2O and 17µl purified template DNA at 100ng/µl per donor (enough for 16 reactions with primers for each KIR). Each KIR primer mix contained between 2 and 4 sequence-specific primers for the KIR of interest and two primers amplifying invariant sequences in HLA-DRA as an internal positive control for each reaction (FDRA 360 and RDRA 595 for reactions 1-15, product size 283bp; FDRA360 and RDRA 633 for reaction 16, product size 608bp). Primer

mixes for each reaction are listed in Table B.2, Appendix B.

Reactions were set up in 200µl capped PCR tubes in strips of 8 forming an 8 by 16 panel of PCR tubes (Figure 2.2). 2µl of 10µM primer mix was aliquoted by multichannel pipette vertically into 8 wells per primer. 8µl template DNA and PCR mastermix was aliquoted horizontally into 16 wells for a final reaction volume of 10µl. Tubes were sealed and gently vortexed and centrifuged prior to thermal cycling.

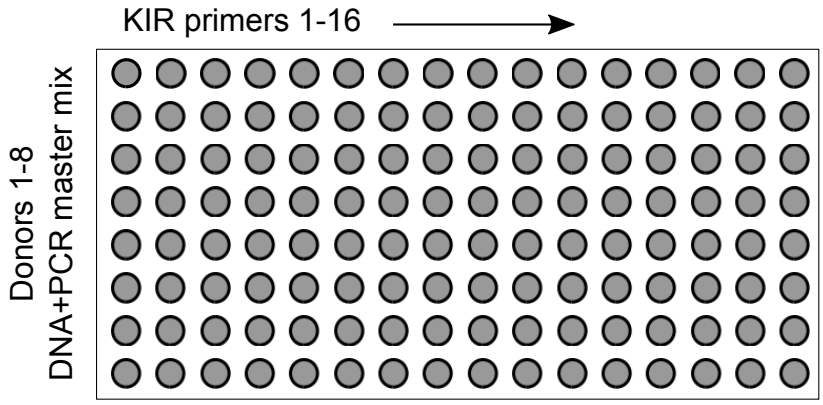

Figure 2.2: **Layout of tubes for KIR PCRs.** Donors were KIR genotyped in batches of 8, with 16 primer combinations per donor.

PCR reactions were run in a thermal cycler with the following program: 15 mins at 94°C; 10 cycles of 94°C for 30 secs and 65°C for 40 secs; 22 cycles of 94°C for 30 secs, 61°C for 30 secs and 72°C for 40 secs; 4°C for 30 secs, and hold at 15°C. Products were electrophoresed with loading buffer on a 3% agarose gel in 1× Tris/Borate/EDTA (TBE) buffer (National Diagnostics) with 2µl ethidium bromide (EtBr) (Sigma) for 45 mins at 150V. Reactions 9 and 16 (2DS4 and 3DP1) were run for an additional 30 mins at 150V for better separation of bands. EasyLadder I (Bioline) was run alongside each set of reactions, with bands at 100, 250, 500, 1000 and 2000 base pairs. Gels were visualised and photographed with a gel doc.

2.8.2.2 NKG2C genotyping

NKG2C deletion was detected by PCR using a Phusion® High Fidelity PCR kit (New England Biolabs) according to a published method [11]. Donors were genotyped for *NKG2C* homozygous presence (++), deletion (−−), or a heterozygous deletion (+−), with product sizes for the deletion and wild-type NKG2C genes of 411bp and 201bp respectively. More details are provided in Chapter 5 and primer sequences are listed in Appendix B. Reactions were run in 96 well plates with each well containing 1µl template DNA, 4µl 5X Phusion High Fidelity buffer, 0.4µl dNTP mix, 0.5µl primers for band 201, 1µl primers for band 411, 0.1µl Taq polymerase, and dH_2O for a total reaction volume of 20µl. PCR reactions were run in a thermal cycler with the following program: 95°C for 3 mins; 10 cycles of 94°C for 30 secs, 65-55°C for 30 secs (starting at 65°C for the first cycle and decreasing by 1°C per cycle), and 72°C for 30 secs; 26 cycles of 94°C for 30 secs, 55°C for 30 secs; hold at 4°C. PCR products were run on a 1.5% agarose gel containing EtBr for 10 mins at 80V, then 1 hr 20 min at 50V before visualisation with a gel doc.

2.8.3 Copy number and structural haplotype of *KIR2DL5*

Analysis of *KIR2DL5* location and copy number was carried out by droplet digital PCR according to the protocol 7.03 Droplet Digital PCR designed by Robert Butcher and Chrissy h. Roberts [207]. Digital droplet PCR uses water and oil emulsion to contain the components of a PCR reaction within individual droplets containing 1 or 0 copies of target DNA, so that successful reactions can be quantified by fluorescence. This procedure and detailed methods are explained in Chapter 6.

Purified DNA from *KIR2DL5*+ donors (as determined by SSP-PCR) was analysed for copy number with reference to the housekeeping gene *RPP30* with invariant copy number of 1. *KIR2DL5* location on the centromeric or telomeric region of the KIR locus was analysed with reference to the KIR genes *KIR2DL2* and *KIR3DS1* respectively, based on linkage between *KIR2DL5* and those genes.

2.9 Statistical analyses

Statistical analysis was performed with Prism 6 (GraphPad), as specified for each experiment. Data were excluded when the gated cell subset contained fewer than 100 cells. All statistical tests are two-sided **** $p \leqslant 0.0001$; *** $p < 0.001$; ** $p < 0.01$; * $p < 0.05$. Statistical tests and sample sizes are stated in the text and in figure legends.

3 | Synergy between common γ_c cytokines and IL-18 potentiates NK cell activation

This chapter is an extended version of a study previously published in *Frontiers in Immunology* as 'Synergy between common γ chain family cytokines and IL-18 potentiates innate and adaptive pathways of NK cell activation' [38] and represents work undertaken jointly with Carolyn M. Nielsen. The published paper is included in Appendix A.

3.1 Introduction

Cytokines are secreted proteins that bind specific receptors and enable communication between cells. The interleukin (IL) family facilitates interactions between leukocytes. There are over forty interleukins, which can be classified into families based on structural and functional homology: the IL-1 family, which includes IL-18 and is generally pro-inflammatory; the common gamma chain (γ_c) family, also known as the IL-2 family, which includes IL-2, IL-15 and IL-21 and has many functions including survival and proliferation of lymphocytes; the IL-12 family, which is also broadly pro-inflammatory; the regulatory IL-10 family; the IL-17 family; the T_H2 family, primarily concerned with helminth infections and allergy; and the chemokines, which induce cell migration after infection or tissue damage (reviewed in [27]).

As cytokines in the same family frequently share subunits of the cytokines themselves or their receptors, there is overlap in many of their functions. Although very few cytokines are thus entirely redundant, there are known detrimental effects of losing most individual cytokines. Studies on mice lacking genes for specific cytokines or their receptors show a range of phenotypes, ranging from phenotypically normal (IL-$6^{-/-}$) to having uncontrollable immune pathology (IL-$10^{-/-}$) (reviewed in [27]). Humans lacking certain cytokines are also affected in a multitude of ways, ranging from increased susceptibility to *Salmonella* and *Mycobacteria* infections (loss of IL-12 [28]) to X-linked severe combined immunodeficiency[1] (loss of IL-2, IL-4, IL-7, IL-9, IL-15 and IL-21, reviewed in [29]). It is clear therefore that the homology between family members is not complete, and although there is likely to be sufficient redundancy between cytokines to allow some degree of function, particularly if the original cytokine is not entirely lost, each cytokine has a specific role in the immune system.

The cytokines that are known to act on NK cells are primarily IL-18, IL-2, IL-15, and IL-12. Other cytokines in these families also activate NK cells, such as IL-23, which has similar effects as IL-12, and IL-21, which is a member of the common γ_c family and shares functions with IL-15. However, these four cytokines activate NK cells in different ways. IL-12 and IL-18 are produced by macrophages and drive IFN-γ production during infection with intracellular pathogens (reviewed in [44]), particularly bacteria and protozoa [25]. Transpresentation of IL-15 by DCs is thought to prime NK cells for activation by lowering the threshold for activation and for driving more cytotoxic NK cell responses [36], as well as survival and maintenance of the NK cell population. IL-2 is crucial for proliferation and survival of T cells and NK cells, particularly during expansion of lymphocyte populations during secondary infections [39, 41].

Cytokine receptors are heterodimers or -trimers, which usually share one or two common subunits (e.g. IL-12 and IL-23 share IL-12Rβ1; the common γ_c family share the γ_c (CD132) alongside a cytokine-specific receptor subunit (e.g. CD25 or IL-15Rα). Sharing receptors can allow faster responses during infection, as many common receptor subunits are con-

[1] The gene *IL2RG* encoding CD132, the common γ_c subunit, is located on the X chromosome [208].

stitutively expressed on the surface of lymphocytes (e.g. CD132 and CD122) [209] and only a few components need to be induced before activation (usually the cytokine-specific subunits, such as CD25). However, the concentration of cytokine required to activate receptors is reduced when the complete receptor is assembled, as in the case of IL-2; the IL-2R$\beta\gamma$ heterodimer is activated by nanomolar concentrations of both IL-2 and IL-15, but the heterotrimer with CD25 allows the receptor to respond to picomolar concentrations of IL-2, and confers specificity on the receptor [210].

3.1.1 Cytokine mediated NK cell activation

Cytokine driven activation of NK cells is well described, but conditions usually involve purified NK cells [22, 32, 211] and comparatively high concentrations of cytokines [22, 33], or else a 'resting' or 'pre-activation' step in IL-2 or IL-15 overnight [212, 213].

Fehniger et al [22] carried out perhaps the most thorough study of the effects of combinations of IL-12, IL-15 and IL-18 on positively-selected NK cells using multiple NK cell readouts: IFN-γ, IL-10, TNF-α, GM-CSF, IL-18R and MIP-1α and MIP-1β. They found that IL-12, IL-15 or IL-18 alone did not induce IFN-γ but that a combination of 10 U/ml (approx. 2ng/ml) IL-12 in combination with either 100ng/ml IL-18 or 100ng/ml IL-15 induced IFN-γ after 24 hours, and that IL-12 with IL-18 was more effective than IL-12 and IL-15. The converse was true for IL-10 induction after 3-6 days, which may indicate that the same cytokines control different NK cell responses at different time points, and therefore perhaps at different points after infection. Both IL-12 and IL-15 induced IL-18Rα (previously known as IL-1Rrp), but not IL-18Rβ (previously AcPL), which they suggest is constitutively expressed. Although this paper looked at combinations of cytokines, the authors did not titrate the cytokine concentrations and there is evidence from other studies, such as Ellery et al [210] and Huang et al [214] that high concentrations of cytokines can either override normal signalling pathways (e.g. high concentrations of IL-2 will bypass signalling via CD25 to use only the IL-2$\beta\gamma$ dimer [210, 211]) or can inhibit signalling *because* of the high concentrations (e.g. IL-12 signals via STAT4, but STAT4 mRNA levels

decrease from the peak with increasing IL-12 stimulation [215]), and therefore the effects they see may not fully correspond with what the cytokine effects would be *in vivo*.

3.1.2 IL-12 and IL-18 are established activators of NK cells

IL-12 is a heterodimer composed of the IL-12p40 and IL-12p35 subunits. IL-12 shares both a ligand and a receptor subunit with IL-23 (IL-12p40 and the β2 receptor subunit respectively) but has distinct functions in both T cell maturation and immune activation and is generally considered obligatory for IFN-γ production (reviewed in [216]). The IL-12R is composed of two subunits, designated beta-1 and beta-2, which are coexpressed and together mediate IL-12 signalling. IL-12Rβ1 alone is capable of binding IL-12 with high affinity but signalling is mediated by IL-12β2; in an IL-12Rβ2 knockout mouse model, splenocytes bound IL-12 but did not induce downstream signalling by STAT4 or produce IFN-γ in response to IL-12 [213]. The β1 subunit is constitutively expressed on NK and T cells whereas the β2 subunit is upregulated during cell activation. Loss of the β1 subunit has been found to be detrimental for the immune response against certain bacterial infections in human populations [28] as is the loss of IL-12 itself; the effect of losing the β2 subunit is not known [216].

During infection, IL-12 is thought to be produced primarily by monocytes and to drive T cell and NK cell IFN-γ production [19]. Past investigations by our group and others have shown that IL-12 alone cannot drive interferon production, but in combination with IL-15 or IL-18 it readily stimulates IFN-γ within 18 hours. Since IL-12 requires other cytokines in order to activate cells, it is of obvious interest to elucidate which cytokines are required and which pathways are used. However, previous *in vitro* work has usually used non-physiologically relevant models, particularly with regard to the concentrations of cytokines. IL-12 is not usually detectable in the serum of healthy individuals [217] as it is highly pro-inflammatory and therefore tightly regulated *in vivo*. These regulatory mechanisms can be overridden by non-physiologically high concentrations of cytokines, obscuring the relevant biological pathways that are activated during infection.

IL-18 was originally named IFN-γ inducing factor by Okamura et al [218] and was thought to be better than IL-12 at inducing IFN-γ. The IL-18R is composed of two subunits. The alpha subunit is thought to recognise and bind IL-18, and is widely expressed on a variety of cells including NK cells, T cells and macrophages [27], whereas the beta subunit signals via the MyD88 pathway [219]; this is shared with related cytokines such as IL-1β, but is distinct from the IL-12 family and the common γ_c family signalling pathways, which use various STAT molecules (reviewed in [41]).

Although the data are somewhat inconsistent [22, 220], the combination of IL-12 and IL-18 is a well established combination for IFN-γ induction. The main source of IL-12 and IL-18 is macrophages, as described in [44], and this combination primarily drives cytokine production, especially IFN-γ and TNFα [22, 218], although it may also drive cytotoxic responses [24]. IL-12 and IL-18, in combination but not alone, were shown to enhance NK cell CD25 expression, IFN-γ production and cytotoxic responses [22, 221, 222] and IL-18 is one of the main pathways for IFN-γ production; on the other hand, IL-2 and IL-12 combined are reported to induce IFN-γ without IL-18 [215].

To summarise, there are many contradictions regarding the effects of IL-12 and IL-18 individually on NK cell function (such as IFN-γ and cytotoxicity), and even more regarding cytokine receptor upregulation (CD25, IL-18R, IL-12R), but it is clear that the combination of the two at high concentrations ($\geqslant$ 1ng/ml IL-12, 50ng/ml IL-18) is a driver of IFN-γ from NK cells.

3.1.3 IL-2 drives T cell and NK cell proliferation

IL-2 is important for T cell proliferation, particularly as part of T cell memory responses. T cells are thought to be the primary source of IL-2 but there is some evidence that DCs also produce small amounts [223]. NK cells also require IL-2 during activation and are capable of responding to it via expression of CD25. CD25 is the ligand-specific alpha chain of the IL-2 receptor and is found on the surface of various lymphocytes, including T cells and NK cells. It is upregulated during activation, potentially to allow greater signalling by IL-2 to further

enhance lymphocyte proliferation and activation. Loss of IL-2 or CD25 is not immediately lethal, but *in vitro* T cell responses are abnormal and serious autoimmune diseases develop [29, 224]. CD4+ CD25+ Foxp3+ regulatory T cells (Tregs) are important producers of IL-10, which mediates immune responses and prevents damage to healthy tissues (reviewed in [225]). IL-2 is therefore important for developing and maintaining peripheral self-tolerance [226]. With regard to NK cells, although IL-2 is important for lymphocyte development in general, IL-15 is thought to be more important for NK development and survival (reviewed in [227]); however IL-2 is an important costimulator for NK cell activation during infection [37].

3.1.4 IL-15 priming and signalling

IL-15 has traditionally been thought of as essential for homeostatic maintenance and survival of NK cells. However, IL-15 also appears to play an important role in enhancing or initiating NK cell activation during some diseases, including malaria [228, 229]. This is thought to be due to NK cell priming by dendritic cells by presentation of IL-15 [35]; this priming response is a precursor to activation rather than an activation signal itself, and allows stronger NK responses to activating signals such as IL-12 or IFN-α than in unprimed NK cells [34, 230]. How priming might work in tandem with NK cell education (described in Introduction, Section 1.1.5) is currently not clear, but is likely to complement a model of an NK cell activation threshold, where IL-15 helps to lower the threshold rather than to drive the NK cell across it.

IL-15 is not freely secreted into blood and therefore is not easily detected in serum [231], but is primarily produced by dendritic cells and is required for both NK cell and T cell homeostasis and maturation [232, 233]. IL-15 signals via the IL-15R, which is composed of the common gamma chain used by multiple cytokine receptors (CD132), a beta chain shared with the IL-2 receptor (CD122), and a private alpha chain specific for IL-15 (IL-15Rα) [234]. Unlike IL-2, IL-15 is capable of binding IL-15Rα with high affinity in the absence of the beta and gamma subunits. This allows IL-15-IL-15Rα complexes to signal via both

cis-presentation, using the IL-15R$\beta\gamma$ complex on the same cell, and trans-presentation, where the IL-15R$\beta\gamma$ subunits are on a different cell (e.g. the T cell or NK cell being signalled; reviewed in [235]). Transpresentation is thought to be most relevant *in vivo* for NK cell activation, but cis-presentation may be important for maintenance of other immune cells and is likely to account for most *in vitro* responses to exogenous IL-15 [235].

Monocytes constitutively express IL-15Rα, and can produce IL-15-IL-15Rα complexes in the endoplasmic reticulum for cell surface expression [49]. In addition to IL-15Rα expression, monocytes can also present a membrane tethered form of IL-15 itself, which is better at activating T cells than soluble IL-15 [236]; however IL-15 is most efficient at signalling when bound to the high affinity IL-15Rα, and the IL-15-IL-15Rα complex activates T and NK cells 50-100 fold more effectively than recombinant uncomplexed IL-15, suggesting that binding IL-15Rα might induce a conformational change that enhances binding to other subunits [237]. Because the effect of IL-15 is greatly enhanced when it is presented on a cell surface, either alone or complexed to IL-15Rα, signalling is generally considered to be contact dependent between monocytes and NK cells and is decreased in the absence of this contact [48].

3.1.5 Aims

The aim of the data presented in this chapter is to characterise NK cell responses to low concentrations of cytokines, both singly and in combination, in order to better understand how NK cells become activated under conditions that mimic events early in infection. We therefore conducted a detailed dose-response analysis of NK cell functional responses and changes in cytokine receptor expression using IL-2, IL-12, IL-15, IL-18, IL-21 and IFN-α at two time points, 6 hours and 18 hours. We also investigated the effect of cytokines on CD16 signalling and degranulation responses.

3.2 Methods

3.2.1 Study subjects

Volunteers were recruited from among staff and students at the London School of Hygiene and Tropical Medicine. All subjects gave written consent under a protocol for recruitment of blood donors approved by the LSHTM ethics committee (reference # 5520) to provide $\leq$ 50ml venous blood.

3.2.2 PBMC preparation and culture

PBMC were isolated from heparinised venous blood on a Ficoll-Hypaque gradient and cryopreserved in liquid nitrogen as described in Methods, Section 2.2). Before use, PBMCs were thawed into complete medium (RPMI 1640, supplemented with 100 U/ml penicillin/streptomycin and 20 mM L-glutamine (Sigma) and pooled 10% human AB plasma (Sigma)), washed, and rested for a minimum of 30 minutes before use.

PBMC (2×10^5/well) were cultured for 6 hours or 18 hours in 5% CO2 at 37°C in 96-well U-bottom plates (Nunc) in complete medium with or without varying concentrations and combinations of recombinant human IL-2, IL-12, IL-15, IFN-α, IL-21 (all from PeproTech), IL-18 (R&D Biosystems) or inactivated influenza virus H3N2 (1μg/ml, NIBSC). GolgiStop (containing Monensin, 1/1500 concentration, BD Biosciences) and GolgiPlug (containing brefeldin A, 1/1000 final concentration, BD Biosciences) were added after 3 or 15 hours (in 6 or 18 hour cultures, respectively) in experiments where intracellular IFN-γ was a read-out. Similarly, anti-CD107a antibody (FITC-conjugated, BD Biosciences) was included in the medium for the entirety of cell culture when CD107a upregulation was a read-out.

For activation via CD16 crosslinking, 96-well flat-bottom plates (Nunc) were coated with anti-human CD16 (BD Biosciences) or an isotype-matched control antibody (mIgG1κ, BD Biosciences) overnight at 4°C. Plates were washed with sterile PBS before addition of 4×10^5 PBMC per well. Cells were cultured in these plates for 6 hours or 18 hours as described

above before harvesting. To harvest cells at the end of culture, plates were incubated at 37°C for 15 minutes with pre-warmed sterile PBS containing 5mM EDTA. PBS with cells was transferred to a 96-well U-bottom plate, centrifuged for 5 minutes at 1800rpm, and washed with FACS buffer before staining with antibodies as above. GolgiStop, GolgiPlug and anti-CD107a were also used as described above.

NK cells were purified from PBMCs using both a StemCell EasySep kit (Stemcell Technologies) as described in Methods, Section 2.2.3 and by magnetic separation column using the NK Cell Isolation Kit (Miltenyi Biotec). The protocol for both uses a mixture of antibodies to bind non-NK cells including T cells, B cells, dendritic cells, monocytes, etc and bind them to magnetic particles. The mixture of cells and magnetic beads is placed against a magnet which draws the bound cells out of solution. The supernatant containing isolated NK cells can then be pipetted off (EasySep) or eluted (MACS column). Purified NK cells were used at a concentration of 2×10^4/well.

3.2.3 Flow cytometry

PBMCs were stained in 96-well U-bottom plates as described in Methods, Section 2.4. Briefly, cells were stained with fluorophore-labelled antibodies to cell surface markers then fixed, permeabilised (Cytofix/Cytoperm, BD Biosciences), and stained for intracellular molecules. The following monoclonal antibodies were used in staining panels for different experiments: anti-CD3-V500, anti-CD57-e450, anti-CD56-PE-Cy7, anti-CD107a-fluorescein isothiocyanate (FITC), anti-IFN-γ-allophycocyanin (APC), anti-CD16-APC-H7, anti-CD16-APC, anti-CD25-PerCP-Cy5.5, anti-IL-18Rα-PE, anti-IL-18Rα-FITC, (all BD or e-Biosciences). Anti-IL-12Rβ2 (R&D Systems) was conjugated to PerCP/Cy5.5 in-house (EasyLink PerCP/ Cy5.5 Abcam). Cells were acquired on an LSRII flow cytometer (BD Biosciences) using FACSDiva software. Data analysis was performed using FlowJo v10 (Tree Star). Gating strategies are detailed in figure legends, with gates set on unstimulated cells (medium alone or isotype controls, with no cytokine stimulation).

3.2.4 Statistical analyses

Statistical analysis of flow cytometry data was performed using Prism 6 (GraphPad), as specified in figure legends. Data were excluded when the gated cell subset contained fewer than 100 cells. Paired Wilcoxon signed rank tests were used to compare responses between stimulation conditions and ANOVA tests for linear trend were used to analyse cytokine titrations. Formal tests for synergy using regression analysis with an interaction term, and linear regression adjusting for confounding factors were performed in STATA (V.14.0). All statistical tests are two-sided **** $p \leq 0.0001$; *** $p<0.001$; ** $p<0.01$; * $p<0.05$. Sample sizes are stated in Figure Legends.

3.3 Results

3.3.1 IL-12 and IL-18: roles in driving IFNγ and CD25

Our first experiment was to titrate IL-12 and IL-18 to clarify the effects of these cytokines. Previous work from our group [6, 17] has used a low cytokine concentration (LCC) combination of 12.5pg/ml IL-12 and 10ng/ml IL-18 to enhance low responses to antigen stimulation, and a high cytokine concentration (HCC) combination of 5ng/ml IL-12 and 50ng/ml IL-18 as a positive control for IFN-γ production. We therefore wished to identify the lowest concentrations of these cytokines that stimulated IFN-γ production and CD25 upregulation after 18 hours using a checkerboard titration with four concentrations of IL-12 and five concentrations of IL-18 (Figure 3.1).

In the absence of cytokine, resting cells show low baseline values of IFN-γ and CD25. IL-18 alone had a dose-dependent effect on CD25 expression (white bars, no IL-12), to which high concentrations of IL-12 (1ng and 10ng/ml, dark red and black bars) had a synergistic effect (Fig. 3.1B). Conversely, IL-18 alone had little effect on IFN-γ production. However, IL-12 alone had no effect on either CD25 or IFN-γ (all bars at 0ng/ml IL-18), and a small amount of IL-18 (5ng/ml) was required in order to see any increase in IFN-γ in addition to IL-12. With a minimum concentration of 5ng/ml IL-18, both 1ng and 10ng/ml IL-12 strongly induced IFN-γ production (Fig. 3.1C).

These data suggest that CD25 is primarily driven by IL-18 alone, although IL-12 can enhance expression. Consistent with published literature, IL-12 drives IFN-γ production, but our data indicate that this requires CD25 expression, as the FACS plots (Fig. 3.1A) show that IFN-γ+ cells are also CD25+ and there are very few IFN-γ+ CD25- cells; there are also far more CD25+ cells than IFN-γ+ cells. We therefore suggest that NK cells are sequentially activated by IL-18, which drives CD25 expression, and then IL-12, which can induce IFN-γ production by CD25+ cells. As CD25 is the high affinity IL-2 receptor, IL-2 may be required for optimal IFN-γ responses, or CD25 expression may correlate with another activation marker required for IL-12 activity.

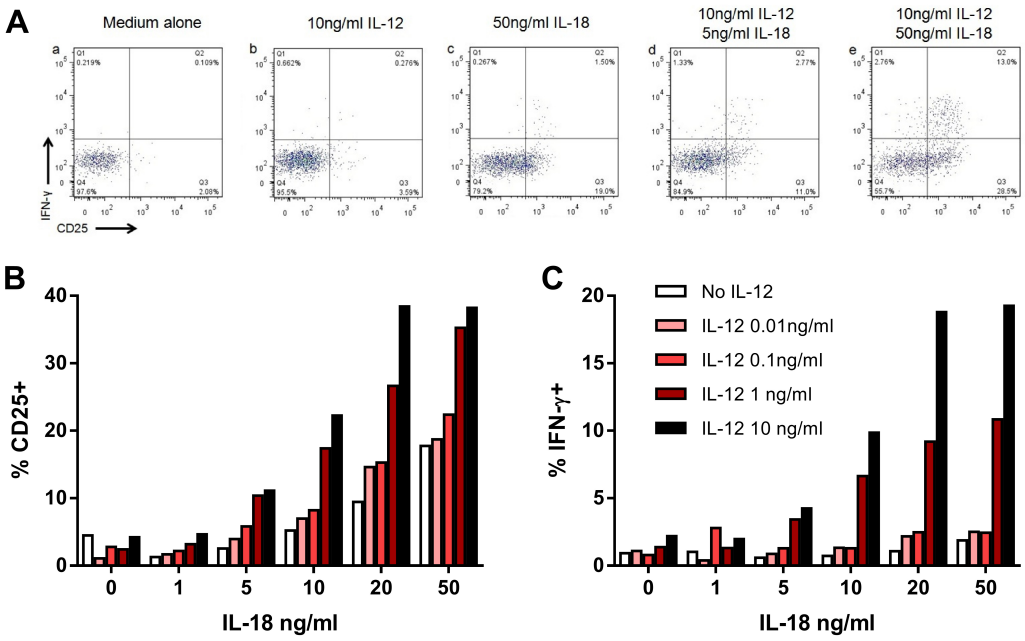

Figure 3.1: **IL-12 and IL-18 drive NK cell responses in a dose-dependent manner.** PBMCs were stimulated with medium alone or with increasing concentrations of IL-12 and IL-18 for 18hrs. Example FACS plots from different conditions showing % IFN-γ+ vs. % CD25+ cells after incubation with medium alone, high conc. IL-12 alone, high conc. IL-18 alone, high IL-12 and low IL-18, and high IL-12 and high IL-18 (A). NK cell CD25 (B) and IFN-γ (C) responses to increasing cytokine concentrations. n= 2, bars represent the mean.

3.3.2 Cytokine-driven functional responses of NK cells

As IL-12 and IL-18 clearly induced IFN-γ and CD25 responses, we next expanded the pool of cytokines to include IL-15, IL-2, IL-21 and IFN-α. For each cytokine we used three concentrations ranging from low to high, where the low concentration was chosen to be as low or lower than concentrations previously described to have minimal effects on NK cell activation (e.g. 12.5pg/ml IL-12, which is used in our lab in the LCC conditions, or 5ng/ml IL-18, which is less than the IL-18 concentration used in LCC). The higher concentrations were chosen by reference to the positive control high concentrations used in our group (HCC), or to the literature, which has frequently reported concentrations of 50ng/ml of IL-15 and IL-18 or higher [22, 33], and between 1 and 10ng/ml IL-12 [22, 33, 238].

3.3.2.1 Increasing concentrations of single cytokines drive IFN-γ and CD25 responses in NK cells

After 6 and 18 hours we analysed CD25 and IFN-γ responses to individual cytokines (IL-2, IL-12, IL-15, IL-18 and IL-21) (Figure 3.2). Both IL-15 and IL-18 independently upregulated CD25 in a dose-dependent manner at both 6 and 18 hours (Fig. 3.2A, B). The CD25 response to IL-15 is higher than the response to IL-18 at 6 hours, which may indicate that cells can respond to IL-15 earlier during infection. After 18 hours, all cytokines except IL-21 show a trend of CD25 upregulation with increasing concentration, but only IL-15 and IL-18 show significant increases in CD25 expression at all concentrations. High concentrations of IL-12 (0.25 and 5ng/ml) do induce CD25 upregulation, consistent with the results in Fig. 3.1B, but this effect is small compared to IL-15 and IL-18-driven CD25 expression. After 6 hours there was little IFN-γ production (Fig. 3.2C), but after 18 hours the highest concentrations of IL-12, IL-15 and IL-18 all significantly and independently upregulated IFN-γ (Fig. 3.2D). The effect of IL-15 alone on IFN-γ production was surprising, but there may be a small amount of endogenous cytokine driving IFN-γ responses after IL-15-induced CD25 upregulation as these assays are carried out with mixed PBMC populations.

3.3.2.2 Combinations of cytokines synergise to drive NK cell responses

From the single cytokine concentration responses, it is clear that NK cells within the PBMC population are responsive to much lower concentrations of cytokines than have been previously used. We therefore looked at combinations of cytokines at these low concentrations to investigate how they might interact to enhance or inhibit NK cell responses and to better model the early NK cell response to cytokine stimulation. PBMCs were stimulated with cytokines for 6 or 18 hours and stained for functional markers and cytokine receptors. In these experiments, we used fixed concentrations of IL-12 (12.5pg/ml), IL-15 (0.75ng/ml) and IL-18 (10ng/ml) either singly or in combinations with each other, and titrated in IL-2 (0, 5 and 50ng/ml) to investigate the effects of IL-12, IL-15 and IL-18 as 'innate'

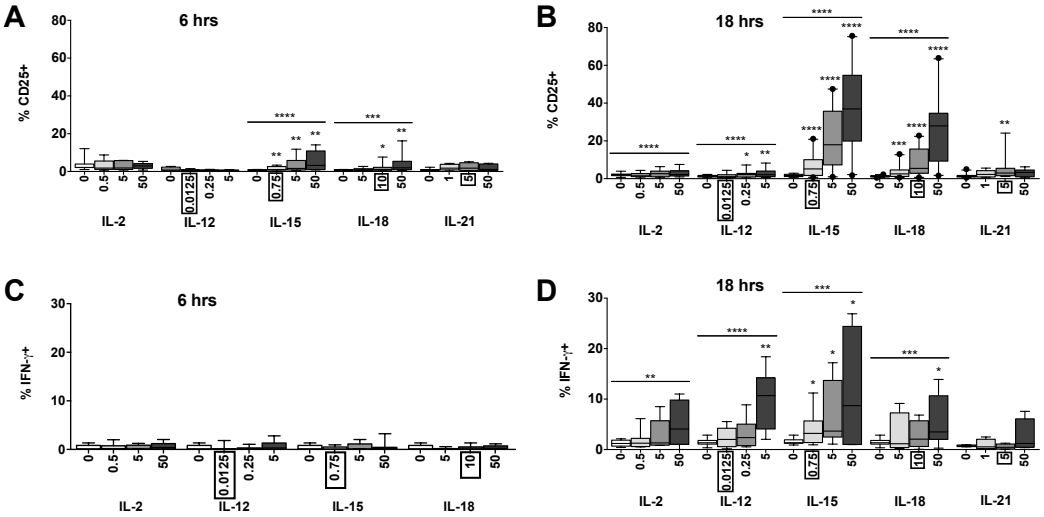

Figure 3.2: **Single cytokine titrations drive CD25 and IFN-γ responses.** Titrations of IL-2, IL-12, IL-15, IL-18 and IL-21 (concentrations ng/ml as labelled) were used to stimulate PBMCs for 6 or 18 hours *in vitro* and the CD25 and IFN-γ responses were measured by FACS. Graphs show the CD25 responses at 6hrs (A) and 18hrs (B), and IFN-γ responses at 6hrs (C) and 18hrs (D). n= 6-22, data from 2-6 experiments. Concentrations in boxes indicate those used in following graphs.

cytokines, with or without help from the 'adaptive' T cell-produced IL-2. We also looked at the interaction of each of these cytokines with IL-21 (5ng/ml) in a separate experiment to investigate whether IL-21 synergises with other cytokines.

CD25 upregulation was driven by IL-18 alone, but was strongly enhanced by a combination of IL-18 and either IL-15 or increasing concentrations of IL-2 (Figure 3.3). Sample FACS plots show CD25 expression in response to medium and 50ng/ml IL-15 (Fig. 3.3A). After 18 hours, IL-15 and IL-18 alone drove CD25, but also strongly synergised to increase CD25 upregulation (test for interaction, p= 0.009) (Fig. 3.3B). IL-12 did not add to IL-18-driven CD25 upregulation, but slightly enhanced responses in the presence of both IL-15 and IL-18. It is clear that IL-2 synergised with IL-18 to drive CD25 responses (trend analysis $p<0.0001$ for IL-18 with increasing IL-2); the combination of IL-2 and IL-12 slightly increased CD25 expression, but this was a very small effect and was not noticeable in combination with IL-18. However, adding IL-2 to combinations involving IL-15 seemed

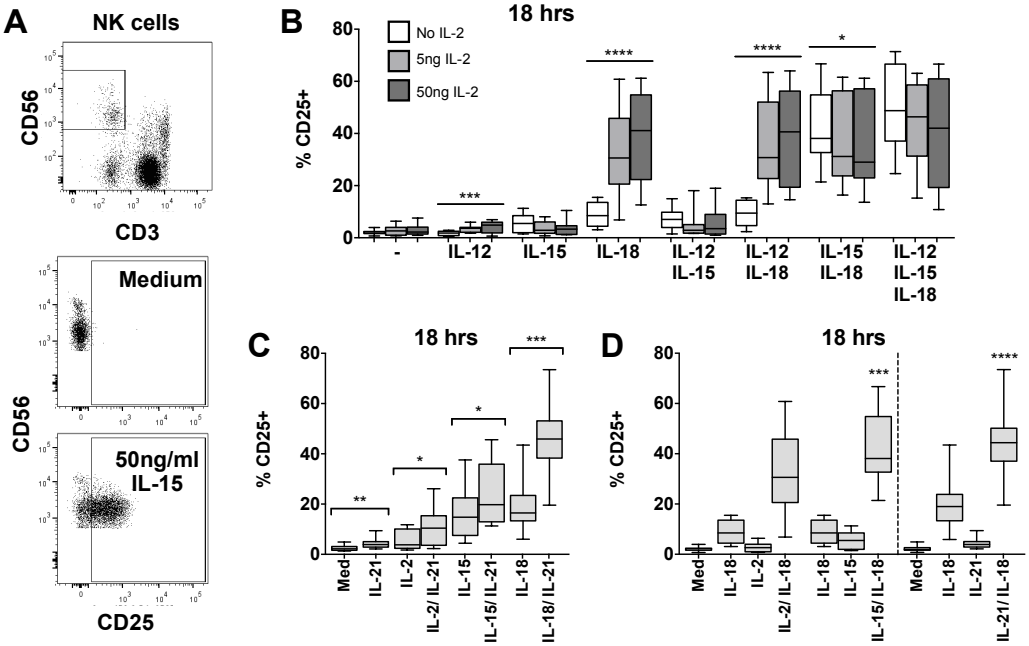

Figure 3.3: **IL-18 synergises with multiple γ_c cytokines to drive CD25 upregulation.** PBMCs were incubated for 18 hours with fixed concentrations of cytokines (IL-12: 12.5pg/ml, IL-15: 0.75ng/ml, IL-18: 10ng/ml, IL-21: 5ng/ml) and 0, 5 or 50ng/ml IL-2. FACS plots of CD56+ CD3- NK cells and CD25 expression after incubation with medium and 50ng/ml IL-15 (A). NK cell responses to combinations of IL-12, IL-15 and IL-18 with different concentrations of IL-2, n= 7-8 (B). NK cell responses to IL-21 in combination with IL-2, IL-15 and IL-18, n= 8 (C). Summary of responses to IL-18 in combination with each of the common γ_c cytokines (D). Box plots represent the 5-95th percentile. Uncapped lines indicate ANOVA tests for linear trend across increasing cytokine concentrations including medium alone, capped lines indicate paired Wilcoxon signed-rank tests.

to reduce CD25 upregulation. There was a non-significant trend for decreasing CD25 when adding IL-2 to IL-15 alone, and adding IL-2 to IL-15 and IL-18 seemed to decrease CD25 expression despite the synergy both IL-2 and IL-15 had with IL-18 (median without IL-2= 38.1%; median with 50ng/ml IL-2= 29.0%, linear test for trend, p= 0.04).

The combination of IL-21 with all of the single cytokines IL-2, IL-15 and IL-18 significantly upregulated CD25 after 18 hours (Fig. 3.3C). This was most noticeable in combination with IL-18, which is consistent with the overlapping functions and signalling pathways of IL-2 and IL-21. It therefore seems that with regard to CD25 upregulation, IL-21 has most in

common with IL-2 rather than IL-15, although all three cytokines are part of the common γ_c family. Most notably from these experiments, it was clear that IL-18 is capable of synergising with all of the common γ_c cytokines to drive CD25 upregulation (summarised in Fig. 3.3D).

IFN-γ responses from the same experiments showed similar trends to CD25 (Figure 3.4). Increasing concentrations of IL-2, IL-12, IL-15 or IL-18 each, individually, induced significant IFN-γ production by NK cells at 18 hours, although the proportions of IFN-γ+ cells rarely exceeded 10% even at the highest cytokine concentrations (see Fig. 3.2). However, it is clear that combining even low concentrations of IL-2 (5ng/ml), which alone did not drive IFN-γ production, with IL-18 (10ng/ml) induced IFN-γ production by a high proportion of NK cells (median: 22.0%) after 6 hours (Fig. 3.4B). At 6 hours this interaction appears to be additive (test for interaction, p= 0.22), and by 18 hours the interaction is highly synergistic (test for interaction, p= 0.006), possibly as a result of IL-18-induced upregulation of CD25, the high affinity IL-2R. The combination of IL-12 and IL-2 also drove IFN-γ production at 18 hours, consistent with [215], although this combination was less effective than with IL-18; the combination of all three cytokines induced IFN-γ production, but not to significantly higher levels than IL-2 and IL-18 together (Fig. 3.4C).

In contrast to our observations for CD25 expression, there was no evidence of antagonism or competition between γ_c cytokines in their induction of NK cell IFN-γ, and there was some evidence of additive interactions of IL-2 enhancing the NK cell IFN-γ responses to the combination of IL-15 and IL-18, particularly at 6 hours. IL-15 plus IL-18 has previously been shown to enhance NK cell IFN-γ, as measured by ELISA, and our data agreed with this, though we saw the effect of this at an IL-15 concentration (0.75ng/ml) much lower than previously described (5ng/ml) [239]. IL-21 alone had no effect on IFN-γ (Fig. 3.4D), nor did we find any significant effect of IL-2 and IL-21 in combination, as has been a point of contention in the literature [240]. However, IL-18 did synergise with IL-21, though to a lesser extent than with IL-2 or IL-15 (summarised in Fig. 3.4E). Our data therefore show that γ_c cytokines (IL-2, IL-15 and IL-21) in combination with IL-18 induce very rapid and extensive IFN-γ production by NK cells. Although IL-2 seems to be the most potent of

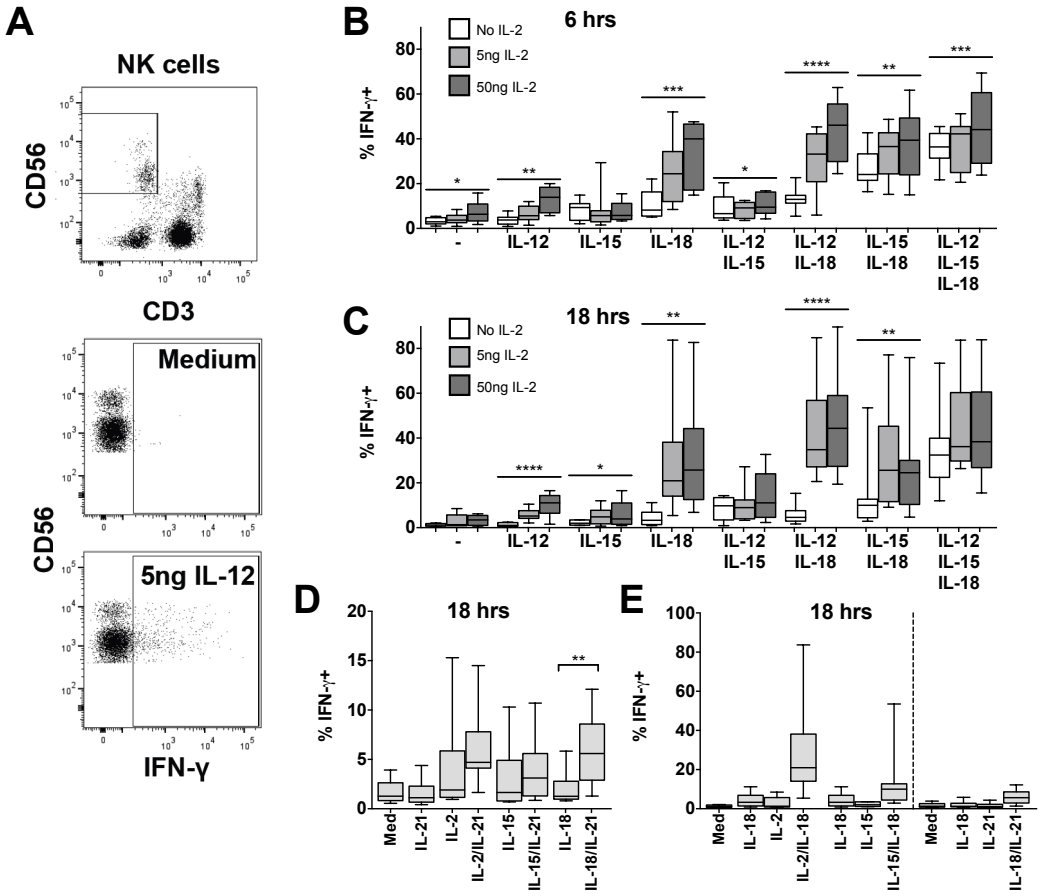

Figure 3.4: **IL-18 synergises with IL-2 or IL-15 to drive IFN-γ production.** PBMCs were incubated for 6 or 18 hours with fixed concentrations of cytokines (IL-12: 12.5pg/ml, IL-15: 0.75ng/ml, IL-18: 10ng/ml, IL-21: 5ng/ml) and 0, 5 or 50ng/ml IL-2 and the intracellular IFN-γ production measured. FACS plots of CD56+ CD3- NK cells and IFN-γ expression after incubation with medium or 5ng/ml IL-12 (A). NK cell responses to combinations of IL-12, IL-15 and IL-18 with different concentrations of IL-2 at 6hrs (B) and 18hrs (C), n= 7-8. NK cell responses to IL-21 in combination with IL-2 (5ng/ml), IL-15 and IL-18 after 18hrs (D), n= 8. IFN-γ expression after stimulation for 18hrs with a combination of IL-18 (10ng/ml) and γ_c cytokines was re-plotted to enable comparison between IL-2, IL-15 and IL-21 working with IL-18 to drive NK cell responses (E). Box plots show the 5-95th percentile range. Data were analysed using paired Wilcoxon signed-rank tests (C: capped lines) or ANOVA tests for linear trend for trend analysis across increasing cytokine concentrations including medium alone (B, C) (uncapped lines). ****p<0.0001, ***p<0.001, **p<0.01, *p<0.05.

these, at least at the cytokine concentrations tested, the ability of IL-15 to augment IFN-γ production offers a route for rapid, innate activation of NK cells prior to the differentiation of IL-2 secreting T cells.

Low concentrations of IL-12 (0.0125ng/ml), alone or in combination with IL-2, had minimal effects on IFN-γ production (Fig. 3.4B, C), but did enhance IFN-γ production in combination with IL-15 and IL-18 at later time points. High concentrations of IL-12 ($\geqslant$ 1ng/ml) synergised strongly with IL-18 to drive both IFN-γ and CD25 (see Fig. 3.1), although we suggest that these do not reflect physiological conditions. Overall, however, as little as 5ng/ml IL-2 in combination with low concentrations of IL-18 (10ng/ml) and IL-12 (12.5pg/ml) was the optimal combination for NK cell IFN-γ induction at 18 hours.

Of interest, given the large body of work describing IFN-γ induction by combinations of IL-12 and IL-18 [22, 33, 211, 220], γ_c cytokines synergise with IL-18 at extremely low concentrations and at very early time points. It is possible therefore that *in vivo* IL-12 may contribute to NK cell IFN-γ production when γ_c cytokines are lacking, such as during primary exposure when IL-2 from antigen-specific T cells may be limited, or at later time points after the initial IFN-γ response has been initiated in order to sustain the response.

3.3.2.3 Functional responses of purified NK cells compared to NK cells within the PBMC population

Although we analysed NK cell responses within the PBMC population rather than using isolated NK cells, we felt confident that these responses were more likely to be representative of *in vivo* NK cell responses. Contact with accessory cells is known to be important during responses to infection, and IL-15, for example, is presented to NK cells from the DC surface. Purifying NK cells therefore removes these important contact signals. The process of purification can also inadvertently activate NK cells or leave a small but highly activated population of T cells, which will confound results. However, to test this we looked at the effect of titrations of single cytokines (IL-2, IL-12, IL-15, IL-18) at 6 hours

and 18 hours on negatively selected, purified NK cells from eight donors, and compared them to PBMCs from the same donors. Purifed NK cells and PBMCs were incubated for 6 and 18 hours and stained for CD25, IFN-γ and CD107a (Figure 3.5). NK cell purity was between 60-80% with some contaminating T cells, which was not optimal, but did remove a significant fraction of accessory cells from the population.

From these data, it is clear that purified NK cells (black) and PBMCs (red) respond in similar manners to cytokine stimulation. CD25 responses are extremely low after 6 hours in both cell populations (Fig. 3.5A), but IL-15 and IL-18 both induced CD25 expression in a dose dependent manner by 18 hours (Fig. 3.5B). CD25 expression was slightly lower on purified NK cells, but this was only significant in the HCC condition (p= 0.031). IFN-γ responses were much more variable in the PBMCs compared to the purified NK cells, but there were no significant differences (HCC, p= 0.094) (Fig. 3.5C, D). The lack of IFN-γ responses to single cytokines differed from our previous results, which may reflect variation between donors.

We also measured CD107a responses, which peaked at 6 hours and were higher and more consistent between donors in PBMCs (Fig. 3.5E) compared to purified NK cells. However, we saw significant trends (analysed by ANOVA tests for linear trend between Med and three cytokine concentrations) in CD107a upregulation in response to increasing concentrations of IL-2, IL-15, and IL-18. After 6 hours, purified NK cells did not upregulate CD107a, but IL-2, IL-15 and IL-18 each drove CD107a expression in PBMCs at both 6 hours (Fig. 3.5E) and 18 hours (Fig. 3.5F) (linear trend at 6hrs: IL-2 and IL-18, $p<$ 0.0001; IL-15, p= 0.0009. At 18hrs: IL-2 and IL-18, $p<$ 0.0001; IL-15, p= 0.0003).

By 18 hours, IL-2 and IL-15 upregulated CD107a expression in purified NK cells as well as in PBMCs, although IL-18 had no effect (IL-2, p= 0.0015; IL-15, $p<$ 0.0001; IL-18, p= 0.643). The effect of cytokines on NK cell degranulation responses therefore do seem to differ in purified and non-purified NK cells, which suggests that degranulation responses by 6 hours depend on signals from other cells in the PBMC population - whether this is indicates that both cell contact and cytokine activation is required for degranulation or

that exogenous cytokines drive accessory cells to trigger NK cell degranulation has yet to be determined. As purified NK cells did upregulate CD107a expression after 18 hours, it is possible NK cells are still capable of a delayed degranulation response in the absence of accessory cells.

From these data, the CD25 and IFN-γ responses of purified and non-purified NK cells are very consistent and show the same trends in response to single cytokines. We therefore feel confident that our results from other experiments are not confounded by endogenous cytokines from accessory cells, and that gating NK cells from the whole PBMC population accurately represents NK cell cytokine responses. However, it is clear that degranulation responses differ in purified or non-purified NK cell populations, and this will be considered later in the context of other experiments looking at NK cell degranulation.

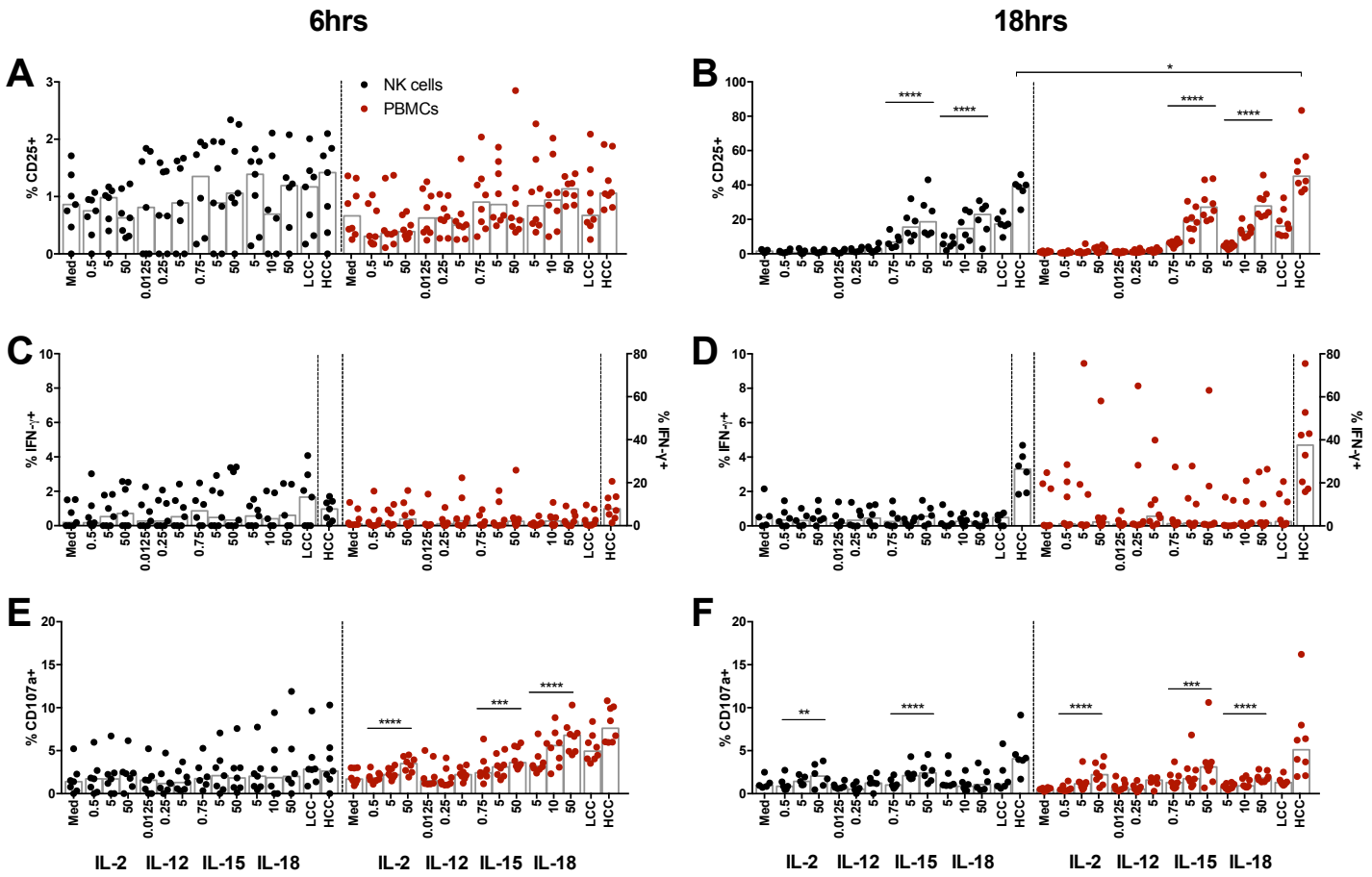

Figure 3.5: **Comparison of NK cell responses in purified NK populations and PBMCs.** Purified NK cells and PBMCs were incubated for 6 or 18 hrs with increasing concentrations of single cytokines (IL-2, IL-12, IL-15, IL-18), and CD25 (A-B), IFN-γ (C-D) and CD107a (E-F) responses were measured (n= 8, from 2 experiments). Bars indicate medians. Uncapped lines indicate ANOVA tests for linear trend across increasing cytokine concentrations including medium. Capped lines indicate paired Wilcoxon signed-rank tests (B). ****p<0.0001, ***p<0.001, **p<0.01, *p<0.05.

3.3.2.4 IFN-α has no effect on IFN-γ or CD25 NK cell responses

IFN-α has traditionally been thought to drive cytotoxic NK cell responses rather than cytokine production, in a model where NK cell responses to viral infection are driven by plasmacytoid DCs and type I interferons (IFN-α and -β) in combination with IL-15 [54]. However, published data also suggest that IFN-α can drive IFN-γ responses [213, 241] under some conditions. We found no effect of IFN-α on CD25, IFN-γ, or CD107a responses. PBMCs were stimulated with 10, 100 or 1000pg/ml IFN-α alone for 6 or 18 hours, and with combinations of IFN-α (10pg/ml) and IL-2, IL-12, IL-15 and IL-18, with medium alone and HCC as negative and positive controls (Figure 3.6). IFN-α alone showed a very small trend in CD25 upregulation that was significant at 6 hours, but this effect was very minor (Fig. 3.6A), and there was no effect of combining IFN-α with any of the other cytokines, including IL-15, in contrast to the existing literature.

3.3.2.5 IL-18 synergises with antibody-driven CD16 downregulation

After vaccination, or upon secondary infection, circulating antigen-antibody complexes binding to FcγRIII (CD16) on NK cells can mediate killing of infected cells via antibody-dependent cellular cytotoxicity (ADCC). As our data suggest that IL-18, in concert with γ_c cytokines, enhances adaptive as well as innate pathways of NK cell activation by working with both IL-2 and IL-15, we wanted to test whether ADCC could be augmented by very low levels of NK cell activating cytokines, as would be present at the site of infection (Figure 3.7).

We found that IL-18, but not IL-12, IL-15, or IL-21, induced rapid (within 6 hours) and sustained (persisting at 18 hours), concentration-dependent downregulation of CD16 expression at the NK cell surface such that cells substantially lost CD16 expression within 6 hours in the presence of 10ng/ml IL-18 (Fig. 3.7B). Our group has previously observed that crosslinking of CD16 with plate-bound anti-CD16 antibody leads to loss of CD16 from the NK cell surface (Goodier et al, unpublished data), and this is consistent with previous reports of CD16 downregulation following CD16 ligation [212]. Adding a high concentration

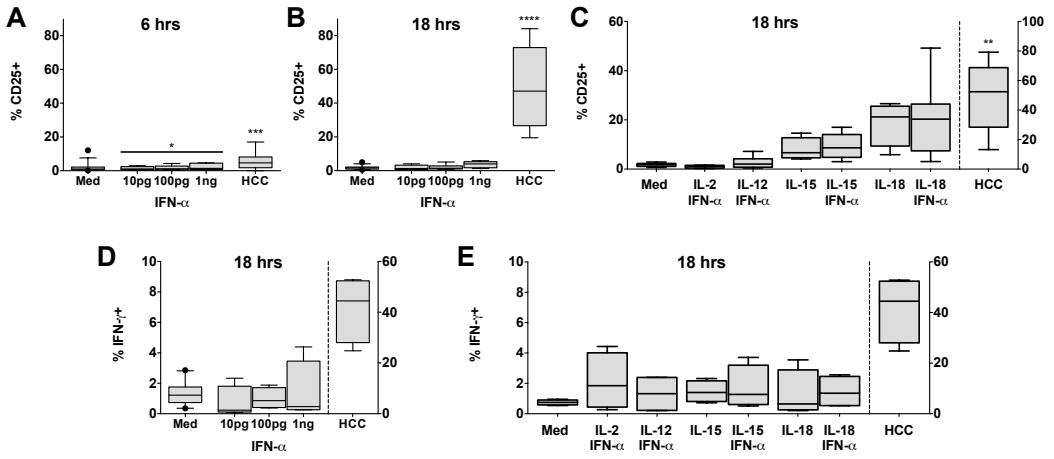

Figure 3.6: **IFN-α does not combine with IL-2, IL-12, IL-15 or IL-18 to drive functional NK cell responses.** CD25 responses after 6 hours (A) or 18 hours (B) were measured after PBMCs were incubated with medium alone, 10, 100 or 1000pg/ml IFN-α or HCC, and after stimulation with dual combinations of IFN-α (10pg/ml) and IL-2 (5ng/ml), IL-12 (12.5pg/ml), IL-15 (0.75ng/ml) or IL-18 (10ng/ml) for 18 hours (C). IFN-γ responses to increasing concentrations of IFN-α (D) and to the same combinations of cytokines (E) were measured after 18 hours. Box plots show the 5-95th percentile range. Data were analysed using paired Wilcoxon signed-rank tests compared to medium alone (HCC conditions, no lines) or ANOVA tests for linear trend for trend analysis across increasing cytokine concentrations including medium alone (A), uncapped lines). ****p<0.0001, ***p<0.001, **p<0.01, *p<0.05.

of IL-12 (5ng/ml) to 50ng/ml IL-18 (HCC) had no greater effect than 50ng/ml IL-18 alone, which further reinforces that IL-18 directly drives CD16 downregulation. Although there was a slight trend for high concentrations of IL-15 to downregulate CD16 at 6 hours, this was not supported at 18 hours or by subsequent experiments.

The effects of IL-18 on CD16 expression were further clarified when measuring CD16 downregulation in response to CD16 crosslinking. Here we observed that IL-18-driven downregulation synergises with the effects of CD16 crosslinking, so that after 6 hours and 18 hours, CD16 expression is lower when NK cells are cultured with a combination of 10ng/ml IL-18 and plate bound anti-CD16 than after culture with either anti-CD16 or IL-18 alone (Fig. 3.7C). Taken together with data indicating that downregulation of CD16 on CD56dim NK cells in response to either CD16 crosslinking or to very high concentrations

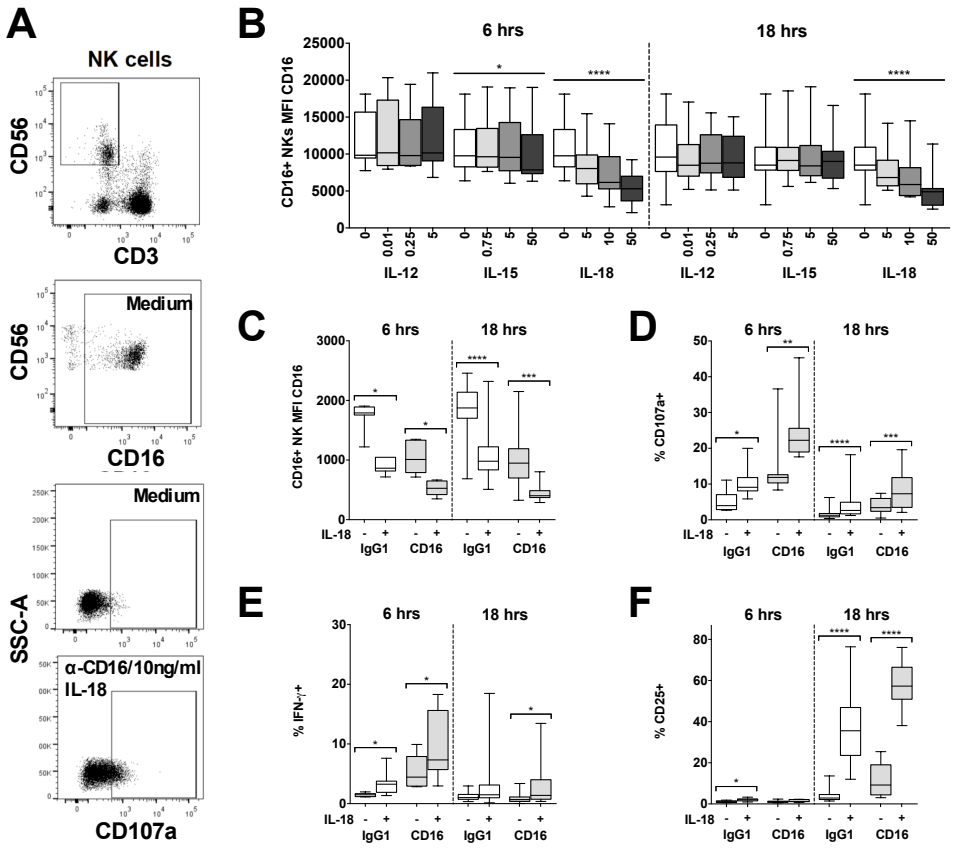

Figure 3.7: **IL-18 enhances responses to CD16 cross-linking and drives CD16 downregulation.** PBMC were stimulated for 6 or 18 hours in vitro and changes in CD16 MFI (mean fluorescence intensity) of CD16+ NK cells were measured in response to Med (medium alone), IL-12, IL-15, or IL-18. Representative FACS show gating of CD56+ CD3- NK cells, and surface expression of CD16 or CD107a on unstimulated cells, or CD107a on NK cells activated with CD16 crosslinking and 10ng/ml IL-18 (A). CD16 MFI on CD56dim CD16+ NK cells was measured after stimulation with Med, IL-12, IL-15, or IL-18 for 6 or 18 hours (B) (n= 9-13, data from 2-3 experiments). For the crosslinking assays, PBMC were stimulated for 6 or 18 hours in vitro with Med (medium alone), α-CD16 or its IgG1 isotype control, with (+) or without (-) 10ng/ml IL-18. CD16 MFI of CD56dim CD16+ NK cells was measured after 6 or 18 hours (C) (n= 7-16, data from 1-2 experiments). Surface expression of CD107a (D), intracellular IFN-γ (E), and CD25 (F) was measured on NK cells after 6 or 18 hours (n= 7-16, data from 1-2 experiments). Box plots show the 5-95th percentile range. Data were analysed using paired Wilcoxon signed-rank tests (C-F: capped lines) or ANOVA tests for linear trend for trend analysis across increasing cytokine concentrations including Med (B, uncapped lines). ****p<0.0001, ***p<0.001, **p<0.01, *p<0.05.

of IL-12 (10ng/ml) plus IL-18 (100ng/ml) can be blocked with a specific inhibitor specific of the metalloprotease ADAM-17 [212], these data raise the interesting hypothesis that the IL-18 and the CD16 signalling pathways may converge to induce metalloprotease-mediated cleavage of CD16 from the cell surface. We could not find any evidence that CD16 crosslinking affects expression of IL-18Rα.

Using crosslinking of cell surface CD16 with plate-bound anti-CD16 antibody as a model of ADCC [212], we next determined the effects of low concentrations of IL-18 on NK cell cytotoxicity (assessed using the CD107a degranulation assay [242, 243] as well as on CD25 and IFN-γ responses. Despite the very rapid downregulation of CD16 by IL-18 and CD16 crosslinking (Fig. 3.7C), we observed that as little as 10ng/ml IL-18 markedly and very rapidly (within 6 hours) augmented NK cell degranulation (Fig. 3.7D) and IFN-γ production in the presence of anti-CD16 antibody (Fig. 3.7E). Furthermore, IL-18 synergised with anti-CD16 to enhance CD25 expression at 18 hours (Fig. 3.7F; test for interaction, p=0.005). These data demonstrate that IL-18 can substantially enhance NK cell ADCC responses and also support the idea that IL-18- and anti-CD16-driven downregulation of CD16 expression is a consequence of activation of signalling pathways downstream of CD16. These degranulation responses after IL-18 stimulation (Fig. 3.7D) are also consistent with the results from Figure 3.5E-F, and suggest that the effects of IL-18 on CD107a expression seen there may be mediated by CD16 signalling and downregulation.

Further work on this subject was done mainly by Carolyn Nielsen, and is described in our paper [38]. Briefly, PBMCs were incubated for 18 hours with or without whole, inactivated H3N2 influenza virus in the presence of plasma that had previously been shown to contain anti-H3N2 IgG and to mediate ADCC [16, 17]. NK cell degranulation, CD25, and IFN-γ responses to H3N2 immune complexes were compared in the presence or absence of exogenous IL-18 (Figure 3.8). We found that IL-18 alone induced modest increases in CD107a, CD25 and IFN-γ expression, and consistent with previously reported data on the H1N1 virus [17], incubation of NK cells with H3N2 virus and plasma containing anti-H3N2 antibodies induced significant degranulation (CD107a expression), upregulation of CD25, and production of IFN-γ. As little as 5ng/ml IL-18 in combination with H3N2 and anti-

H3N2 was sufficient to markedly augment CD107a, CD25 and IFN-γ expression; the effects of the combination of IL-18 plus H3N2/anti-H3N2 were additive for CD107a expression, but synergistic for CD25 and IFN-γ.

In summary, therefore, IL-18 synergises with CD16 mediated signals to augment NK cell ADCC activity and indicates that IL-18 may play an important role in driving NK cell cytotoxicity as well as cytokine production.

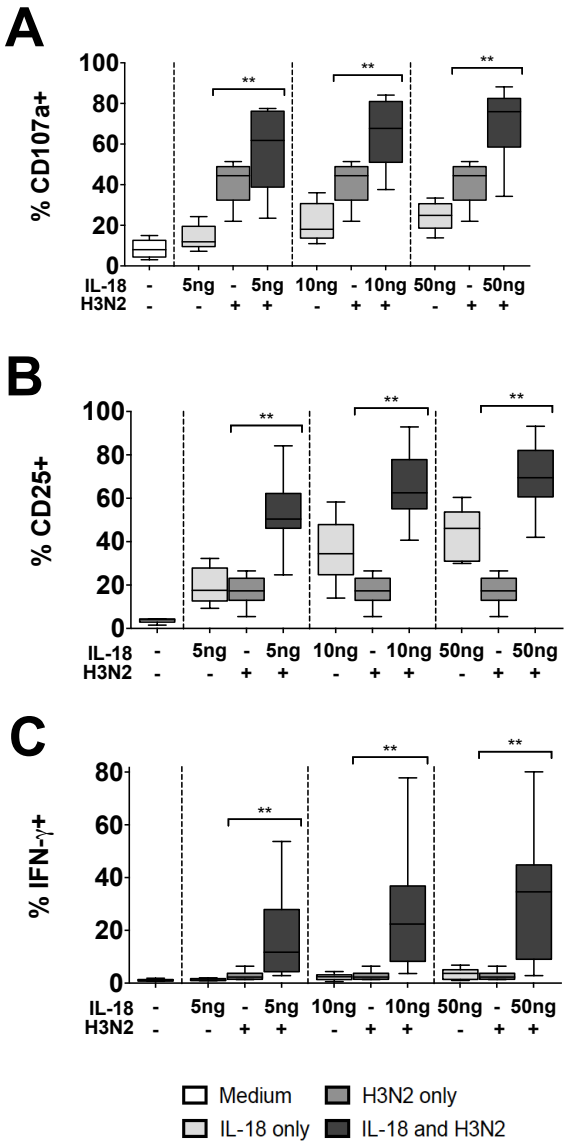

Figure 3.8: **Antibody and IL-18 synergise in response to H3N2.** PBMC were stimulated for 18 hours *in vitro* with Med (medium alone), 5, 10, 50ng/ml IL-18, with or without 1 μg/ml inactivated influenza virus H3N2. Responses were measured as the percentage of NK cells expressing surface CD107a (A), surface CD25 (B), or intracellular IFN-γ (C) (n= 7-8, data from one experiment). Box plots show the 5-95th percentile range. Data were analysed with paired Wilcoxon signed rank tests. ****$p<0.0001$, ***$p<0.001$, **$p<0.01$, *$p<0.05$.

3.3.3 Cytokine-driven changes in cytokine receptor expression

3.3.3.1 IL-18R expression is driven by IL-18 in a positive feedback loop

As IL-18 alone is able to induce both CD25 and IFN-γ expression within 6 hours (Figure 3.2), we hypothesised that maintaining the capacity for IL-18 signalling might be required for optimal NK cell activation and therefore that sustained or enhanced expression of the IL-18R may contribute to the synergy between IL-18 and γ_c cytokines. To determine whether, and if so which, cytokines regulate IL-18R expression, NK cell surface expression of IL-18Rα (CD218a, the receptor component required for signalling [244]) was measured after 6 hours or 18 hours of PBMC culture with IL-2, IL-12, IL-15, IL-18, IL-21 or IFN-α, alone and in combination (Figure 3.9). It was immediately obvious that resting levels of IL-18Rα expression are extremely variable between donors with the proportion of resting NK cells expressing the receptor varying from approximately 20% to greater than 80% (Fig. 3.9B, C). Polymorphisms affecting DNA methylation within the promoter region of IL18R1, the gene encoding IL-18Rα, and subsequent transcription of the gene have been reported and may in part explain this variation [245, 246] and we have previously observed lower levels of IL-18Rα expression in human cytomegalovirus (HCMV)-infected individuals than in HCMV-uninfected individuals [17]. Despite this inter-individual variation, resting levels of IL-18Rα expression are very high in comparison to resting levels of the high affinity IL-2R (as defined by expression of the IL-2Rα chain, CD25; see Figures 3.2A, B, and 3.3) and fully functional IL-12R (as defined by expression of IL-12R-β2; see Figure 3.11) and may explain the very rapid (within 6 hours) NK cell response to exogenous IL-18. Indeed, we observed a weak but statistically significant correlation between resting levels of NK cell IL-18Rα expression and upregulation of CD25 following IL-18 stimulation (n= 18, 50ng/ml IL-18, linear regression (adjusting for use of PE- and FITC-conjugated anti-IL-18Rα) R= 0.241, p= 0.046).

Contrary to previously published data indicating that IFN-α [219] and IL-12 [22, 33, 219, 238] can individually induce IL-18R mRNA [22, 219], IL-18Rα protein expression [33], or IL-18R expression [238] in human NK cells, and that IL-12/STAT4 signalling induces IL-

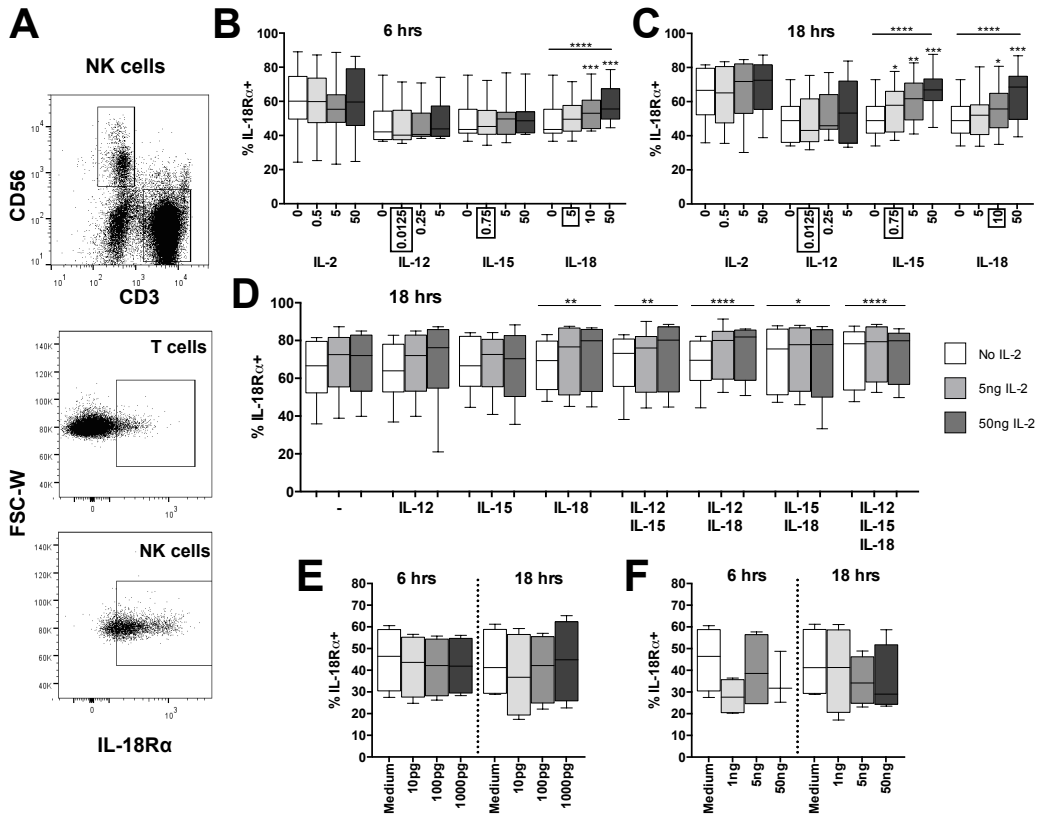

Figure 3.9: **Positive feedback from IL-18 induces IL-18R.** PBMC were stimulated for 6 or 18 hours *in vitro* and changes in NK cell surface expression of IL-18Rα was measured in response to Med (medium alone), IL-2, IL-12, IL-15, IL-18, or IL-21. Representative flow cytometry plots show gating of CD3+ T cells, CD3-CD56+ NK cells, and surface expression of IL-18Rα on unstimulated T cells and NK cells for IL-18Rα-FITC (N.B. as used in D; IL-18Rα-PE used in B-C) (A). IL-18Rα expression on NK cells was measured after stimulation with Med, IL-2, IL-12, IL-15, IL-18, or IL-21 (concentrations per ml as labelled) for 6 (B) or 18 hours (C) (n= 7-11, data from 1-2 experiments). Concentrations in boxes indicate those used in following graphs. IL-18Rα expression on NK cells was also measured after stimulation with a titration of IL-2 (0, 5, 50ng/ml) in combination with IL-12 (12.5pg/ml), IL-15 (0.75ng/ml), and/or IL-18 (10ng/ml) after 18 hours (D), (n= 8, data from 2 experiments). IL-18Rα expression on NK cells was measured after stimulation with single cytokine concentrations of IFN-α (E) or IL-21 (F) after 6 or 18 hrs (n=4, data from one experiment). Box plots show the 5-95th percentile range. Data were analysed using paired Wilcoxon signed-rank tests (B-D: no lines; compared to Med) or ANOVA tests for linear trend for trend analysis across increasing cytokine concentrations including Med (B-D, uncapped lines). ****p<0.0001, ***p<0.001, **p<0.01, *p<0.05.

18Rα expression in mice [247, 248], we found no increase in surface expression of IL-18Rα in response to increasing concentrations of either IL-12 (Fig. 3.9B-D) or IFN-α (Fig. 3.9E) with or without IL-2 (Fig. 3.9D). There are several likely explanations for this discrepancy. For example, in previous studies, exogenous IL-2 was routinely added to NK cell cultures and IFN-α was used at much higher concentrations [219]; NK cells were stimulated with very high concentrations of IL-12 [22, 33]; IL-18R mRNA was assessed rather than IL-18R protein [22, 219]; NK cells were purified by positive selection which may, in itself, contribute to subsequent activation [22, 33]; or components of the IL-18R other than IL-18Rα were measured [22, 219, 238]. Nevertheless, our data suggest that at physiological concentrations, IL-2, IL-12 and IFN-α have little, if any, effect on IL-18Rα expression. We also observed no effect of IL-21 on IL-18Rα expression (Fig. 3.9F).

By contrast, we found clear evidence of concentration-dependent upregulation of NK cell IL-18Rα expression in response to IL-15 alone and IL-18 alone (Fig. 3.9B, C). 10ng/ml of IL-18 was sufficient to upregulate IL-18Rα within 6 hours (Fig. 3.9B) (p= 0.001) and this effect was sustained at 18 hours (Fig. 3.9C) (p= 0.0003). IL-15 had no effect on IL-18Rα expression at 6 hours, but as little as 0.75ng/ml IL-15 was sufficient to upregulate IL-18Rα expression by 18 hours (Fig. 3.9B, C) (p= 0.019). Overall, IL-15 and IL-18 each increased the proportion of NK cells expressing IL-18Rα by approximately 15% (median percentage of IL-18Rα+ NK cells: 50.1% medium only; 64.6% with 50ng IL-18; 66.8% with 50ng IL-15). The ability of IL-18 to rapidly augment expression of its own receptor is suggestive of a positive feedback loop, allowing for enhanced IL-18 signalling, continued synergism with other signalling pathways and efficient induction of NK cell effector functions in the first few hours of infection.

We next considered whether other cytokines might synergise with IL-18 to further enhance IL-18Rα expression. Increasing concentrations of IL-2, either alone or in combination with IL-12 or IL-15 had no significant effect on IL-18Rα expression at either 6 hours (not shown) or 18 hours (Fig. 3.9D). However, IL-2 modestly but significantly enhanced the effects of IL-18 in a dose dependent manner and there was an additive effect of combining IL-15 and IL-18 in the absence of IL-2. Addition of other cytokines to the IL-18 plus IL-2 cocktail

did not further enhance IL-18Rα expression. Although at the low cytokine concentrations used in these experiments (0.0125ng/ml IL-12, 10ng/ml IL-18) we saw no additive or synergistic effect of adding IL-12 to IL-18, at much higher concentrations (5ng/ml IL-12 and 50ng/ml IL-18) we did observe a significant ($p< 0.0001$) additive effect of these two cytokines increasing IL-18Rα expression. These data support our contention that IL-18 is the key cytokine in initiating and sustaining NK cell responses under physiologically relevant conditions such as very early infection, and that NK cell responses that can be induced with very high (non-physiological) cytokine concentrations *in vitro* may not be relevant *in vivo*.

In summary therefore, low concentrations of IL-18 rapidly and significantly upregulate the IL-18Rα subunit and this effect is augmented by low concentrations of IL-15 and IL-2. Given that IL-18 alone is sufficient to induce expression of the high affinity IL-2R (CD25), it seems that IL-18 and IL-2 synergistically and reciprocally upregulate their own and each other's receptors in a potent positive feedback loop. The minimal role of low concentrations of IL-12 in this process may explain the limited synergies of exogenous IL-12 in the early NK cell IFN-γ response (see Figure 3.4).

3.3.3.2 IL-15R expression is variable and rapidly downregulated after 6 hours

As IL-15 appears to be one of the cytokines driving early NK responses, we looked at expression of the IL-15Rα subunit that is specific for IL-15 signalling and works in combination with the β and γ chains shared with IL-2 (Figure 3.10). PBMCs were stimulated with IL-2, IL-12, IL-15, IL-18, IL-21 and IFN-α alone and in combination for 6 and 18 hours, and the percentage of IL-15Rα+ cells measured. It was immediately clear that IL-15Rα expression varied greatly between donors (from 1-15%), and that while expression was clearly detectable at 6 hours, by 18 hours expression was not detectable for most conditions (Fig. 3.10B). The data did not reveal any strong upregulatory effects of any cytokines at 6 hours, but IL-18 showed what appears to be a dose-dependent effect of maintaining if not increasing IL-15Rα expression. This is particularly noticeable at 18 hours (grey bars

in Fig. 3.10B), where 50ng/ml IL-18 was the only stimulus where IL-15Rα expression was maintained.

Titrating IL-2 into the combinations of IL-12, IL-15 and IL-18 had variable effects on IL-15Rα expression. On the whole, there was no significant effect of adding IL-2, but for both IL-2 alone and conditions containing IL-12 but not IL-18 (i.e. IL-12 and IL-12+IL-15 with or without IL-2) there was a trend towards downregulation of IL-15Rα. Unfortunately we were unable to confirm these results with more donors as subsequent batches of IL-15Rα antibody did not give consistent results, possibly due to manufacturing issues. If this were correct, it would be consistent with some published observations that IL-2 inhibits signalling by other γ_c cytokines [41, 249].

3.3.3.3 IL-12R expression is limited at early time points

For completeness, we also examined expression of IL-12Rβ2 in response to single cytokines or cytokine combinations (Figure 3.11). The proportion of NK cells expressing IL-12Rβ2 was transiently (seen at 6 hours but not at 18 hours) and only modestly enhanced by 10-50ng/ml IL-18 and by 50ng/ml IL-15 at both time points; however the biological relevance of such small effects is unclear. There was no effect of exogenous cytokines on IL-12Rβ2 expression at the level of individual cells (as measured by MFI), and we therefore suggest that IL-12 plays a limited role in NK cell activation at very early time points (as shown by the previous figures) in part because of the lack of receptor expression at these times.

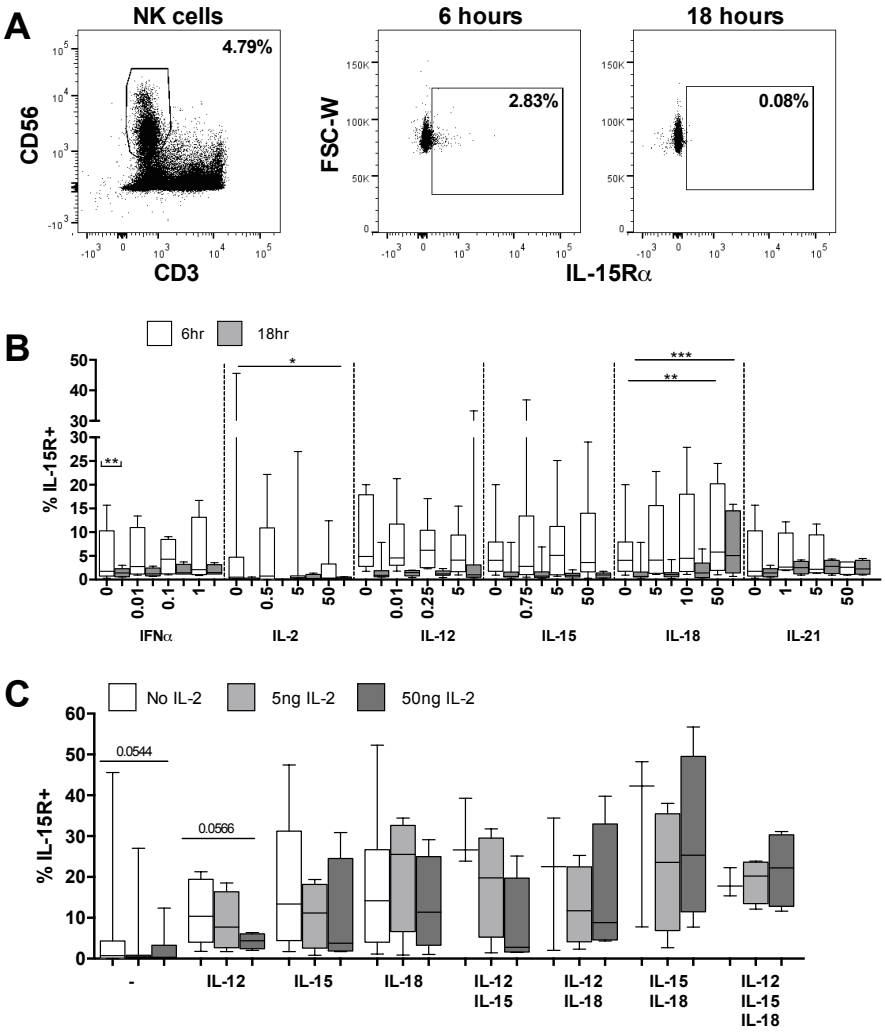

Figure 3.10: **IL-15Rα is maintained by IL-18 and might be downregulated by IL-2.** PBMC were stimulated for 6 or 18 hours in vitro and changes in NK cell surface expression of IL-15Rα was measured in response to Med (medium alone), IFN-α, IL-2, IL-12, IL-15, IL-18, or IL-21. Representative flow cytometry plots show gating of CD3-CD56+ NK cells and surface expression of IL-15Rα on unstimulated NK cells after 6 hours (A). IL-15Rα expression on NK cells was measured after stimulation with Med, IFN-α, IL-2, IL-12, IL-15, IL-18, or IL-21 (concentrations per ml as labelled) for 6 (white bars) or 18 hours (grey bars) (n= 7-11, data from 1-2 experiments) (B). Concentrations in boxes indicate those used in following graphs. IL-15Rα expression on NK cells was also measured after stimulation with a titration of IL-2 (0, 5, 50ng/ml) in combination with IL-12 (12.5pg/ml), IL-15 (0.75ng/ml), and/or IL-18 (10ng/ml) after 6 hours (C), (n= 4, data from 1 experiment). Box plots show the 5-95th percentile range. Data were analysed using paired Wilcoxon signed-rank tests or ANOVA tests for linear trend for trend analysis across increasing cytokine concentrations including Med (B-C, uncapped lines). ****p<0.0001, ***p<0.001, **p<0.01, *p<0.05.

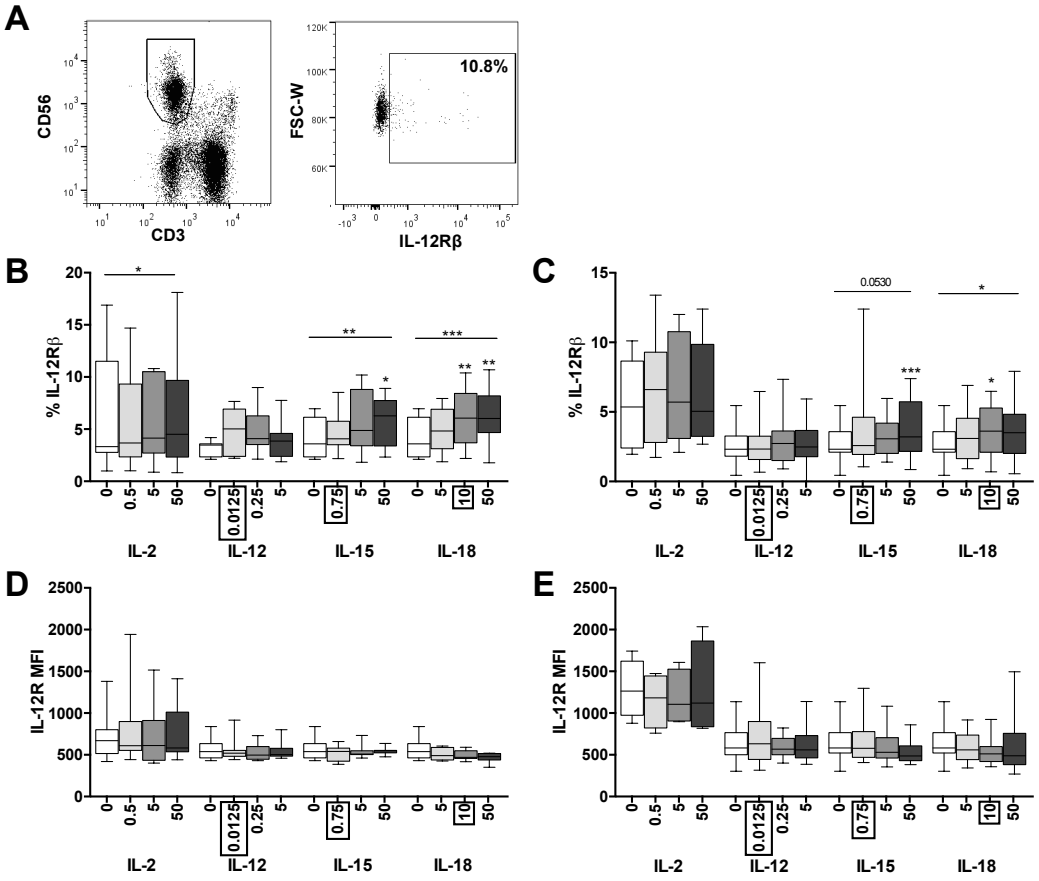

Figure 3.11: **Low level IL-12Rβ2 upregulation following IL-15 or IL-18 stimulation.** PBMC were stimulated for 6 or 18 hours in vitro and changes in NK cell surface expression of IL-12Rβ2 was measured in response to Med (medium alone), IL-2, IL-12, IL-15, or IL-18. Representative flow cytometry plots show gating of CD3-CD56+ NK cells and surface expression of IL-12Rβ2 on unstimulated cells (A). IL-12Rβ2 expression on NK cells was measured after stimulation with Med, IL-2, IL-12, IL-15, IL-18 (concentrations in ng/ml as labelled) or HCC after 6 hours (B) (n= 7-16, data from 1-3 experiments) or 18 hours (C) (n= 8-18, data from 2-3 experiments), with mean fluorescence intensity (MFI) of IL-12Rβ2 expression on NK cells for the same experiments at 6 hours (D) and 18 hours (E). NB: IL-2 titrations were performed using a different batch of anti-IL-12Rβ2-PerCP/Cy5.5 conjugated antibody. Data were analysed using paired Wilcoxon signed-rank tests (B-C: no lines; compared to Med) or ANOVA tests for linear trend for trend analysis across increasing cytokine concentrations including Med (B-C, uncapped lines). ***$p<0.001$, **$p<0.01$, *$p<0.05$.

3.4 Discussion

The role of NK cells as early responders during infection has been described in multiple disease models [25, 37, 250]. However, although NK cells can be stimulated to produce cytokines or cytotoxic responses *in vitro* by a variety of cytokines at high concentrations, it is the early *in vivo* conditions that are most relevant to any model of NK cells as functional responders. The capacity of NK cells to become activated within minutes or hours of stimulation with very low concentrations of innate cytokines is therefore the key to their role as early responders duing infection.

In an attempt to conduct a more physiologically relevant analysis of NK cell-cytokine interactions, we have conducted a systematic analysis of the roles of different cytokines and cytokine combinations in NK cell activation and their interaction with adaptive immune responses. We have demonstrated that NK cells can respond, within hours, to concentrations of cytokines that are orders of magnitude lower than previously appreciated and that NK cells can integrate signals, synergistically, from multiple cytokine receptors and FcγRIII, enabling them to respond quickly and effectively to extremely low concentrations of pro-inflammatory stimuli.

Previous investigations have almost exclusively used purified NK cells, which has the advantage of precisely controlling cytokine concentrations but lacks other activation stimuli found *in vivo*, namely cell-cell contacts and, in secondary responses, antibody crosslinking of Fc receptors. Direct contact between NK cells and DCs in order to trans-present IL-15 via IL-15-IL-15Rα complexes has been well described to be far more potent than free IL-15 or soluble IL-15Rα complexes [234, 251], and so the concentrations required to activate an isolated NK cell are far in excess of the picomolar amounts required in a biological system. Similarly, interactions with macrophages (reviewed in [44]) via NK cell receptors (e.g. NKG2D) [250, 252] and adhesion molecules (e.g. ICAM-1-LFA-1; reviewed in [253]) are well-established requirements for NK cell activation in multiple infection models. Additionally, few studies have evaluated combinations of more than two cytokines and none have carefully titrated cytokine concentrations within these combinations. Thus, although

we have abundant information about which cytokines and other signals can, under certain conditions, activate NK cells, we have a much less clear picture of which signals and which combinations of signals most efficiently activate NK cells in physiologically relevant conditions. The use of low concentrations of cytokines is particularly relevant because there is evidence that high cytokine concentrations may override natural homeostatic mechanisms that regulate the extent and duration of NK cell activation. Additionally, while we fully accept that in our assays exogenous cytokines might induce other cells in the PBMC population to express accessory molecules or produce cytokines that augment NK cell responses, and indeed this may explain the rather limited contribution of exogenous IL-12 in our assays, we argue that this better reflects the *in vivo* situation and the true potential of NK cells.

Our data point to IL-18 as the key component of the initial inflammatory response that 'primes' NK cells to respond to other cytokines and to FcγRIII/CD16-mediated signals. In accordance with published data [211] we show that 50ng/ml IL-18 is sufficient to induce CD25 expression on >40% of NK cells within 18 hours; however we extend these data to reveal significant upregulation of CD25 within 6 hours at IL-18 concentrations as low as 10ng/ml. Rapid IL-18-induced upregulation of CD25 explains the synergistic interaction we observed between IL-18 and IL-2; this has been reported previously [32] but only at IL-18 concentrations that are 100-fold higher than the concentration used here. Moreover, our data extend these findings to demonstrate that synergy between IL-18 and IL-2 enhances IFN-γ production (irrespective of the presence of IL-12 or IL-15) and we confirmed the importance of IL-18 in enhancing ADCC responses to influenza virus via naturally occurring anti-H3N2 antibodies in normal human plasma. Taken together, these data place IL-18 at the interface of innate and adaptive activation of NK cells.

Particularly of note, the enhanced IL-18-driven responses in the presence of common γ_c family cytokines (i.e. IL-15, IL-21, and IL-2) are remarkably consistent to an extent not previously appreciated. These cytokines signal via the common γ_c (CD132) (reviewed in [41]), and IL-15 and IL-2 also share the receptor beta subunit (CD122). IL-2 and IL-15 in particular are thought to have highly overlapping functions and are sometimes used

interchangeably during cell culture experiments. However, we have found that their effects on NK cells during activation are not identical [40] and, in fact, when used in combination, they may interfere with each other.

In cultures containing IL-18 with either IL-2 or IL-15, we observed no additional benefit of adding the third cytokine (either IL-15 or IL-2). Although IL-15 and IL-18 both individually and synergistically upregulate CD25 expression, and IL-18 subsequently synergises with IL-2 to increase IFN-γ production, there is no such synergy between IL-15 and IL-2. Rather, adding IL-2 to any cytokine cocktail containing IL-15 reduces CD25 expression and has little if any beneficial effect on IFN-γ. This is perhaps unsurprising given the shared receptor components of IL-15 and IL-2 but may also reflect a more complex feedback mechanism. IL-2 inhibits IL-7Rα, another member of the common γ_c family, during T cell activation [249], and our own unpublished data suggest IL-2 might also downregulate IL-15Rα on NK cells (Fig. 3.10). If our data are correct and IL-2 does downregulate IL-15Rα, this lends credence to the theory that the γ_c cytokines have distinct temporal expression patterns, as described by [39, 41]; if IL-15Rα is constitutively expressed at early time points to allow IL-15 signalling that drives CD25 expression, then is downregulated by IL-2 itself or another intermediary, this allows the shared beta and gamma receptor subunits to form a highly sensitive IL-2R with CD25 instead of IL-15Rα. Downregulation by IL-2 may therefore be a method for limiting the competition for the common receptor subunits and downstream signalling molecules from related cytokines, thus allowing one member of the family to predominate at different stages of infection. This is consistent with the pre-activation 'priming' role proposed for IL-15 [234], an 'adaptive' T cell-driven role for IL-2, and potentially a secondary infection/memory-like role for IL-21, although the effects of IL-21 on NK cells are much less clear than its effects on T cells.

This competition for cell signaling components may extend to the STAT pathways in addition to receptor subunits, as both IL-2 and IL-15 utilise STAT5 (reviewed in [41] and [29]). This is in contrast to IL-21, which shares the common γ_c but signals via STAT3 [240], and IL-12, which has a distinct signalling pathway involving STAT4 and belongs to the pro-inflammatory family that includes IL-23 (reviewed in [216]). There is additionally

some evidence that IL-15 induces STAT5 binding to CD25 [239], and also that IL-15Rα is less stable in formation with the beta and gamma subunits than CD25 [209]; all of this suggests that IL-15 is not able to take part in sustained signalling responses throughout the course of infection.

These shared pathways are logically consistent with the ability of IL-18 to synergise with all of the common γ_c cytokines, as we have shown here; IL-18 signalling begins early and is sustained throughout the course of infection, and is capable of modulating the immune response via interactions with different cytokines and of controlling the receptor expression of multiple signalling partners (CD25, IL-15Rα, IL-18Rα itself), with the added effect of IL-12 later in infection. Again, these data confirm that IL-18 is at the interface between the innate and adaptive immune system. The fact that these effects also happen at significantly lower concentrations than have previously been described suggests that previous work may have been affected by the use of purified NK cells, which, although not influenced by endogenous cytokines, also lack the normal cell contacts which may permit thresholds for cytokine signalling to be reached even at very low concentrations.

3.4.1 Proposed model for activation and cytokine receptor upregulation

Taken together, our data lead us to propose the following model of early NK cell activation (Figure 3.12). At the start of a primary infection, the initial colonising pathogens induce transpresentation of constitutively expressed IL-15, activation of constitutively expressed IL-18 precursor and secretion of bioactive IL-18, and transcription and translation of IL-15 and IL-18 by dendritic cells and macrophages (reviewed in [222, 230, 254]). The synergistic interaction of IL-15 and IL-18 rapidly induces NK cells to produce IFN-γ within 6 hours; this response may be further augmented by IL-12 and is sustained for at least 18 hours by a positive feedback loop in which IL-18 and possibly IL-15 sustain expression of IL-18Rα. At the same time, induced expression of CD25 allows the formation of the high affinity IL-2R, priming the NK cells to take part in T cell-mediated adaptive immune responses. As

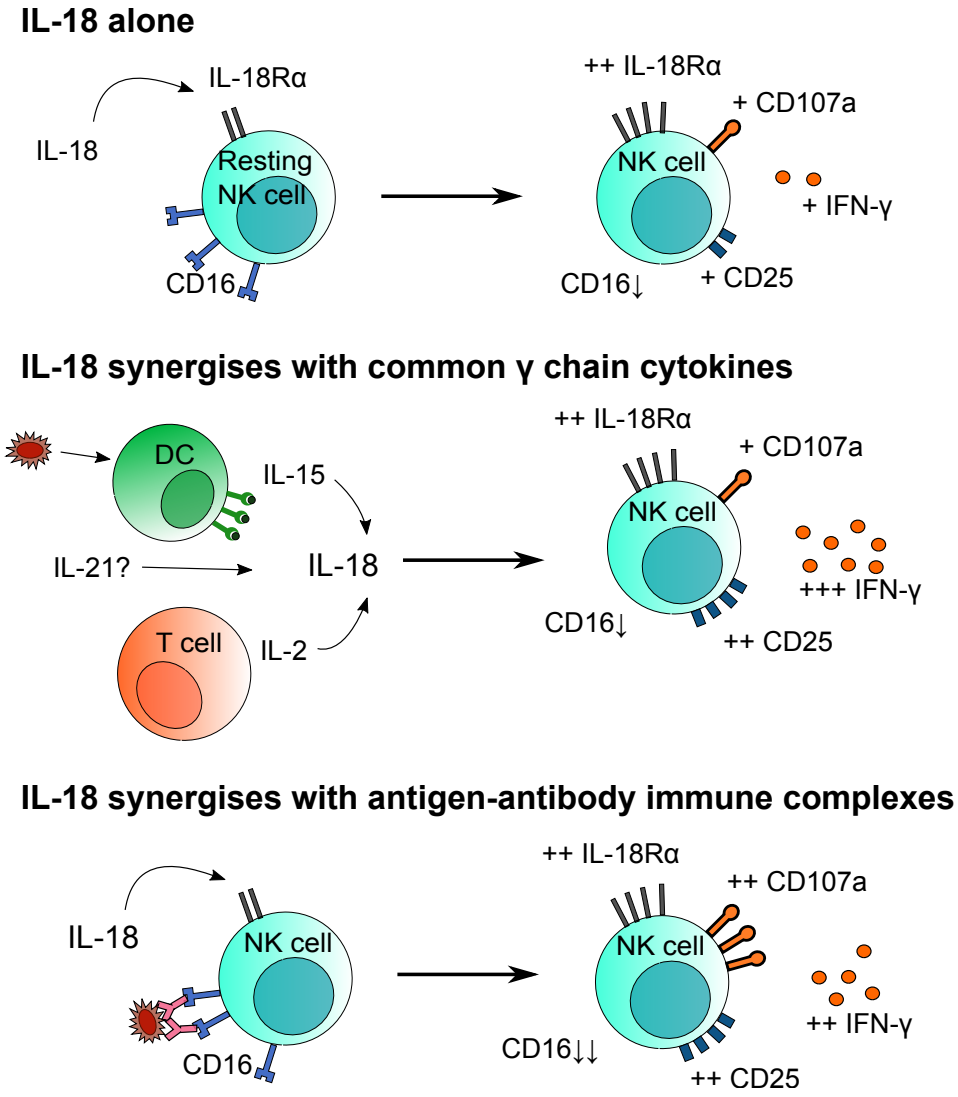

Figure 3.12: **A proposed model of NK cell activation by cytokines with rapid IL-18 driven activation of NK cells.** The schematic shows a proposed model of NK cell activation by IL-18 and its synergies with γ_c cytokines or antigen-antibody immune complexes during primary or secondary immune responses. Within 6 hours of stimulation, IL-18 drives IL-18R upregulation and modest increases in CD25, IFN-γ and degranulation, as well as downregulation of FcγRIII (CD16). In combination with IL-15 or IL-21 from accessory cells, or with T cell-derived IL-2, IL-18 drives much stronger CD25 and IFN-γ responses, measurable at 6 hours and peaking at 18 hours. Antigen-antibody complexes cross-link CD16 and synergise with IL-18 to drive ADCC and IFN-γ production after 6 and 18 hours.

IL-2 becomes available, IL-15R expression decreases through a combination of competition for receptor subunits and STAT molecules; IL-15 itself may further drive this process by upregulating CD25 expression and encouraging downstream signalling molecules to bind the IL-2R complex. Later in infection, or during re-infection after the differentiation of antigen-specific T helper cells and production of antibodies, IL-18 synergises with IL-2 and with antibody-antigen complexes to enhance ADCC and IFN-γ production. The immediate availability of IgG antibodies allows ADCC reactions to occur within 5 hours [212], and subsequent rapid downregulation of FcγRIII/CD16 by IL-18 and/or CD16 crosslinking brings the reaction to a close, thereby preventing immune pathology. IL-2Rα expression is now sustained by IL-18 and IL-2, further enhancing NK cell sensitivity to IL-2 and, in synergy with IL-12, maximising IFN-γ production [211].

In summary, therefore, we have shown that IL-18 synergises with components of both the innate (IL-15, IL-12) and the adaptive immune response (IL-2, antibody) to very rapidly induce antimicrobial NK cell responses (IFN-γ and ADCC). The extremely low concentrations of cytokines that are required for this process, and the speed with which it happens, identify IL-18 as a key 'first responder' at the intersection of innate and adaptive immune responses to infection.

4 | Functional responses of NK cells to malaria-infected red blood cells

4.1 Introduction

4.1.1 IFN-γ responses against malaria are associated with protection

A strong and early IFN-γ response is considered essential for control of parasitaemia during malaria infection. Much of the work on cytokine responses to malaria has been done in mouse models, which have shown a crucial role for IFN-γ in parasite control and clearance ([161, 255]; reviewed in [141]), but also the importance of IL-10 in preventing immunopathology due to unregulated inflammation and in promoting resolution of the immune response [157, 162, 256]. Similarly, blockade of the regulatory receptor CTLA-4 exacerbates pathology in mouse models with a lethal strain of malaria, but mediates lower peak parasitaemia and swifter parasite clearance in a non-lethal model [257]. However, while most models suggest that inflammatory cytokines, and TNFα in particular, can cause immunopathology including severe anaemia and cerebral malaria [158, 159], overexpression of IL-10 at early and mid time points impedes parasite clearance [165] and may allow low levels of parasites to persist as a compromise between sterile protection and immunopathology. Information on which immune cells are required for control of disease in the early, mid and late stages of infection has also predominantly come from mouse models [178, 185, 186].

Data from human populations also indicate that IFN-γ is protective during malaria infec-

tion (reviewed in [258]). IFN-γ production by PBMCs was associated with mild rather than severe malaria in children [259], and children with mild malaria who had detectable IFN-γ responses also had delayed incidence of reinfection within one year of the study. After experimental vaccination and challenge with whole sporozoites under drug cover [188], volunteers had enhanced IFN-γ and IL-2 T cell recall responses *in vitro* 2.5 years after infection [260]; likewise, after vaccination with *P. falciparum* antigens, IFN-γ responses correlated with memory responses after 3 months post-immunisation [261]. However, most of these studies have focused on T cells (or presumed T cells) as the source of IFN-γ and have only performed limited analyses on the cellular sources of IFN-γ. Additionally, the time points used for *in vitro* stimulation in the studies have ranged from 24 hours to 3 days, which is long after the early response time of NK cells [37, 183].

As in mouse models, higher levels of proinflammatory cytokines appear to be associated with clinical disease in humans. A high ratio of TNFα to IL-10 has been linked to severe malaria in children [160], and higher proinflammatory responses were linked to symptomatic malaria compared to lower inflammatory responses in individuals with asymptomatic malaria ([201, 262]; reviewed in [263]). However, overexpression of regulatory cytokines including TGF-β was also linked to higher parasitaemia in infected individuals and therefore poorer outcomes [173]. In these human studies, however, IFN-γ still appeared to correlate with protection [259] (whereas TNFα in particular was associated with pathology [157, 168]), and the role of IL-10 as a regulatory cytokine was unclear [262].

IFN-γ from CD8 T cells and NK cells, along with TNFα [264], is thought to control parasitaemia in the pre-erythrocytic stages by inducing infected hepatocytes to produce intracellular nitric oxide (NO) and reactive oxygen species (ROS) [199, 265, 266]. Blood stage IFN-γ responses are IL-12 dependent [267] and are thought to primarily activate macrophages to phagocytose and kill infected RBCs through intracellular NO production [42]. Within the spleen in mouse models, DCs and macrophages have been shown to phagocytose iRBCs and merozoites and to contribute to IFN-γ production by CD4 T cells [186] and NK cells [268]. There appears to be considerable redundancy in the cellular

sources of IFN-γ (NK cells, CD4 and CD8 T cells, γδ T cells, NK T cells), which is biologically sound but occasionally leads to contradictions in the literature. However, the role of NK cells as contributors to IFN-γ production is rarely challenged, and the existing literature on NK cell responses to malaria will be described in the next section.

4.1.2 Previous studies on functional NK cell responses to malaria

A function for NK cells as early responders in malaria infection was suggested early in the 1980s in humans [269] and mice [270]. IL-12-dependent IFN-γ production by NK cells was shown to control parasitaemia in mice during blood stage [184] and pre-erythrocytic infections [199], which has further been shown to require cross-talk with DCs [34, 268]. Studies on early pre-erythrocytic immune responses also suggested that NK cells are important for amplifying initial CD8 T cell responses by producing IFN-γ, which in turn drives synthesis of NO [199].

Data on NK cell responses in humans are predominantly *in vitro*, but a few *in vivo* studies in infected individuals have looked at both IFN-γ production and cytotoxic responses [271–273]. *In vitro* studies of NK cell activation have found that iRBCs can activate NK cells at early time points [18] to produce IFN-γ and require contact with live iRBCs [183, 201], contact with accessory cells [26, 42, 43], and activation with IL-12, IL-18 [183] and IL-2 [37]. There is also some evidence that NK cells can directly kill iRBCs [142, 274], although the receptors mediating this interaction are still unclear despite some proposed candidates [42, 274, 275]. However, the ability of NK cells to directly interact with iRBCs is supported by several *in vitro* studies [42, 43, 200], which will be examined further in Chapter 5. Antibodies binding iRBCs may also mediate NK cell cytotoxicity by ADCC during blood stage infection.

Much of the literature looking at *in vivo* IFN-γ production described above acknowledges NK cells as a source of IFN-γ, although the proportion of the cytokine response ascribed to NK cells or T cells varies based on the time point of the study (reviewed in [258]). NK cells are also thought to undergo degranulation during the late liver stage and the erythrocytic

stage, based on circulating soluble granzyme levels in infected malaria naive volunteers and Cameroonian children [273] and *in vitro* killing of schizonts by NK cells from malaria infected Kenyan children and adults [276]. There is additionally some evidence that NK cells have T cell dependent 'memory-like' immune responses, dependent on both IL-2 and T cell contact [272], where NK cells showed enhanced IFN-γ production in experimentally infected individuals up to 20 weeks after infection.

4.1.3 Long-term NK cell immunity to malaria

The existence of NK cell 'memory' is still controversial, and not well substantiated in any disease model other than murine cytomegalovirus (MCMV) (reviewed in [277]). The ability of NK cells to directly recognise specific pathogens is also not clear, although the existence of the KIR repertoire and other NK cell receptors does provide a potential mechanism for such a response and there is some evidence of direct NK-iRBC interactions [42, 200]. There have been few studies comparing NK cell responses in malaria naive and exposed populations from an 'adaptive' perspective [272, 278]. Immunity to malaria is known to be both slow to develop and heavily dependent on a broad antibody repertoire (reviewed in [145] and Introduction, Section 1.2.3), but the role of NK cells has been comparatively overlooked, although NK cells may work with antibody to clear iRBCs by ADCC. As mentioned above, studies on the profiles of cytokine responses in naive and symptomatic or asymptomatic malaria infected individuals have shown contradictory results, but appear to link lower production of inflammatory cytokines with asymptomatic infection and incidence of less severe malaria (reviewed in [263]). As NK cells contribute to cytokine production that is immunologically useful but can also cause immunopathology, such as IFN-γ production, the role of NK cells in reccurrent infection is of interest depending on whether they exhibit a greater capacity to respond upon restimulation or if any IFN-γ response is entirely taken over by the classic adaptive T cell responses. The role of NK cells upon secondary infection or in the later stages of primary infection could also shift from cytokine production to a more direct role in killing infected cells [142, 273, 276].

4.1.4 Enhancing NK cell responses with exogenous cytokines

As previously described in Chapter 3, cytokines play an important role in both priming and activating NK cells. IL-15 is most commonly considered to be important for priming NK cells [36, 279], which is supported by our findings that IL-15 drives early CD25 and cytokine production and decreases in importance over time as other cytokines (such as IL-2) begin to direct the immune response instead [38]. Likewise, IL-12 and IL-18 are thought to be key cytokines produced by monocytes which drive IFN-γ responses in NK cells and T cells. The roles of these cytokines may vary based on multiple factors, including NK subsets and their responsiveness, the priming state of NK cells, the available accessory cells, and possibly even previous exposure of NK cells to the pathogen. Much of the literature regarding NK cell responses to cytokines does not use an antigen in addition to exogenous cytokine, but there are a few groups that have looked at a combination of cytokines and non-viral pathogens including Longhi et al (2012), *Paracoccidioides brasiliensis* [280], Lapaque et al (2009), *Salmonella enterica* [25], and Klezovich-Bernard et al (2012), anthrax spores [250].

The rationale for using cytokines to enhance the NK cell responses to iRBCs is mainly to compensate for suboptimal accessory cell signalling *in vitro* so as to better measure the optimal responses of NK cells themselves. As NK cell IFN-γ responses to iRBCs in LSHTM donors are rarely above 10% and are often less than 2%, it is difficult to discriminate between donor responses although there is strong evidence that genetic differences may underlie these differences (reviewed in [281] and [61]). Boosting the NK cell responses with, for example, a low concentration of IL-12 and IL-18 (LCC) to enhance vaccine recall responses [17], could allow for better understanding of the differences in response to iRBCs. Previous work from other groups has found that various cytokines including IL-15 [228], IFN-α [276] and IL-12 [184] enhance NK cell responses to malaria.

4.1.5 Aims

The aim of this chapter is to examine the functional NK cell response to *P. falciparum*-infected RBCs of malaria naive and malaria exposed donors from LSHTM and Uganda respectively, focusing on IFN-γ production, CD25 upregulation, and degranulation responses (measuring CD107a expression). I aim to look at the variation in NK cell response within each population and to compare the two groups. I will also analyse whether NK cell responses of some of the Ugandan donors are affected by active parasitaemia at the time of blood collection or by parasitaemia within the last year. This work therefore focuses on the functional responses of NK cells to iRBCs in two populations who differ in previous exposure to malaria, but also in age, genetic background, and environmental factors, particularly exposure to other common infections such as HCMV. It also focuses on the effects of exogenous cytokines (IL-12, IL-15 and IL-18) on NK cells in the presence of iRBCs, which both continues from the work in Chapter 3 and attempts to optimise the culture conditions for detecting NK cell responses to iRBCs.

4.2 Methods

4.2.1 Study subjects

For the malaria naive donors (n= 46), volunteers were recruited from among staff and students at the London School of Hygiene and Tropical Medicine. All subjects gave written consent under a protocol for recruitment of blood donors approved by the LSHTM ethics committee (reference # 5520) to provide $\leq$ 50ml venous blood. Donors ranged in age from 23.7 to 61.9 years (mean age 36.7 years). Donors were asked about their previous exposure to malaria, and were excluded if they had ever had a diagnosed or suspected malaria infection.

Malaria-exposed donors (n= 53) were recruited from two sites in Uganda, Nagongera and Walukuba, as part of the PRISM cohort at the Infectious Diseases Research Collaboration. Ethical approval was obtained from the Makerere University School of Medicine Research and Ethics Committee (REC REF 2011-203), the Uganda National Council for Science and Technology (HS 1074), the LSHTM ethics committee (reference # 6012), and the University of California, San Francisco Committee on Human Research (reference 027911). Donors had an age range of 1.4 to 68.2 years of age (mean age 13.7 years), divided into three groups of under 5 (n=20), 5-11 (n=21), and 20-70 years old (n=12). 10 donors had detectable blood-stage parasites on the day of blood collection as determined by thick blood smear; 21 individuals had had at least one episode of clinical malaria or asymptomatic parasitaemia in the previous 365 days. More information is detailed in Methods, Section 2.1. Table 4.1 contains greater detail about age and parasitaemia.

4.2.2 PBMC preparation and culture

For donors from LSHTM, PBMCs were isolated from whole blood by Histopaque separation as described in Methods, Section 2.2, and used on the day of donation. Remaining PBMCs were frozen in 10% DMSO and stored in liquid nitrogen for future use. Isolated

Age group	Nagongera (n)	Walukuba (n)	Mean age (years)	Parasitaemia (n)	Malaria in last 365 days (n)
<5	10	10	3.05	3	11
5-11	11	10	7.64	7	10
20-70	4	8	41.87	0	0
Total	25	28	13.70	10	21

Table 4.1: **Summary of Ugandan donors.** Donors are grouped by age (<5 years, 5-11 years, 20-70 years). Columns show the number of donors from Nagongera and Walukuba, the mean age of each age group, the number of donors with parasitaemia at the time of collection, and the number of donors with episodes of malaria in the past 365 days.

PBMCs were resuspended in culture medium containing 10% FCS and 2mM L-glutamine in RPMI. Frozen PBMCs from Ugandan donors were defrosted in 20ml warm RPMI and washed twice (see Methods, Section 2.2.2), then rested for 1-2 hours at room temperature in culture medium containing 10% FCS and 2mM L-glutamine in RPMI. No antibiotics (penicillin/streptomycin) were used in culture.

PBMCs (2×10^5/ml) were incubated for 18 hrs in 5% CO_2 at 37°C in 96-well U-bottom plates (Nunc) in complete medium with uninfected RBCs or MACS-purified schizont stage infected RBCs (described in Methods, Section 2.3) at a ratio of 1:3 PBMCs to RBCs. Recombinant IL-12, IL-15 (both Peprotech) or IL-18 (R&D Biosystems) was added to cultures as described per experiment. Optimised functional assays contained PBMCs with medium only, uRBCs or iRBCs, with or without 0.75ng/ml IL-15, and 5ng/ml IL-12 and 50ng/ml IL-18 as a positive control (HCC). Brefeldin A at a final concentration of 3µg/ml was added for the last three hours of culture (i.e. at 15 hours). Anti-CD107a antibody (FITC-conjugated, BD Biosciences) was included in the medium for the entirety of cell culture when CD107a upregulation was a read-out.

Two strains of *P. falciparum* parasites were used in culture. Strain 3D7A was used for all experiments with donors from LSHTM. Strain 3D7HT-GFP is a transgenic parasite line expressing cytosolic green fluorescence protein (GFP) further described and validated in

Target	Fluorophore	Vol. per sample (μl)	Cat. no.	Company
CD3	V500	1	561416	BD Horizon
CD56	PE-Cy7	0.5	335826	BD Bioscience
CD57	e450	1	48-0577-42	eBioscience
CD25	PE	0.5	12-0259-42	eBioscience
CD107a	FITC	0.5	555800	BD Pharmingen
IFN-γ	APC	0.25	554702	BD Pharmingen

Table 4.2: FACS antibody panel for functional responses of LSHTM donors.

Chapter 5, Section 5.3.1.2, and was used in experiments with donors from Uganda.

4.2.3 Flow cytometry

PBMCs were stained in 96-well U-bottom plates as described in Methods, Section 2.4. Briefly, after 18 hours cells were stained with fluorophore-labelled antibodies to cell surface markers then fixed, permeabilised (Cytofix/Cytoperm, BD Biosciences), and stained for intracellular molecules. After permeabilisation but prior to intracellular staining, cells were washed with Permwash (BD Biosciences) until all red blood cells were lysed and no longer visible in the wells (usually 2-4 washes to remove RBCs from uRBC controls). Different panels of monoclonal antibodies were used to stain PBMCs from LSHTM (Table 4.2) and Ugandan (Table 4.3) donors due to a change in parasite strain. The 3D7HT-GFP *P. falciparum* strain fluoresces in the FITC channel, which required revision of the antibody panel. Frozen PBMCs from a previously characterised malaria naive UK donor were used as a control during each experiment with Ugandan donors as a control for differences in methodology between experiments.

4.2.4 Statistical analyses

Statistical analysis of flow cytometry data was performed using Prism 6 (GraphPad). Data were excluded when the gated cell subset contained fewer than 100 cells. Paired Wilcoxon

Target	Fluorophore	Vol. per sample (μl)	Cat. no.	Company
CD3	V500	1	561416	BD Horizon
CD56	PE-Cy7	0.5	335826	BD Biosciences
CD16	APC-H7	0.5	560195	BD Pharmingen
CD25	PE-Cy5	1	45025942	eBioscience
CD57	PE	1	12057742	eBioscience
CD107a	e450	2	48107942	eBioscience
Parasites	GFP	n/a		
IFN-γ	APC	0.25	554702	BD Pharmingen

Table 4.3: FACS antibody panel for functional responses of Ugandan donors.

signed rank tests were used to compare responses between stimulation conditions. Unpaired Mann-Whitney t tests were used to compare LSHTM vs. Ugandan donors, or donors with or without parasitaemia. Analysis of variance (ANOVA) tests were used to compare multiple data sets and correct for multiple comparisons as described in each experiment. All statistical tests are two-sided **** $p \leq 0.0001$; *** $p<0.001$; ** $p<0.01$; * $p<0.05$.

4.3 Results

4.3.1 Exogenous cytokines boost NK cell responses from frozen PBMCs

From inital experiments with donors from LSHTM, frozen PBMCs seemed to make lower responses to iRBCs than fresh PBMCs, although frozen PBMCs are commonly used in other assays within our group without problems [11, 17, 38]. As it has been established that multiple signals are required for NK cell activation by iRBCs [26, 37], it was possible that certain cell populations or cytokine stimuli were being lost during the freezing process, which has been reported by other groups [282, 283]. One such population has been suggested to be monocytes, which may be less robust than lymphocytes and therefore less likely to recover from the freezing process. Important cytokines known to affect NK cell activation produced by these accessory cells include IL-12, IL-15 and IL-18 [26]. I therefore decided to investigate whether responses of frozen cells to iRBCs could be rescued by exogenous cytokines by comparing NK cell responses to iRBCs using fresh and frozen PBMCs from the same donors. Cytokines were chosen based on previous work from our group [6, 17] using a low concentration of IL-12 (12.5pg/ml) and IL-18 (10ng/ml) (LCC) to boost responses from frozen cells during restimulation with vaccine antigens, and low concentrations of IL-15 for its role in 'priming' NK cells.

PBMCs from six donors were collected and frozen. Cells were thawed at 3 or 6 weeks after freezing and incubated with 3D7A-iRBCs for 18 hrs as previously described to measure IFN-γ, CD25 and CD107a upregulation. Fresh PBMCs were collected from the same donors at each time point and analysed alongside the frozen cells so that the responses of fresh and frozen PBMCs to iRBC and cytokine stimulation could be compared (Figure 4.1).

Responses from fresh and cryopreserved NK cells were compared after incubation with a low concentration of IL-15 (1.5ng/ml) or IL-12 and IL-18 (LCC), with or without uRBCs and iRBCs (Fig. 4.1B). Although there was a trend for NK cell responses to be lower in the frozen PBMCs for all conditions, this was not statistically significant for any comparison

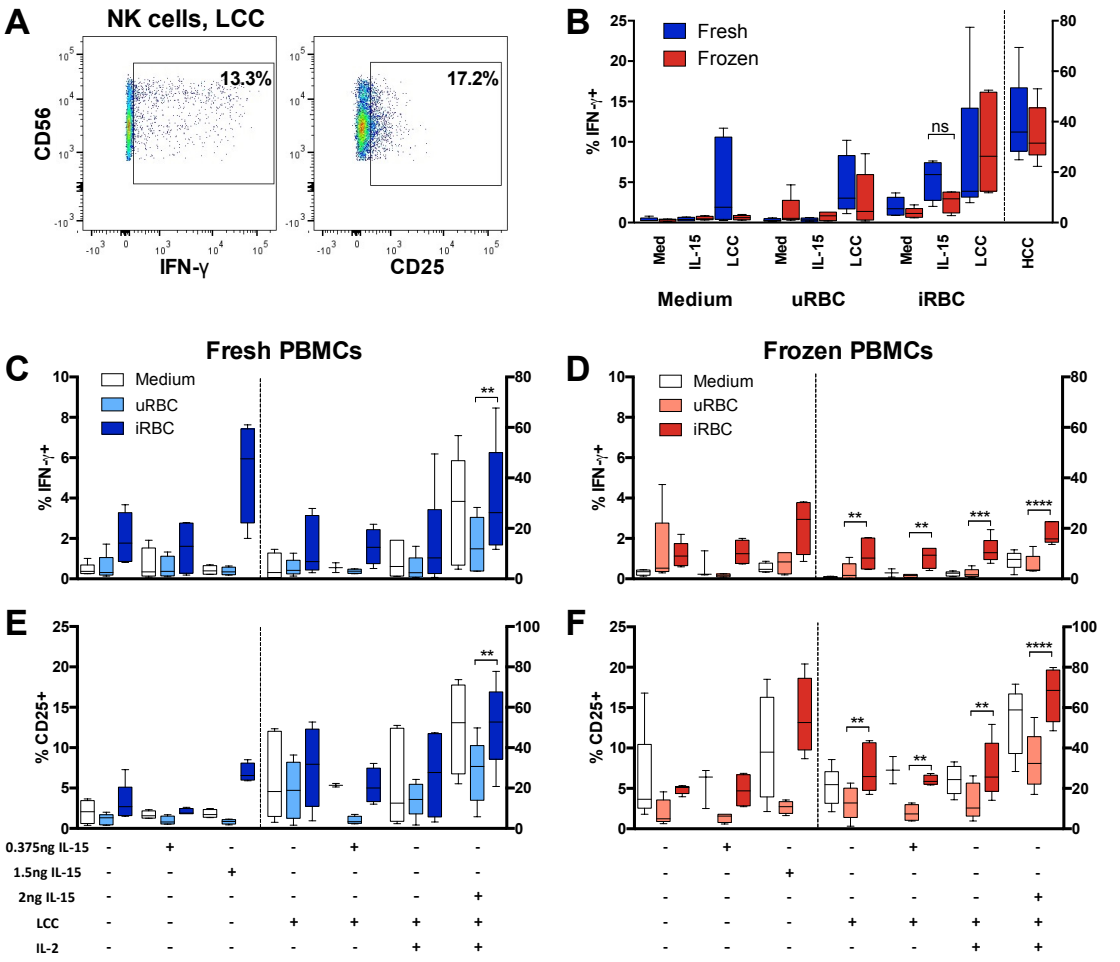

Figure 4.1: **Comparing NK cell responses from fresh and frozen cells.** Paried fresh and frozen PBMCs from the same LSHTM donors were incubated with medium alone, uRBCs, or iRBCs, with different cytokines: IL-15 (0.375, 1.5, 2.0ng/ml), LCC (12.5pg/ml IL-12, 10ng/ml IL-18), or IL-2 (50 U/ml) in the combinations indicated. HCC was used as a positive control. FACS plots show IFN-γ and CD25 responses on fresh NK cells stimulated with LCC (A). Differences in IFN-γ production by NK cells from fresh (blue) and frozen (red) cells to medium alone, 1.5ng/ml IL-15 or LCC, with uRBC or iRBC (B) (n= 5). Fresh and frozen cells were incubated with medium, uRBCs or iRBCs with cytokines as indicated in +/− table and measured for IFN-γ (C-D) and CD25 upregulation (E-F) (n= 5, two experiments). Broken lines indicate data are plotted on different y-axes. Capped lines indicate comparisons between uRBC and iRBC for the same cytokine conditions. Statistical analyses were carried out by unpaired t tests with Holm-Sidak correction for multiple comparisons. * $p \leq 0.05$, ** $p < 0.01$, *** $p < 0.001$ **** $p < 0.0001$.

(multiple t tests, Holm-Sidak correction). Adding low concentrations of IL-15 (0.375 and 1.5ng/ml), IL-12 and IL-18, or a combination of these enhanced IFN-γ (Fig. 4.1C, D) and CD25 (Fig. 4.1E, F) responses to iRBCs in both fresh and frozen PBMCs. The lowest concentration of IL-15 (0.375ng/ml) had no effect on IFN-γ or CD25 upregulation, but adding 1.5ng/ml IL-15 to culture with iRBCs enhanced the IFN-γ and CD25 responses in fresh and frozen cells. IL-15 alone enhanced responses in combination with iRBCs, but not with medium or uRBCs (1.5ng/ml IL-15: IFN-γ on fresh cells, $p= 8.4 \times 10^{-5}$. Frozen cells, $p= 0.004$. CD25 on fresh cells, $p= 0.0006$. Frozen cells, $p= 0.0044$. Unpaired t tests, Holm-Sidak correction). Adding LCC to culture enhanced IFN-γ and CD25 responses to iRBCs (IFN-γ on fresh cells, $p= 0.002$. Frozen cells, $p= 0.0002$. CD25 on fresh cells, $p= 0.016$. Frozen cells, $p= 2.2 \times 10^{-5}$), but also strongly enhanced CD25 upregulation to uRBCs (CD25 on fresh cells, $p= 0.024$. Frozen cells, $p= 0.032$, all unpaired t tests, Holm-Sidak correction). Other combinations of cytokines that included LCC also drove strong NK cell responses in the presence of iRBCs, but showed the same background upregulation in response to medium and uRBCs. Therefore, although the difference in IFN-γ and CD25 expression between iRBCs and medium/uRBCs was increased by using LCC, allowing more discrimination between the responses, LCC increased the background NK cell response while 1.5ng/ml IL-15 did not. Adding further cytokines (IL-2 or IL-15) to LCC conditions had no detectable effect compared to LCC, possibly because the upregulatory effect of LCC masked any differences. When comparing the responses of fresh and frozen cells to the same cytokine stimulation, there were no statistically significant differences in the IFN-γ or CD25 responses. Median responses to iRBCs were higher than responses to uRBCs and medium for all conditions, although this did not reach statistical significance in conditions without LCC (indicated on graphs).

In conclusion, 1.5ng/ml IL-15 specifically enhanced NK cell IFN-γ and CD25 responses to iRBCs. LCC also enhanced NK cell responses but induced background CD25 upregulation in medium and uRBC conditions. Although frozen PBMCs gave lower IFN-γ responses, they did not respond significantly less well to iRBCs than fresh PBMCs, especially when aided by exogenous cytokines.

4.3.2 IL-15 boosts NK cell responses to iRBCs with low background activation

From these cytokine combinations, it appeared that low concentrations of IL-15 could enhance NK cell responses to iRBCs, while the combination of IL-12 and IL-18 (LCC) increased the background CD25 and IFN-γ responses. I next tested the effects of increasing concentrations of single cytokines (IL-12, IL-18 and IL-15) and iRBCs on NK cell responses. Cryopreserved PBMCs were incubated for 18 hours with IL-12, IL-18 or IL-15 with medium, uRBCs, or 3D7A-iRBCs (Figure 4.2). FACS plots show the gating strategy for IFN-γ and CD25 responses on NK cells (Fig. 4.2A). IL-12 induced strong IFN-γ responses (Fig. 4.2B) in the presence of iRBCs at high concentrations (0.25 and 5ng/ml) (compared to no IL-12: $p= 1.5 \times 10^{-7}$ and $p= 1.3 \times 10^{-8}$, unpaired t tests, Holm-Sidak correction), and only induced background IFN-γ responses at the highest concentration (medium, $p=$ 0.023; uRBC, ns).

IL-12 only statistically significantly increased CD25 expression at the highest concentration (5ng/ml) (Fig. 4.2C), and had little effect on background CD25 production. Increasing concentrations of IL-18 had a much smaller effect on IFN-γ production, but also appeared to specifically enhance responses to iRBCs (compared to no IL-18: 10ng/ml, $p=$ 0.006; 25ng/ml, $p=$ ns; 50ng/ml, $p=$ 0.010). However, IL-18 also increased CD25 expression in all conditions in a dose-dependent manner (consistent with our results from Chapter 3). CD25 responses in conditions containing uRBCs appeared slightly reduced, which is consistent with data from [284], but this was not statistically significant. IL-15 was used at a lower range of concentrations and had the smallest effect in increasing both IFN-γ and CD25 responses, but specifically enhanced NK cell responses to iRBCs and had a minimal effect on medium or uRBC conditions (iRBC responses, IFN-γ: 1.5ng/ml IL-15, $p=$ 0.004. CD25: 0.75ng/ml, $p=$ 0.0012; 1.0ng/ml, $p= 3.4 \times 10^{-6}$; 1.5ng/ml, $p= 9.7 \times 10^{-7}$). 0.75ng/ml IL-15 also appeared to upregulate responses to iRBCs ($p=$ 0.026), but this was not significant after correcting for multiple comparisons. Therefore, although all three single cytokines appeared to enhance IFN-γ responses to iRBCs specifically, this effect

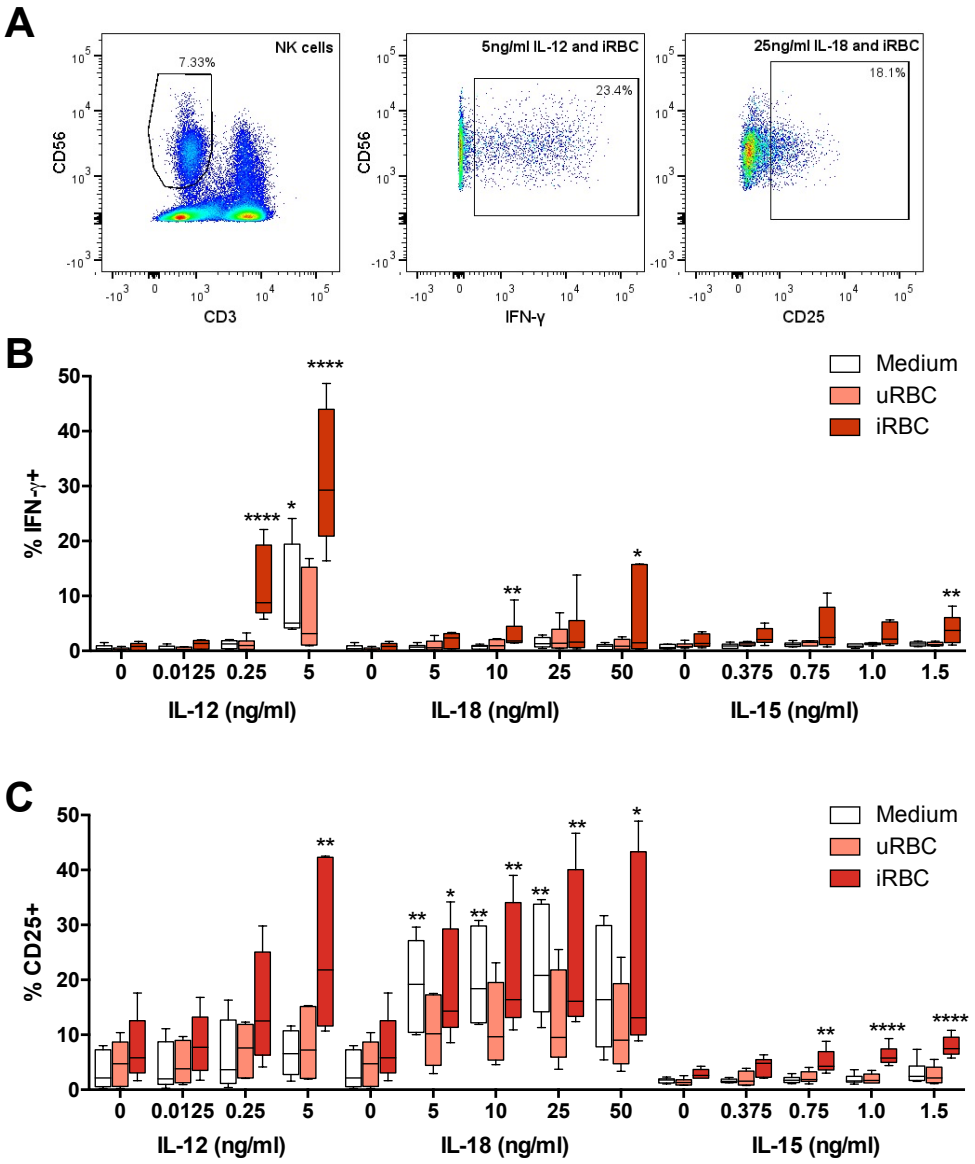

Figure 4.2: **Single cytokine titrations drive IFN-γ and CD25 NK cell responses to iRBCs.** Cryopreserved PBMCs were incubated with increasing concentrations of single cytokines in combination with medium, uRBCs, or iRBCs for 18 hours. FACS plots show gating for IFN-γ and CD25 on NK cells stimulated with iRBCs and IL-12 or IL-18 respectively (A). Increasing concentrations of IL-12, IL-18 and IL-15 (ng/ml as indicated) were incubated with medium alone (white), uRBCs (orange) or iRBCs (red) and IFN-γ (B) and CD25 (C) responses measured (n= 6). Box and whisker plots show min-to-max values. Statistics indicate comparisons to medium/uRBC/iRBC without cytokines (0ng/ml). Statistical analyses were carried out by unpaired t tests with the Holm-Sidak correction for multiple comparisons. * $p \leq 0.05$, ** $p < 0.01$, *** $p < 0.001$ **** $p < 0.0001$.

was only seen at relatively high concentrations of IL-12 (0.25ng/ml), which is likely to represent non-physiological conditions, and IL-18 drove CD25 upregulation at all tested concentrations without being affected by iRBC presence or absence. Conversely, very low concentrations of IL-15 appeared to slightly enhance responses to iRBCs without driving background CD25 expression.

To determine the optimal concentration of exogenous IL-15 for priming NK cells without creating a non-specific response, PBMCs were titrated with increasing concentrations of IL-15 both with or without iRBCs (Figure 4.3). Fresh PBMCs from two donors were incubated with increasing IL-15 concentrations without iRBCs for 18 hours (Fig. 4.3A). Increasing concentrations of IL-15 only (light blue bars) showed no effect on IFN-γ production by NK cells even at 25ng/ml, but adding a fixed concentration of IL-12 (12.5pg/ml) and IL-18 (10ng/ml) (LCC) (dark blue bars) to IL-15 induced a clear dose-dependent IFN-γ response with increasing IL-15 concentration. IL-15 alone appeared to induce CD25 expression with increasing concentrations, and LCC had an additive effect on this upregulation (Fig. 4.3B). In addition, low concentrations of IL-15 (0.375, 0.75, 1.0, 1.5 ng/ml) combined with iRBCs drove NK cell IFN-γ responses in some donors but not others (n= 6) (Fig. 4.3C). These differences were not evident in the CD25 responses, where IL-15 had similar effects in all six donors (Fig. 4.3D). Donors with IFN-γ responses to iRBCs even in the absence of IL-15 are shown in dark blue (585F and 596M), donors who had IFN-γ responses only after stimulation with exogenous IL-15 in light blue (586M and 596M), and donors who did not produce IFN-γ even with IL-15 are shown in white (591F and 636F).

The iRBC-specific effects of IL-15 may correspond with a model of NK cell priming by IL-15 [35]. Instead of activating an NK cell, priming lowers the threshold for NK cell activation so that cells are able to respond to low levels of further stimulation with antigen or other cytokines. This would be consistent with the data shown in both Figures 4.2B-C and 4.3, where low concentrations of IL-15 drive CD25 and IFN-γ responses only in the presence of iRBCs or LCC, but not with uRBCs or IL-15 alone. By contrast, IL-12 and IL-18 activated NK cells even in the absence of iRBCs, consistent with their roles as independent activating signals during infection [26].

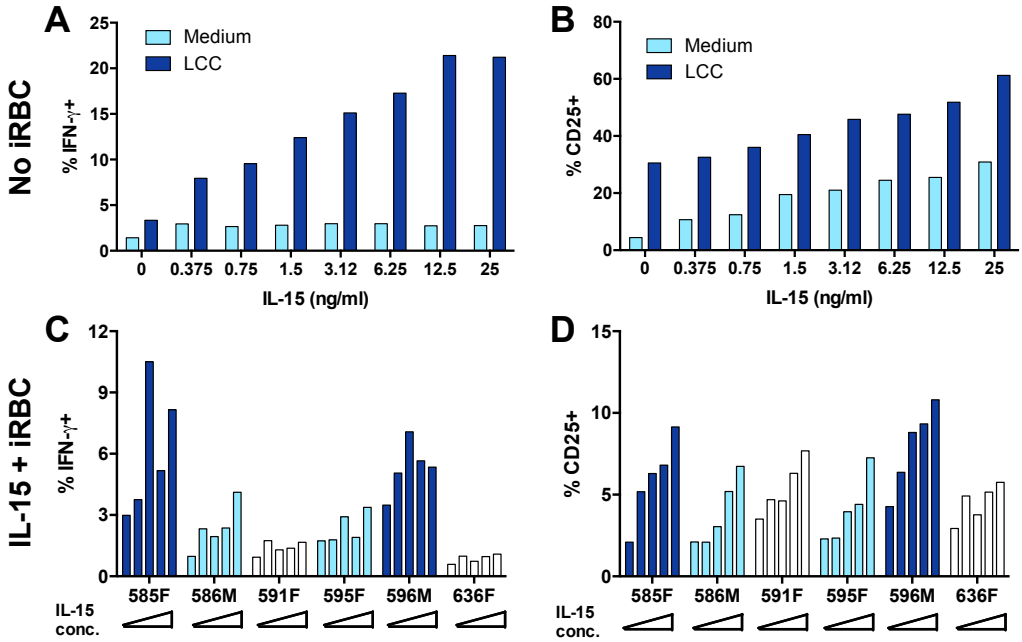

Figure 4.3: **Low concentrations of IL-15 do not drive background NK cell activation but do enhance responses to iRBCs.** Fresh PBMCs were incubated with concentrations of cytokines for 18 hours. Increasing concentrations of IL-15 with (dark blue) or without (light blue) 12.5pg/ml IL-12 and 10ng/ml IL-18 (LCC) (without uRBCs or iRBCs) drove IFN-γ (A) and CD25 (B) NK cell responses (n= 2). Low concentrations of IL-15 (0, 0.375, 0.75, 1.0, 1.5ng/ml, increasing concentration indicated by triangles) and iRBCs drove IFN-γ (C) and CD25 (D) responses in some donors but not others (n= 6).

In summary, therefore, IL-15 boosted NK cell responses to iRBCs at a concentration of 0.75ng/ml, enhancing IFN-γ and CD25 responses. IL-12 and IL-18 were only effective at high concentrations which also increased background levels of NK cell activation. An IL-15 concentration of 0.75ng/ml was chosen for future experiments on the basis that it was the lowest concentration that reliably upregulated IFN-γ and CD25 responses.

4.3.3 Validation of NK cell responses to 3D7HT-GFP parasite strain

Experiments investigating the role of NK-iRBC conjugates (described in Chapter 5) required the use of the *P. falciparum* strain 3D7HT-GFP in order to better characterise

conjugate formation. This led to a change in methodology between assaying NK cell responses from LSHTM and Ugandan donors, as mentioned in the Methods of this chapter. In order to determine whether this parasite strain was equivalent to the 3D7A strain used for experiments with LSHTM donors, I tested NK cell IFN-γ and CD25 functional responses with both parasite strains. Freshly isolated PBMCs from six LSHTM donors were incubated for 18 hours with medium alone, uRBCs, MACS-isolated 3D7A iRBCs (iRBCs), or MACS-isolated 3D7HT-GFP iRBCs (GFP iRBCs) with or without 0.75ng/ml IL-15, or high concentration IL-12 and IL-18 (HCC). BfA was added for the last three hours of incubation. PBMCs were stained for intracellular IFN-γ production and surface CD25 upregulation (Figure 4.4).

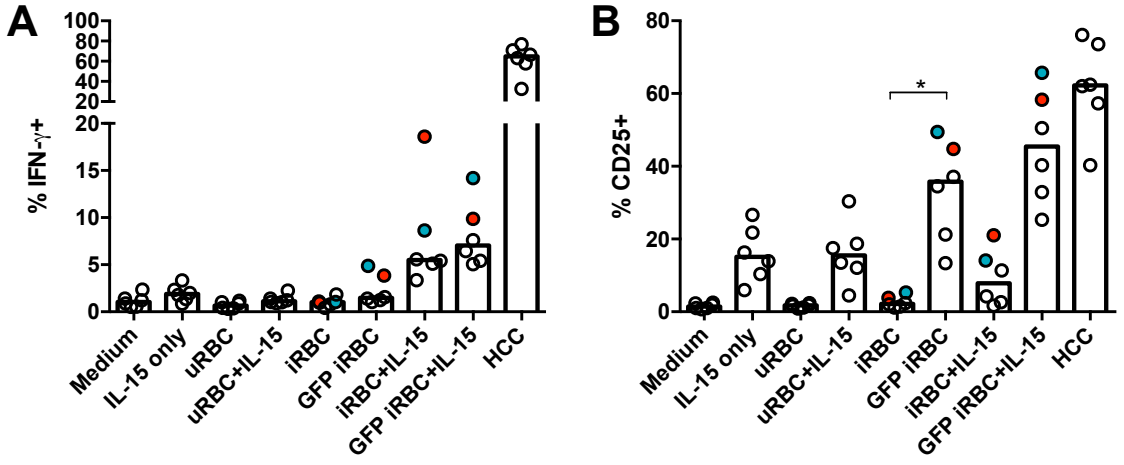

Figure 4.4: **3D7HT-GFP parasites induce similar NK cell responses as 3D7A parasites.** Fresh PBMCs from six donors from LSHTM were stimulated for 18 hours with medium, uRBCs, 3D7A iRBCs or 3D7HT-GFP iRBCs with or without IL-15, or with HCC, and IFN-γ production (A) and CD25 upregulation (B) was measured by FACS. Statistical analyses by Friedman tests with Dunn's correction for multiple t tests * $p \leq 0.05$, ** $p < 0.01$, *** $p < 0.001$ **** $p < 0.0001$.

There were no significant differences in the IFN-γ responses between the parasite strains (Fig. 4.4A), and the responses of individual donors were similar (Friedman tests for multiple comparisons, Dunn's correction). Two high responding donors (219F and 267M) are marked in blue and red respectively. The 3D7HT-GFP strain appeared to significantly

upregulate CD25 expression compared to the 3D7A strain (p= 0.043) without IL-15, but this difference was not significant in the presence of IL-15 (p= 0.08) (Fig. 4.4B). The apparent increase in CD25 expression may be due to emission spectra overlap of the GFP into the PE channel (and therefore CD25 measurement). Further experiments did not show increased CD25 in response to the GFP parasites. The consistency of the IFN-γ responses indicates that there are no significant differences in the NK cell responses to the parasite strains. I therefore concluded that 3D7HT-GFP iRBCs could be used for future experiments concerned with conjugation, and functional responses were comparable with data that used 3D7A iRBCs.

4.3.4 Functional NK cell responses in a malaria-naive and a malaria-exposed population

The variability in NK cell responses to iRBCs between individuals in a population has been well described [26, 200, 202], but the reasons for this variability are still unclear. I therefore compared NK cell responses from a malaria naive group from within LSHTM and a malaria exposed group from Uganda. This provided an opportunity to look at two populations of different environmental and genetic backgrounds and analyse their responses to iRBCs, as well as to compare them based on prior exposure to parasites. Although donors from LSHTM are not all from the same country, the majority of donors are white and Caucasian (92%), and therefore are likely to have similar genetic backgrounds.

PBMCs were stimulated with iRBCs in two assays: firstly for 18 hrs as previously described, with or without a low concentration of IL-15 (0.75ng/ml), and secondly for a two hour assay to characterise conjugate formation with iRBCs and a variety of phenotypic markers on the NK cell surface. The data from the conjugation assay are described in Chapter 5. Donors were also genotyped for NKG2C and a variety of KIR genes, which will also be covered in Chapter 5. 3D7A-iRBCs were used for experiments with LSHTM donors and 3D7HT-GFP-iRBCs were used for experiments with Ugandan donors. All experiments measuring NK cell responses of Ugandan donors also included frozen PBMCs from a previously characterised

LSHTM donor as a control in order to ensure that differences potentially caused by a change in parasite strain or by freezing of PBMCs would not skew the results. NK cell responses from these control LSHTM donors were consistent with their previously collected data.

4.3.4.1 NK cells from different populations show heterogeneous IFN-γ, CD25 and CD107a responses

After 18 hours, NK cell responses of donors from LSHTM to iRBCs varied, but there was significant upregulation of both IFN-γ and CD25 in response to iRBCs compared to uRBCs. FACS plots show NK cell responses to iRBCs and IL-15 (Fig. 4.5A). Both IFN-γ and CD25 responses are significantly enhanced in the presence of IL-15 (Fig. 4.5B, C). Cells from all donors responded well to the positive control ($>$ 20% IFN-γ in response to HCC), and the background responses to medium alone ($<$ 1.8% IFN-γ) and uRBCs ($<$1.9% IFN-γ) were low. Background IFN-γ and CD25 responses were statistically significantly upregulated by IL-15 with both medium and uRBCs (IFN-γ, p= 0.016 and $p<$ 0.0001; CD25, p= 0.002 and $p<$ 0.0001), but responses were low (IFN-γ $<$ 5%, CD25 $<$ 7.5%). Stimulation with iRBCs did not appear to strongly drive degranulation responses, although CD107a was upregulated significantly by iRBCs compared to uRBCs with or without IL-15 (p=0.008, p=0.034 respectively) (Fig. 4.5D); this is consistent with the idea that NK cells primarily respond by producing cytokines to kill malaria parasites, though also allows for the possibility of contact dependent killing.

NK cell responses from Ugandan donors to iRBCs were much lower than responses from the LSHTM group (Figure 4.6). FACS plots show NK cell responses to positive control (HCC) (Fig. 4.6A). IFN-γ responses were very low (Fig. 4.6B), although there was a small but significant increase in IFN-γ production after stimulation with iRBC alone compared to uRBC (p= 0.021, Wilcoxon signed rank test), although not when comparing the two in the presence of IL-15 (p= 0.254), which suggests that the effect of IL-15 may obscure any subtle responses to iRBCs in this population. In the presence of 0.75ng/ml IL-15, IFN-γ

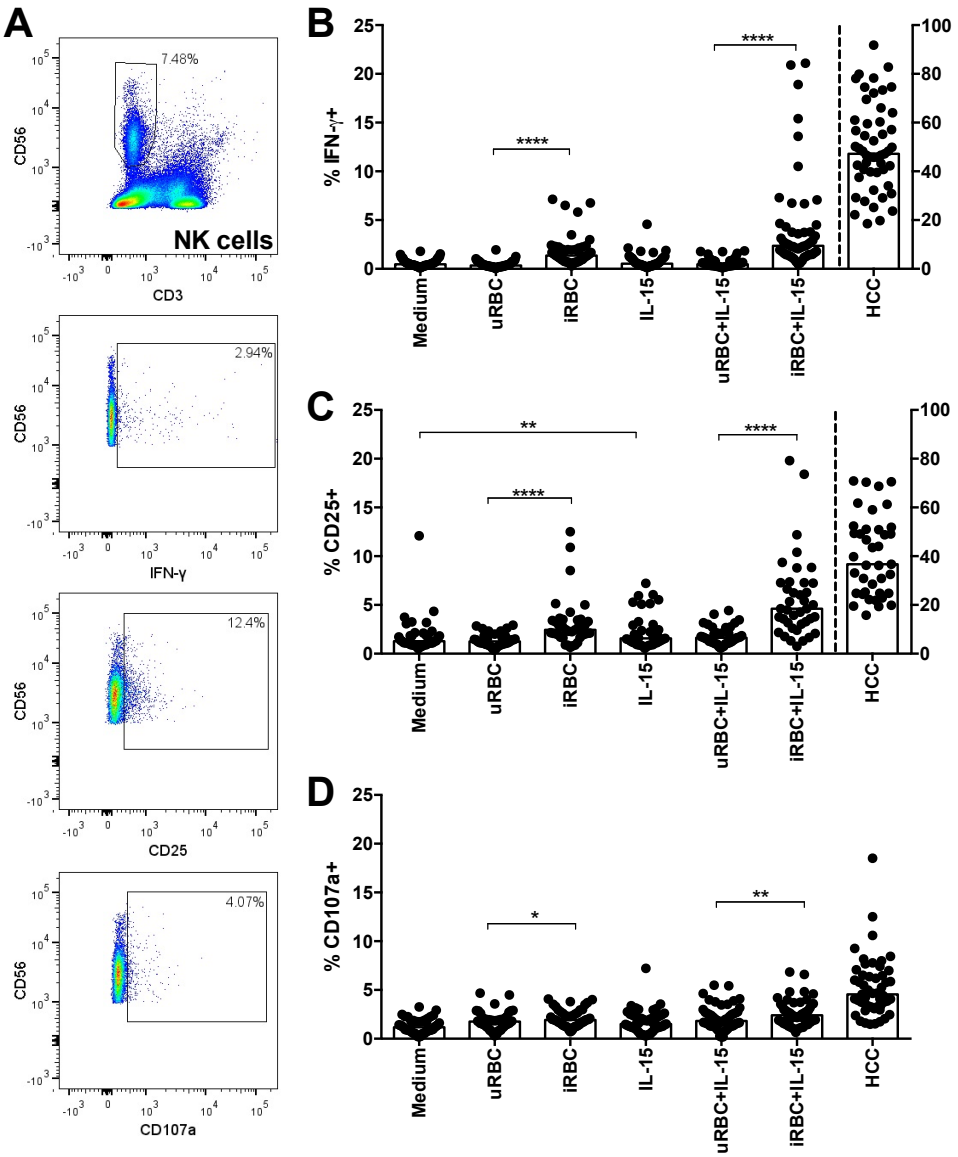

Figure 4.5: **Functional responses of malaria naive donors from LSHTM.** Fresh PBMCs from malaria naive LSHTM donors were incubated with iRBCs with or without 0.75ng/ml IL-15 for 18 hrs. FACS plots show NK cells and gating strategies for IFN-γ, CD25 and CD107a in response to iRBCs+IL-15 (A). IFN-γ (B), CD25 (C) and CD107a (D) responses for each donor are shown as scatter plots (n= 39-46). Bars indicate the median. Dotted lines indicate positive control (HCC) responses plotted on the right hand y-axis. Statistical analyses were carried out by Wilcoxon signed rank tests. * $p \leq 0.05$, ** $p < 0.01$, *** $p < 0.001$ **** $p < 0.0001$.

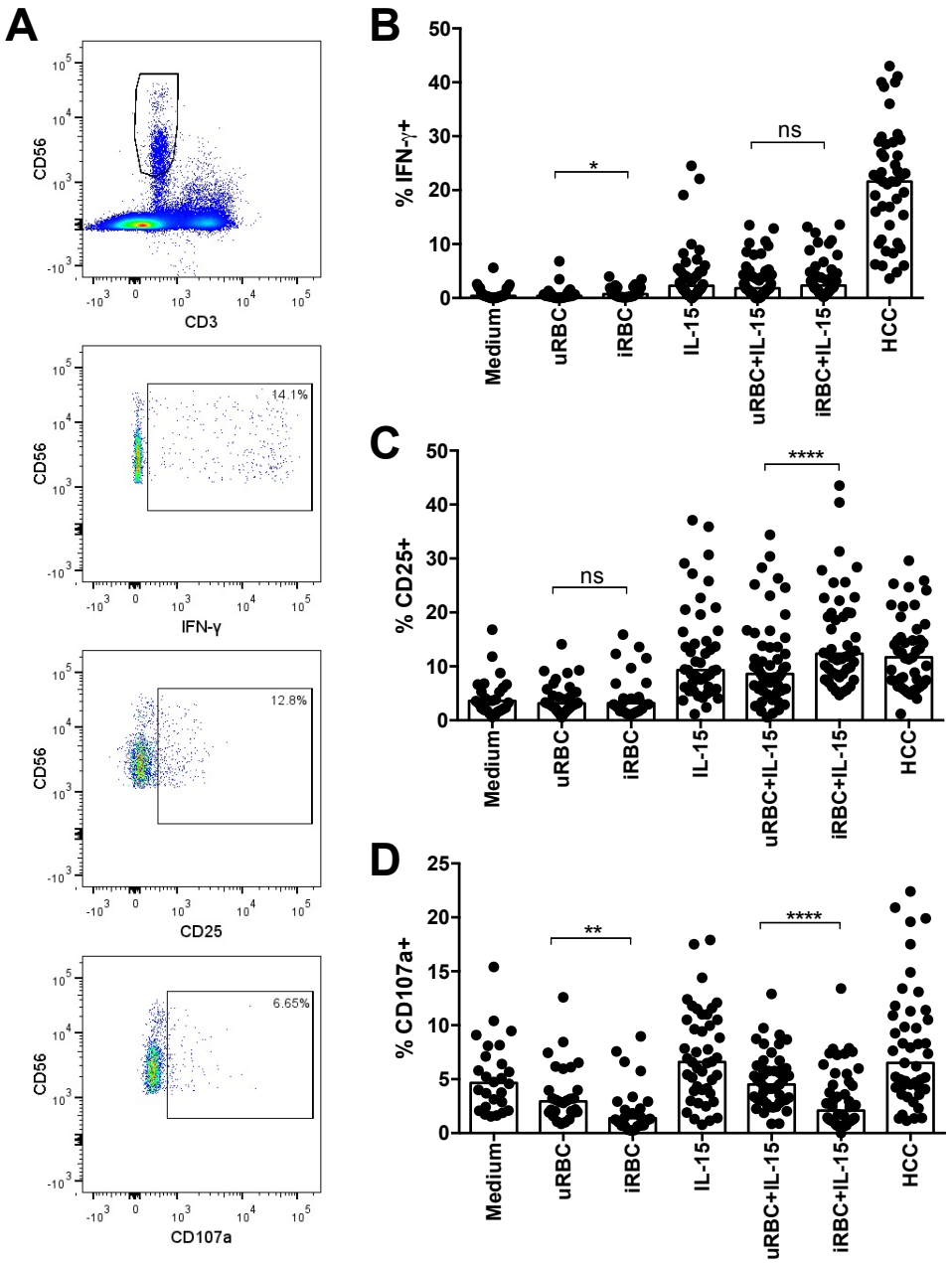

Figure 4.6: **Functional responses of malaria exposed donors from Uganda.** Frozen PBMCs from malaria exposed Ugandan donors were incubated with iRBCs with or without 0.75ng/ml IL-15 for 18 hrs. FACS plots show NK cells and gating strategies for IFN-γ, CD25 and CD107a in response to positive control (HCC) (A). IFN-γ (B), CD25 (C) and CD107a (D) responses for each donor are shown as scatter plots (n= 53). Bars indicate the median. Statistical analyses were carried out by Wilcoxon signed rank tests. * $p \leq 0.05$, ** $p < 0.01$, *** $p < 0.001$ **** $p < 0.0001$.

was high (0-15%), but this appears to be entirely cytokine driven and is probably linked to the extremely high CD25 expression on these cells after IL-15 stimulation. Conversely, CD25 responses were significantly higher after stimulation with iRBCs+IL-15 compared to uRBCs+IL-15 ($p< 0.0001$), but not in the absence of IL-15 ($p= 0.252$) (Fig. 4.6C). Of interest, CD107a responses in Ugandan donors appeared to be inhibited by iRBCs (Fig. 4.6D). Responses to iRBCs were significantly lower than responses to uRBCs ($p= 0.01$), although the median responses for both conditions were low (uRBC= 2.96%, iRBC= 1.39%). IL-15 slightly upregulated CD107a expression in all conditions, but this was not enough to rescue the CD107a response to iRBC.

Direct comparison of IFN-γ, CD25 and CD107a responses showed that the largest difference between the groups is the background upregulation of all responses from Ugandan donors with IL-15 (Figure 4.7). Donors from LSHTM had a small but significantly higher IFN-γ response to iRBCs alone than the Ugandan group ($p= 0.010$, LSHTM median: 1.36%, Ugandan median: 0.73%) (Fig. 4.7A), which may be consistent with studies that found that proinflammatory cytokine responses to malaria were lower after multiple infections (reviewed in [263]). However, although Ugandan donors had strong responses to IL-15, IFN-γ and CD107a responses to iRBCs+IL-15 were not significantly different between the two groups ($p= 0.63$, $p= 0.52$. Mann-Whitney t tests) (Fig. 4.7E), which may reflect iRBC-specific boosting of NK cell responses by IL-15 in the LSHTM population.

Ugandan donors had higher background CD25 responses than LSHTM donors for all conditions (medium alone, LSHTM median: 1.28%, Ugandan median: 3.60%) except iRBCs without IL-15 (p= 0.097) (Fig. 4.7C). However, although responses to IL-15 from Ugandan donors were higher, both IFN-γ and CD25 responses to IL-12 and IL-18 (HCC) were much lower than in LSHTM donors, indicating major differences in basic NK cell responses between these donors. In addition, CD107a background expression was high in Ugandan donors, which may indicate preactivation by other infections. Comparing responses between LSHTM donors and Ugandan adults only (both groups over 20 years old) showed similar trends as the comparison between LSHTM and the total Ugandan population, but Ugandan adults had significantly higher background CD107a responses than LSHTM

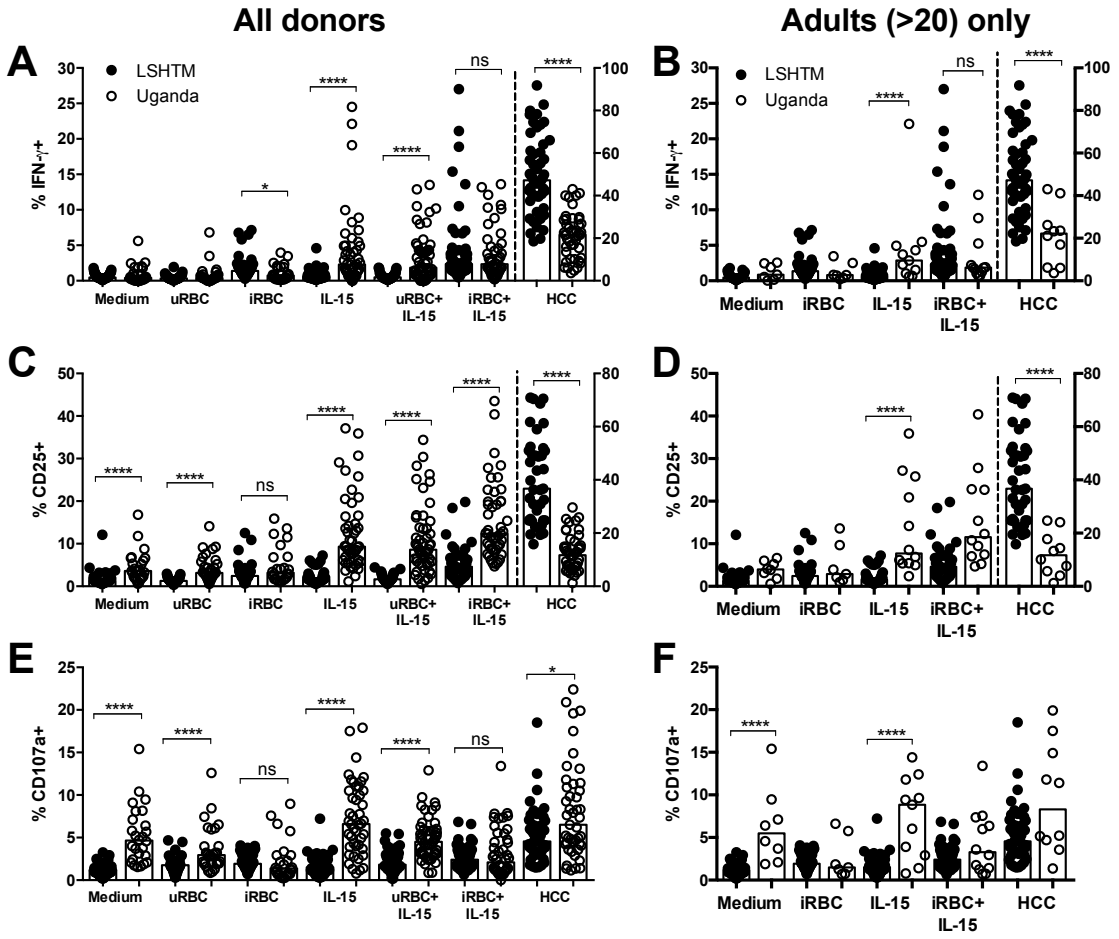

Figure 4.7: **Comparing NK cell responses in malaria naive and malaria exposed populations.** Comparing NK cell responses of LSHTM (filled circles) and Ugandan donors (empty circles) after 18 hrs of incubation with medium, uRBC or iRBC +/− 0.75ng/ml IL-15, or positive control (HCC) by IFN-γ (A-B), CD25 (C-D) and CD107a (E-F) expression. Graphs show comparisons of LSHTM (n= 45) and all Ugandan donors (n= 53), and LSHTM and adult Ugandans only (>20 years old, n= 10). Bars represent the population median. HCC IFN-γ and CD25 responses are plotted on the right hand y-axis. Stastistical analyses carried out by Mann-Whitney tests. * $p \leq 0.05$, ** $p < 0.01$, *** $p < 0.001$ **** $p < 0.0001$.

donors after stimulation with medium alone or IL-15 (Fig. 4.7F), which may be due to a higher frequency of mature cytotoxic NK cells in these donors. Responses of adults only to uRBCs and uRBCs+IL-15 are not shown, as there were no significant differences between responses by adults and the total Ugandan group. There were also no significant differences

in CD25 responses to iRBCs+IL-15 between the groups of adults, possibly indicating that younger Ugandan children are responsible for the high NK cell responses to IL-15 and high CD25 expression.

4.3.4.2 NK cell responses of Ugandan donors by age and site

IFN-γ, CD25 and CD107a responses to iRBCs and iRBCs+IL-15 in Ugandan donors were analysed by age group (under 5 years, 5-11 years and 20-70 years; mean age of each group was 3.05 years, 7.64 years and 44.0 years respectively) and by the location the samples were collected from, Nagongera or Walukuba (Figure 4.8). The 5-11 age group had the highest IFN-γ and CD25 responses to both iRBCs only and iRBCs+IL-15, although this was only statistically significant for IFN-γ responses to iRBC+IL-15 (p= 0.007) (Fig. 4.8A). However, these responses are iRBC-specific rather than IL-15-driven (ANOVA test for differences in IL-15 only responses, p= 0.099; iRBC only responses, p= 0.075). There were no significant differences in CD107a upregulation between age groups (Fig. 4.8C, E), or correlations between IFN-γ or CD107a responses and age (Fig. 4.8D, E). Dividing donors of all ages by location showed no significant differences in IFN-γ production (to iRBCs+IL-15) between the populations (p= 0.41) (Fig. 4.8F). Likewise, comparing the NK cell responses between age groups in each location showed no significant differences (<5, p= 0.79, 5-11, p= 0.12, >20, p= 0.81). However, higher IFN-γ responses in the 5-11 age group appear to be predominantly from donors in the high-endemnicity site Nagongera (ANOVA test, p= 0.028), although the median response from 5-11 year olds from Walukuba was also higher than in other age groups (ANOVA test, p= 0.30). As there were no significant differences in responses from each site between age groups or in the total population, grouping the two sites does not affect the analysis of this data. Splitting the donors into age groups (Figure 4.8A, F) did indicate that 5-11 year olds had higher IFN-γ and CD25 responses than the other age groups, which may be linked to the likelihood of infection in children of this age.

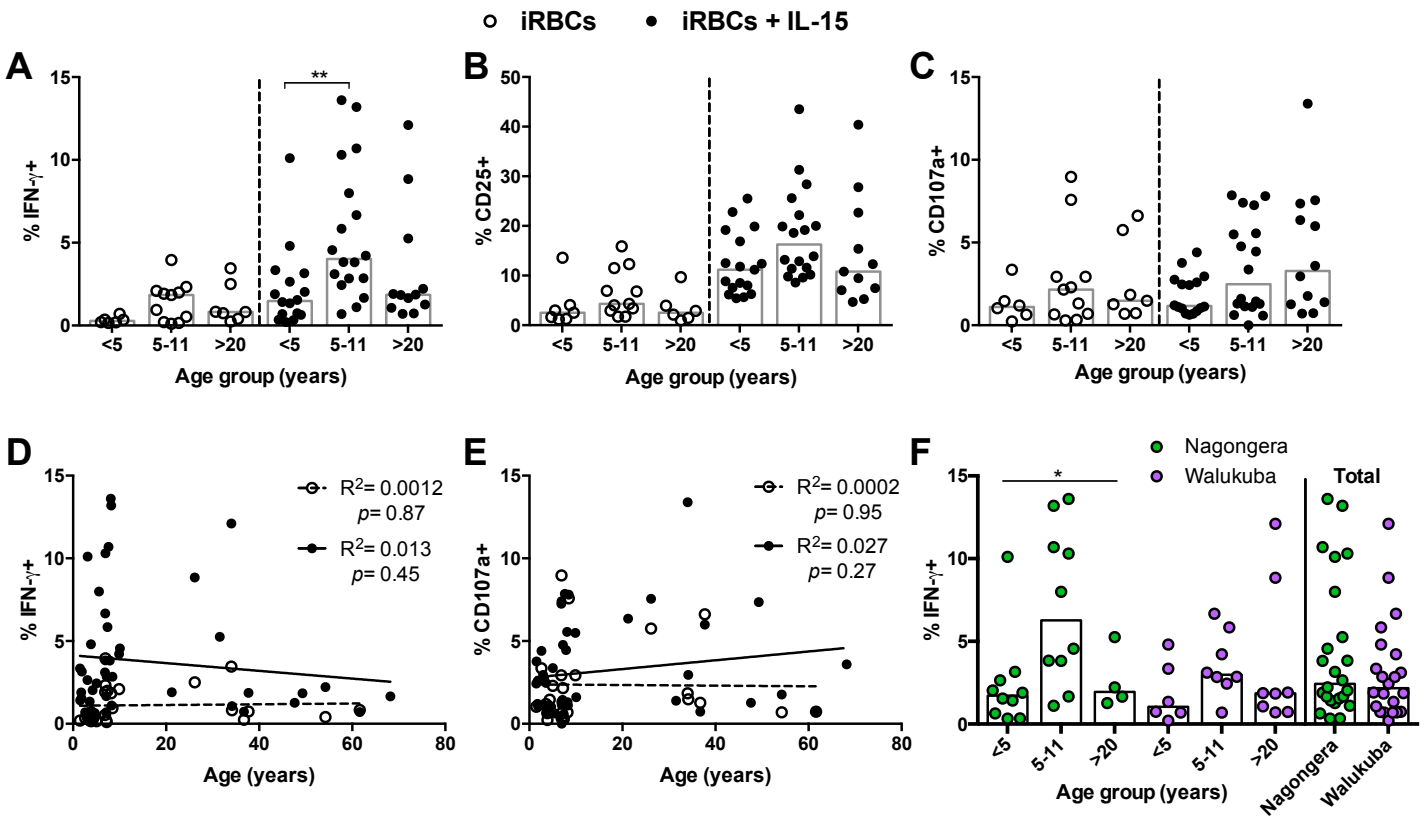

Figure 4.8: **NK cell responses of Ugandan donors by age and site.** Frozen PBMCs from Ugandan donors were incubated with iRBCs (empty circles) or iRBCs+IL-15 (filled circles) for 18hrs and gated for NK cell responses. IFN-γ (A), CD25 (B) and CD107a (C) responses were split into three age groups (<5 years (n= 16), 5-11 years (n= 18), 20-70 years (n= 12)). Correlations between IFN-γ (D) or CD107a (E) responses and age (n= 46) with linear regression (iRBC broken line, iRBC+IL-15 unbroken line). IFN-γ responses to iRBC+IL-15 split by age group and collection site (F) (Nagongera, green circles n= 24, Walukuba, purple circles n= 22). Responses for all age groups divided by location are shown under 'total'. Bars represent medians. Uncapped lines show Kruskal-Wallis ANOVA tests. * $p \leq 0.05$, ** $p < 0.01$, *** $p < 0.001$ **** $p < 0.0001$.

4.3.4.3 Current or recent infection with *P. falciparum* did not significantly affect NK cell responses

Ugandan donors were grouped by history of parasitaemia in the last year to investigate the effect of recent infection on NK cell responses. Donors were sorted by presence (+) or absence (−) of parasites as determined by blood film on the day of blood collection (Figure 4.9), and by parasitaemia in the last 365 days before collection (Figure 4.10). n= 10 had parasites on the day of collection and n= 21 had had parasitaemia in the last year. All but one donor from the first group were also represented in the second. All donors with parasitaemia either in the recent past or present were under 11 years old; the majority of the group with current parasitaemia were between 5 and 11 (in Nagongera, 30% (3/10) of under fives had parasitaemia and 54.5% (6/11) of 5-11 year olds; in Walukuba, 1/10 under fives had parasitaemia), and 90.5% (19/21) of the children in Nagongera had a history of parasitaemia in the last year. All individuals were non-symptomatic at the time of blood collection.

Of the individuals with parasitaemia on the day of collection (Fig. 4.9), parasitaemic donors appeared to have a slightly higher IFN-γ responses in all conditions except HCC, but there were no statistically significant differences after correcting for multiple comparisons (Dunn's t tests). There were no significant differences between the groups in CD25 or CD107a upregulation, although IL-15-driven CD25 responses appeared to be lower in donors with parasitaemia. Although 10 individuals had parasitaemia, some data were excluded due to low cell count (<100 events in the NK gate), particularly in the conditions without IL-15, and therefore sample sizes are too small for meaningful statistical analysis.

Individuals with parasitaemia in the last year had similar NK cell responses to those without parasitaemia for IFN-γ, CD25 and CD107a (Figure 4.10). There were no significant differences between the groups, although CD25 responses to IL-15 also appeared to be lower in individuals with a history of parasitaemia (not statistically significant). This suggests that if NK cells contribute to memory-like responses, this assay was not capable of

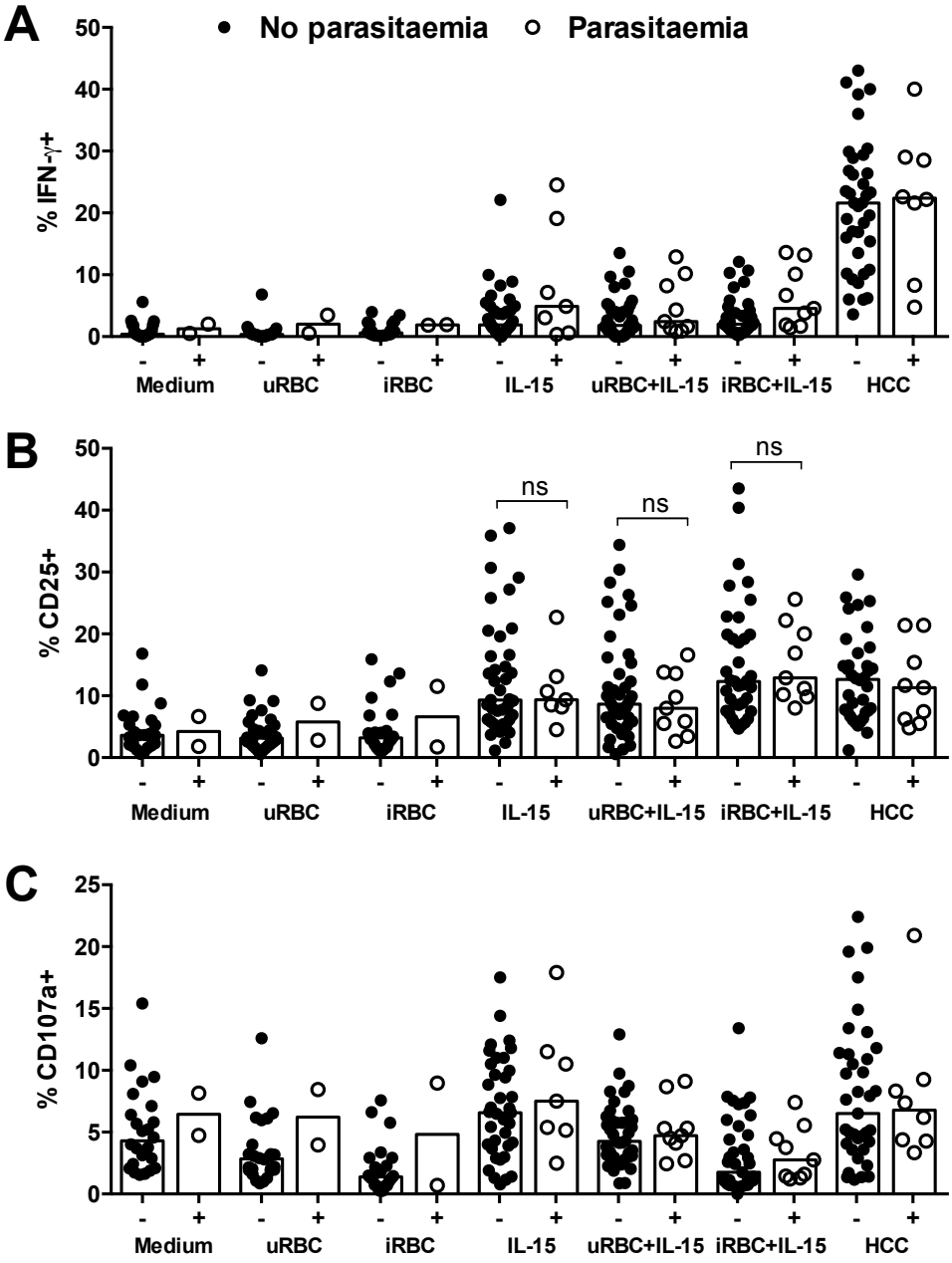

Figure 4.9: **NK cell responses of Ugandan donors by parasitaemia at time of collection.** IFN-γ (A), CD25 (B) and CD107a (C) responses split by presence ($n \leqslant 10$) or absence ($n \leqslant 43$) of malaria parasites at the time of blood collection. Frozen PBMCs were incubated with medium alone, 0.75ng/ml IL-15, uRBCs, uRBCs+IL-15, iRBC, iRBC+IL-15, or HCC for 18 hrs. Bars represent medians. Statistical analyses carried out by Dunn's multiple comparisons tests. No statistically significant results.

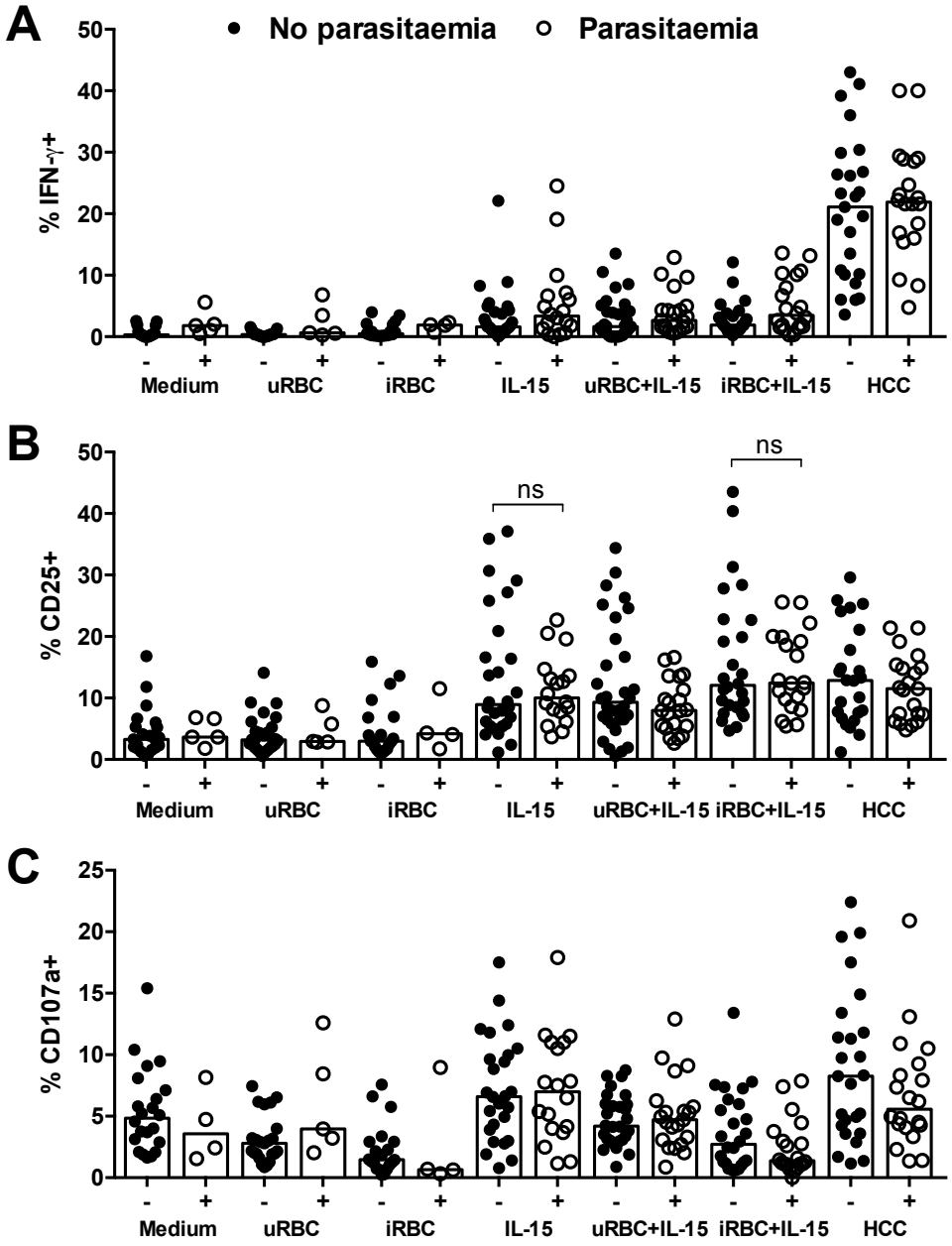

Figure 4.10: **NK cell responses of Ugandan donors with parasitaemia in the last 365 days.** IFN-γ (A), CD25 (B) and CD107a (C) responses split by presence ($n \leqslant 20$) or absence ($n \leqslant 28$) of parasitaemia within the last 365 days. Frozen PBMCs were incubated with medium alone, 0.75ng/ml IL-15, uRBCs, uRBCs+IL-15, iRBC, iRBC+IL-15, or HCC for 18 hrs. Bars represent medians. Statistical analyses carried out by Dunn's multiple comparisons tests. No statistically significant results.

detecting the responses and a larger study is required to investigate differences in age, location and the effect of current or past malaria infections.

4.3.4.4 Effect of NK cell maturity on IFN-γ and CD25 expression

As described in Introduction, Section 1.1, the maturation state of NK cells using the CD56 bright/dim paradigm and the marker CD57 allows classification of NK cell populations into the least mature CD56 bright CD57- cells ('CD56 brights'), through CD56 dim CD57- cells ('CD57-') and CD56 dim CD57 intermediate cells ('CD57int'), to the most mature CD56 dim CD57+ cells ('CD57+') [4–6]. The more mature CD57int and CD57+ subsets accumulate with age, and therefore young children tend to have more CD56 brights and CD57- NK cells, whereas adults have more CD57+ NK cells. The functional capacities of these subsets differ, where CD56 bright and CD57- cells are more responsive to cytokines and in return produce more cytokines upon stimulation; CD57+ cells are considered more cytotoxic and able to directly kill target cells, as well as being more responsive to ADCC upon CD16 crosslinking (reviewed in [5]), but do not produce IFN-γ in response to cytokine stimulation. HCMV infection is thought to drive expansion of CD57+ NK cell subsets and to induce more 'mature' NK cell populations. It is important to note that the prevalence of HCMV in African populations is high from an early age (an estimated 95% of children in the Gambia are seropositive by the age of three [11]), whereas HCMV prevalence is much lower in the UK population and increases only slowly with age [285]; the Ugandan donors are therefore very likely to be HCMV+. It is therefore likely that the distribution of NK cells between less mature and more mature subsets varies between Ugandan and LSHTM donors.

Comparing the proportions of NK cell subsets between LSHTM and Ugandan donors showed several differences in functional responses (Figure 4.11). The percentage of cells per subset for each donor was gated after incubation with medium alone. Donors from the Ugandan group had significantly higher proportions of CD57- NK cells than LSHTM donors (median percentages: LSHTM, 35.5%, Ugandan, 47.6%, $p = 0.002$) (Fig. 4.11B). However,

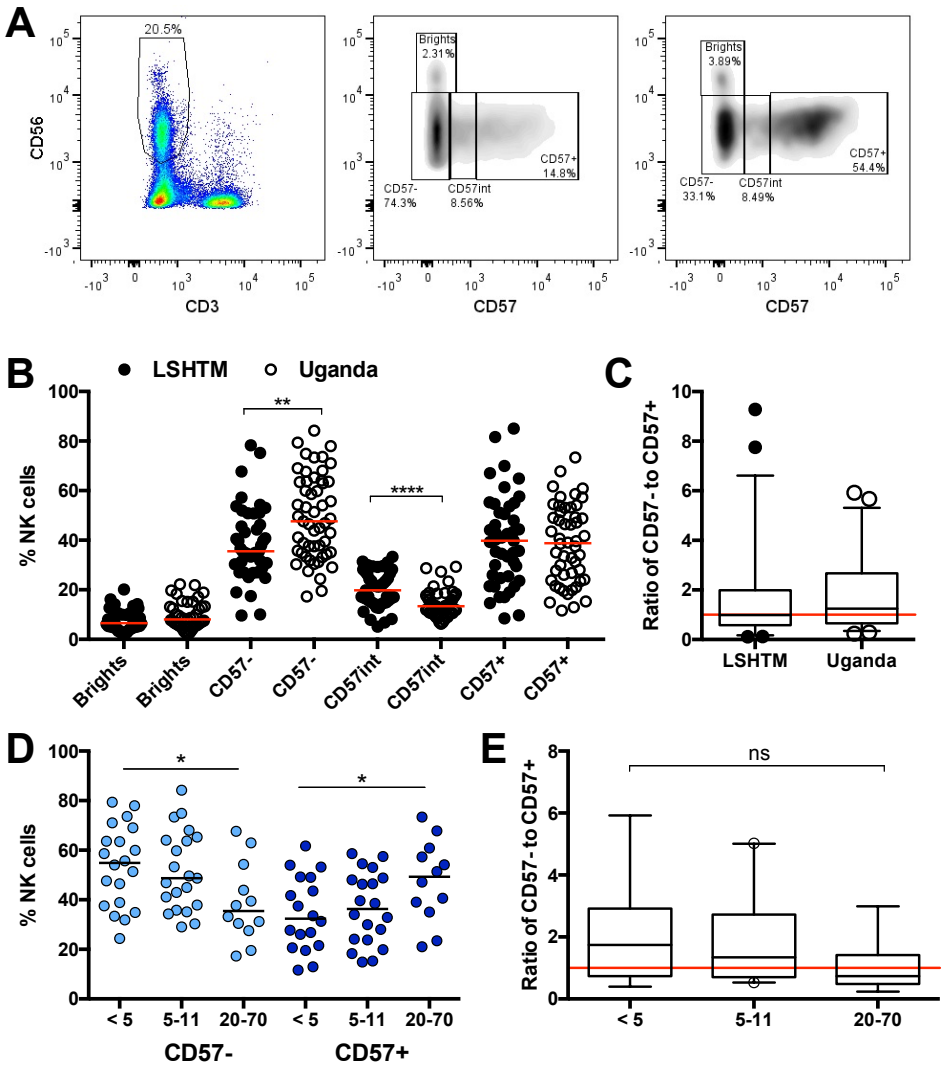

Figure 4.11: **NK cell maturation subsets show minor differences between LSHTM and Ugandan populations.** NK cells are divided into CD56 bright, CD57-, CD57intermediate and CD57+ subsets. FACS plots show NK cell gating and CD57 subset gating for a typical LSHTM and Ugandan adult donor (A). Comparison of the percentage of NK cells each subset represents in LSHTM (n= 45) and Ugandan donors (n= 53) (B). Each circle represents a donor, red lines show the median. Box-and-whisker plots represent the ratio of CD57- to CD57+ NK cells for each group of donors (C). Whiskers indicate the 5-95th percentiles, red line indicates a ratio of 1.0 (equal proportions of CD57- and CD57+ cells). Proportions of CD57- and CD57+ NK cells differ with age in Ugandan donors (D), and the ratio of CD57- to CD57+ NK cells decreases in adults (E). Statistical analyses carried out by unpaired parametric t tests with Holm-Sidak correction for multiple comparisons, or ANOVA tests for linear trend. * $p \leq 0.05$, ** $p < 0.01$, *** $p < 0.001$ **** $p < 0.0001$.

although LSHTM donors had higher percentages of CD57int NK cells ($p< 0.0001$), both populations had the same proportions of CD57+ NK cells (median percentages: LSHTM, 39.8%, Ugandan, 38.8%, $p= 0.83$). The ratio of CD57- to CD57+ NK cells for each donor was calculated and shown as box-and-whisker plots (Fig. 4.11C). Ratios >1.0 represent higher proportions of CD57- NK cells and vice versa. There was no significant difference between the overall ratios of the two groups ($p= 0.19$), although the median of the Ugandan group was slightly higher (1.24) than the LSHTM group (0.98). The range of values for each group between individuals also indicates that the proportion of each subset can vary greatly. As the majority of the Ugandan donors were children, the proportion of CD57- and CD57+ NK cells were compared in different age groups (under 5 years old, 5-11 year olds, 20-70 year olds). The percentage of CD57- NK cells decreased with age and CD57+ NK cells increased accordingly (Fig. 4.11D), but there were no statistically significant differences in the ratio of CD57- to CD57+ NK cells between the age groups (<5 vs. 5-11: $p= 0.68$, 5-11 vs. 20-70: $p= 0.064$, <5 vs. 20-70: $p= 0.053$) (Fig. 4.11E). The increase in CD57+ NK cells with age is consistent with observations from our group and others [6, 10], while the effect of HCMV infection is likely to be driving NK cell maturation in younger children and increasing their proportion of CD57+ NK cells [17].

To investigate the contribution of each NK cell subset to the total IFN-γ, CD25 and CD107a responses, NK cell responses of the LSHTM donors were broken down by subset (Figure 4.12). IFN-γ responses were low in all subsets in the absence of iRBCs or HCC, although all conditions showed a significant trend where IFN-γ production decreased with increasing CD57 expression (ANOVA test for linear trend). The most responsive subsets are the CD56 bright and CD57- NK cells, which is most striking for the responses to HCC, where 70-100% of the CD56 bright cells but only 5-40% of CD57+ cells are IFNγ+. A similar effect can also be seen in both the iRBC alone and iRBC+IL-15 conditions, where the CD56 bright subset responds most highly. However, as the mean percentage of CD56 bright cells in these donors was 7.49% compared to a mean of 38.6% CD57- cells (see Fig. 4.11), the majority of IFN-γ producing cells were CD57- cells. Comparing the responses of the CD57int and CD57+ subsets to iRBCs vs. uRBCs also shows a small increase in

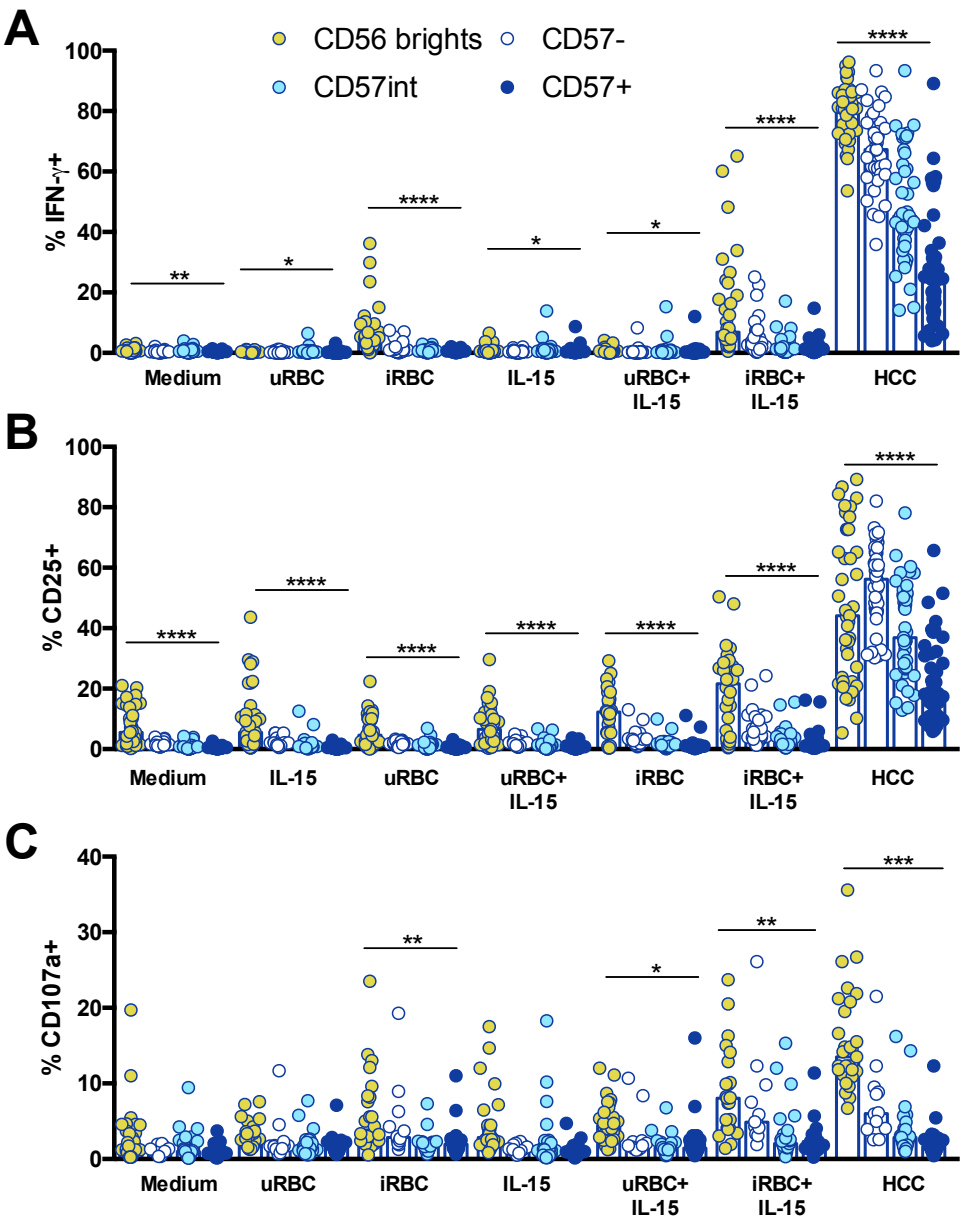

Figure 4.12: **CD57 subset analysis in LSHTM donors.** NK cells were gated into four subsets, CD56 brights (yellow), CD57- (clear), CD57int (light blue) and CD57+ (dark blue), and analysed for IFN-γ (A), CD25 (B) and CD107a (C) responses after 18hrs (n= 35-41). Bars represent medians. Statistical analyses carried out by one-way ANOVA with Geisser-Greenhouse correction and tests for linear trend (uncapped lines). * $p \leq 0.05$, ** $p < 0.01$, *** $p < 0.001$ **** $p < 0.0001$.

IFN-γ production (both subsets $p< 0.0001$), indicating that more mature NK cells are still capable of limited cytokine production, and also suggests that the IFN-γ response is not entirely cytokine driven. CD25 was constitutively expressed on CD56 bright NK cells, and decreased with increasing CD57 expression (test for both ANOVA and linear trend for all conditions were $p<0.0001$) (Fig. 4.12B). However, CD57int and CD57+ cells were capable of upregulating CD25 expression in response to iRBCs with or without IL-15. Although CD107a and cytotoxic responses are associated with more mature NK cells and CD57 expression, there was no clear trend towards increased CD107a expression in CD57+ subsets, and instead CD56 bright cells appeared to upregulate CD107a in response to iRBCs (Fig. 4.12C). Less mature subsets also upregulated CD107a in response to HCC. From these data, NK cell subset had no clear effect on CD107a expression other than in cytokine-driven responses (predominantly HCC); assays involving a MHC-deficient target cell rather than cytokine-driven activation may provide a clearer picture of degranulation responses [242, 286].

Gating of NK cell subsets from Ugandan donors showed similar trends as in the LSHTM group (Figure 4.13). Due to low cell numbers during freezing of PBMCs, functional responses of the CD56 bright subset were not analysed as few donors had more than 100 cells in this subset.[1] IFN-γ responses were clearly dominated by CD57- cells for all conditions, and CD57- cells showed higher background IFN-γ responses than CD57- subsets from LSHTM donors. It was also clear that CD57- cells were the main producers of IL-15-driven IFN-γ, and IFN-γ production, even in response to IL-15 stimulation, decreased sharply with increasing CD57 expression.

CD25 responses of CD57- NK cells showed high background levels of expression and decreased with increasing CD57 expression. However, CD57int cells also upregulated CD25 expression in response to IL-15 at higher levels than LSHTM donors (mean CD57int CD25 response to IL-15: LSHTM, 1.45%, Ugandan, 4.88%), which may indicate a different and

[1] Although the percentage of CD56 bright cells in the total NK cell population could be calculated (as in Figure 4.11), analysis of functional responses was not carried out as one event in the positive gate (e.g. IFN-γ+) would represent more than 1% of the population, thus potentially skewing the data due to background staining or noise.

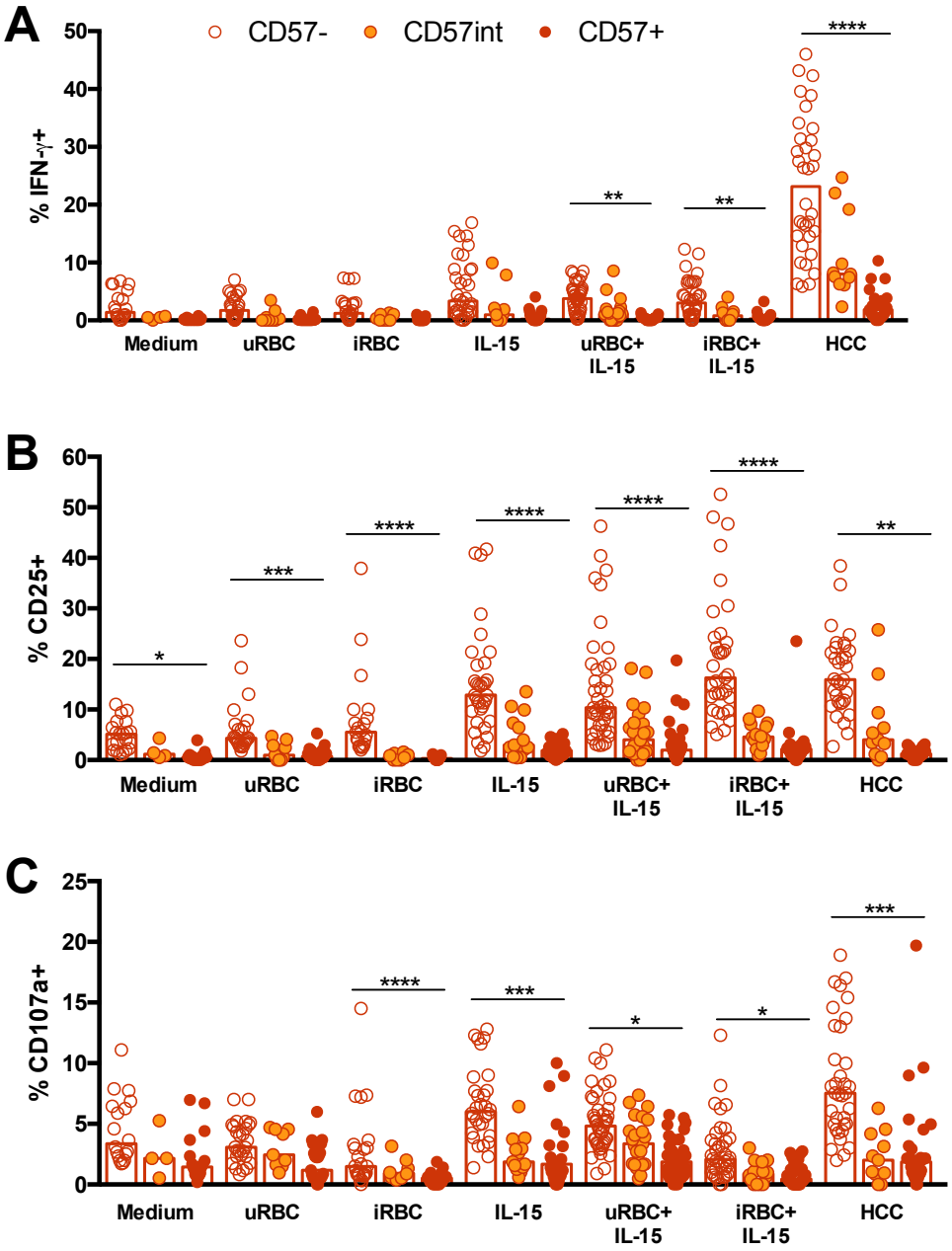

Figure 4.13: **CD57 subset analysis in Ugandan donors.** NK cells were gated into four subsets. CD56 brights were excluded due to insufficient cell numbers, and three subsets, CD57- (clear), CD57int (light blue) and CD57+ (dark blue), were analysed for IFN-γ (A), CD25 (B) and CD107a (C) responses after 18hrs (n= 4-42). Bars represent medians. Statistical analyses carried out by ANOVA tests for linear trend (uncapped lines). * $p \leq 0.05$, ** $p < 0.01$, *** $p < 0.001$ **** $p < 0.0001$.

more cytokine-responsive phenotype of the CD57int subset in Ugandan donors compared to LSHTM donors. It is also interesting that CD57+ cells from Ugandan donors showed almost no IFN-γ or CD25 response to HCC stimulation, whereas CD57+ cells from LSHTM donors, while responding at lower frequencies than CD57- or CD57int cells, still had median IFN-γ responses of 23.5% and CD25 responses of 18.9% (compared to medians of 1.86% and 1.24% respectively in Ugandan donors). CD107a responses showed a clear decreasing trend with increasing CD57 expression, but as responses were generally low this effect was small. The apparent depression in CD57- CD107a expression after incubation with iRBCs contrasts with the increased expression seen in LSHTM donors, but is not otherwise explained by the subset analyses. As low levels of CD107a can be driven by stimulation with IL-12 and IL-18, the increased responsiveness of CD57- NK cells to these cytokines may account for the higher CD107a expression compared to CD57+ NK cells in this assay.

4.3.4.5 Proportions of CD57- NK cells correlate with IFN-γ and CD25 expression

To test for the effects of age in the Ugandan donors that might affect the ability of NK cell subsets to respond to activation, the functional responses of CD57- NK cells in different age groups (under 5 years, 5-11 year olds, 20-70 year olds) were compared. CD57- NK cells were gated as in Figure 4.11 and IFN-γ, CD25 and CD107a responses from these cells were measured by FACS. CD57- NK cell responses to IL-15, iRBCs, iRBCs+IL-15 or HCC did not significantly differ between age groups (Figure 4.14), indicating that CD57- NK cells from all donors have a similar capacity for activation and CD57- NK cells from younger donors are not 'more functional' than those from older individuals.

Comparing these two populations makes it clear that the Ugandan CD57- subset had high background levels of both IFN-γ and CD25, which appears to primarily account for the background levels of the total NK population. As CD57- NK cells seemed likely to drive the majority of IFN-γ and CD25 upregulation in both groups of donors, total NK cell

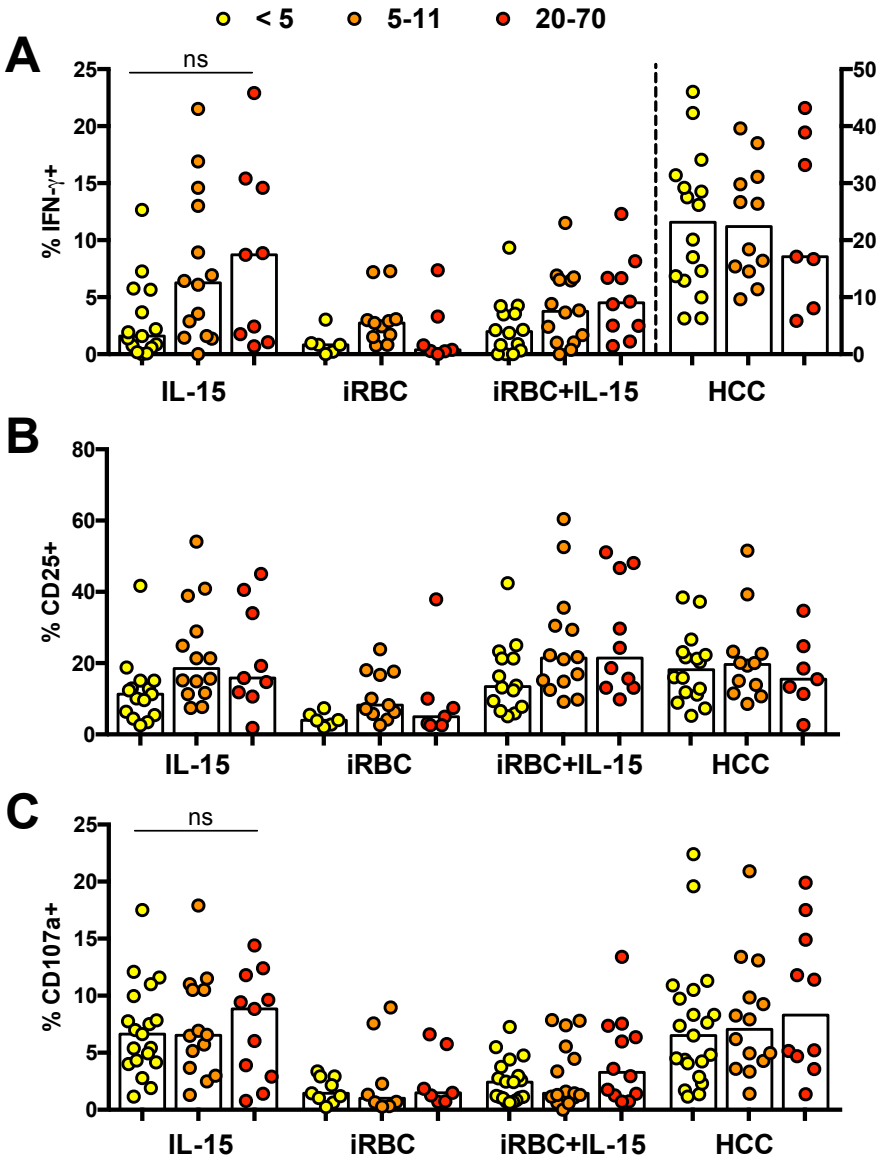

Figure 4.14: **CD57- NK cell function does not differ by age.** Functional responses of CD57- NK cells from Ugandan donors (using frozen PBMCs) were divided by age and analysed for IFN-γ (A), CD25 (B) and CD107a (C) after 18hrs. Age groups were under 5 years (n=16, yellow), 5-11 year olds (n=14, orange) and 20-70 year olds (n=10, red). Bars represent medians. Statistical analyses carried out by ANOVA tests for linear trend (uncapped lines), no statistically significant results.

responses were tested against the percentage of CD57- cells in donors from each group to see whether increased proportions of CD57- correlated with increased IFN-γ, CD25 or CD107a responses (Figure 4.15).

NK cells from LSHTM donors showed no correlations between IFN-γ, CD25 or CD107a responses and proportions of CD57- cells. However, IFN-γ responses from Ugandan donors to iRBCs alone significantly correlated with CD57- percentages (R^2= 0.23, p= 0.019). CD25 responses to both iRBCs and iRBCs+IL-15 also significantly correlated with CD57- proportions (iRBCs, R^2= 0.31, p= 0.005; iRBCs+IL-15, R^2= 0.093, p= 0.039), consistent with the data suggested in Fig. 4.13B. The lower correlation in the presence of IL-15 for both IFN-γ and CD25 responses is interesting, and perhaps could be related to increased responsiveness of CD57int cells to IL-15, so that non-specific IL-15-driven IFN-γ and CD25 responses overwhelm iRBC-specific activation. CD107a responses showed a small but non-significant correlation with increasing CD57- proportions, but the trends are too small to draw further conclusions from these data.

As higher production of IFN-γ and CD25 appeared to correlate with increasing proportions of CD57- NK cells, functional responses were again correlated with percentages of CD57- NK cells after stimulation with high concentrations of IL-12 and IL-18 (5ng/ml and 50ng/ml respectively) (HCC) (Figure 4.16). The percentage of CD57- NK cells strongly correlated with IFN-γ responses in both LSHTM and Ugandan donors (R^2= 0.20 and 0.32 respectively) (Fig. 4.16A), as did CD25 responses (R^2= 0.16 and 0.19 respectively) (Fig. 4.16B). This is likely to be due to the expression of IL-12R and IL-18R on CD57- NK cells allowing these cells to produce a large proportion of IFN-γ upon stimulation with cytokines. However, CD107a upregulation did not correlate with CD57- NK cells (Fig. 4.16C), which is consistent with a model where NK cell cytotoxicity and degranulation responses are driven by other stimuli such as CD16 crosslinking, which is mainly found on CD57+ NK cells.

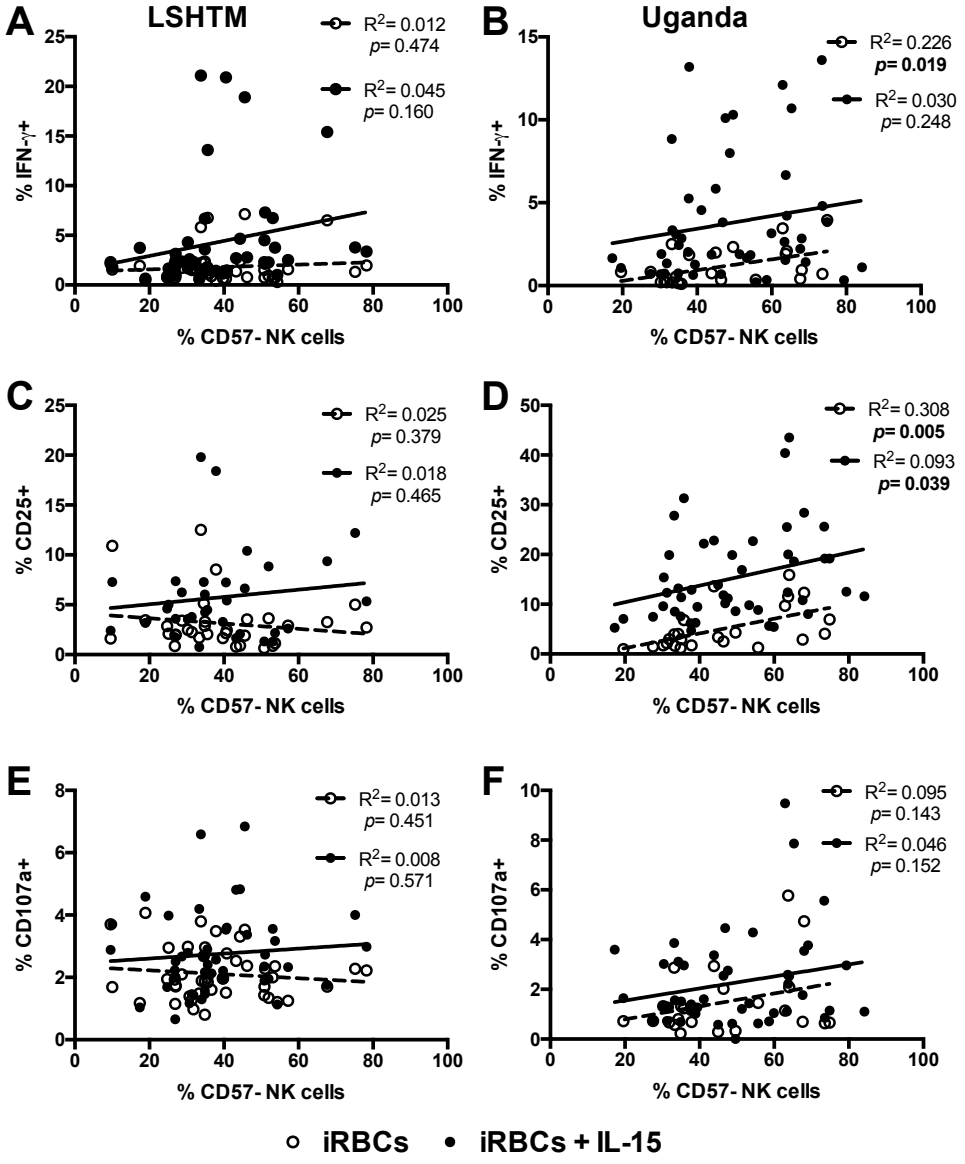

Figure 4.15: **Proportions of CD57- NK cells correlate with IFN-γ and CD25 responses.** CD57- NK cell percentages were plotted against total NK cell IFN-γ (A-B), CD25 (C-D) and CD107a (E-F) responses to iRBCs (clear circles) (n= 24) or iRBCs+IL-15 (filled circles) (n= 46) in LSHTM or Ugandan donors. R^2 and p values are indicated on each plot. Statistically significant p values are shown in bold. Statistical analyses carried out by linear regression.

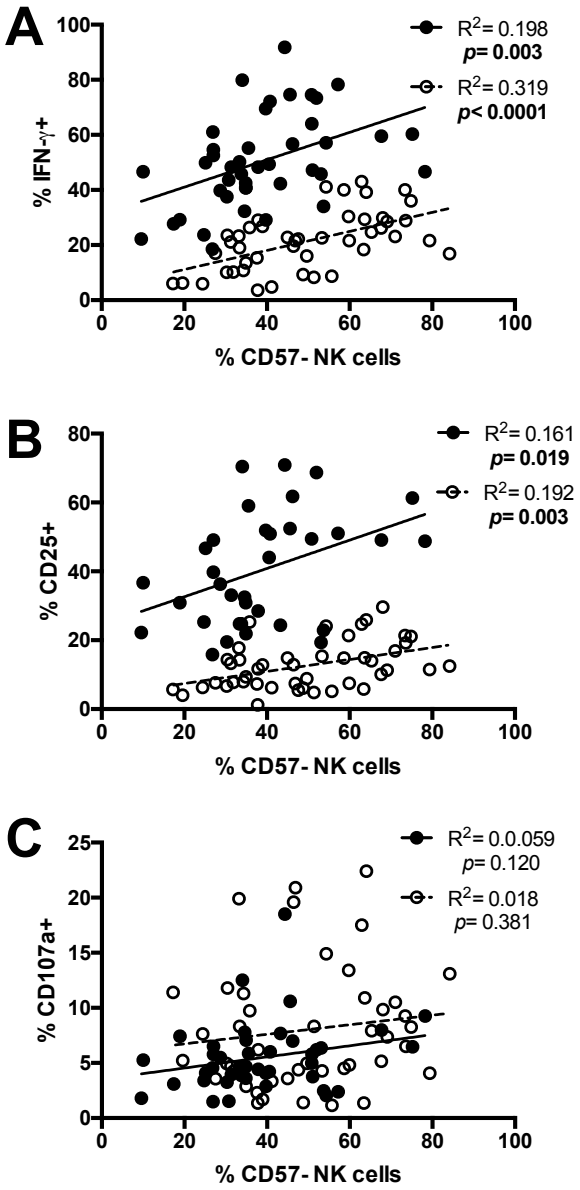

Figure 4.16: **Proportions of CD57- NK cells correlate with IFN-γ and CD25 responses to IL-12 and IL-18.** CD57- NK cell percentages were plotted against total NK cell IFN-γ (A), CD25 (B) and CD107a (C) responses to high concentration IL-12 and IL-18 (HCC). Responses from LSHTM (n= 45) and Ugandan (n=51) donors are plotted on the same graphs by filled and empty circles respectively. R^2 and p values are indicated on each plot. Statistically significant p values are shown in bold. Statistical analyses carried out by linear regression.

4.4 Discussion

NK cell responses to malaria are well-established as highly variable within a group of individuals [200], but are less well described between two populations from different backgrounds. There are obvious problems with comparing different populations, several of which are present within this study; the most obvious is the disparity in age between the populations, followed by differences in environmental exposure. Factors such as HCMV status, which has been found to impact NK cell responses to cytokine stimulation [17], have not been taken into account when analysing these data, and it is likely that most, if not all, of the individuals from Uganda are HCMV seropositive. Serum samples were not available to analyse HCMV infection in this group of donors, but studies of HCMV prevalence in both Tanzania and the Gambia indicate almost universal infection at a young age [11, 287]. However, despite these caveats, the differences in responsiveness to all stimuli between these two populations are interesting. The most noticeable differences between the two groups in this study are increased responsiveness to IL-15 and high background CD25 expression in the Ugandan donors.

IFN-γ, CD25 and CD107a responses of malaria naive donors from LSHTM were upregulated by iRBCs and low levels of exogenous IL-15 enhanced these responses in an antigen-specific manner. Conversely, responses of malaria exposed Ugandan donors to iRBCs were low in the absence of IL-15, and the addition of IL-15 drove strong non-specific NK cell responses. Although CD57 expression has a clear effect on IFN-γ and CD25 production, the proportions of CD57- and CD57+ NK cells within each group of donors were similar. Analysis of the contribution of each subset to cytokine production showed that CD57+ responses, while the least responsive subset in both groups, contributed almost no IFN-γ in responses by Ugandan donors. This suggests that CD57 expression alone does not determine the NK cell capacity for cytokine production, and will be investigated further in Chapter 5.

4.4.1 PBMCs from Ugandan donors are more sensitive to IL-15 and express high background CD25

Heterogeneity of IFN-γ responses to iRBCs in malaria naive individuals has been previously described [200], but the difference in responsiveness to IL-15 raises the possibility that one contributing factor to this range is an intrinsic difference in the activation threshold at which NK cells begin to respond. The function of IL-15 as 'priming' rather than activating may be particularly relevant here, whereby it lowers the activation threshold of a cell rather than itself driving cell activation to cross the threshold [35, 36]. This would account for the generally low levels of background activation seen in the IL-15 alone and uRBC+IL-15 conditions in these donors, whereas both IL-12 and IL-18 had little effect at low concentrations in enhancing responses to iRBCs, and at higher concentrations or in combination drove IFN-γ and CD25 responses themselves.

By contrast, IL-15 drove IFN-γ and CD25 responses in the Ugandan population very strongly, which was unanticipated. This could be due to polymorphisms in the IL-15R between the populations, perhaps reducing the threshold of IL-15 needed to activate cells, or higher constitutive IL-15R expression on NK cells and therefore enhanced ability to respond quickly. Ugandan donors had a higher baseline CD25 expression than LSHTM donors, which suggests a greater capacity to respond to low levels of stimulation, especially to IL-2. As IL-15 and IL-2 share the β and γ receptor subunits CD122 and CD132 (but not CD25), it could be that IL-15 bound the low- and medium-affinity components of the IL-2R, thus triggering cytokine-driven IFN-γ by bypassing the normal mechanisms for activation or priming by IL-15. iRBCs themselves did not appear to have any effect on CD25 upregulation in this population when compared to medium or uRBCs; the greatest effect by far was of IL-15, which was comparable to the effect of HCC (there were no significant differences between CD25 NK cell responses to any conditions with IL-15 and HCC). For comparison, the difference in the percentage of CD25+ NK cells between IL-15 alone and HCC in the LSHTM group was 34.3% ($p< 0.0001$).

It is also interesting that while Ugandan IFN-γ responses to IL-15 were higher than LSHTM

responses, IL-12 and IL-18 driven activation was consistently lower in both the total NK population and each of the CD57 subsets. Previous studies have also reported lower exogenous IL-12 and IL-18 driven IFN-γ responses in African populations than in European populations [11]. Reduced responsiveness to cytokines has been observed in HCMV+ individuals due to the expansion of the less-responsive CD57+ subset, but although many of the Ugandan donors are likely to be HCMV seropositive [11, 288], there was still a clear trend for increased CD57+ NK cells in adults compared to children. However, the only statistically significant differences in IFN-γ responses between age groups was increased IFN-γ production in 5-11 year olds compared to the under fives, and the reasons for the overall reduction in responsiveness to cytokine stimuli in Ugandan donors compared to LSHTM donors are still unclear, especially as this seems to contrast with high CD25 expression. Ugandan donors did not appear to upregulate CD25 in response to iRBCs compared to uRBCs in the absence of IL-15, but did show an iRBC-specific CD25 response with IL-15. Whether this is linked to the higher levels of background CD25 expression in the population, so that NK cells are constitutively sensitive to IL-2 stimulation (and thus secondary 'recall' responses) and are enhanced further by the presence of antigen and IL-15 in combination, has yet to be determined, and it would have been interesting to titrate IL-2 into culture with PBMCs from Ugandan donors to compare these responses with LSHTM donors, who had minimal responses to IL-2 alone compared to IL-15.

The difference in mean age of LSHTM and Ugandan donors (23.0 years) was reflected in the higher proportion of CD57- NK cells in Ugandan donors. However, IFN-γ responses to iRBCs and HCC by LSHTM donors were generally higher than the responses from Ugandan donors, which was surprising as a less mature NK cell population is usually also associated with higher capacity to produce IFN-γ [6, 38]. IFN-γ and CD25 responses were lower in Ugandan donors even when the proportion of CD57- NK cells were similar to LSHTM donors, which indicates a reduced responsiveness of their NK cells distinct from expression of CD57.

4.4.2 NK cell 'memory' responses to iRBCs

This possible responsiveness to IL-2 naturally suggests the potential for secondary responses, where activated T cells might produce IL-2 upon restimulation with iRBCs. Endogenous cytokines from memory responses did not appear to drive NK cell responses as IFN-γ and CD107a responses were very low in the absence of exogenous IL-15, even in the presence of iRBCs. Analysis of responses of donors with parasitaemia on the day of blood collection is limited by low numbers of donors, and so firm conclusions cannot be drawn from this analysis. Donors with parasitaemia within the last year, if not at the time of collection, had marginally higher background IFN-γ responses than those who had not, but there were no statistically significant differences in the conditions with iRBCs, which either suggests that NK cells do not have a memory response to iRBCs, or else that, as it is likely that all of these individuals will have had malaria at some point, NK cell responses are long-lived enough that it makes no difference when they last had malaria. It may be also interesting that there were no differences in the HCC responses from donors with or without current parasitaemia.

If NK cell from the parasitaemic group are more highly activated to produce IFN-γ, adding IL-12 and IL-18 does not enhance this activation. Whether there could be some benefit in a weaker response to IL-12 and IL-18 is debatable. Downregulation of the IL-12 and IL-18 receptors on NK cell populations could be beneficial in limiting immunopathology, particularly if sufficient IFN-γ might come from another source, or if IFN-γ is only of limited use after 24 hours; conversely, this lowered responsiveness could be a side effect of other infections, such as HCMV or helminths, which might be detrimental. I did not collect data on the expression of the cytokine receptors in the Ugandan population, which might indicate if there is any polymorphism in receptor function or expression that could account for a reduced effect of these cytokines. Immunity to malaria in high transmission areas becomes sufficiently effective to heavily reduce the clinical symptoms of malaria at an early age (reviewed in [129]), and therefore IFN-γ responses in Ugandan donors may become lower relatively early (by age 10) due to repeated exposure. This may also be

one reason that IFN-γ responses were lower in the Ugandan population than in the naive LSHTM group.

Considering these factors, it does not seem likely that NK cells show a classical 'memory' response to malaria parasites. It is possible that the NK cells of the Ugandan population are in a higher state of activation, or have a lower threshold for activation because of the pathogens, environmental or malarial, that they have been exposed to compared to donors from LSHTM, but NK cells do not appear to take part in specific recall responses to iRBCs (unless only a small proportion of NK cells take part in this and the effect is lost in the total population). It is possible that NK cells contribute to adaptive immune responses in a more supporting role by producing other cytokines (e.g. to stimulate T cell responses) rather than IFN-γ, or require other signals not provided here, such as T cell help via IL-2 production over a longer period of time [272].

4.4.3 CD57 subsets do not explain differences in NK cell responsiveness between groups of donors

As previously mentioned, the proportions of CD57 subsets differed between the groups, but the median and mean percentages of CD57+ NK cells were almost identical for both LSHTM and Ugandan donors (38-39%). This is likely to be due to an infection-driven (e.g. HCMV) expansion of CD57+ NK cells in the Ugandan population, as seen in other African populations [11], which is countered by the lower age of the Ugandan donors and the higher frequency of CD57- NK cells in younger individuals [4]. Interestingly, the CD57int subset is smaller in Ugandan donors, which may indicate that HCMV infection leads to rapid acquisition of CD57 on the NK cell surface while CD57+ expansion due to ageing moves cells through the intermediate subsets more slowly. CD57- and CD57+ subsets were compared as a ratio because these populations tend to comprise the majority of NK cells (CD56 bright cells are typically under 10% of NK cells and CD57int cells are between 5-15% of NK cells).

Despite the similarities in proportions of NK cell subsets, Ugandan donors had overall

lower IFN-γ expresison than LSHTM donors. This decreased response was not caused by age variation within the Ugandan donors, as CD57- NK cells from all age groups in the Ugandan donors had similar capacities for IFN-γ and CD25 production. Likewise, when comparing total IFN-γ and CD25 responses to the proportion of CD57- NK cells in both LSHTM and Ugandan groups, LSHTM donors had higher NK cell responses than Ugandan donors with comparable percentages of CD57- NK cells. CD57- subsets from both groups had comparable median IFN-γ responses to both iRBCs and iRBCs+IL-15, but the range of IFN-γ responses to iRBCs+IL-15 in LSHTM donors was nearly double that of Ugandan donors. Likewise, although CD57+ cells are less responsive to cytokine stimulation because they express lower levels of IL-18R and IL-12R [6], they were still stimulated to produce IFN-γ and upregulate CD25 expression by HCC in LSHTM donors. By contrast, CD57+ cells from Ugandan donors had extremely low IFN-γ, CD25 and CD107a responses to almost all stimuli, except for CD107a responses to HCC.

It is possible that this is a mechanism to prevent immunopathology after recurring exposure to malaria parasites, but it also implies that the functional capacity of each phenotypically defined subset differs from those seen in European adults, and that increased CD57 subset percentages alone are not the cause of this low IFN-γ production. Whether certain subsets are significantly affected due to viral infection (other than CD57 expansion with HCMV) or prior exposure to malaria is unclear. Phenotypic analyses of both KIR molecules and NCRs were carried out and are described in Chapter 5 and compared to functional responses, which provides some information on this question, but the possibility of further inhibitory molecules (comparable with CTLA-4 or PD-1 expression on T cells, reviewed in [289]) that induce a blanket downregulation of NK cell proinflammatory responses could be explored further. Other immune regulatory mechanisms, such as IL-10 produced by regulatory T cells, may also downregulate NK cell responses to prevent pathology, and therefore measuring cytokines released by PBMCs during culture might indicate whether NK cell responses themselves are reduced or whether other anti-inflammatory immune mechanisms are responsible for IFN-γ downregulation.

4.4.4 Conclusions

In conclusion, the NK cell responses from LSHTM and Ugandan donors varied significantly, both to malaria infected red blood cells and to a variety of cytokines. It seems likely that previous infections, either viral or malarial, in the Ugandan population have influenced NK cells to produce less IFN-γ to both iRBCs and IL-12 and IL-18, but to express higher levels of 'adaptive' cytokine receptors (CD25 for responding to IL-2) and respond strongly to low levels of IL-15. These mechanisms for quickly upregulating both IFN-γ and CD107a responses may enable NK cells to respond swiftly to frequent infections, and may indicate a 'memory-like' response of constant pre-activation [16, 211], rather than an antigen-specific 'memory' mechanism of activation. Malaria naive donors did not show these levels of preactivation, and so NK cell responses were more consistent with the previous *in vitro* work carried out with other antigen stimulation [17]. However, the role of IL-15 in priming NK cells showed a clear iRBC-specific response in malaria naive donors, which is consistent with an infection model where DCs transpresent IL-15 to drive NK cell responses to pathogen [35]. Although I did not observe strong IFN-γ responses to iRBCs in the malaria exposed Ugandans, stimulation in an assay better modelling T cell help (such as adding exogenous IL-2 or incubation over a longer time period) or with antigen-specific IgG to induce ADCC responses might better indicate a role for NK cell responses during secondary malaria infection. Therefore, while NK cell responses to repeated malaria infection are still unclear, the changes in NK cell profile driven by malaria and other infections clearly affect the type and magnitude of NK cell responses in different populations of indiviuals.

5 | KIR and NKG2C genotyping and phenotyping and NK-iRBC conjugate formation

5.1 Introduction

The role of NK cells as cytotoxic effector cells capable of directly interacting with target cells is mediated by a wide variety of NK cell receptors. These include inhibitory molecules such as the killer lectin-like receptor (KLR) NKG2A and inhibitory KIRs, and activating receptors including NKG2C, activating KIRs, and natural cytotoxicity receptors (NCRs) including NKp46 and NKp30. During these interactions, NK cells form an immune synapse with a target cell, where surface molecules on both cells migrate to the site of contact (reviewed in [290]) and determine a net activating or inhibitory signal after interacting with ligands on the target cell, as described in Introduction, Section 1.1.3 (reviewed in [62]). Cytotoxic killing involves localised secretion of lytic granules containing perforin and granzyme across the cytotoxic immune synapse. During formation of an immune synapse, two concentric rings form the supramolecular activation cluster (SMAC) with a peripheral ring (pSMAC) of adhesion molecules such as ICAM-1 and LFA-1 that stabilise cell-cell interactions, and a central ring (cSMAC) of inhibitory and activating NK cell receptors (e.g. KIRs, NCRs) which determine the outcome of the immune synapse [291]. Immune synapses have been primarily studied in CD8 T cells, but are also well documented in NK cells, where each synapse can last for several minutes, during which NK cells test the ratio

of activating to inhibitory signals [290].

5.1.1 Killer Immunoglobulin-like Receptors

5.1.1.1 KIR expression patterns and determinants

The structure and known interactions of KIRs and HLA have been covered in Introduction, Section 1.1.4.3. All KIRs except KIR2DL4 and the pseudogenes are clonally expressed on subsets of peripheral blood NK cells. The proportion of NK cells with surface expression of each KIR varies based on a number of factors, including KIR allele (some alleles are not expressed on the NK cell surface at all, e.g. *KIR2DL5B* [292] or *KIR3DL1*004* [104]), KIR copy number (e.g. higher copy numbers of *KIR2DL2* and *KIR2DL3* are associated with higher proprtions of 2DL2+ or 2DL3+ NK cells [293]), and expression of other KIRs (e.g. expression of KIR2DL2 reduces the frequency of KIR2DL1 expression [84]). However, KIR expression on an individual NK cell is thought to be stochastic and dependent on the probability of expression of each KIR [115], although there are contradictory data on whether expression of the relevant HLA ligand for inhibitory KIRs (e.g. HLA-C2 for KIR2DL1, HLA-C1 for KIR2DL2 or 2DL3) influences KIR expression [84, 115]. Most NK cells express at least one inhibitory KIR [115] and 66% express more than one [294], although populations of self tolerant peripheral NK cells without inhibitory KIRs have been described [295]. Expression of inhibitory KIRs may be acquired sequentially, which may determine how many inhibitory KIRs are expressed on an individual NK cell and predispose NK cells to express KIRs that will recognise self-HLA ligands [84].

KIR expression is highly variable and appears to be heavily determined by promoter variation. Promoter methylation status is thought to be a major determinant of activity [296, 297], and there is evidence that expression of KIRs that are not expressed on peripheral mature NK cells including *KIR2DL5B* [87] and *KIR3DL3* [298] can be induced by *in vitro* demethylation of the promoter region, indicating that the gene itself is not defunct. Promoter regions may also contain bidirectional promoters that create antisense transcripts

to inhibit promoter activity and reduce KIR expression, and the overall strength of each promoter (sense transcription increasing expression vs. antisense transcription inhibiting expression) may determine the level of expression for each KIR [105]. An additional mechanism seen in *KIR3DL1* and *KIR3DS1+* donors showed what the authors called a 'genotype-driven expansion' of KIR3DS1+ cells based on the number of copies of *KIR3DL1*, so that having two copies of 3DL1 enhanced 3DS1 expression [89]. The possible interactions of KIRs with each other (also potentially seen by KIR2DL2-mediated downregulation of 2DL1 expression [84]) may be a major additional determinant of KIR expression.

5.1.1.2 KIR haplotype is associated with disease and protection

There are two distinct KIR haplotypes which are designated 'A' and 'B', comprising a combination of KIRs commonly inherited together. The A haplotype consists of a defined set of KIR genes: 2DL1, 2DL3, 2DL4, 2DS4, 2DP1, 3DL1, 3DL2 and 3DL3, which can contain all of these genes or fewer. The B haplotype by definition includes any of the other KIRs, and can also include any of those in the A haplotype [98]. The classic A haplotype genes are inhibitory (except for 2DS4), and it has been suggested that AA homozygotes tend to respond less strongly to pathogen-associated signals from malaria [202]; however, other studies looking at control of viral infections such as HCV found that the homozygous A haplotype was beneficial and could confer resistance to disease (reviewed in [83]). These differences may hinge on the type of NK cell response required to confer protection, where NK cells licensed by inhibitory KIRs are capable of anti-viral cytolytic activity but may have reduced cytokine production in response to malaria [183, 202], and activating KIRs 'turn down' these cytotoxic responses without affecting the capacity for cytokine production ([118], reviewed in [117]). Alternatively, there is evidence that 'unlicensed' NK cells that are unable to mediate missing-self cytotoxicity, comprising a non-trivial subset of the total NK population [84, 295], may still be activated by inflammatory cytokines and participate in anti-pathogen responses [2] including IFN-γ production [299].

The protective effects of individual KIR receptors are difficult to acertain because the

strength of protection may depend on carriage of a KIR and its HLA ligand, both of which may be epitope specific. For example, having all three of *KIR3DS1*, *KIR3DL1* and a particular HLA-B epitope, *HLA-Bw4*^{80I} has been shown to be protective against HIV infection [81]. However, having *KIR3DS1* without *KIR3DL1* or *HLA-Bw4*^{80I} was not protective, and may be associated with greater susceptibility to HIV [89].

With regard to malaria infection, heterozygous carriage of the AB KIR haplotypes appears to be associated with increased IFN-γ production *in vitro* compared to IFN-γ responses of NK cells from either AA or BB homozygous individuals [202]. Similarly, AB heterozygosity has been suggested to be protective during clinical malaria infection, as Olaniyan et al found that individuals carrying c-AB2/t-AA (i.e. individuals with heterozygous A and B centromeric KIR genes in combination with telomeric A family genes), were more likely to have asymptomatic malaria infections rather than uncomplicated or severe symptomatic malaria cases and that KIR2DL5, 2DS3 and 2DS5 might be protective against symptomatic malaria [300]. As carriage of both A and B haplotypes is likely to increase the total number of different KIR receptors that can be an expressed by an individual, heterozygosity may increase the proportion of NK cells that express a KIR capable of binding self-HLA and are therefore licensed (reviewed in [2, 111]) and therefore may be more responsive to activation by pathogens. Conversely, in a Gambian population, Yindom et al suggested that an AA KIR haplotype may be protective during malaria infection and that carriage of activating KIRs is associated with higher mortality [301]; this may suggest that NK cell responses contribute to the inflammatory responses that are associated with severe disease, either because they express a particular activating KIR that recognises a currently unknown ligand on infected erythrocytes or because the balance of activating to inhibitory KIR expressed by B haplotype-bearing NK cells lowers the threshold for activation (reviewed in [117]).

To date, the largest genetic association study of KIR and malaria susceptibility, conducted in Thailand, reported that KIR2DL3 in association with its ligand HLA-C1 is associated with risk of cerebral malaria compared to uncomplicated malaria, and that this combination of KIR2DL3-HLA-C1 is significantly less common in malaria-endemic areas than might be

expected; the authors proposed that this was evidence of natural selection against carriage of HLA-C1 [302]. One hypothesis that might unify all of these findings is that protection is mediated by KIR2DL2 (a B haplotype KIR), which binds HLA-C1 with higher affinity than KIR2DL3 (an A haplotype KIR) [109]; thus carriage of a single copy of the centromeric B haplotype may confer protection against severe malaria by preventing interactions between KIR2DL3 and HLA-C1 through preferential expression of KIR2DL2. However, larger studies of KIRs that take into account the genetic background of the population and the allelic diversity of both KIR and HLA Class I molecules are needed to determine whether KIR receptors do in fact influence malaria disease progression. Additionally, tools for detection of KIR and HLA expression at the cellular rather than genetic level are limited and so the majority of studies focusing on KIRs and disease have used KIR gene carriage to determine associations between susceptibility or protection rather than detectable KIR expression, leading to interesting but difficult to prove hypotheses.

5.1.1.3 KIR variation in different populations

KIR genes in African populations have been found to be considerably more diverse than those found in European populations, which is borne out by the large number of unique KIR haplotypes detected only in African individuals [303–305]. A major study on KIR gene frequency carried out by Nakimuli et al in Uganda showed that both KIR3DS1 and KIR2DS1 were significantly less frequent than in European populations, and that Ugandans have higher frequencies of the centromeric B region but lower frequencies of the telomeric B region than Europeans [304]. Allelic variation is also higher in African populations [102, 303], which is an important consideration during KIR genotyping as some uncommon alleles may not be detected by standard KIR primer sequences, particularly if the primers are optimised to detect KIR alleles more common in Europeans. Linkage disequilibrium between KIR genes also appears to be weaker in African populations, so that genes that are in strong linkage disequilibrium in European individuals are less strongly associated in African individuals [304, 305]. The location on the centromeric or telomeric regions of certain KIR genes also differs between populations, such as KIR2DS5 and KIR2DS3;

although these two genes appear to be confined to the telomeric and centromeric regions exclusively in Caucasian populations [306], this does not hold true in African populations and there appears to be an important role for centromeric KIR2DS5 in protection against pre-eclampsia in pregnant women [95]. It is therefore important to take this diversity into account when attempting to draw conclusions about KIR genes in African populations, which are less well characterised than their European counterparts, as assumptions about gene linkage and allelic frequencies may not apply to these individuals.

5.1.2 NKG2A and NKG2C receptors on natural killer cells

NKG2A and NKG2C are KLRs that form signalling complexes with CD94 and bind the non-classical MHC molecule HLA-E [68]. The NKG2A/CD94 dimer is inhibitory and prevents NK cell lysis, and has been shown to be expressed inversely proportionally to KIRs before licensing [294], providing an important role in ensuring self-tolerance prior to KIR expression [307]. However, NKG2C/CD94 binding HLA-E induces NK cell activation, and is primarily of interest because of the expansion of NKG2C+ NK cells during HCMV infection [74]. There is some evidence that HCMV viral proteins suppress NK cell activation via the NCR NKp30 [308] and downregulate classical MHC class I molecules while maintaining expression of HLA-E, which may be an immune evasion response targeted at binding inhibitory NKG2A [309]. By increasing NKG2C expression, NK cells are able to target these HLA-E expressing infected cells and control HCMV infection.

5.1.2.1 NKG2C expansion and NK cell maturation

NKG2C is found on NK cells and some CD8+ T cell subsets. In NK cells, NKG2C is associated with increased NK cell maturity as defined by CD57 expression [11] (where NK cells gain CD57 expression with increasing maturity, shifting from cytokine production to cytotoxic functions [5]). Young children have high proportions of CD56bright CD57- NKG2A+ NK cells whereas older adults have much higher proportions of CD56dim CD57+ NKG2C+ cells, and a progression from one to the other can be observed in the age groups

in between. However, whether this maturation is driven purely by age, by exposure to infection throughout life or by both is unclear [11]. HCMV is thought to be a major driver of NK cell maturation, partially because it is associated with large expansions in CD57+ NKG2C+ populations [17] and other changes in NK cell phenotype [15]. HCMV prevalence varies by population, where 80% of the UK population is seropositive by age 65 [285], but 94% of children in the Gambia are seropositive by age 3 [11]. The accelerated maturation of the expanded NKG2C+ subset is thought to be useful for controlling HCMV infection but may be beneficial or detrimental for other immune responses. In environments with multiple immune stimuli, such as rural Africa, it may be beneficial to have more mature and cytotoxic NK cells at a young age; however, cytokine production is lower in this subset, including during responses to vaccination which may reduce protection [6, 17] (A. Darboe, unpublished).

HCMV is of particular interest in the study of NK cells because the murine NK cell receptor for MCMV is Ly49H; the Ly49 family is analogous to the human KIR family but with completely distinct structures and evolutionary lineage. Ly49H specifically binds the MCMV m157 protein on infected cells ([310], reviewed in [311]). It is therefore of significant interest to determine if a similar antigen specificity is observed in human NK cells to HCMV or otherwise, raising the possibility of NK cell adaptive immunity. However, as described in Chapter 4, this has not yet been established, although NKG2C has been suggested as the Ly49H equivalent for recognition of HCMV [311].

5.1.2.2 NKG2C deletions and effect on disease

Non-expression of *NKG2C* due to deletion of the locus has been observed in many populations [11, 17, 312], but frequencies of this deletion appear to be higher in certain populations. *NKG2C* deletion in individuals from the Gambia was found to be as high as 36.2%, whereas in Tanzanian individuals the deletion frequency was 20.9%, comparable with other global populations [313]. Heterozygous (+/−) individuals have slightly lower expression of NKG2C but appear to control HCMV infection as well as +/+ homozygotes [314]. Gam-

bian children under 10 years old with a homozygous NKG2C deletion had significantly lower frequencies of CD57+ NK cells and higher anti-HCMV antibody titres than *NKG2C* +/+ or +/− children, which may suggest that children without NKG2C expression are less able to control HCMV viral load [11]. This effect disappeared in older age groups, suggesting that alternative mechanisms for controlling HCMV infection develop with age. One such mechanism may involve expansions of KIR+ NK cells; it has been suggested that KIR2DL1- or KIR2DL3-licensed NK cells may control HCMV infection [14], or that activating KIRs may mediate effector functions in the absence of NKG2C [315]. There is also evidence that KIR2DL1 is coexpressed on NKG2C expanded cells in donors with an AA KIR haplotype (Uhrberg et al, unpublished). Taken together, these data suggest that NKG2C and KIR expression control NK cell activation and response to infection in combination. This may be relevant to NK cell responses during malaria infection as these expanded subsets of NKG2C+ CD57+ NK cells are thought to express lower levels of cytokine receptors [6], and so may be less responsive to IL-12 and IL-18 activation by macrophages during malaria infection [26].

5.1.3 NK-iRBC conjugate formation

The possibility of NK cell conjugation with iRBCs is of obvious interest due to the possibility of direct killing of iRBCs by NK cells as a result of these conjugates. As described in Chapter 4, Introduction, there is some evidence of NK cell-derived granzyme upregulation during blood stage malaria infections both *in vivo* [273] and *in vitro* [200], which implies NK cell cytotoxic activity against iRBCs. Similarly, there is *in vitro* evidence of iRBC killing by NK cells [275, 276], although it is unclear how relevant these experimental models are *in vivo*. However there is also some evidence that iRBC-NK cell contact is an important requirement for NK cell activation and cytokine production, and that dead or lysed iRBCs do not fully activate NK cells [18, 201].

NK-iRBC conjugate formation has been seen and described by several groups, most notably in papers by Baratin et al (2005) [42] and Korbel et al (2005) [200] (Figure 5.1). Baratin

and colleagues found that NK92 cells (an NK cell line) selectively interacted with infected RBCs but not uninfected RBCs (Fig. 5.1A), which they termed 'rosettes' (distinct from the malaria pathology of rosetting, where an iRBC is surrounded by uRBCs). Korbel et al observed conjugate formation between iRBCs and freshly isolated human NK cells from multiple individuals, a subset of whom showed evidence of NK cell actin rearrangement at the contact site with iRBCs (Fig. 5.1B). Actin rearrangement is likely to indicate NK cell polarisation to form the SMAC [291], and therefore strongly supports the possibility of immune synapse formation, although does not indicate what the functional outcome of the synapse might be (cytotoxicity or survival). Artavanis-Tsakonas and colleagues also detected NK-iRBC conjugates in a stable percentage of NK cells for up to 90 minutes [183] by measuring CD56+ Glycophorin A+ events by flow cytometry (glycophorin A is a red blood cell membrane protein found on all RBCs), which implies either stable NK-iRBC conjugate formation, or transfer of RBC membrane proteins to the NK cell surface.

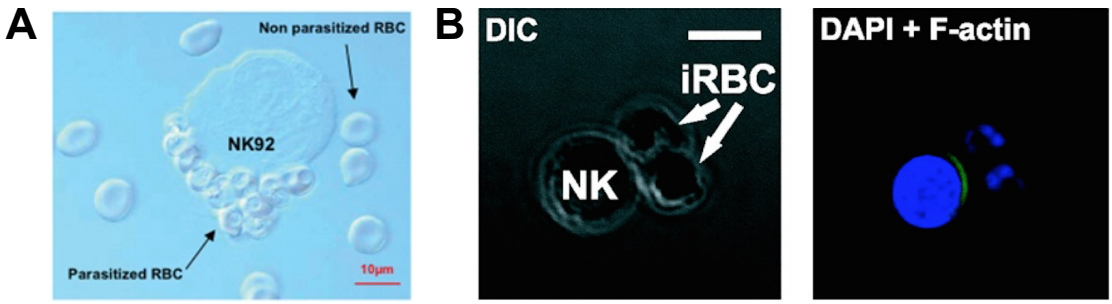

Figure 5.1: **Contact between a NK92 cell and iRBCs.** Baratin and colleagues found that infected, but not uninfected, RBCs formed stable contacts with the human cell line NK92, which they termed 'rosettes' (A). Figure from Baratin et al, 2005, *PNAS* [42]. Korbel et al saw actin relocalisation in NK cells to the point of contact with iRBCs (B). NK cells are stained blue with DAPI, F-actin shown in green. Figure from Korbel et al, 2005, *J Immunol.* Copyright 2005. The American Association of Immunologists, Inc. [200].

Despite the evidence for NK-iRBC interactions, the functional outcome of these conjugates are unclear. Chen et al (2014) [142] have described a humanised mouse model in which interactions with NK cells led to the death of iRBCs. However, iRBC death has not been observed after incubation with primary human NK cells, and the iRBC molecules with

which the NK cell might interact are unknown. Although healthy RBCs do not express inhibitory MHC/HLA, they also do not appear to express activating NK cell ligands and therefore are generally thought to go unnoticed by NK cells. Ligands on iRBCs mediating interactions with NK cells may therefore be RBC-surface expressed parasite proteins (reviewed in [152, 316]), which also form targets for blood stage antibody development (potentially leading to ADCC), or host-derived stress signals from the RBC itself [275]. There have been some proposed candidates for these ligands, including the parasite protein PfEMP1 [274], a major virulence factor responsible for parasite sequestration and immune evasion [152, 268], but Baratin et al [43] found that PfEMP1 was not a key factor in conjugate formation, although it did interact with ICAM-1 on NK cells and CD36 on both monocytes and NK cells. Likewise, heat shock protein (Hsp)70 has been suggested as an erythrocyte stress signal [275], but this has not been verified by other studies. The receptors on both NK cells and iRBCs mediating conjugate formation are therefore still a mystery.

5.1.4 Aims

The aim of this chapter is to detect and measure possible interactions of iRBCs and NK cells in NK-iRBC conjugates, to determine whether these interactions occur in both the LSHTM and Ugandan donors, and to characterise the phenotypic profiles of donor NK cells to establish possible causes of the inter-donor variation in NK cell responses described in Chapter 4. I therefore first measured and compared NK-iRBC conjugate formation in both populations, and then used flow cytometry and PCR to determine KIR and NKG2C phenotype and genotype on NK cells. This also allowed a comparison of both KIR gene carriage and KIR surface NK cell expression in two different populations of variable genetic and environmental background.

5.2 Methods

5.2.1 3D7HT-GFP parasite validation

The 3D7HT-GFP *P. falciparum* transgenic parasite line constitutively expresses cytosolic green fluorescent protein (GFP) that can be detected by flow cytometry and is stable in culture over time [203]. To better detect NK-iRBC conjugate formation by directly detecting the malaria parasite rather than the red blood cell, 3D7HT-GFP parasites fluorescing in the FITC channel were hypothesised to be preferable to α-glycophorin A staining of iRBCs [183]. This parasite strain was compared to the normal 3D7A strain to determine whether NK cell responses were the same against both parasite strains, focusing on functional markers including IFN-γ, CD25 and CD107a in an 18 hour assay (as described in Chapter 4); PBMCs were also incubated with both parasite strains for 2 hours and stained for NK surface markers and glycophorin A to determine successful conjugate formation.

For confocal microscopy, 1×10^6 PBMCs were coincubated with 3×10^6 iRBCs in 40µl culture medium (RPMI, 10% FCS, L-glutamine) for 15-30 mins at 37°C in a U-bottom plate (Nunc), then fixed in 100µl 1.5% formaldehyde and 0.1% glutaraldehyde dissolved in PBS for 30 mins at room temperature. Fixation was stopped with 100µl washing buffer (1x PBS, 0.1% Tween 20) and samples were centrifuged for 5 mins at 500g and washed again before blocking for 30 mins in 100µl blocking solution (PBS, 10% FCS) and washed again. Actin staining was carried out using phalloidin-AlexaFluor 594 (Life Technologies), diluted 1:40 in PBS and incubated for 20 mins at room temperature. Samples were washed again, then stained with 300nM DAPI (Life Technologies) for 5 mins. Samples were then thoroughly washed at least twice with washing buffer and finally with PBS, resuspended in 10µl and pipetted onto a glass coverslip with a drop of Vectashield (Vector Laboratories) mounting medium. Coverslips were then mounted on slides and sealed with nail polish. Images were taken using a Zeiss LSM510 at 40× and 100× magnification.

NK-iRBC interactions were imaged with an ImageStream Mark II Imaging Flow Cytometer (Amnis) to look for conjugates in greater numbers of cells. ImageStream uses similar

principles as flow cytometry, where cells are stained with fluorescent antibodies and run in a single-cell stream past a series of lasers. In addition to this, two cameras take images of the cells within the stream so that fluorescent staining can be seen on individual cells and can be overlaid with phase-contrast images during analysis, thus combining flow cytometry and basic confocal microscopy. ImageStream images were taken by Samuel Sherratt.

5.2.2 KIR genotyping

DNA was extracted from whole blood aliquots as described in Methods, Section 2.8.1. Samples were typed for KIR genes according to published protocols [205, 206], as described in Methods, Section 2.8.2.1, and summarised below. Presence or absence of 17 KIR genes (2DL1, 2DL2, 2DL3, 3DL1, 3DL2, 2DS1, 2DS2, 2DS3, 2DS4, 2DS5, 3DS1, 2DP1, 3DL3, 3DX1, 2DL4, 2DL5, 3DP1) was detected by sequence-specific primer PCR using the primer sequences in Table B.1, Appendix B. Each gene was detected in a separate PCR reaction, except for KIR3DL3 and 3DX1, which were combined in reaction 13.

Each PCR reaction contained 5µl HotStarTaq Mastermix (Qiagen) (containing Taq polymerase, buffer and dNTPs), 0.3µl 25mM $MgCl_2$, 1.7µl nuclease-free dH_2O, 2µl of 10µM primer mix and 1µl template DNA at 100ng/µl in a final reaction volume of 10µl. Primer mixes contained between 2 and 4 sequence-specific primers for the KIR of interest and an internal positive control (HLA-DRA) for each reaction. Primer mixes for each reaction can be found in Appendix B [206]. PCR reactions were run in a thermal cycler with the following program: 15 mins at 94°C; 10 cycles of 94°C for 30 secs and 65°C for 40 secs; 22 cycles of 94°C for 30 secs, 61°C for 30 secs and 72°C for 40 secs; 4°C for 30 secs, and hold at 15°C. Products were electrophoresed with loading buffer on a 3% agarose gel in 1× Tris/Borate/EDTA (TBE) buffer with 2µl ethidium bromide (EtBr) for 45 mins at 150V. Reactions 9 and 16 (2DS4 and 3DP1) were run for an additional 30 mins at 150V for better separation of bands. EasyLadder I was run alongside each set of reactions, with bands at 100, 250, 500, 1000 and 2000 base pairs. Gels were visualised and photographed with a gel doc.

Presence of the amplified gene is shown as a band on the gel, falling below the control sequence at 283bp. For reaction 9, further electrophoresis allows separation of the PCR product into a full (133bp) or deleted (111bp) form of *KIR2DS4*. Prior to genotyping the unknown samples from both LSHTM and Uganda, this protocol was tested on four DNA samples from the 33rd UCLA International KIR Exchange [317] (KDNA# 129, 130, 131 and 132). The KIR Exchange program ships four DNA samples to all participating labs for genotyping, and all results are compiled and published. My results were therefore checked against the published genotypes for each samples and agreed with the consensus results [318].

5.2.3 KIR phenotyping by FACS

KIR expression on the NK cell surface was determined by FACS. Anti-KIR antibodies are commercially available but tend to be cross-reactive for multiple KIRs, and therefore are usually used in combinations. Process of elimination by combining flow cytometry data with genotyping data is also useful. Some KIRs have more than one antibody clone available, but the panels used here were optimised by Martin Goodier.

NK cell phenotype data were collected from donors in two sets of experiments, using slightly different panels and staining protocols. The first experiments comprise the donors from LSHTM and used the 3D7A *P. falciparum* line. The second experiments encompasse all the Ugandan donors, as well as four LSHTM donors from experiment I with known phenotypes, who were used as controls to ensure consistency of results, and used the 3D7HT-GFP *P. falciparum* line unless otherwise stated. Changes in the protocol were made because the intial fixation to preserve the NK-iRBC conjugate formation affected antibody binding and staining profiles, and antibody panels were modified to incorporate the GFP parasites (FITC channel) and replace antibodies with poor staining.

For the first experiments with LSHTM donors, 4×10^5 PBMCs were incubated with medium, uRBCs or MACS-purified iRBCs at a 1:5 ratio for 2 hours at 37°C (MACS purification as described in Methods, Section 2.3). Cells were washed with FACS buffer,

centrifuged at 500g for 5 mins, and fixed in 100µl 4% paraformaldehyde for 15 mins at room temperature. Cells were then washed twice with FACS buffer and stained with 10µl surface antibodies for 20 mins at 4°C, washed again and resuspended in 250µl FACS buffer.

For the second experiments with Ugandan donors, 4×10^5 PBMCs were incubated with medium, uRBCs or MACS-purified iRBCs at a 1:5 ratio for 2 hrs at 37°C. Cells were washed with FACS buffer, centrifuged at 500g for 5 mins, and stained with 10µl surface antibodies for 20 mins at 4°C, washed again, then fixed with 70µl BD Cytofix/Cytoperm for 30 mins at room temperature in the dark. Cells were washed twice with BD Permwash, then resuspended in 250µl FACS buffer. To determine NK-iRBC conjugate formation, separate wells with PBMCs and uRBCs or iRBCs at the same concentrations were incubated during the same time period, washed with FACS buffer, centrifuged at 500g for 5 mins, and fixed in 100µl 4% paraformaldehyde for 15 mins at room temperature before washing with FACS buffer, staining with surface antibodies, and washing and resuspension in FACS buffer.

BD CompBeads were stained with single antibodies as compensation controls. GFP compensation controls were made by mixing 1ml of 3D7HT-GFP parasites and 1ml non-fluorescent 3D7A parasites together and fixing with 4% paraformaldehyde for 30 mins before washing and resuspending in 400µl FACS buffer. All samples were run on a BD LSR II Flow Cytometer, and analysed using FlowJo.

α-KIR antibodies used are shown in Tables 5.1 (LSHTM donors) and 5.2 (Ugandan donors). Table 5.3 shows the KIRs for which I have phenotyping data, the known cross-reactivity of the antibodies (mainly between homologues), alternative names (by cluster of differentiation), the antibody clone, and the manufacturer. A complete list of antibodies, manufacturers, and catalogue numbers can be found in Appendix B.

Panel 1		Panel 2		Panel 3		Panel 4	
Marker	Fluor	Marker	Fluor	Marker	Fluor	Marker	Fluor
CD16	APC-H7	CD56	APC-V770	CD56	APC-V770	CD56	APC-V770
CD3	V500	CD3	V500	CD3	V500	CD3	V500
CD235a	PerCP-e710	CD235a	PerCP-e710	CD235a	PerCP-e710	CD235a	PerCP-e710
NKG2A	FITC	CD94	FITC	-	FITC	2DL4	FITC
NKG2C	APC	NKG2A	APC	NKG2D	APC	3DL1/S1	APC
2B4	PE	2DS4	PE	2DL5	PE	-	PE
CD57	e450	CD57	e450	CD57	e450	3DL1	vioblue
CD56	PE-Cy7	2DL1/S1	PC7	2DL2/3/S2	PC7	-	PE-Cy7

Table 5.1: FACS antibody panels for LSHTM donor phenotyping.

Panel 1		Panel 2		Panel 3	
Marker	Fluor	Marker	Fluor	Marker	Fluor
CD56	APC-V770	CD16	APC-H7	CD56	APC-V770
CD3	V500	CD3	V500	CD3	V500
-	PE-Cy5	-	PE-Cy5	2DL3	PerCP-Vio700
parasites	FITC	parasites	FITC	parasites	FITC
2DL5	APC	3DL1/S1	APC	NKG2A	APC
2DS4	PE	-	PE	NKG2C	PE
CD57	e450	3DL1	vioblue	CD57	e450
2DL1/S1	PC7	CD56	PE-Cy7	2DL2/3/S2	PC7

Table 5.2: FACS antibody panels for Ugandan donor phenotyping.

KIR	Cross-reactivity	Alt. name	Referred to as	Clone	Manufacturer
2DS1	2DL1	CD158a,h	2DL1_S1	EB6B	Beckman Coulter
2DL2	2DS2, 2DL3	CD158b1,b2	2DL2_L3_S2	GL183	Beckman Coulter
2DL3		CD158b2	2DL3	REA147	Miltenyi Biotec
2DS4		CD158i	2DS4	FES172	Beckman Coulter
2DL5		CD158f	2DL5	UP-R1	Miltenyi Biotec
3DL1		CD158e	3DL1	DX9	Miltenyi Biotec
3DS1	3DL1	CD158e1,e2	3DL1_S1	Z27.3.7	Beckman Coulter

Table 5.3: Table of KIR antibodies, cross-reactivity, and clone.

5.2.4 NKG2C genotyping and phenotyping

NKG2C deletion was detected by PCR using a Phusion® High Fidelity PCR kit (New England Biolabs) according to a published method [11]. All donors were genotyped for NKG2C homozygous presence (++), deletion (−−), or a heterozygous deletion (+−). Reactions were run in 96 well plates with each well containing the following (Table 5.4):

Reaction mix	volume/µl
Phusion (HF) buffer 5x	4
dNTP mix	0.4
pF201 10uM	0.5
pR201 10uM	0.5
pF411 10uM	1
pR411 10uM	1
dH_2O	11.5
Taq polymerase	0.1
DNA template	1
Total volume:	20

Table 5.4: Master mix of primers and reagents for NKG2C genotyping.

DNA was used at between 10-100ng/µl as measured by NanoDrop. Primer sequences are listed in Table B.3, Appendix B. Reaction volumes were mixed by pipetting, sealed with a clear plastic film, briefly centrifuged and run in a thermal cycler on the 'touchdown_AG' program: 95°C for 3 mins; 10 cycles of denaturation at 94°C for 30 secs, annealing from 65-55°C for 30 secs (starting at 65°C for the first cycle and decreasing by 1°C per cycle), and extension at 72°C for 30 secs; 26 cycles of 94°C for 30 secs, 55°C for 30 secs; hold at 4°C. PCR products were run with loading buffer on a 1.5% agarose gel with 2µl EtBr for 10 mins at 80V, then 1 hr 20 min at 50V. EasyLadder I was run alongside each gel, with bands at 100, 250, 500, 1000 and 2000bp. Gels were visualised in a gel doc. The product sizes for the deletion and wild-type NKG2C genes are 411bp and 201bp respectively.

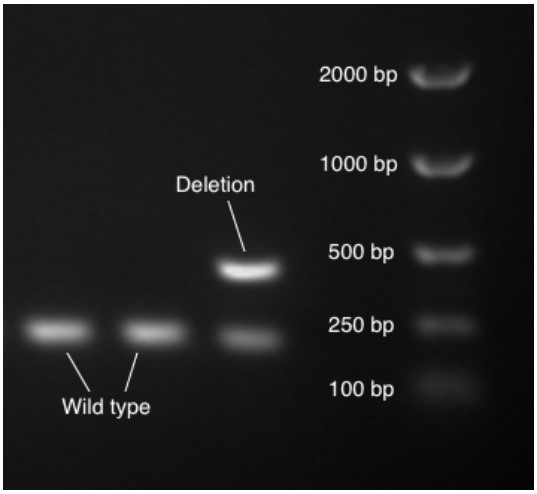

Figure 5.2: **NKG2C genotyping PCR products.** Agarose gel showing NKG2C genotyping bands from three donors. Donors 1 and 2 are wild type NKG2C carriers (band at 201bp), donor 3 has a heterozygous deletion as shown by the two bands (411 and 201bp). DNA ladder bands are 2000, 1000, 500, 250 and 100bp.

5.3 Results

5.3.1 NK-iRBC conjugate formation

Based on the protocol from Artavanis-Tsakonas et al [183], NK-iRBC conjugate formation was detected and measured by FACS. Conjugates were defined as CD3- CD56+ glycophorin A+ (also known as CD235a) events using parasite strain 3D7A, or in later experiments as CD3- CD56+ GFP+ events when using a 3D7HT-GFP parasite strain. PBMCs were incubated with medium alone, uRBCs or MACS-purified schizonts for two hours. Cells were then stained for phenotypic markers, including the panels in Tables 5.1 and 5.2.

5.3.1.1 Time course of conjugate formation.

A short time course was conducted to test how quickly NK-iRBC conjugates were formed and how long they lasted in culture (Figure 5.3). Fresh PBMCs from three donors were incubated with medium, uRBCs, or MACS-purified iRBCs at 30 min intervals for up to 150 min before fixation and staing for FACS analysis. At 90 and 150 min, the medium and uRBC control incubations were also measured. Cells were stained for CD56+CD3- NK cells, glycophorin A (CD235a), CD25 and CD69. Conjugate formation (CD56+ CD235a+ events) was detected after 30 mins of incubation, and increased until 60 mins, after which it was maintained past 2.5 hours. Background 'conjugate' formation between uRBCs and NK cells was measured at 90 and 150 mins, where it increased with time (light blue bars). However, as the iRBCs are MACS-purified prior to incubation and have a purity of $\geq$90%, uninfected cells are not a large proportion of conjugates in the iRBC wells. As the percentage of NK cells in conjugates was stable over time, a 90-120 minute incubation was used for future experiments. Whether the individual conjugates were maintained throughout the incubation or if the rate of conjugation formation and dissociation reached equilibrium is not clear. CD25 and CD69 expression did not change over the timeframe of this experiment, consistent with data that CD25 is not upregulated within 6 hours of stimulation [38].

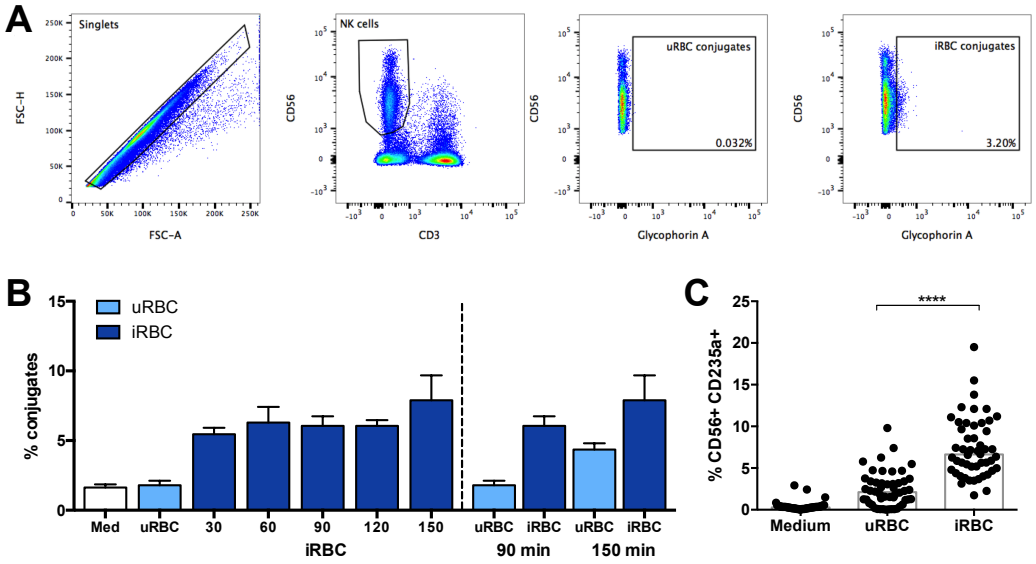

Figure 5.3: **NK-iRBC conjugate formation is rapid and sustained for at least two hours**. Fresh PBMCs were incubated with medium alone (white bar), uRBCs (light blue bars) or purified iRBCs (dark blue bars) and conjugate formation measured after fixation at half hour intervals. FACS gating shows singlets (FSC-H vs. FSC-A), NK cells (CD56+ CD3-), and CD56+ glycophorin A+ events after PBMC incubation with uRBCs and iRBCs (A). Conjugate formation over time is shown at time intervals up to 150 mins (B). Bars on the right of the dotted line compare conjugate formation between uRBCs and iRBCs after 90 and 150 mins. From a different experiment, (C) compares conjugate formation in uRBCs and iRBCs across the whole LSHTM population after 2 hrs (n= 53). Statistical analysis by Wilcoxon signed rank tests, **** p< 0.0001.

5.3.1.2 Validation of 3D7HT-GFP parasites for eliciting NK cell responses.

Although the percentage of uRBCs forming conjugates with NK cells was low, I decided it would be better to detect the parasite itself rather than the RBC to ensure only true NK-iRBC conjugates were measured. The 3D7HT-GFP *P. falciparum* strain, which expresses cytosolic GFP and is detectable by FACS and confocal microscopy, was tested for fluorescence stability and its ability to activate NK cells in the same way as the 3D7A strain (Figure 5.4). Parasites in culture (not MACS-isolated) from both 3D7A (Fig. 5.4A) and 3D7HT-GFP strains (Fig. 5.4B) were fixed for 30 mins in 4% paraformaldehyde and analysed by flow cytometry. Parasitaemia of the GFP strain was 10.1% by FACS and

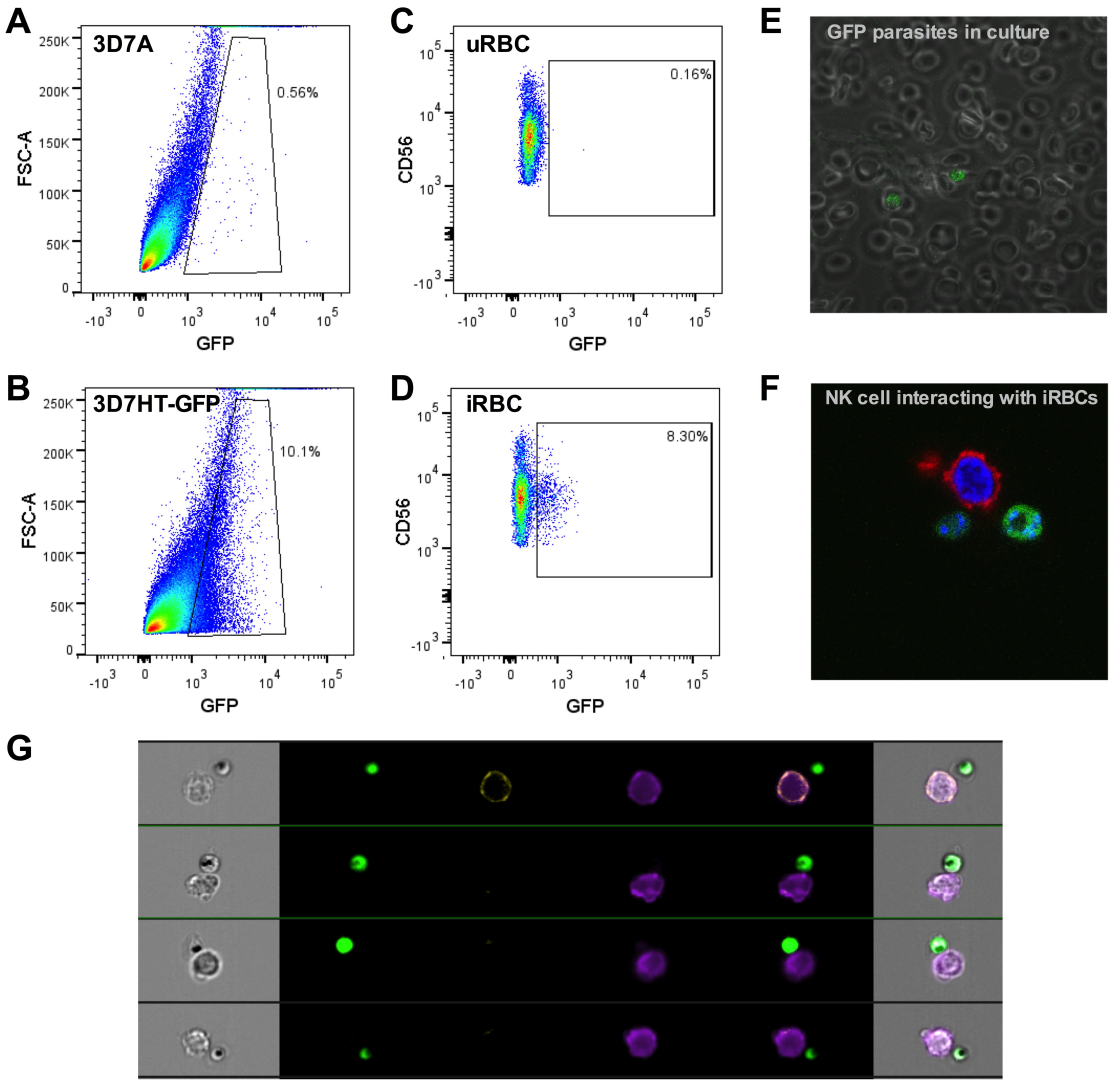

Figure 5.4: **3D7HT-GFP parasites and NK cell conjugates are detectable by FACS and fluorescence microscopy.** Fixed whole parasite cultures from 3D7A (A) and 3D7HT-GFP (B) were analysed by FACS. Gating was set on the 3D7A plot, and the 3D7HT-GFP parasitaemia compared to counts from thin blood films by light microscopy. Fresh PBMCs and uRBCs (C) or iRBCs (D) were incubated for 2 hrs before staining with NK cell markers and fixation and measured for conjugate formation. FACS plots are from one representative donor. Confocal microscopy was used to image fixed 3D7HT-GFP parasites in culture without staining (E) and a mix of PBMCs and iRBCs (F) after staining for DNA with DAPI (blue) and F-actin with AlexaFluor 594 (red). Conjugates were observed after 2 hrs incubation by ImageStream (G) for four different cells. From left to right, images show the same cells in phase-contrast, GFP, CD56 (yellow), CD57 (purple), fluorescence overlay (green, yellow, purple), and total overlay (phase contrast and fluorescence). ImageStream images were taken by S. Sherratt.

9.7% by light microscopy from a thin blood film, which indicates that all parasites in the culture express GFP and are detectable by flow cytometry within a mix of uRBCs, the fluorescence is stable after fixation in 4% formaldehyde, and background fluorescence is low. NK-RBC conjugate formation after 2 hours incubation of PBMCs and uRBCs (Fig. 5.4C) or MACS-purified iRBCs (Fig. 5.4D) is clearly measurable with low background from NK-uRBC conjugates. Confocal microscopy also showed clear parasite GFP expression even when in a mix of uRBCs (Fig. 5.4E), and after incubation with PBMCs and additionally stained for DNA and F-actin with DAPI (blue) and phalloidin-AF594 (red) respectively (Fig. 5.4F). Lastly, conjugates were observed by ImageStream (an imaging flow cytometer) (Fig. 5.4G) after PBMCs and iRBCs were co-incubated for 2 hrs and stained for NK cell markers (CD56 is shown in yellow, CD57 in purple, iRBCs in green). These data show that CD3- CD56+ GFP+ NK-iRBC conjugates can be accurately measured by FACS without a background signal or response from uRBCs, meaning that 3D7HT-GFP iRBCs can be used for future experiments concerned with conjugation. Functional responses are comparable with past data that used 3D7A iRBCs, as validated in Chapter 4.

5.3.1.3 Comparing conjugate formation between populations.

After validating the methods for detecting NK-iRBC conjugates, using either glycophorin A or GFP parasites, NK cells from all donors from both the LSHTM and Ugandan study groups were measured for conjugate formation after two hours of incubation. The percentage of NK cells forming conjugates differed between individuals from around 2-24%, but cells from all donors appeared to be capable of forming at least some conjugates. It was therefore of interest to determine whether there were population differences in the percentage of conjugates formed, which could be due to genetic profiles or to prior exposure to malaria. CD56+ GFP+ conjugates for each donor are shown for the LSHTM (n= 32) (Figure 5.5A) and Ugandan (n= 53) (Fig. 5.5B) populations. Gates for CD56+ GFP+ events were set on the uRBC control as shown in Figure 5.4C. Conjugate formation in the LSHTM group was originally measured using glycophorin A and was repeated with GFP iRBCs in 32 donors, who are shown here for comparison with the Ugandan group. The range of each group were similar (LSHTM, 1.1-24.7%, Uganda, 2.6-23.4%), but the median conjugate formation of each group appeared to be higher in Ugandan donors than in LSHTM donors (7.53 vs. 6.87%), although this did not reach statistical significance (p= 0.059), Mann-Whitney test).

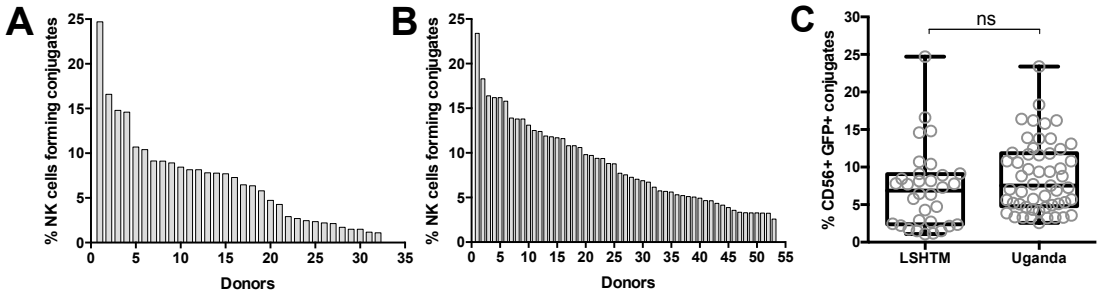

Figure 5.5: **Comparing NK-iRBC conjugate percentages between two populations.** PBMCs were incubated with GFP-iRBCs for 2hrs before FACS staining and fixation. Histograms represent the percentage of NK cells forming conjugates in the LSHTM (A) and Ugandan groups (B), where each bar is one donor. Box-and-whisker plots indicate the min-to-max values, interquartile range, and medians (C). Statistical analyses by Mann-Whitney tests.

As Ugandan donors had marginally higher conjugate formation, it was important to discover whether conjugate formation correlated with other functional markers, or whether the conjugate formation itself had a function (e.g. leading to degranulation and target cell killing). The percentage of NK cells producing either of two functional markers, IFN-γ and CD107a, in response to iRBCs (A, C) or iRBCs with IL-15 (B, D) after 18 hours were therefore plotted against conjugate percentage after 2 hours to test for correlation (Figure 5.6). Linear regression was used to determine correlation for each population individually (dark blue circles and dashed lines indicate LSHTM donors, light blue circles and dotted lines indicate Ugandan donors) and the groups combined (unbroken lines). Neither IFN-γ production nor CD107a expression correlated with conjugate formation in either population or when all donors were considered together. R^2 values are shown next to each graph, but none reach significance ($p< 0.05$). This suggests that forming conjugates may not be required for NK cell activation, but also does not inhibit activation. There were also no differences between the populations, indicating that the functional differences observed in Chapter 4 are not influenced by conjugate formation.

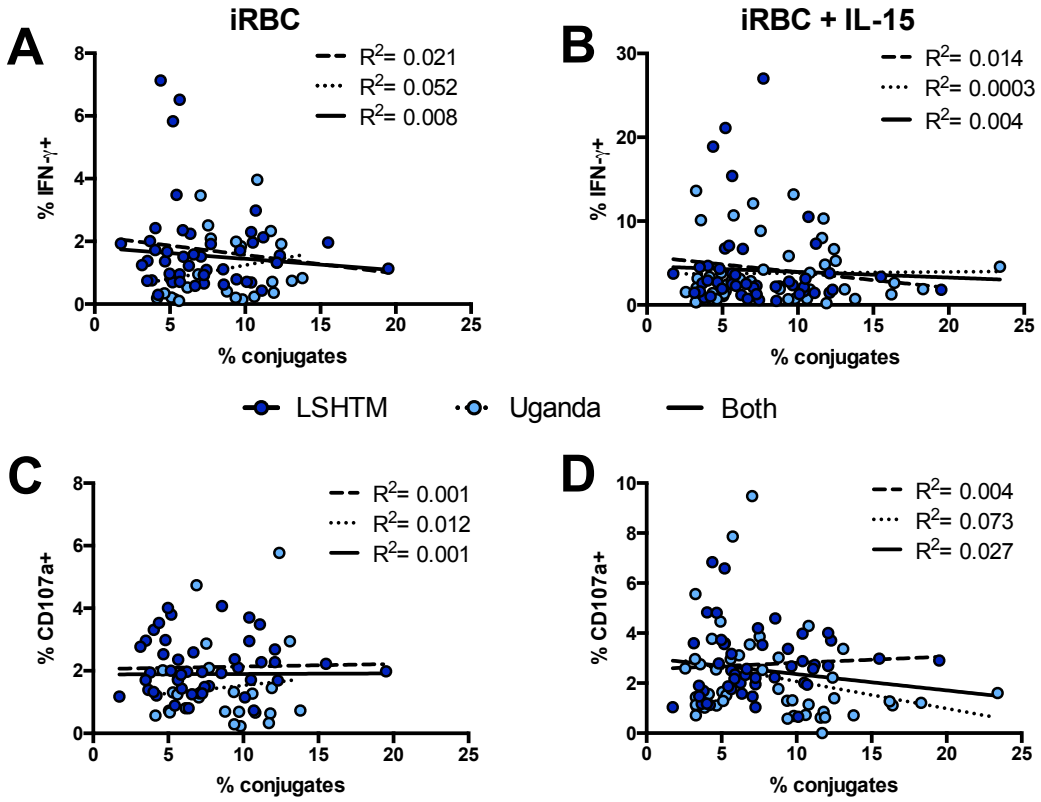

Figure 5.6: **Functional markers of activation do not correlate strongly with conjugate formation**. IFN-γ (A, B) and CD107a (C, D) responses of donors to iRBC alone and iRBC+IL-15 after 18 hrs were plotted against conjugate formation after 2 hrs. LSHTM (dark blue) and Ugandan (light blue) responses are plotted on the same graphs with R^2 values shown accordingly. Black lines show the linear trend of both groups combined. Statistical analyses by linear regression.

5.3.2 KIR genotype and expression patterns differ between populations and affect functional NK cell responses

5.3.2.1 Genotyping reveals different frequencies of KIR genes in LSHTM and Ugandan populations

As conjugate formation had no apparent effect on NK cell function, I looked further into the overall NK cell phenotype, focusing on the KIR genes. DNA was extracted from whole blood and genotyped for 17 KIR genes using sequence-specific primer PCR. Table 5.5 summarises the frequency of individual KIR genes in each population. LSHTM donors (n= 48) and a subset of Ugandan donors were genotyped for all KIR genes, and gene frequencies are calculated on these donors. DNA yields were low for most of the Ugandan donors, so full KIR genotyping was only carried out with samples with DNA concentrations of 25ng/µl or higher (n= 16). The entire Ugandan population (n= 53) was genotyped for *KIR2DL2, 2DL5* and *3DS1* (marked with a star), and recalculated gene frequencies are shown in brackets. Percentages represent the proportion of individuals with the gene within each genotyped population (n). Fisher's exact test (a χ^2 test) was used to test for significant differences in gene frequency between the populations. The full genotype results of each donor are listed in Appendix C.

From Table 5.5, the gene frequencies in each population can be compared. The framework KIRs delineating the centromeric and telomeric regions, KIR3DL2, 3DL3 and 3DP1, are present in all donors. KIR2DL4 is the fourth framework KIR, and is present in all genotyped Ugandan donors but missing in three LSHTM donors; however, this may be an error in my genotyping, as deletion of this gene is extremely rare [319]. *KIR3DS1* frequency was significantly lower in the Ugandan population (p= 0.017), consistent with published data [304]. This was further investigated in the following chapter. Additionally, although the overall frequency of *KIR2DS4* was similar in both populations, the deletion variant was notably less common in the Ugandan population compared to the LSHTM population (50.0% vs. 86.4%). This difference did not reach significance (p= 0.051), but most likely would have in a larger sample size.

KIR gene	LSHTM (n=48)		Ugandan donors (n= 16)		p value
	No. donors	%	No. donors	%	
2DL1	47	97.9	15	93.8	0.44
2DL2	25	52.1	9	56.25 (60.4)	0.31
2DL3	45	93.8	13	81.3	0.16
3DL1	46	95.8	16	100.0	1.00
3DL2	48	100.0	16	100.0	1.00
2DS1	19	39.6	3	18.8	0.22
2DS2	25	52.1	7	43.8	0.77
2DS3	19	39.6	4	25.0	0.38
2DS4	44	93.8	13	81.3	0.16
full	17	37.5	7	43.75	0.77
del	38	86.36	8	50	0.051
2DS5	16	33.3	7	43.8	0.55
3DS1	21	43.8	2	12.5 (20)	0.017
2DP1	48	100.0	14	87.5	0.060
3DL3	48	100.0	16	100.0	1.00
3DX1	48	100.0	16	100.0	1.00
2DL4	45	93.8	16	100.0	0.57
2DL5	32	66.7	9	56.3 (68)	1.00
3DP1	48	100.0	16	100.0	1.00

Table 5.5: **KIR gene frequency in the LSHTM and Ugandan populations.** Donors from LSHTM (n= 48) and Uganda (n= 16) were genotyped for 17 KIR genes. Recalculated gene frequencies for *KIR2DL2, 2DL5* and *3DS1* in Ugandan donors (n= 53) are shown in brackets. KIR2DS4 genotype is split by full and del variants. Differences in gene frequency for each gene was calculated by Fisher's exact test, and is listed as a p value.

From the genotyping data, putative KIR haplotypes (AA homozygous or Bx homozygous or heterozygous) can be assigned to each donor (Table 5.6). For the LSHTM donors, all KIR genes have been typed and therefore gene presence or absence is known for all these donors. For the Ugandan donors, complete presence/absence genotyping is only known for 16 donors. However, presence or absence of *KIR2DL2, 2DL5* and *3DS1* is known for all 53 donors (all of which are found on the B haplotype). *KIR2DL2* is the archetypal centromeric B haplotype gene, whereas *KIR3DS1* is found on the telomeric B haplotype and *KIR2DL5* is promiscuous and can be found on both regions. Donors missing all of these genes have been assigned an AA haplotype, and any donor with one or more of these an Bx haplotype. It is possible to have B haplotypes without these three genes (e.g. containing *KIR2DS1* but not *KIR2DL2, 3DS1* or *2DL5*), but is rare [304, 320].

Haplotype	LSHTM (%)		Uganda (%)	
AA	11	(20.2)	10	(18.9)
Bx	41	(78.8)	41	(77.4)
Unknown	0	(0)	2	(3.77)
Total	52		53	

Table 5.6: **Putative KIR haplotypes (AA, Bx) in each population.** Haplotypes are based on genotyping of 17 KIR genes in the LSHTM population, and 3 KIR genes (2DL2, 2DL5, 3DS1) in the Ugandan population. Numbers show the donors with that haplotype; percentages represent this in the total population. DNA from two Ugandan donors was of insufficient quality to determine any genotype or haplotype.

5.3.2.2 KIR expression is variable between individuals and populations and changes with NK cell maturation

As part of the conjugate formation and phenotyping panels, NK cell KIR expression after 2 hours was measured on all donors from both populations using the antibodies described in Table 5.3. Because of the cross-reactivity of the KIR antibodies, expression levels of KIR2DL1, 2DL2, 2DS1 and 3DS1 have been calculated by comparing two populations through FACS and by process of elimination based on presence/absence genotyping. Ex-

pression levels of KIR3DL1, 2DS4 and 2DL5 have been measured directly based on the FACS gating (Figure 5.7).

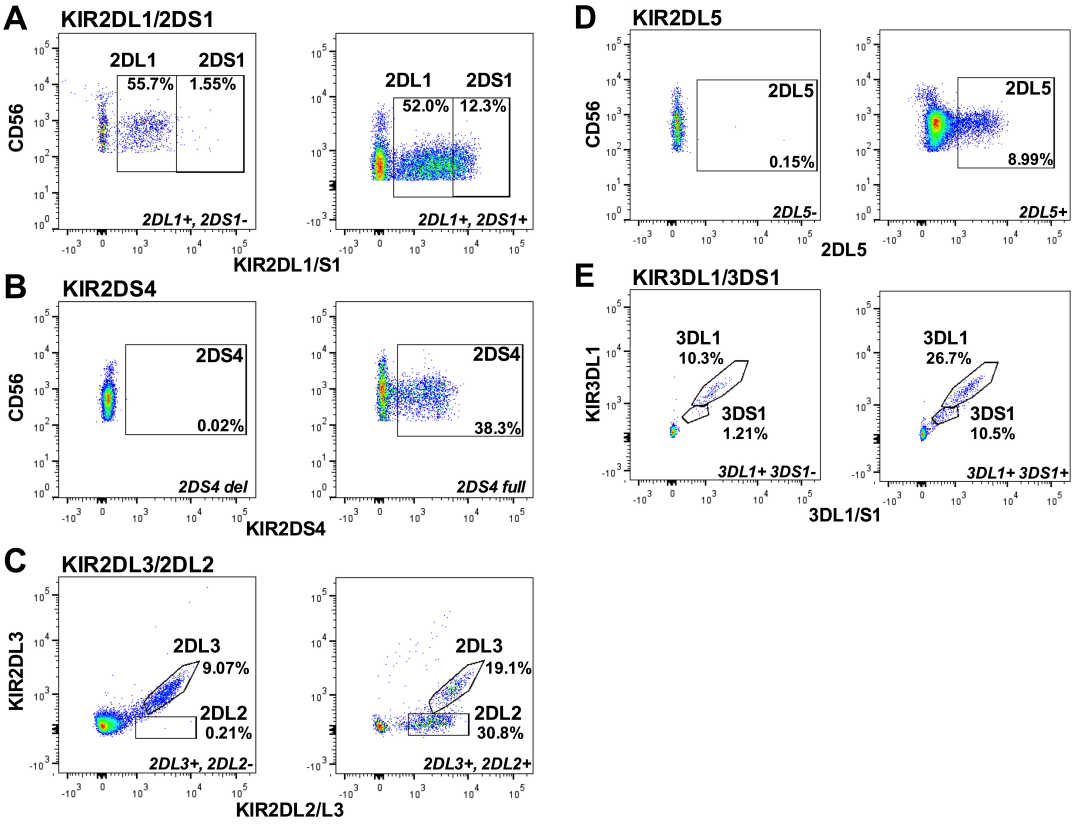

Figure 5.7: **FACS gating for KIR expression on NK cells**. FACS plots show gating for KIR2DL1 and 2DS1 (A), 2DS4 (B), 2DL2 and 2DL3 (C), 2DL5 (D), and 3DL1 and 3DS1 (E), using the antibodies listed on the axes. Donor genotype is denoted in the bottom corner of each plot.

Table 5.7 summarises the percentage of gene positive donors with NK cell surface expression of that KIR. As previously mentioned, KIR gene expression is complex and controlled by multiple factors, especially upstream promoter regions. Pseudogenes (e.g. *KIR2DP1*) and some alleles (e.g. *KIR2DS4* del, *KIR2DL5B*) are not expressed on mature peripheral NK cells, and therefore some individuals carrying a KIR gene do not express it. Table 5.7 shows the number of donors with KIR expression as measured by FACS (KIR expression), the number of donors who carry that gene according to PCR genotyping data (*KIR+*, and the percentage of donors with the gene who express surface KIR (%). All the data are present

for LSHTM donors, but genotyping data is not available for all the Ugandan donors, and therefore donors without KIR expression cannot be divided into those without the gene and those with a non-expressed gene. Genotype data for all donors (n= 53) is available for KIR2DL2, 2DL5 and 3DS1, and so exact expression frequencies can be calculated for these genes as shown. Gene carriage for 2DL1, 2DS1, 2DS4, 2DL3 and 3DL1 is unknown (listed as n/a).

For KIR2DL5, 2DL2 and 3DS1, expression frequency is listed for LSHTM and Ugandan donors, and compared for differences in the proportions of donors with surface expression of these KIRs by Fisher's exact test. Significant p values are in bold. As shown by the gating strategy (Fig. 5.7A, C, E), expression of KIR2DL1, 2DS1, 2DL2, 2DL3 and 3DS1 can be ambiguous due to antibody cross-reactivity, and requires cross-referencing to genotyping data for process of elimination.

KIR	LSHTM (n= 46)			Uganda (n= 52)			p value
	KIR expression (n)	*KIR+* (n)	% expressors	KIR expression (n)	*KIR+* (n)	% expressors	
2DL1*	33	33	100	52	n/a		
2DS1*	13	13	100	10	n/a		
2DS4	19	45	42.2	38	n/a		
2DL5	13	31	41.9	5	34	14.7	**0.025**
2DL2*	24	24	100	31	31	100	1.00
2DL3*	26	26	100	41	n/a		
3DL1	36	46	78.3	46	n/a		
3DS1*	13	21	61.9	8	10	80.0	0.43

Table 5.7: **Frequency of surface KIR expression in gene positive donors.** Percentages represent the number of *KIR+* donors with surface KIR expression. p values are calculated by Fisher's exact test; significant values are in bold ($p \leq 0.05$). * indicates that antibodies for these KIRs are cross-reactive and expression may include cells costained for other KIRs (as indicated by previous gating strategy).

From this table, there were clearly significant differences in 2DL5 expression between the groups. KIR2DL5 expression among *KIR2DL5* carriers was much lower in the Ugandan population (14.7% vs. 41.9%, p= 0.025) although the gene frequency was the same (68.0% vs. 66.7%, p= 1.00). As the non-expressed *KIR2DL5B* gene is reported to be more common in African populations [321], this is consistent with existing literature. Further analysis of KIR2DL5 expression and structural haplotyping was carried out and is described in Chapter 6.

All donors with *KIR2DL2* expressed KIR2DL2 (total for both groups, n= 55). Both groups had *KIR3DS1*+ individuals who did not express surface KIR3DS1. Both KIR3DL1 and 3DS1 are known to be highly polymorphic, and some alleles of 3DL1 have been shown not to bind the 3DL1-specific antibody DX9 that was used here [322], which may account for the lack of detectable expression in some LSHTM donors (the null phenotype). Although an exact percentage of KIR2DS4 expressors cannot be calculated for the Ugandan donors as *KIR2DS4* genotype is not known, 38/53 Ugandan donors had clear KIR2DS4 expression on NK cells (usually >15% positive NK cells), which indicates a higher proportion of *KIR2DS4 full* in this population compared to the LSHTM donors, of whom 19/45 *KIR2DS4*+ donors expressed 2DS4. This is consistent with the decreased frequency of *KIR2DS4 del* seen in Table 5.5 and suggests that 2DS4 is more commonly expressed in Ugandan donors compared to the predominantly Caucasian LSHTM donors. The percentage of NK cells expressing each KIR can be highly variable, which is primarily linked to promoter variation and gene copy number [89, 321, 322]. The range of KIR+ NK cells within groups of *KIR*+ donors can be variable (Fig. 5.8) and differ between population.

The data appear to be consistent with KIR+ NK cell frequencies reported in the literature: 2DL1, 15-25% [79, 323]; 2DS4, 1.28-46.8% [94]; 2DL5, under 10% [99]; 2DL2, 25-45% [323, 324]; 2DL3, 15-40% [293]; 3DL1, 1.6-32.2% [325]. However, there were some significant differences in expression levels of KIR+ NK cells between the populations, where LSHTM donors had larger populations of 2DS4+, 2DL3+ and 3DL1+ NK cells than Ugandan donors (Fig. 5.8A). The reasons for these differences are unclear, but could be due to the difference in age between these groups of donors, as KIR expression is higher on more

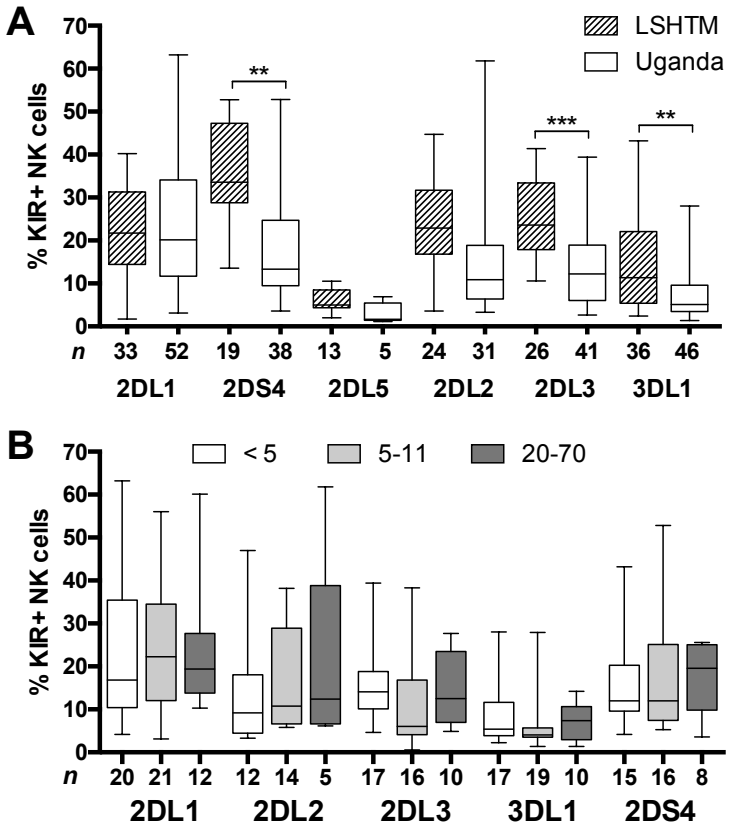

Figure 5.8: **Expression of KIR molecules on NK cells varies between donors.** Box-and-whisker plots showing the range of KIR expression on the NK cell surface for individuals carrying that KIR gene. LSHTM and Ugandan donors for each KIR are shown side by side (A). KIR expression for Ugandan donors grouped by age (< 5 years, 5-11 years, 20-70 years) (B). n underneath the bars indicate the number of individuals represented in each bar, whiskers indicate the minima and maxima. Statistical analyses by Mann-Whitney t tests (A) and ANOVA tests for linear trend (B). * $p \leq 0.05$, ** $p < 0.01$, *** $p < 0.001$ **** $p < 0.0001$.

mature NK cells which accumulate with age. However, there were no significant differences in KIR expression between Ugandan donors of different ages (Fig. 5.8B), although there was a trend for increased expression of 2DL2 and possibly 2DS4 in older donors. This trend may have reached statistical significance with a greater sample size (n is indicated for each group on the x-axis). Apart from genetic factors controlling KIR expression, such as promoter variation and the influence of self-HLA on NK cell licensing, environmental

factors may also influence KIR expression, such as HCMV-driven 2DL1+ and 2DL3+ NK expansions [13, 323], and it is likely that the Ugandan donors have been exposed to a greater number of environmental pathogens [11], which may account for the increased frequency of KIR+ NK cells in some Ugandan donors.

As KIR expression is thought to be acquired with increasing maturity, KIR expression on each of the four CD57 subsets was analysed (CD57 subsets as described in Introduction, Section 1.1 and analysed in Chapter 4) (Figure 5.9). NK cells were categorised as CD56 bright, CD57-, CD57int or CD57+ by FACS gating (Fig. 5.9A). Expression of KIR2DL1, 2DS1, 2DS4, 2DL5, 2DL2 and 2DL3 was analysed on the NK cell surface after 2 hours incubation with medium only in both LSHTM (Fig. 5.9B) and Ugandan donors (Fig. 5.9C).

Expression of KIR2DL1, 2DS4, 2DL2 and 2DL3 on the NK cell surface clearly increased with CD57 expression. Consistent with published data [202], CD56 bright cells expressed very low levels of KIR molecules, although in the Ugandan group a small percentage of CD56 brights appeared to express KIR2DL1, which may indicate that these cells were becoming more mature. Interestingly, in Ugandan and LSHTM donors expression of KIR2DS1 did not appear to increase with NK cell maturity, although the sample size is small (both n= 7). KIR2DL5 expression, as an inhibitory KIR, is likely to increase with CD57 expression and in LSHTM donors there was a slight increase in 2DL5+ NK cells with increasing CD57 expression (p= 0.016). 2DL5 expression in Ugandan donors suggests a similar trend, but there are too few donors to determine whether this is the case (n= 5) and the population of 2DL5+ NK cells is small (<10% of NK cells). CD57 and KIR3DL1 and KIR3DS1 were not analysed in the same FACS panel and so CD57 subset data are not shown. The mechanisms by which NK cell licensing occurs are not known, so it is unclear whether NK cells in peripheral blood show a steady increase in KIR expression over time or some trigger induces a change in KIR and CD57 co. From these data, CD57- NK cells do express KIRs at a lower frequency than CD57+ NK cells and at a higher frequency than CD56 brights, but it is not possible to say in what way KIR expression might be acquired.

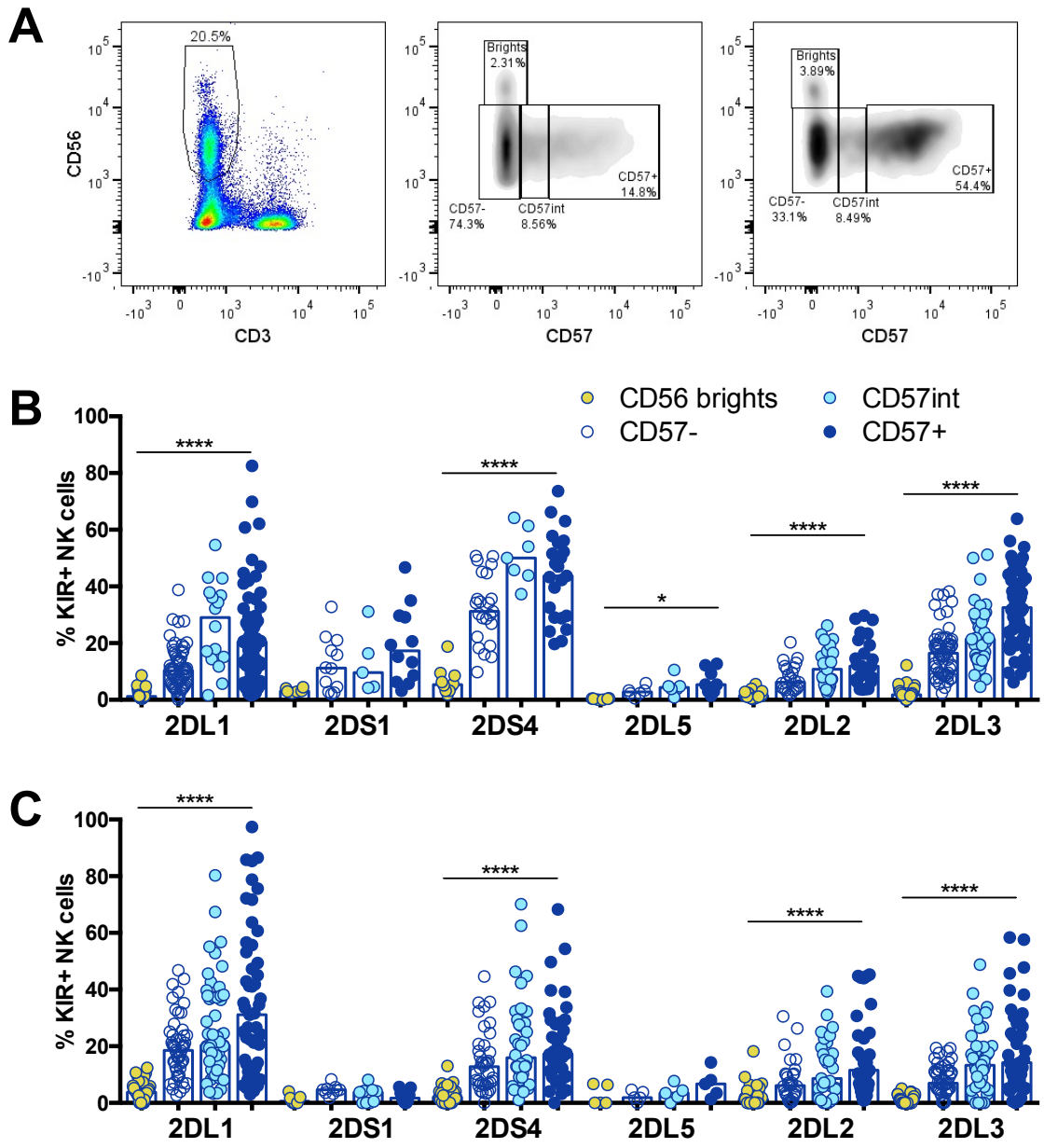

Figure 5.9: **Expression of KIR molecules on NK cells increases with NK cell CD57 expression.** NK cells were incubated with medium alone for 2 hours and gated for maturation subset and KIR expression. Gating strategy for NK cells and CD57 expression on a LSHTM and a Ugandan donor (A). Expression of KIR2DL1, 2DS1, 2DS4, 2DL5, 2DL2 and 2DL3 on each CD57 subset (CD56 bright (yellow), CD57- (white), CD57int (light blue), CD57+ (dark blue)) in LSHTM (B) and Ugandan (C) donors. Uncapped lines indicate linear trends across subsets for each KIR. Statistical analyses by ANOVA tests for linear trend. * $p \leq 0.05$, ** $p < 0.01$, *** $p < 0.001$ **** $p < 0.0001$.

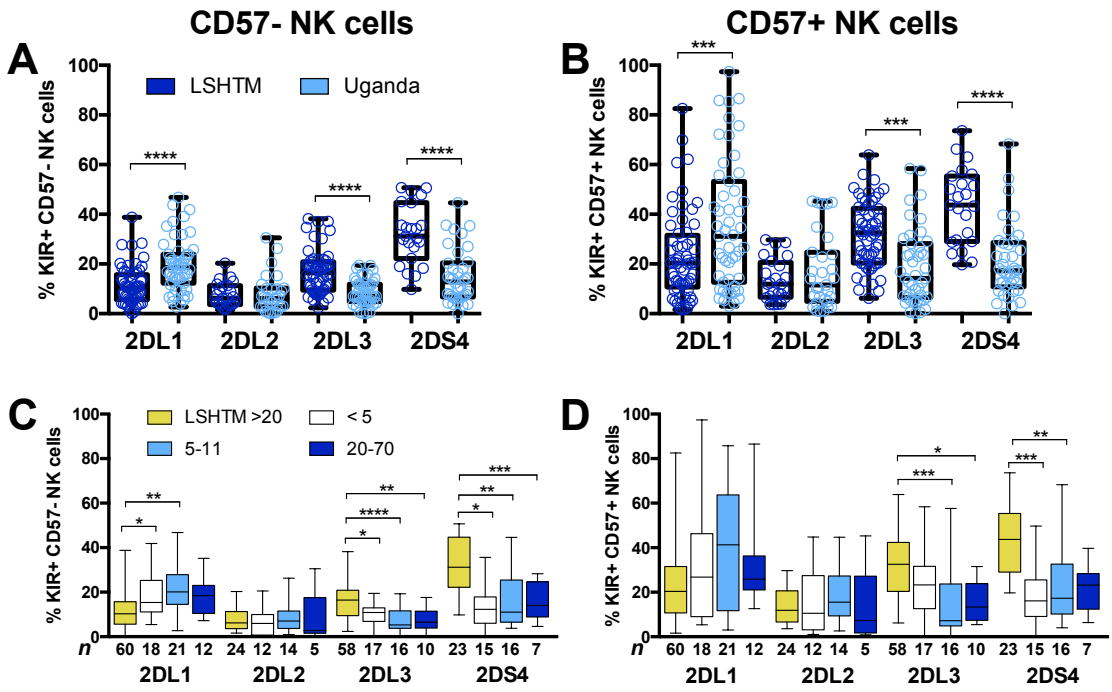

Figure 5.10: **KIR expression on CD57 NK cell subsets differs between LSHTM and Ugandan donors.** NK cells were incubated with medium alone for 2 hours and gated for maturation subset (CD57- or CD57+) and KIR expression. Comparing proportions of KIR2DL1+, 2DL2+, 2DL3+ or 2DS4+ NK cells by CD57- (A) and CD57+ (B) subsets for LSHTM and Ugandan donors. Comparing the percentage of KIR+ NK cells between different age groups (LSHTM adults 20-70 years old, yellow; Ugandans: <5 years old, white; 5-11 years old, light blue; 20-70 years old, dark blue) in CD57- (C) and CD57+ (D) subsets. Statistical analyses by Dunn's multiple comparisons tests. Whiskers indicate maxima and minima, n for each bar is indicated on the x-axis. * $p \leq 0.05$, ** $p < 0.01$, *** $p < 0.001$ **** $p < 0.0001$.

To test whether the differences in KIR expression between the groups of donors was due to CD57 NK cell subset, NK cells were gated by CD57 and KIR expression, and then compared between LSHTM and total Ugandans, or grouped by age into total LSHTM (all donors over 20 years old), and Ugandans under five years old, 5-11 years of age, and over 20 years old. CD57- and CD57+ NK cell subsets were examined in order to compare KIR expression on each subset (Figure 5.10). When considering KIR expression on CD57- and CD57+ subsets, there was a clear increase in 2DL1 expression in Ugandan donors compared to LSHTM donors in both these subsets (Fig. 5.10A, B), which appeared to

be primarily observed in Ugandan children (Fig. 5.10C, D). Conversely, percentages of NK cells expressing either 2DL3 or 2DS4 was higher in LSHTM donors, consistent with KIR expression patterns observed in the total NK cell population. The reasons for these differences in KIR expression are not clear, but may indicate that factors driving KIR expression (such as self-HLA genotype) differ between the groups of donors. There were no significant differences in the proportion of KIR+ CD57- or KIR+ CD57+ NK cells between different age groups within the Ugandan donors, indicating that these NK cell subsets show similar phenotypes between different ages and the trend for increasing KIR expression with age is likely due to the accumulation of CD57+ NK cells in older people, rather than increased KIR expression within a CD57 NK cell subset.

5.3.2.3 KIR expression affects NK cell functional responses

Previous work had suggested that KIR haplotype (AA or Bx) might influence NK cell functional responses and that individuals with an AB haplotype had higher IFN-γ responses to multiple pathogens after *in vitro* stimulation than AA or BB homozygotes [202]. Donors were grouped by haplotype and analysed for IFN-γ, CD25 and CD107a responses to iRBC+IL-15 after 18 hours and conjugate formation after 2 hours by KIR haplotype (Figure 5.11). None of the NK cell responses were significantly linked to haplotype, although Bx donors in both populations appeared to make more IFN-γ, and in the Ugandan population this approached significance (p= 0.064, Mann-Whitney t test). This is consistent with the observations by Korbel et al [202], but may require a larger study size to test whether there are truly differences between haplotypes as the number of AA haplotype donors was small in both populations (n= 11 and 10). It was not possible to distinguish between AB and BB individuals (the Bx group), which might further stratify the data. Combining the LSHTM and Ugandan groups did not show a significant difference in IFN-γ production (p= 0.069). Therefore KIR haplotype alone did not account for the differences in NK cell responses to iRBCs, nor did it influence the number of NK-iRBC conjugates formed.

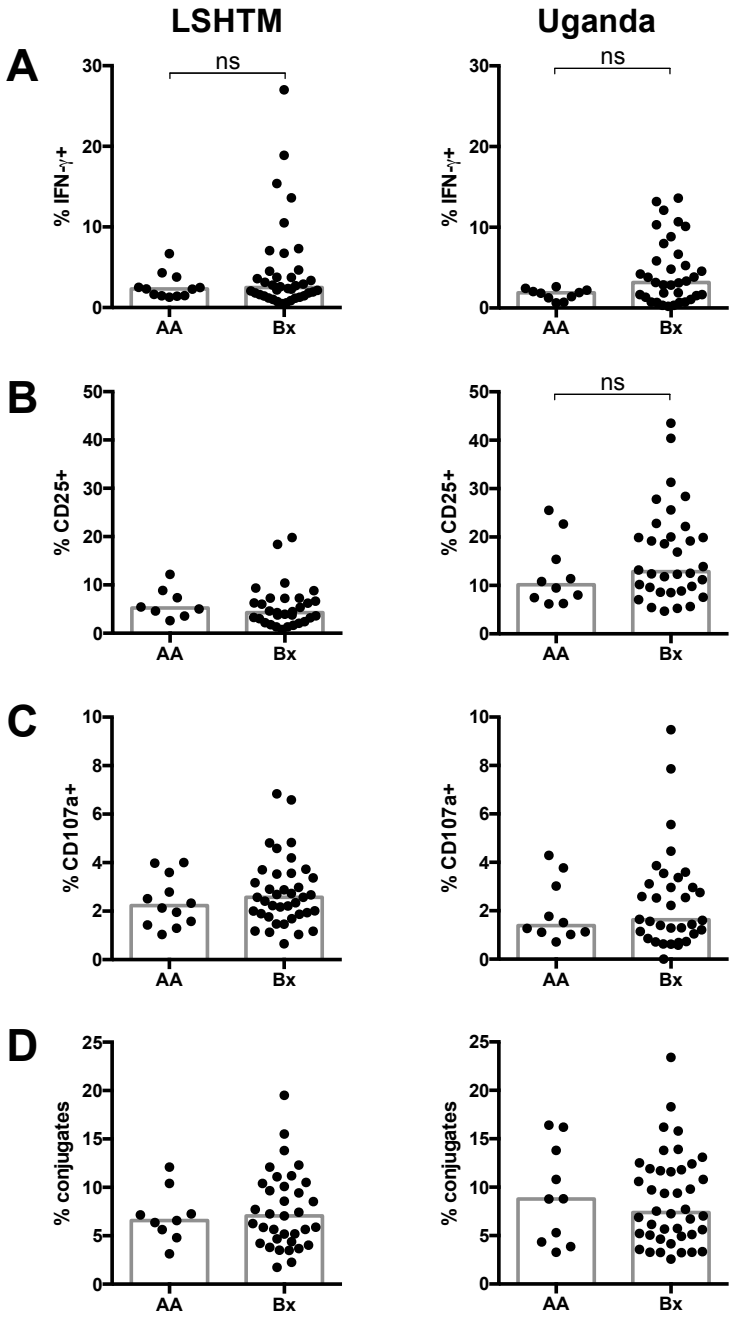

Figure 5.11: **KIR haplotype does not significantly influence NK cell functional markers.** Donors from the LSHTM and Ugandan populations were grouped by AA or Bx haplotype and IFN-γ (A), CD25 (B), CD107a (C) and conjugate formation (D) was measured. Statistical analyses by Mann-Whitney t tests, no significant differences.

Although KIR expression is broadly stable in individuals over time, various factors can drive changes in the NK cell subsets expressing certain KIRs, such as NK cell maturation with age or HCMV infection. Therefore KIR expression was measured on NK cells after incubation for 2 hours with medium alone, uRBCs or iRBCs and compared (Figure 5.12). Expression levels were broadly consistent across the different conditions, and there were no significant differences between uRBC and iRBC conditions. However, in two donors (one LSHTM and one Ugandan) there was a large upregulation of KIR2DL5 after incubation with iRBCs from 0% to greater than 20% which could not be accounted for by experimental error. This was therefore explored in more detail as described in Chapter 6. Preliminary experiments also appeared to indicate that KIR2DL5 was modestly upregulated on the NK cell surface after iRBC incubation in more donors, although this difference was not significant in the final analysis.

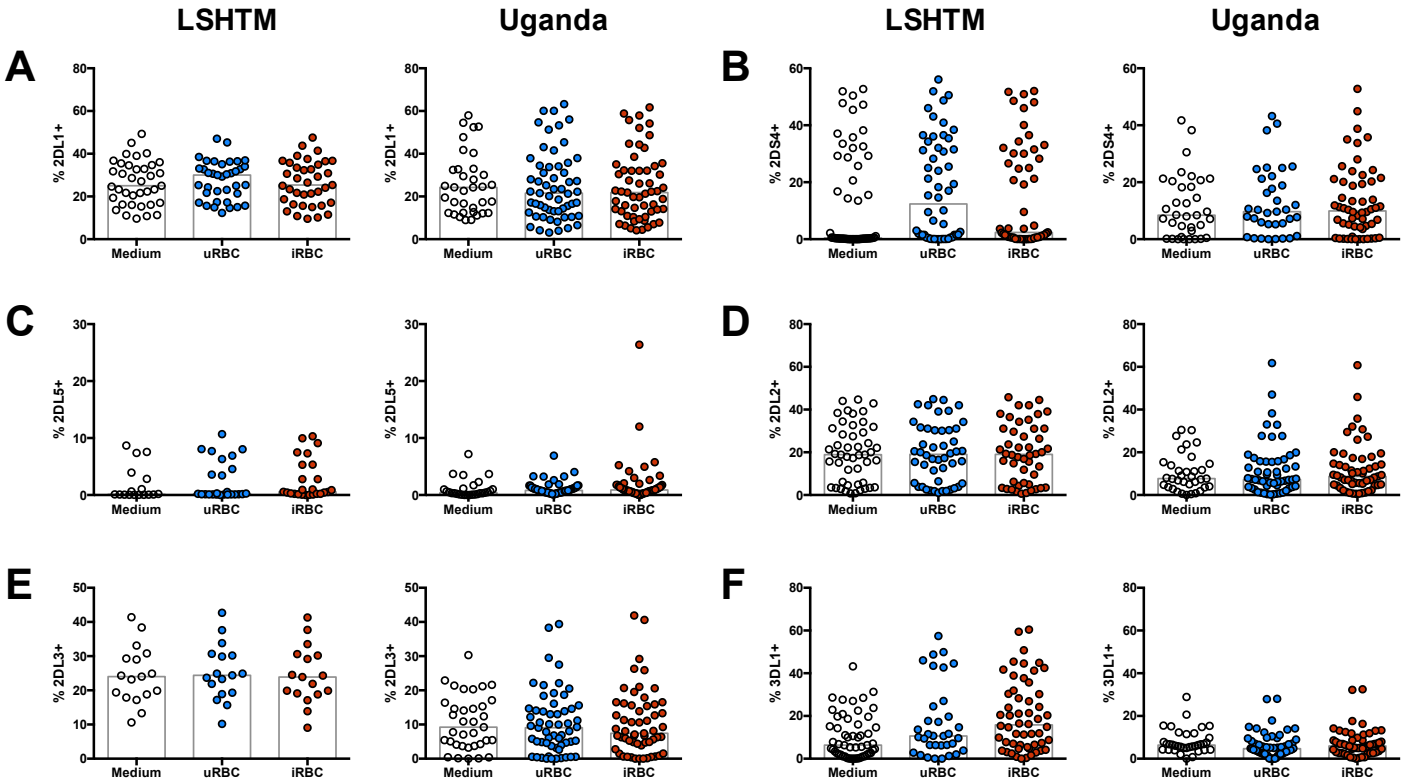

Figure 5.12: **KIR expression on the NK cell surface after incubation with iRBCs.** PBMCs were incubated with medium alone (white), uRBCs (blue) or iRBCs (red) for 2 hrs and stained for KIR expression. Bars indicate median values and were compared using Wilcoxon signed-rank tests. No significant differences.

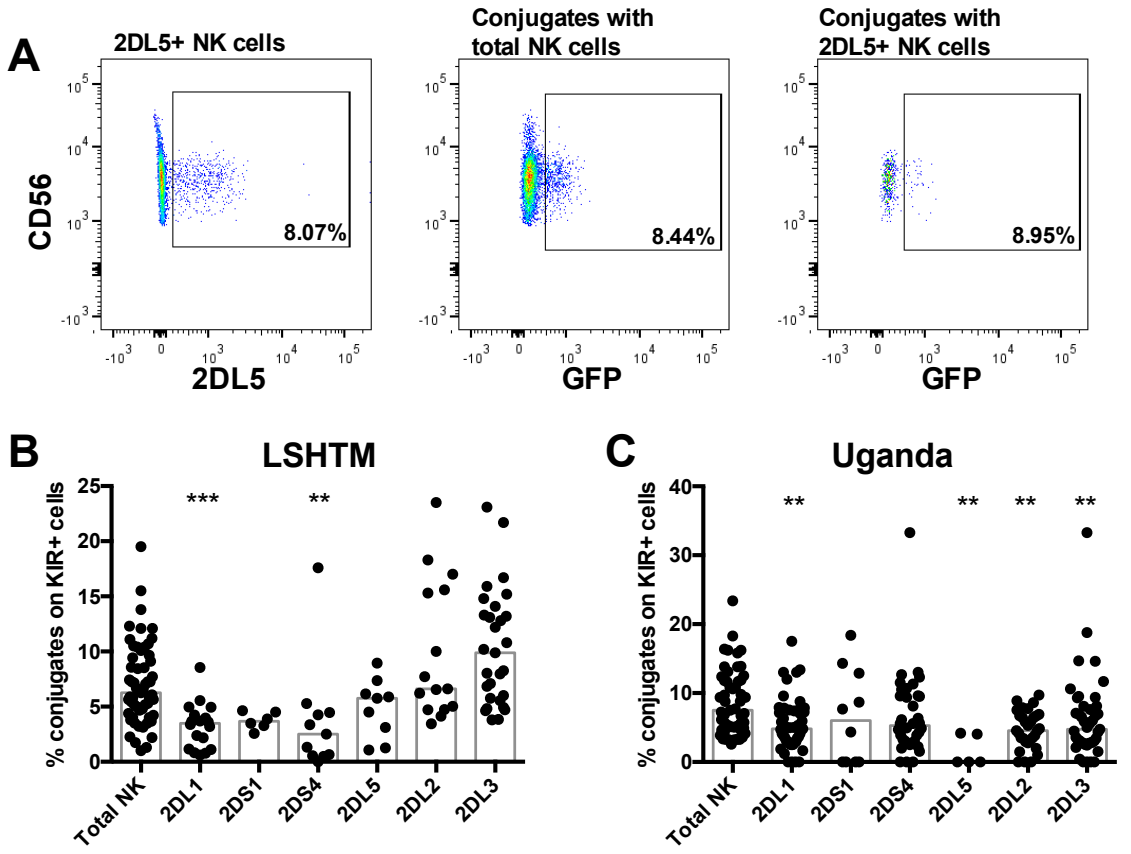

Figure 5.13: **NK-iRBC conjugate formation differs with KIR expression.** NK cells were incubated with iRBCs for 2 hours and KIR expression and NK-iRBC conjugate formation. Sample FACS gating of KIR+ NK cells (here 2DL5+ cells), NK-iRBC conjugate formation in the total NK cell population, and the percentage of KIR+ cells that form NK-iRBC conjugates (A). The percentage of NK-iRBC conjugates that KIR+ NK cells formed is shown compared to the total percentage of NK-iRBC conjugates in LSHTM (B) and Ugandan (C) donors. Statistical analyses by Kruskal-Wallis tests for multiple comparisons compared to Total NK. * indicate comparisons of KIR+ cells with the Total NK percentage. * $p \leq 0.05$, ** $p < 0.01$, *** $p < 0.001$ **** $p < 0.0001$.

To determine whether KIR expression affected NK-iRBC conjugate formation, the percentage of conjugates was calculated after gating for KIR+ NK cells (Figure 5.13). There were some significant differences in conjugate formation in KIR+ NK cells compared to the overall NK cell population, but these differences were not consistent between the groups of donors. LSHTM donors had statistically significantly lower conjugate formation in

KIR2DL1, 2DS1 and 2DS4+ NK cells compared to the number of conjugates formed by the total NK cell population. However, donor numbers in both KIR2DS1 and 2DS4+ populations are low (n= 10 and n= 6 respectively), compared to the total NK group (n= 50). Conversely, Ugandan donors had statistically significantly lower conjugate formation in KIR2DL1, 2DL2, 2DL3 and 2DL5+ NK cells compared to the total NK population, which indicates that expression of inhibitory KIRs may reduce conjugate formation with iRBCs.

5.3.3 NKG2C genotyping and expression

NKG2C and NKG2A are expressed on the NK cell surface at different stages of maturity, which is consistent with their roles as activating and inhibitory receptors sharing the same coexpression receptor (CD94). NKG2A is expressed on less mature, KIR- NK cells including the CD56 bright subset. As NK cells mature and gain CD57 expression, the overall population of NK cells loses NKG2A expression and gains NKG2C, although it is unclear whether individual NK cells undergo this process or whether a smaller population of NKG2C+ NK cells undergo clonal expansion and form a larger proportion of NK cells over time. Detection of NKG2A and NKG2C by flow cytometry shows what fraction of the NK cell population expresses each receptor and how this differs between donors (Figure 5.14).

NKG2C expression clearly varies between healthy donors. Mature peripheral NK cells express a high frequency of NKG2A+ NKG2C- and NKG2A- NKG2C- NK cells (Fig. 5.14B), but these populations undergo large reductions in donors with NKG2C+ expanded subsets (Fig. 5.14C). However, in donors with a homozygous *NKG2C* deletion, the NKG2A+ subset may be reduced but NKG2C is not expressed, and the percentage of NKG2A- NKG2C- NK cells increases (Fig. 5.14D). HCMV status is not known for any donors in this study, but based on FACS data from previous studies [11, 17], Fig. 5.14B is likely to be HCMV- and Fig. 5.14C is likely to be HCMV+.

5.3.3.1 NKG2C deletion frequency is similar in LSHTM and Ugandan groups

NKG2C genotype for both LSHTM (n= 44) and Ugandan donors (n= 53) was analysed by PCR. Percentages of *NKG2C* +/+, *NKG2C* +/− and *NKG2C* −/− individuals are summarised in Table 5.8 for both groups. Donors from Uganda were additionally split by age group (<5 years (n= 20), 5-11 years (n= 21), 20-70 years (n= 12)). The frequency of the *NKG2C* deletion allele was calculated for each population as a whole.

From Table 5.8, frequency of *NKG2C* −/− genotype was low in both populations. *NKG2C*

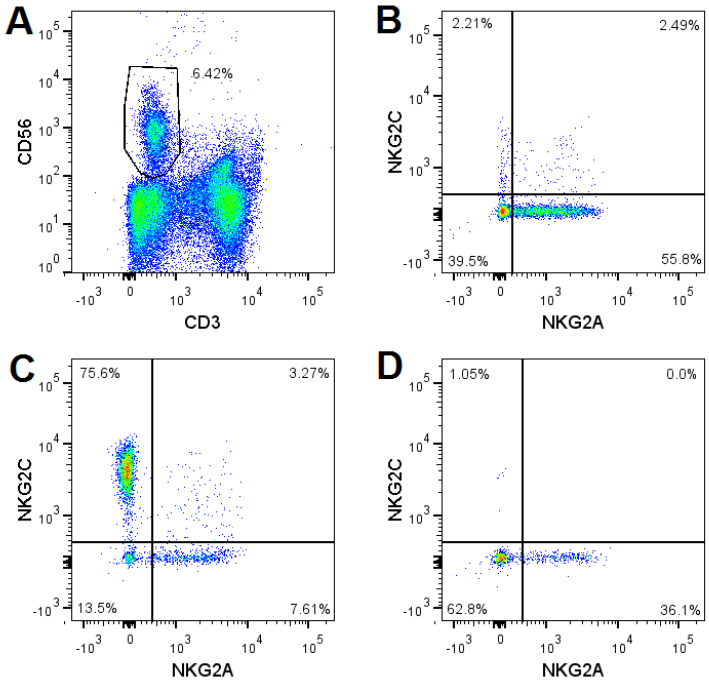

Figure 5.14: **NKG2A and NKG2C FACS gating on NK cells.** FACS gating for CD56+ CD3- NK cells (A) and NKG2C vs. NKG2A expression on NK cells (B-D). Plots B-D are from three different Ugandan donors: a healthy adult with some NKG2C expression (B), an individual with an expanded NKG2C population (C), and an *NKG2C* negative donor with no NKG2C expression. Percentages of cells in each gate or quadrant are indicated on the plots.

NKG2C genotype	LSHTM/ % donors (n)	Uganda/% donors (n)			
		Total	<5 (n= 20)	5-11 (n= 21)	20-70 (n= 12)
+/+	65.9 (29)	47.2 (25)	50.0 (10)	38.1 (8)	58.3 (7)
+/−	29.5 (13)	45.28 (24)	40.0 (8)	52.4 (11)	41.7 (5)
−/−	4.54 (2)	7.6 (4)	10.0 (2)	9.5 (2)	0.0 (0)
NKG2C (−) freq.	19.3%	30.2%			

Table 5.8: **NKG2C genotyping data from all donors.**

+/+ was the most common genotype in both populations, and in this small sample size there were no significant difference in the proportion of homozygous or heterozygous NKG2C+ individuals between the two populations (Fisher's exact test, p= 0.091). There was no significant difference in the frequency of the deleted allele in each population (p=

0.098), although there was a slight trend towards increased frequency of the deletion allele in the Ugandan group. This is consistent with other published data, which found a deletion allele frequency of approximately 38% in West Africans, but is higher than the frequency of the deletion found in nearby Tanzania (20.9%) [11, 313]. Within the Ugandan group, dividing donors by age group showed no significant differences in distribution of genotype by age (χ^2 test).

5.3.3.2 NKG2C and CD57 expression are higher in *NKG2C*+ donors

NKG2C is known to be coexpressed with CD57 in HCMV-expanded NK cell populations. Percentages of NKG2C+ and CD57+ NK cells were therefore measured by flow cytometry in the Ugandan group both singly and in combination (Figure 5.15). Typical FACS plots from three Ugandan individuals from Nagongera in the <5 year old age group are shown with gating for NK cells, NKG2C on NK cells, and CD57+ NK cells within the CD56 dim subset. Donor 384 (Fig. 5.15D) was homozygous for *NKG2C* deletion and did not express NKG2C, along with a relatively small CD57+ population (12.4%). Donor 401 (Fig. 5.15E) was heterozygous and had expression of both NKG2C and CD57, though the population of NKG2C+ CD57+ cells was low (5.48%). By contrast, donor 14 (Fig. 5.15F) was *NKG2C*+/+ and had strong expression of NKG2C both singly (NKG2C+ CD57-, 31.3%) and with CD57 (NKG2C+ CD57+, 23.5%).

Similar patterns of NKG2C and CD57 expression were observed in the whole population (Figure 5.16). There was a clear dose effect of *NKG2C* so that *NKG2C* +/+ individuals (Fig. 5.16A) had significantly higher percentages of NKG2C+ cells overall compared to the groups of individuals with either heterozygous (p= 0.034) or homozygous deletions (p= 0.0038, Kruskal-Wallis tests). There was also a trend towards decreasing mean fluorescence intensity for NKG2C expression per cell with loss of *NKG2C*, although this was not statistically significant. The same pattern was seen in CD57 (Fig. 5.16B) where *NKG2C* +/+ individuals had higher proportions of CD57+ NK cells (median 44.7%) and *NKG2C* −/− donors had significantly lower proportions of CD57+ NK cells (median 13.3%) (p=

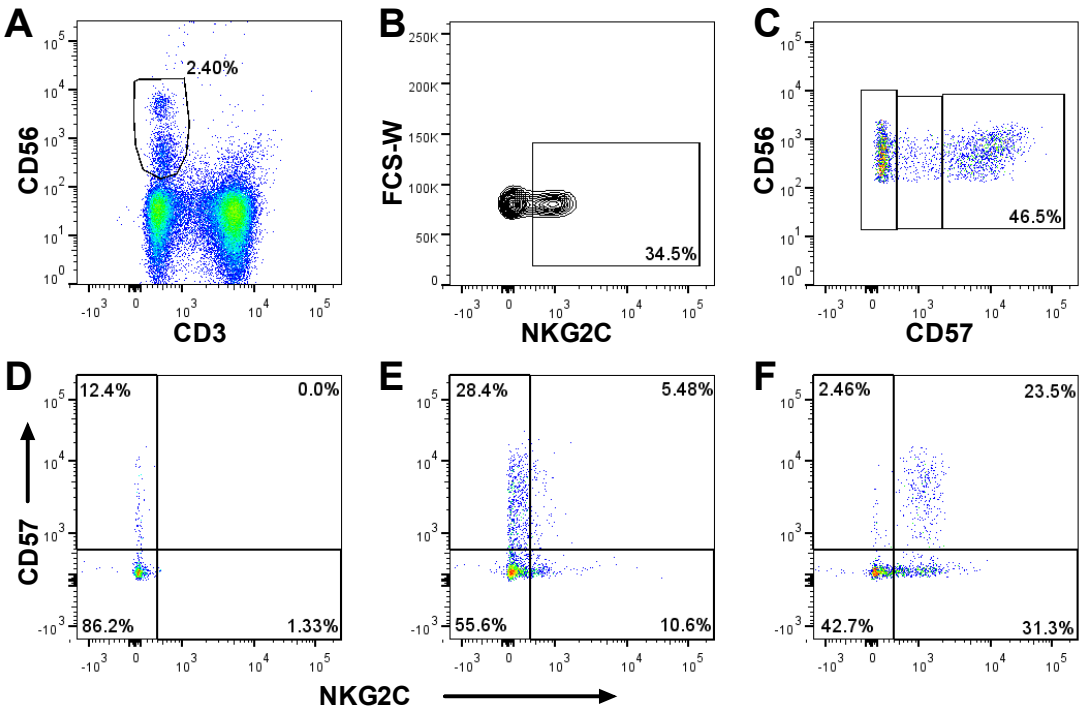

Figure 5.15: **NKG2C and CD57 coexpression in donors with different NKG2C genotype.** FACS gating for CD56+ CD3- NK cells (A), NKG2C+ NK cells (B) and CD57+ NK cells (C). Coexpression of CD57 and NKG2C is shown by FACS plots from three typical Ugandan donors in the <5 age group with *NKG2C* −/− (D), +/− (E) and +/+ (F) genotype. Percentages of cells in each gate or quadrant are indicated on the plots.

0.0097). CD57 MFI was also lower on NK cells from *NKG2C* −/− donors compared to +/+ donors (p= 0.024), but CD57 MFI in +/+ and +/− donors was similar (+/+ median, 7175, +/− median, 6660). Consistent with these trends, percentages of NKG2C+ CD57+ NK cells were highest in +/+ donors and non-existent in −/− donors, with intermediate proportions in heterozygotes.

There was also no evidence of NKG2C expression differing between age groups (Figure 5.17). Expression of NK cell NKG2C, CD57 and NKG2C+ CD57+ in all genotypes was split by age group (<5, 5-11, 20-70 years) (Fig. 5.17A). There were no *NKG2C* −/− donors in the 20-70 year old group, indicated as 'n/a'. NKG2C expression was not affected by age (ANOVA test for linear trend, p= 0.80), but the percentage of CD57+ NK cells did increase

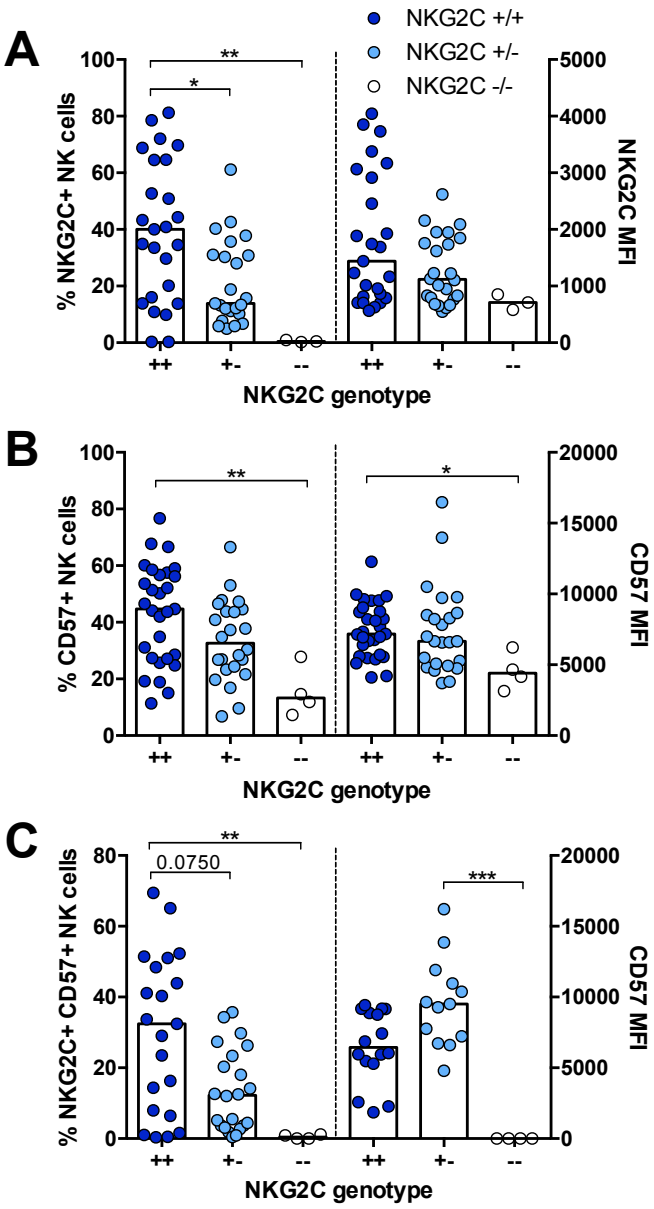

Figure 5.16: **NKG2C and CD57 expression is lower in donors heterozygous for NKG2C.** PBMCs from all Ugandan donors (n= 53) were incubated for 2 hours in culture medium and NK cells analysed for NKG2C expression, CD57 expression and NKG2C+ CD57+ coexpression with MFI. Donors were split by NKG2C genotype and the percentage of NKG2C+ (A), CD57+ (B) and NKG2C+ CD57+ (C) NK cells and the MFI of each donor is shown as a circle. Bars indicate medians. Statistical analyses by Kruskal-Wallis tests for multiple comparisons. * $p \leq 0.05$, ** $p < 0.01$, *** $p < 0.001$ **** $p < 0.0001$.

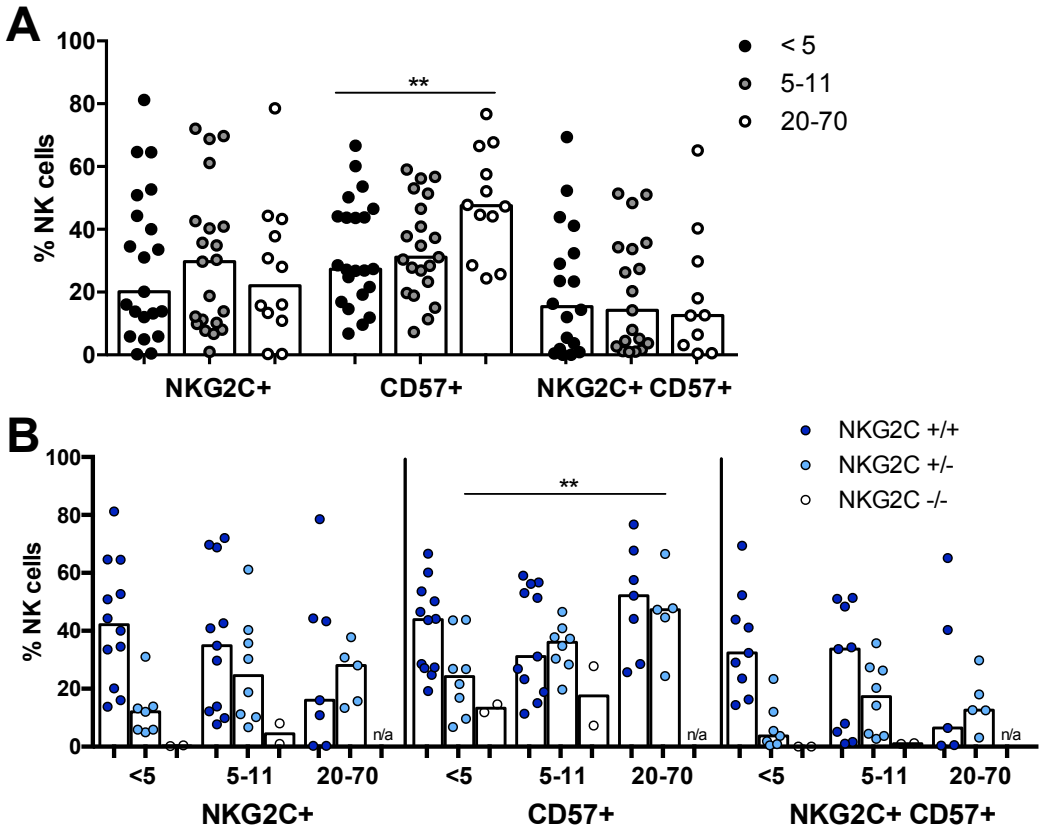

Figure 5.17: **CD57 expression in different age groups varies by NKG2C genotype.** NKG2C and CD57 expressing NK cells from the PBMC population were divided by age group (<5, 5-11, 20-70) and NKG2C genotype. Percentages of NKG2C+, CD57+ and NKG2C+ CD57+ NK cells by age group (A), and by NKG2C genotype (+/+ (dark blue), +/− (light blue) and −/− (clear)) for each age group (B). Uncapped lines indicate linear trend by ANOVA. Statistical analyses for differences between groups by Kruskal-Wallis test and ANOVA tests for linear trend between left to right columns. * $p \leq 0.05$, ** $p < 0.01$, *** $p < 0.001$ **** $p < 0.0001$.

with age (ANOVA test for linear trend, $p = 0.0084$), consistent with literature describing CD57 as a maturation marker [4, 5]. Further subdividing donors by NKG2C genotype within each age group (Fig. 5.17B) indicated that increasing CD57 expression with age in this group of donors was primarily driven by NKG2C heterozygotes ($p = 0.0064$, $R^2 = 0.35$, ANOVA test for linear trend). CD57 expression in *NKG2C* +/+ individuals did not differ between age groups (test for linear trend, $p = 0.27$, $R^2 = 0.043$). These differences may be

due to faster HCMV-driven expansion of NKG2C+ cells in homozygous individuals and therefore an associated early increase in CD57 expression, whereas NKG2C heterozygotes have smaller NKG2C+ subsets and acquire CD57 more slowly with age. There were no age-based differences in NKG2C+ or NKG2C+ CD57+ expression, and the trends within each age group for decreasing NKG2C+ or NKG2C+ CD57+ populations are consistent with data shown in Figure 5.16.

5.3.3.3 NKG2C genotype drives expansions of KIR+ NK cells in putative HCMV-infected donors

Coexpression of NKG2C and KIR molecules was not measured due to limitations of the antibody panels, but expression of KIR2DL1, 2DL3, 3DL1 and 2DS4 in LSHTM and Ugandan donors was grouped by NKG2C genotype (Figure 5.18) (only KIRs with sufficient numbers of donors were analysed by *NKG2C* genotype). Donors expressing KIRs (as gated from Figure 5.7) were split into *NKG2C* +/+, +/− and −/− groups, and differences in expression were analysed by ANOVA tests for linear trend. There were no differences between NKG2C genotypes in LSHTM donors (Fig. 5.18A), which is likely to be linked to the low incidence of HCMV in this group and non-expanded NKG2C+ subsets. In the Ugandan group, KIR2DL1+ NK cell subsets were significantly expanded in *NKG2C*+/+ individuals compared to +/− or −/− individuals (test for linear trend, p= 0.0096, R^2= 0.12) (Fig. 5.18B), which is consistent with studies suggesting that KIR+ expanded subsets might control HCMV infection [14]. Additionally, the effect of *NKG2C* +/+ or +/− genotype suggests that KIR2DL1 and NKG2C may be coexpressed on these cells, which would be consistent with expansions of mature KIR-licensed cytotoxic NK cells in HCMV individuals. Interestingly, other inhibitory KIRs (2DL3 and 3DL1) showed no effect of NKG2C genotype, perhaps suggesting that these KIRs are less associated with HCMV control. Conversely, KIR2DS4, an activating KIR, indicated a slight trend towards increased expression in the NKG2C +/− which would be consistent with a model requiring increased expression of activating KIRs to compensate for non-expression of NKG2C [315]. However, more donors are needed to test this hypothesis. There was no significant differ-

ence between KIR2DS4 expression in +/+ and +/− individuals (p= 0.11, Mann-Whitney t test).

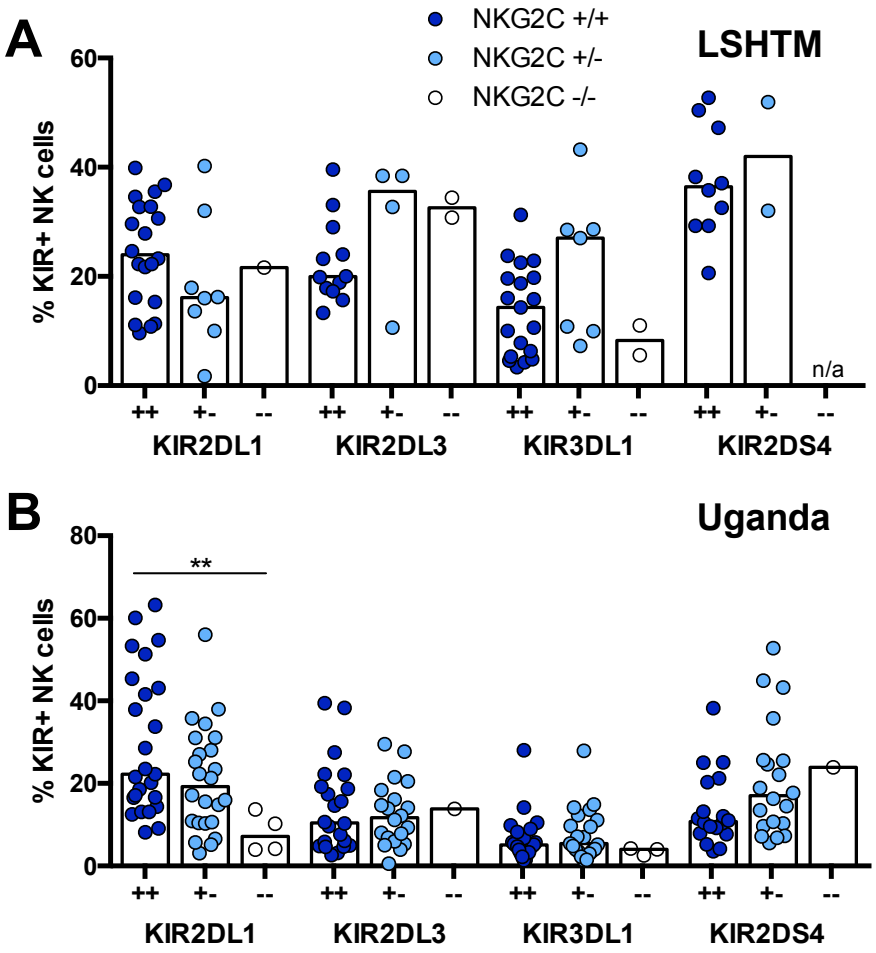

Figure 5.18: **Expression of KIR2DL1 on NK cells is higher in *NKG2C*+ Ugandan donors.** Percentages of KIR2DL1, 2DL3, 3DL1 or 2DS4 expressing NK cells were divided by *NKG2C* genotype (+/+ (dark blue), +/− (light blue) and −/− (clear)) for LSHTM (A) and Ugandan (B) donors. Uncapped lines indicate linear trend by ANOVA. Statistical analyses for differences between groups by Kruskal-Wallis tests and ANOVA tests for linear trend between left to right columns. * $p\leq$ 0.05, ** $p<$ 0.01, *** $p<$ 0.001 **** $p<$ 0.0001.

5.3.3.4 NK cell functional responses are not affected by NKG2C genotype

To test whether NKG2C genotype affected NK cell functional responses, IFN-γ production, CD107a expression and NK-iRBC conjugate formation were assessed by NKG2C genotype in both LSHTM and Ugandan donors (Figure 5.19). PBMCs were incubated with iRBCs, iRBCs with 0.75ng/ml IL-15, or 5ng/ml IL-12 and 50ng/ml IL-18 (HCC) for 18 hours and stained for IFN-γ (Fig. 5.19A, B) and CD107a expression (Fig. 5.19C, D). PBMCs were also incubated with iRBCs for 2 hours and assessed for conjugate formation (Fig. 5.19E, F). There was no statistically significant effect of NKG2C genotype on any functional readout in either group of donors. IFN-γ responses were not affected in LSHTM donors, but IFN-γ responses to HCC in Ugandan donors showed a slight increase in *NKG2C* $-/-$ individuals. This may be linked to smaller populations of mature (NKG2C+ CD57+) NK cells in these donors and therefore greater responsiveness to IL-12 and IL-18 on less mature cells. However this effect was not statistically significant in this small number of *NKG2C* $-/-$ donors. No effect of NKG2C genotype was seen in iRBC or iRBC+IL-15 IFN-γ responses, suggesting that responsiveness to IL-15 is not changed in these donors and the high Ugandan IFN-γ responses from Chapter 4 are not dependent on NKG2C genotype. Similarily, CD107a responses to HCC in Ugandan donors showed a slight trend towards greater CD107a expression in *NKG2C* $-/-$ donors (Fig. 5.19D), but this was not significant due to low numbers of donors.

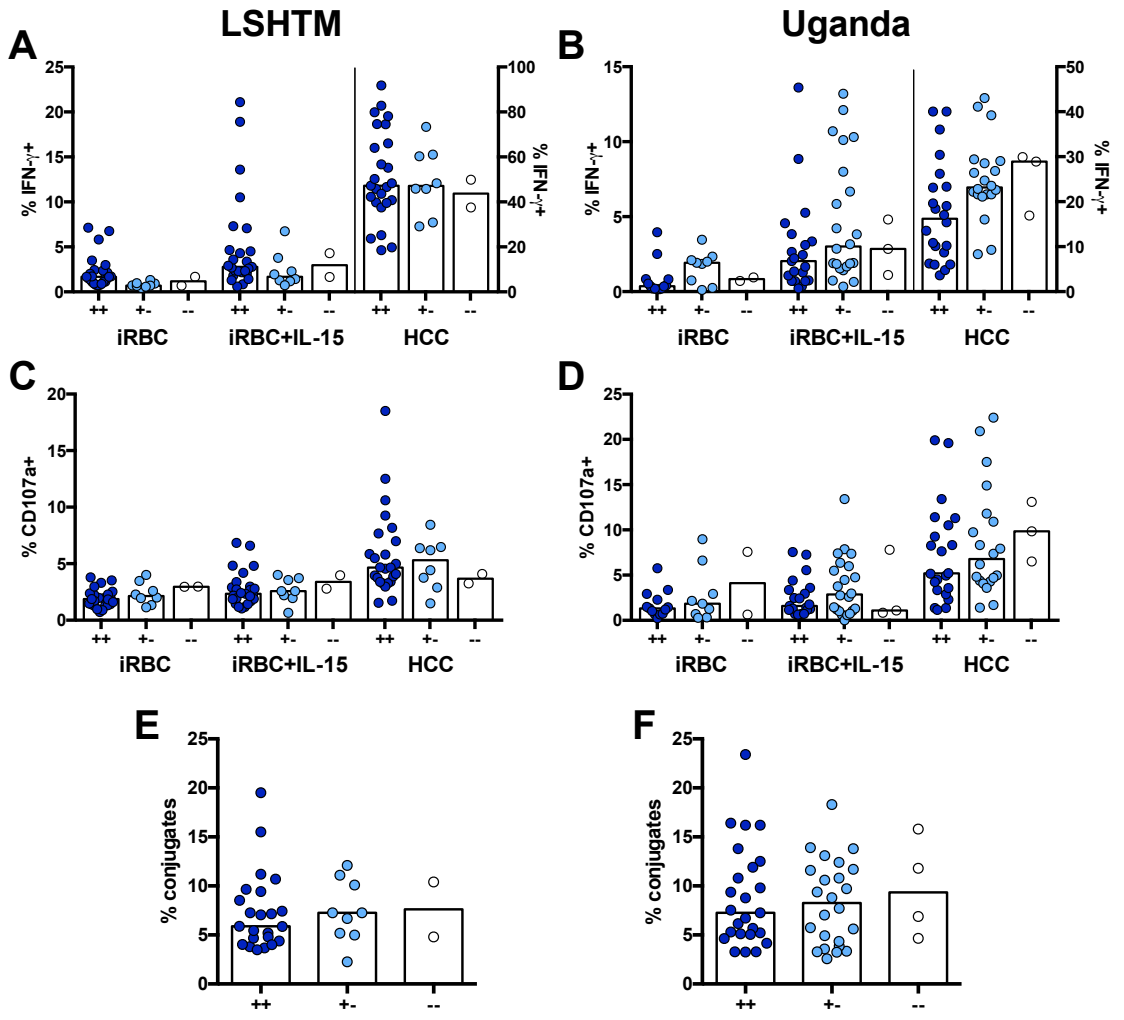

Figure 5.19: **NKG2C genotype has no effect on NK cell functional responses to malaria iRBCs.** PBMCs from LSHTM and Ugandan donors were incubated with iRBCs, iRBCs+IL-15 (0.75ng/ml), or HCC (5ng/ml IL-12, 50ng/ml IL-18) for 18 hours and stained for IFN-γ (A-B) and CD107a (C-D) responses. PBMCs were also incubated with iRBCs for 2 hours and stained for NK-iRBC conjugates (E-F). Responses were divided into NKG2C genotype (+/+ (dark blue), +/− (light blue) and −/− (clear)). Statistical analyses for differences between groups by Kruskal-Wallis test and ANOVA tests for linear trend between left to right columns. No significant results.

5.4 Discussion

5.4.1 NK-iRBC conjugate formation does not correlate with functional NK cell responses

Interactions between NK cells and iRBCs during conjugate formation have been observed by several groups by both microscopy and flow cytometry. So far only one group [142] has seen clear evidence of NK cell killing of iRBCs (in a humanised mouse model), although Korbel et al [200] observed actin rearrangement which may be a precursor to a functional immune synapse. The fact that conjugate formation did not correlate with any of the functional markers used in these experiments, particularly IFN-γ and CD107a, suggests that conjugates do not in themselves enhance or inhibit functional responses. Conjugate formation was seen in all donors to some extent, consistent with observations by Korbel et al, although that may not necessarily lead to immune synapse formation. More importantly, the receptors and ligands interacting within the immune synapse will control the outcome of the contact, and therefore the KIR profile of each cell may be a bigger determinant in its functional capabilities. Although RBCs do not express HLA molecules, alternative molecules on the iRBC that are currently unidentified might act as ligands for some KIRs (e.g. activating KIRs, KIR2DL5, KIR2DL4), or else the effect of licensing via KIR expression may tune NK cell subsets to become more or less responsive to iRBCs. NK cells expressing multiple KIRs were not looked at in detail from these experiments as the antibody panels required that most KIRs were on different panels (most antibodies were on the fluorophores PE, PE-Cy7, or APC). Individuals in the Ugandan group had a significantly higher proportion of NK-iRBC conjugates compared to LSHTM donors, which was not accounted for by genetic factors including KIR and NKG2C genotype, or by maturation phenotype (NKG2C and CD57 expression on NK cell subsets). There did appear to be differences in conjugate formation based on KIR expression, although results differed between the groups of donors. Conjugate formation by NK cells from Ugandan donors appeared to be reduced on NK cells expressing 2DL1, 2DL2, 2DL3 and 2DL5, all of which are inhibitory KIRs. This suggests NK cells expressing inhibitory KIRs may in-

teract less with iRBCs, which could indicate that activation of NK cells during malaria is suppressed by inhibitory KIR expression. Conversely, this may indicate that licensed, inhibitory KIR-expressing, cytotoxic NK cells are not interacting with iRBCs and therefore iRBC killing does not occur. This also raises the possibility that NK cells might interact with iRBCs via an activating KIR not measured in this experiment. Ligands for activating KIRs are mostly unknown [118] and so iRBCs may express one such ligand.

5.4.2 KIR and NKG2C genotypes and expression are associated with NK cell maturity and differ between populations

Individual KIR genes and AA/Bx haplotypes are conserved in all human populations, but the frequencies of KIR genes and haplotypes differ between populations [82, 83]. Genotyping of both the LSHTM and Ugandan groups showed similar frequencies of most KIR genesm but expression patterns of KIRs showed differences in the frequency of donors expressing KIR2DL5 and KIR2DS4 between the groups, which both have known non-surface expressed alleles (*KIR2DL5B* alleles are transcriptionally suppressed [87, 99], *KIR2DS4* deletion variants are expressed as soluble forms unbound to the NK cell surface [103]). African populations have been reported to have a higher diversity of *KIR2DL5* alleles [303], many of which are *KIR2DL5B* and therefore not expressed. Similarly, as the α-KIR2DL5 mAb is reported to only bind one KIR2DL5 allele, other expressed alleles may not be detected. However, the reasons for the high frequency of a non-expressed gene are not clear. As this KIR appeared to be influenced by iRBC exposure and there is some literature linking it to malaria outcomes [300], it was explored in much greater detail in the next chapter. I also acknowledge that the LSHTM donors are not a homogenous population, and therefore comparing gene frequencies between these donors and Ugandans has limitations as a 'population' comparison. However, 46/50 (92%) of the LSHTM donors were white Caucasian individuals (from the UK, Europe, North America and Australia), and so these donors are likely to have many similarities in genetic background.

KIR2DS4 deletion alleles have been reported at high frequencies (80%) in British-Caucasian

populations [103], which is consistent with the frequency in the LSHTM population here (86.36%). 18.8% of donors were heterozygous for full and deletion *KIR2DS4* variants, so 42% of LSHTM donors expressed KIR2DS4 on NK cells. Although genotyping data was not available for many Ugandan donors, 76% of donors expressed 2DS4 on the NK cell surface, which implies that expressed *KIR2DS4* alleles are more common in Uganda than in Caucasian populations. Studies on *KIR2DS4* frequency in other populations included Brazilians with similar expression frequencies as Caucasians [326] and west African and Asian populations, where *KIR2DS4* gene frequency was 0.82 and 0.56 respectively (allele and expression were not measured in this study) [305]. *KIR2DS4* deletions have been suggested to be less common in populations where *2DS4* is the only activating gene and AA haplotypes predominate [103], but this Ugandan group is not one of those populations (77% of donors have Bx haplotypes).

Expression of KIR2DL1, 2DL2, 2DL3 and 2DS4 on mature NK cells was seen in both groups of donors and was strongly linked with increasing CD57 expression, so that CD56 bright NK cells showed very little KIR expression (KIR2DL4, which is expressed on all NK cells, was not analysed in these experiments) and CD57+ NK cells were predominantly KIR+. Expression of KIR2DS1 and 2DL5 did not significantly increase with CD57 subset, which is likely to be due to the low number of donors expressing either of these KIRs, and because the percentage of NK cells expressing these KIRs is naturally low. KIR2DS1 expression has been reported at between 5-15% NK cells [327], and KIR2DL5 is expressed on under 10% of healthy NK cells [87]. However, it may also indicate that NK cell subsets expressing these KIRs do not expand in the same way as, for example, KIR2DL1 during maturation or HCMV infection.

This evidence of greater KIR expression with increasing NK cell maturity further agrees with the model of NK cell licensing and a shift towards greater cytotoxicity, where more mature NK cells are permitted to interact with and potentially kill target cells.

In Ugandan donors there was a clear expansion of NKG2C+ CD57+ NK cells which is likely to be due to HCMV infection, and KIR2DL1 in particular was expanded in the same

donors. This is consistent with studies that have found that KIR2DL1 and NKG2C are coexpressed on NK cells during HCMV infection [14], but other inhibitory KIRs including KIR2DL3 showed little expansion despite suggestions in the literature that this was the case. It would be interesting to examine whether this selective expansion of KIR2DL1+ cells might be linked to HLA-C expression in these donors, as HLA-C2 is more common in Ugandan populations [302, 304], and therefore whether KIR+ NK cell expansions occur in the absence of their cognate ligand. As NKG2C, CD57 or KIR2DL1+ NK cell populations were not expanded to the same degree in LSHTM donors, despite the many differences between these populations it is likely that HCMV infection is responsible for the increased frequency of these cells in Ugandan individuals. The frequency of *NKG2C* deletions in Ugandan donors appeared to be slightly higher than in LSHTM donors, although this did not reach statistical significance. This is consistent with data from the Gambia which suggested that African populations had higher frequencies of *NKG2C* $-/-$ [11, 313]. NKG2C+ was expressed on NK cell subsets in a dose-dependent manner so that +/+ homozygotes had higher proportions of NKG2C+ cells than heterozygotes, which concurs with existing studies [11, 314].

5.4.3 KIR haplotype may affect NK functional responses in a larger population

Although grouping donors by KIR AA or Bx haplotype did not reveal any significant differences in NK cell function (IFN-γ, CD25, CD107a or conjugate formation), some donors with a Bx haplotype did appear to produce more IFN-γ, which may reach significance in a larger population. Bx haplotypes contain more activating KIRs, which might influence the amount of IFN-γ production either by directly activating the NK cell, or indirectly by interacting with another immune cell that then activates the NK cell. As has also been shown, NK-iRBC direct contact is required for strong cytokine responses along with other activating signals [183]. Whether the contact requirement involves KIR molecules is unclear from these experiments as there are other NK cell receptors capable of mediating

these responses (e.g. natural cytotoxicity receptors). Therefore, although conjugate formation cannot be interpreted as a productive response (either to enhance or prevent target cell killing and/or cytokine production), it may still be a useful marker of direct NK cell responses to iRBCs in the absence of a more specific NK-iRBC interaction.

Analysis of individual KIR gene presence or absence suggested that having KIR2DL2 (a B haplotype gene) was associated with increased IFN-γ production, but this was not statistically significant for responses to iRBCs only (p= 0.40) or iRBCs+IL-15 (p= 0.15). Other KIR genes showed no effect on functional NK cell responses. It is possible that, as KIR2DL2 and KIR2DS2 are in close linkage disequilibrium, an increased IFN-γ response in individuals with this gene is due to the activating KIR2DS2 rather than inhibitory KIR2DL2, and these effects might be statistically significant in a larger study.

5.4.4 Conclusions

In conclusion, NK cells from LSHTM and Ugandan donors had similar genetic profiles, both in KIR gene carriage and KIR haplotype, but had very different expression and functional NK cell profiles. This appears to be heavily linked to maturation status of NK cells so that NKG2C-driven CD57+ and KIR2DL1+ subsets were increased in Ugandan individuals despite their young age compared to LSHTM donors, and is most likely to be a direct consequence of HCMV infection. Formation of NK-iRBC conjugates was variable in both populations and is not clearly explained by expression patterns of either KIRs or NKG2C, although there may be a link between inhibitory KIR expression and reduced proportions of NK-iRBC conjugation. However, it does appear that NK cells can and do interact with iRBCs in two different populations, although how this may occur and what implications it might have for immunity to malaria are still unclear.

6 | Evaluating the role of KIR2DL5 in NK cell recognition of *Pf*-iRBCs

6.1 Introduction

This chapter focuses on the carriage and expression of *KIR2DL5* in the LSHTM and Ugandan groups, with a focus on whether this KIR might play a role in the detection of malaria parasites by NK cells. The rationale for this investigation was the striking difference in the frequency of NK cell surface KIR2DL5 expression between these two groups of individuals as described in the previous chapter, despite very similar frequencies of *KIR2DL5* carriage, which provided an opportunity to explore the differences in expression of this gene based on its centromeric or telomeric location. Additionally, KIR2DL5 expression appeared to be strongly and selectively upregulated in two donors after a short incubation with *P. falciparum* infected red blood cells, raising the possibility that iRBCs might influence NK cell receptor expression and function. These data are shown at the end of this chapter.

KIR2DL5 was first described by Parham et al [86] as a novel gene expressed on NK cells and T cells with structural similarities to KIR2DL4. Orthologues of the gene have been found in several non-human primate species, but activating homologues have not been described [99] (KIR2DS5 is not a homologue). *KIR2DL5* actually consists of two highly homologous but distinct genes classified by their chromosomal location and designated *KIR2DL5A*, found in the telomeric region of the KIR complex, also referred to as the KIR2DL5-T locus, and *KIR2DL5B*, found in the centromeric region, also referred to as

the KIR2DL5-C locus [85]. *KIR2DL5* is found in all human populations, with the frequency of carriage of at least one copy ranging from 26-86%, and there are 21 described alleles, although many of these are only found at extremely low frequencies in African populations [303]. The majority of *KIR2DL5* alleles in both Asian and Caucasian populations are *KIR2DL5A*001* and *KIR2DL5B*002*, with frequencies of 25-31% and 28% of Caucasians and 43-60% and 20% of east and Southeast Asians estimated to be carriers of the respective alleles [87, 303]. *KIR2DL5A*005* is the second most commonly expressed telomeric allele, found in approximately 10% of Caucasians [87, 321].

Of particular importance, *KIR2DL5A*001* is the only KIR2DL5 protein detectable by flow cytometry by the α-2DL5 antibody UP-R1 [328]. *KIR2DL5A*005* is not detected by this antibody, although mRNA transcription has been detected [328]. *KIR2DL5B* genes are thought to be constitutively non-expressed [87, 292] and so are not detected on the cell surface apart from the centromeric alleles *KIR2DL5B*003/00602*, which are found at extremely low frequencies in African populations [303]. Table 6.1 summarises *KIR2DL5* gene frequency in a selection of the existing literature.

Author	Year	Reference	No. donors	Population	KIR2DL5+/%	*KIR2DL5A*/%	*KIR2DL5B*/%
Vilches	2000	[86]	108	Caucasian	51.9	n/a	n/a
Gomez-Lozano	2002	[85]	112	Caucasian	52.7	33.0	30.4
Yawata	2006	[297]	132	Japanese	18.5	15.9	2.6
Gomez-Lozano	2007	[87]	92	Caucasian	56.5	42.4	27.2
Santin	2007	[329]	71	Caucasian	78.9	56.3	22.5
Du	2008	[303]	250	Caucasian	48.4	34.0	28.4
			96	Asian-Indian	84.4	64.7	56.3
			32	African-American	56.3	18.8	50.0
			35	Asian	57.1	51.5	20.0
Mulrooney	2008	[321]	77	Caucasian	48.1	40.0	
Hou	2010	[102]	100	African-American	55.0	31.0	82.0
Kimoto	2010	[330]	256	Japanese	50.4	n/a	n/a
Garcia-Leon	2011	[331]	200	Caucasian	46.0	n/a	n/a
Jiang	2012	[101]	2999	Caucasian	30.2	n/a	n/a
Olaniyan	2014	[300]	554	African	76.7	n/a	n/a

Table 6.1: *KIR2DL5* frequency in different populations from selected publications. Percentages indicate the proportion of individuals with at least one copy of the gene, as stated by the authors. Proportions of *KIR2DL5A* and *KIR2DL5B* are included where available.

6.1.1 Copy number variation of *KIR2DL5*

Exchange of centromeric or telomeric regions occurs around the point of reciprocal recombination between *KIR3DP1* and *KIR2DL4* and generates new KIR haplotypes that may contain different KIR genes to the previous haplotype (described in Introduction, Section 1.1.4.3, reviewed in [3]), although genes are not duplicated or deleted by this exchange. However, KIR copy number can be highly variable within a haplotype due to non-reciprocal recombination during meiosis which leads to loss, duplication or recombination of genes [101, 332, 333]. Variable copy number has been seen frequently with B haplotypes but is comparatively rare in A haplotypes. The reasons for this are unclear, but greater variety in B haplotypes may be beneficial either during reproduction or during infection based on carriage of activating KIR genes [101]. The *KIR2DL5* duplication leading to *KIR2DL5A* and *KIR2DL5B* in different regions is thought to have occurred around 1.7 million years ago and is not seen in non-human primate species [90]. As the genes are on different regions of the chromosome, they are not in linkage disequilibrium and are subject to presence/absence variation, and so carriage of both *KIR2DL5A* and *2DL5B* together is estimated at around 12.5% in Caucasian populations [329] and 7% in African-Americans [102]. Copy number variation (CNV) therefore derives from reciprocal recombination events leading to both centromeric and telomeric gene carriage or duplication of *KIR2DL5* at the same locus, and therefore could result in CNV= 4 when both parental chromosomes are taken into account. However, in Caucasian populations estimated *KIR2DL5* CNVs are 24.7% CNV= 1, 5.43% CNV= 2 and 0.03% CNV= 3 (where the remainder are *KIR2DL5*-) [101]. It would be possible to carry four copies of *KIR2DL5*, but this would occur at extremely low frequencies in a population.

6.1.2 Association of *KIR2DL5* on the KIR locus

KIR2DL5 is in strong linkage disequilibrium with other some B haplotype KIR genes depending on both locus and allele. The most common centromeric allele, *KIR2DL5B*002*, is

associated with *KIR2DS3*001*, whereas *KIR2DL5A*001* is usually linked with *KIR2DS5*002*, leading to a broad association of centromeric *KIR2DL5* with *2DS3* and telomeric *KIR2DL5* with *2DS5* [99]. However, other common *KIR2DL5* alleles are often associated with other alleles of *KIR2DS3* and *KIR2DS5* which may reverse this association, including *KIR2DL5A*005* with *2DS3*002*. Therefore *KIR2DL5A* and *KIR2DL5B* both associate with *KIR2DS3* and *KIR2DS5* in the telomeric and centromeric regions [90]. Although KIR2DL5, 2DS3 and 2DS5 show the strongest linkage and are commonly cited as a cluster in disease association studies, due to their duplication and variable location it is difficult to pinpoint their location on the KIR locus. However, *KIR2DL5B* is 2030bp downstream of *KIR2DL2*, which is always confined to the centromeric region, and likewise *KIR2DL5A* is downstream of *KIR3DS1* on the telomeric region [292] (Figure 6.1). *KIR2DL2* and *KIR3DS1* have well-defined loci near the framework genes at the beginning of each KIR region (*KIR3DL3* and *KIR2DL4* respectively) and can be used as indicators of centromeric or telomeric region, and linkage of *KIR2DL5* with both genes has been established in multiple studies [102, 292]. These linkages allow for characterisation of *KIR2DL5* at the centromeric or telomeric locus by structural haplotype determination as described in [334]. However, it is also important to note that linkage disequilibrium between KIR genes has been found to be weaker in African populations, and so exceptions to these associations are possible [304].

6.1.3 Control of KIR2DL5 expression

In PBMC populations of individuals who express KIR2DL5, the subset of KIR2DL5+ NK cells is typically less than 10% of NK cells [328]. KIR2DL5 can be coexpressed with other inhibitory KIRs or found as the only inhibitory KIR on an NK cell [99, 328]. However, not all alleles of *KIR2DL5* are expressed due to methylation of the promoters upstream of the gene [87], which adds an additional level of complexity to KIR2DL5 expression patterns. Coding sequences of *KIR2DL5* are very similar and show no evidence of loss of function mutations (e.g. a stop codon) [87], but there are three structurally divergent

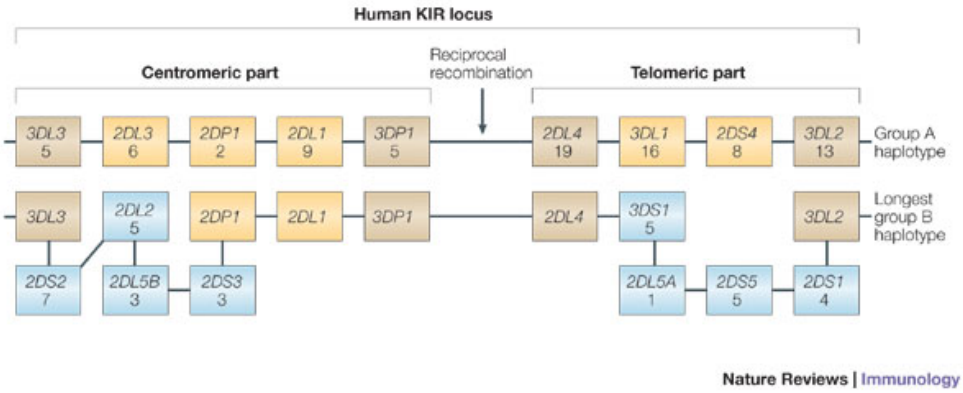

Figure 6.1: **Arrangement of *KIR2DL5* on the A and B haplotypes.** *KIR2DL5* genes are found on both the centromeric and telomeric regions of the KIR locus downstream of *KIR2DL2* and *KIR3DS1* in association with *2DS3* or *2DS5* respectively. Figure from Parham P, 2005, Nat. Rev. Immunol. [3].

promoters which regulate *KIR2DL5* expression, labelled as type I, II or III promoters [292]. Promoter types I and III allow clonal expression of 2DL5, but mRNA of 2DL5 alleles controlled by the type II promoter is undetectable (reviewed in [99]). Relatedly, the pseudogene *KIR3DP1* is controlled by the same type II promoter and is transcriptionally silent [335]. The type II promoter has a mutated binding site for the RUNX transcription factors that was suggested to be the barrier to transcription, but experiments showed that demethylation of the promoter site permitted transcription of *KIR2DL5*, suggesting that epigenetic methylation rather than the RUNX mutation prevents transcription of certain *KIR2DL5* alleles [87, 336]. However, as antisense transcripts from promoter regions have been suggested to regulate promoter function [337] and such antisense transcripts for *KIR2DL5B* have been detected in CD56 bright NK cells [105] (i.e. inhibiting promoter activity in NK cells that do not express KIRs), it has been suggested that the RUNX site downregulates the antisense promoter activity and permits gene transcription [337]. The non-expressed *KIR2DL5B* alleles are therefore constitutively turned off, rather than non-functional [87]. Additionally, after *in vitro* demethylation of promoter regions, type II promoters appeared to have greater activity than functional type I or III and induced higher levels of 2DL5 mRNA transcripts [87, 321].

6.1.4 Role as an inhibitory receptor and associations with malaria and autoimmune diseases

Although the functions of KIR2DL5 are unknown, KIR2DL5 contains ITIM domains and is thought to inhibit NK cell activation via recruitment of Src homology 2-containing protein tyrosine phosphatases -1 and -2 (SHP-1 and SHP-2) [338]. The role of KIR2DL5 in pathology has been explored for several autoimmune diseases including multiple sclerosis [331], celiac disease [329], and systemic lupus erythematosus (SLE) [330]. However, the results of these studies have varied by disease. Santin et al [329] found that carriage of *KIR2DL5B* without *KIR2DL5A* was associated with increased risk of celiac disease in Basque patients, which they suggest may be because KIR2DL5 expression is beneficial and inhibits NK cell cytotoxicity. Conversely, García-León et al [331] found that *KIR2DL5A* in combination with *KIR3DS1* (which suggests that 2DL5 is expressed) was associated with increased susceptibility to multiple sclerosis in Spanish individuals and potentially faster progression in disease pathology. Kimoto et al [330] found that carriage of *KIR2DL5* (without testing for *KIR2DL5A* or *KIR2DL5B*) was protective against SLE in Japanese subjects but associated with an increased risk of infection. All of these studies used comparatively small numbers of subjects (under 200 individuals), and it is difficult to draw any conclusions about whether 2DL5 is the underlying driver of either protection or pathology.

With regard to infectious diseases, carriage of *KIR2DL5* with *KIR3DS1* was suggested to be protective during hepatitis B infection in a Chinese population [339], although this has not been further substantiated. However, in malaria infection the *KIR2DL5/S3/S5* cluster has been suggested to be protective against symptomatic and severe malaria. Olaniyan et al [300] found that the combination of *KIR2DL5*, *2DS3* and *2DS5* was significantly more common in children with asymptomatic malaria than with uncomplicated or severe cases (defined as either cerebral malaria or severe anaemia), and furthermore that *KIR2DS3* and *2DS5* were more common in the uncomplicated malaria cases than in the severe cases. Although the authors did not test for *KIR2DL5A* or *KIR2DL5B* outright, centromeric and telomeric haplotypes were defined to some extent and c-AB2/t-AA individuals (car-

rying centromeric *KIR2DL2, 2DL5, 2DS3* and *2DS5* and telomeric AA haplotype genes excluding *KIR3DS1*) were protected against symptomatic malaria. This therefore suggests that *KIR2DL5B* is present in these donors, but *KIR2DL5A* (and *KIR2DS3/S5*) is not described in any of the telomeric haplotypes, which suggests either total absence of this gene or an oversight in the study analysis. Additionally it would be presumptuous to assume that *KIR2DL5B* is not transcribed as some alleles found in African populations are expressed [303]. The authors suggest that carriage of both A and B haplotype genes may be mediating protection against malaria, consistent with other studies also describing the 'heterozygote advantage' of KIR haplotypes [183, 202, 340], although another group have suggested that the AA haplotype may be protective against malaria in the Gambia [301]. None of these studies investigated either mRNA transcription or surface expression of 2DL5.

In conclusion therefore, the role of *KIR2DL5* in disease is still unclear. Expression of 2DL5 may be beneficial or detrimental during autoimmune diseases depending on the disease, which is likely to be consistent with the different pathologies of celiac disease and multiple sclerosis. In malaria infection, it seems that carriage of both A and B haplotypes is an advantage and that there may be a protective effect of centromeric *KIR2DL5* and *KIR2DS3/S5* genes, but these studies acknowledge their limitations in terms of haplotype resolution and numbers of individuals involved.

6.1.5 Aims

The aim of the work presented in this chapter is to explore the differences in gene frequency and expression levels of KIR2DL5 in both LSHTM and Ugandan donors by using droplet digital PCR to determine CNV and structural haplotype of *KIR2DL5*, and by flow cytometry to measure expression of 2DL5 on the NK cell surface. I have also tried to examine the effects of *KIR2DL5* gene carriage and expression on the interactions of NK cells with iRBCs to determine whether this KIR is involved in NK-iRBC conjugate formation or NK cell production of IFN-γ or degranulation responses.

6.2 Methods

6.2.1 DNA digestion by enzyme restriction

DNA was purified from whole blood as described in Methods, Section 2.8.1. Prior to analysing *KIR2DL5* copy number, DNA was digested by EcoRI restriction endonuclease so that each copy of the gene would be encapsulated in a separate droplet during ddPCR droplet generation. DNA from each donor was digested with EcoRI (New England Biosciences). 5µl of 100ng/µl DNA was incubated with 0.5µl EcoRI, 2µl 10x EcoRI buffer, and 15µl dH_2O at 37°C for 60 minutes in a water bath, then the digestion stopped by heating to 65°C for 20 minutes in a heating block. Samples were stored at 4°C.

6.2.2 Structural haplotype and copy number analysis by ddPCR

KIR2DL5 copy number variation (CNV) and haplotype (whether the gene is located in the centrometric or telomeric region) was determined by droplet digital PCR (ddPCR) according to a protocol designed by Chrissy h. Roberts and Robert Butcher (SOP 7.03 Droplet Digital PCR). ddPCR uses a water-oil emulsion to contain the reagents of a PCR reaction in a limiting dilution within c. 20,000 individual droplets, each of which contain one or zero copies of the DNA PCR target. The ddPCR reaction simultaneously detects two targets using fluorescent probes (here, fluorescein (FAM) and hexachloro-fluorescein (HEX)). Droplets are read in a flow cytometer-like droplet reader that measures and quantifies the number of PCR-positive and -negative droplets, allowing quantification of DNA copies per sample without needing reference to reference samples or calibration curves [341]. Droplets can be single or double positive, indicating which PCR reaction resulted in amplification. This method is explained and validated for KIR CNV and structural haplotype analysis in [334]. For KIR2DL5 copy number analysis, a probe for an internal reference gene of invariant copy number, *RPP30*, was included in the HEX channel and *KIR2DL5* was assayed on the FAM channel. The ratio of positive KIR target-droplets to positive *RPP30* targets was calculated and multiplied by two to correct for diploidy in KIR CNV estimates. Structural

haplotype analysis was based on linkage disequilibrium between KIR2DL5A and KIR3DS1 in the telomeric region and KIR2DL5B and KIR2DL2 in the centromeric region, as described above. As DNA targets are present at a limiting dilution in the ddPCR mixture, it is possible that two independent, physically unlinked DNA targets might be randomly confined in the same droplet, causing a double FAM+ HEX+ event, but the incidence of double positive events within a droplet will be much higher if the DNA targets are not independent and are physically linked, such as two KIR genes in close proximity on the same chromosome. Donors were genotyped for all KIR genes by SSP-PCR (described in Chapter 5, Methods) and *KIR2DL5+* donors were analysed for structural haplotype with either *KIR2DL2* or *KIR3DS1* as appropriate. Donors with both genes were assayed for linkage of *KIR2DL5* with each gene in two separate reactions. KIR2DL5 was assayed on the FAM channel and KIR2DL2 or KIR3DS1 was assayed on the HEX channel. Linkage was automatically calculated by the QuantaLife software by estimating the number of molecules in the assay carrying both target genes based on the number of double positive droplets. Linkage between *KIR2DL5* and *KIR2DL2* or *3DS1* can be abrogated by restriction endonuclease digestion, which reduces the linkage calculation as a control for whether gene linkage is actually present in double positive droplets. EcoRI digested DNA was used for copy number analysis, and for initial analyses of structural haplotype alongside uncut DNA as a proof of concept; uncut DNA was used for the majority of structural haplotype analysis (Figure 6.2).

Samples were prepared for droplet generation using a master mix of 10µl 2× SuperMix (Qiagen), 1µl primer mix (final primer concentration 0.3µM), 2.5µl DNA at 10ng/µl and 8.5µl dH_2O in a final volume of 22µl per well (shown in Table 6.2). Primer sequences are listed in Appendix B. Samples were mixed throughly but not vortexed to prevent shearing of the DNA. 20µl of sample and 70µl Droplet Generation Oil (BioRad) were loaded into the droplet generation cartridge (BioRad) in columns of eight. The cartridge was sealed with a rubber gasket and placed in the droplet generator (QX200 AutoDG Droplet Digital PCR System, BioRad). Target-free ddPCR mixtures and dH_2O only controls were included in each plate.

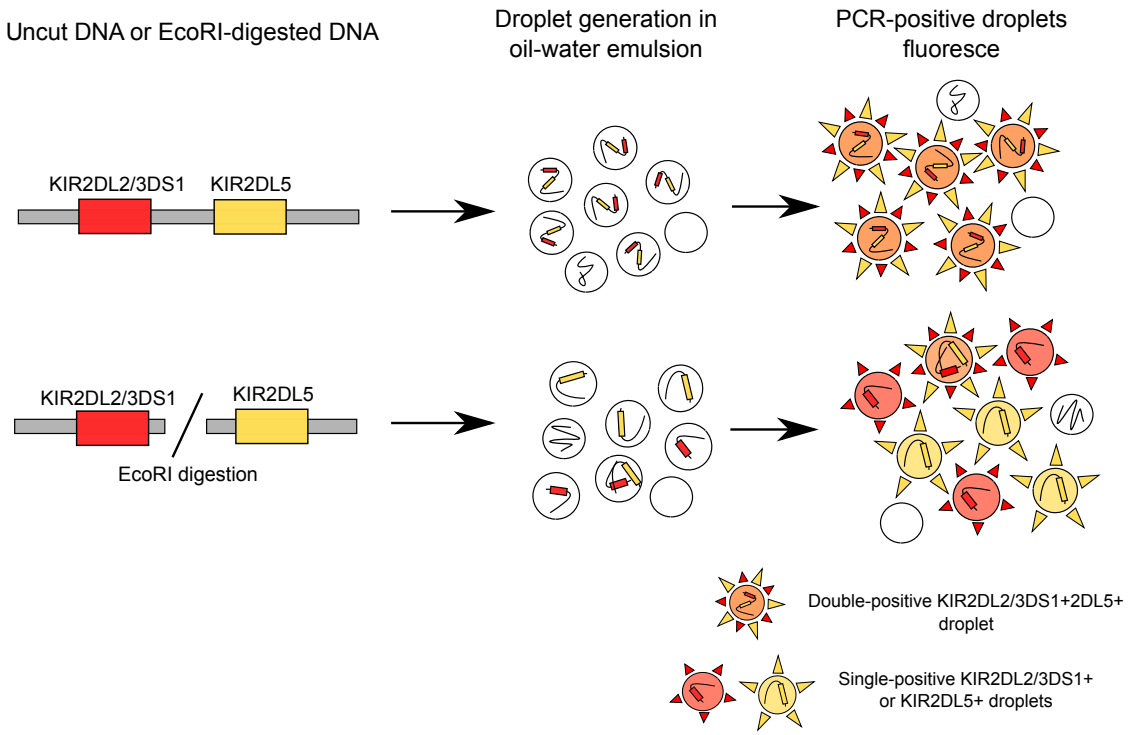

Figure 6.2: **Structural haplotype analysis by droplet digital PCR.** Droplet digital PCR uses oil to emulsify components of the PCR reaction into droplets each containing 1 or 0 copies of template DNA. For structural haplotyping, *KIR2DL2-2DL5* and *KIR3DS1-2DL5* are in close proximity on the KIR locus, but this linkage can be broken by digestion with EcoRI (*KIR2DL2/3DS1* shown in red, *KIR2DL5* in yellow). When confining the PCR reagents into droplets, linked DNA targets are likely to be encapsulated in the same droplet, whereas unlinked DNA templates are more likely to be separated. After the PCR, PCR-positive droplets fluoresce and are detectable by a droplet reader. Double positive fluorescent droplets (orange) indicate both genes are present, which is more probable if genes are linked, whereas single positive droplets contain only one gene.

After the droplets had been generated, samples were transferred to a clean PCR plate (Eppendorf) and heat sealed with foil. Samples were run in a thermal cycler (Applied Biosystems) under the program 'DDPCR', which consists of 10 mins at 95°C, 40 cycles of 15 seconds at 95°C and 1 min at 60°C, 10 mins at 98°C, and hold at 12°C. Droplets were counted immediately in a droplet reader (QX200 Droplet Reader, BioRad) and analysed with QuantaSoft software.

	Reagent	Volume/µl	Final conc.
Copy number variation	ddSupermix	11	1×
	KIR2DL5/RPP30 FAM/HEX primer	1	0.3µM
	dH_2O	8.5	
	DNA (EcoRI digested, 10ng/µl)	2.5	25ng/reaction
	Total	23	
Structural haplotype	ddSupermix	11	1×
	KIR2DL5-FAM primer	1	0.3µM
	KIR2DL2/KIR3DS1-HEX primer	1	0.3µM
	dH_2O	7.5	
	DNA (uncut, 10ng/µl)	2.5	25ng/reaction
	Total	23	

Table 6.2: ddPCR reaction mixtures

DNA samples with known *KIR2DL5* copy numbers were used as controls for copy number analysis. Samples KDNA0123, 0127, and 0128 were obtained from the UCLA International KIR Exchange [317] by Chrissy Roberts and were confirmed to have copy numbers of 3, 2 and 1 respectively [334].

6.2.3 Flow cytometry

PBMCs were stained in 96-well U-bottom plates as described in Methods, Section 2.6. After 2 hours cells were stained with fluorophore-labelled antibodies to cell surface markers then fixed, permeabilised (CytoFix/CytoPerm, BD Biosciences), and stained for intracellular molecules. Antibodies used were CD56-PE-Cy7, CD3-V500 (both BD Bioscience), KIR2DL5-APC or PE (clone UP-R1, Miltenyi Biotec, see Antibody Data Sheet in Appendix B for manufacturers' details), and 3D7HT-GFP parasites. Data were analysed with FlowJo, TreeStar. Statistical analyses were carried out by GraphPad Prism, version 6.0.

6.2.4 KIR2DL5 reporter cell line

A reporter cell line constitutively expressing KIR2DL5 was used to test for iRBC-2DL5 binding. 2B4 T cell hybridoma cells stably transfected with a NFAT-GFP reporter construct (first described in [342]) expressing 2DL5 on the cell surface will express GFP when bound to the 2DL5 ligand via a modified intracellular tail region. The positive control M2 antibody induces GFP expression by cross-linking the FLAG-tag on the modified 2DL5 tail. The reporter cell line was kindly provided by the Trowsdale group, Cambridge [343].

4×10^4 reporter cells were incubated for 18 hours with medium, 2×10^5 uRBCs, 2×10^5 iRBCs or M2 antibody, in triplicate. Cells were washed with FACS buffer and fixed with CytoFix/CytoPerm (BD Bioscience) for 30 minutes to fix iRBCs, then analysed for GFP expression by flow cytometry. For the positive control, flat-bottomed wells were coated with goat anti-mouse antibodies and incubated with M2 antibody for 30 minutes before washing with PBS. PBS was used as a negative control for the M2 antibody incubation. Reporter cells were separately incubated with medium, uRBCs or iRBCs for 18 hours and stained with α-2DL5-APC to test the stability of 2DL5 expression and analysed by FACS.

6.3 Results

6.3.1 Expression of KIR2DL5 via FACS

Expression of KIR2DL5 on the NK cell surface is highly variable due to promoter variation. However, the majority of studies on KIR2DL5 have used mRNA to determine expression and the expression per cell has been difficult to assess. The anti-KIR2DL5 antibody for flow cytometry, UP-R1, was first described by Estefania et al in 2007 [328]. UP-R1 recognises the most commonly expressed form of KIR2DL5, KIR2DL5A*001, but not KIR2DL5A*005 or any of the KIR2DL5B proteins. PBMCs were incubated for 2 hours with medium and stained for NK cell expression of KIR2DL5 (Figure 6.3). Expression patterns are shown for six donors of known genotype. *KIR2DL5-* donors showed no background 2DL5 staining (Fig. 6.3A), and some *KIR2DL5+* donors had no 2DL5+ NK cells (Fig. 6.3B), low percentages of 2DL5+ NK cells (Fig. 6.3C), or high percentages of 2DL5+ NK cells (Fig. 6.3D). No donors had greater than 10% 2DL5+ NK cells, consistent with the literature [99, 328]. The same patterns were seen in Ugandan donors where *KIR2DL5+* donors did (Fig. 6.3F) or did not (Fig. 6.3E) express surface 2DL5. This staining suggests that the UP-R1 antibody is specific for KIR2DL5, but cannot guarantee that the antibody has stained all 2DL5+ cells.

Of individuals expressing 2DL5, there was a significant difference in the percentage of 2DL5+ NK cells between LSHTM and Ugandan groups (p= 0.014, Mann-Whitney t test) (Figure 6.4A). Numbers of individuals were low (n= 13 and n= 5 for LSHTM and Uganda respectively), but may indicate that within the Ugandan group even 2DL5 expressors have lower proportions of 2DL5+ NK cells than LSHTM donors. Likewise, mean fluorescence intensity (MFI) of 2DL5 on NK cells was lower in Ugandan donors, which may also indicate that 2DL5 expression is lower on individual NK cells (p= 0.0025, Mann-Whitney test) (Fig. 6.4B). However, donor numbers were small and further investigation is required to test whether expression levels differ between these populations (not all LSHTM data are shown for MFI as different fluorophores (2DL5-PE or APC) were used for some experiments, MFI

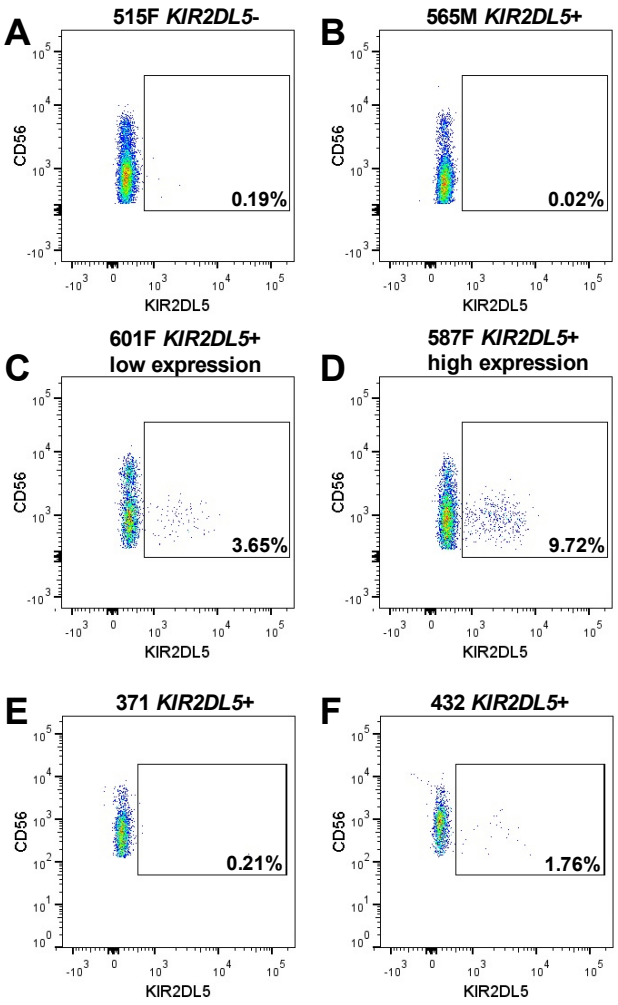

Figure 6.3: **Expression of KIR2DL5 on NK cells by FACS.** FACS plots showing KIR2DL5 staining on NK cells with the KIR2DL5-specific UP-R1 antibody on four LSHTM donors: a *KIR2DL5* negative donor (A), a *KIR2DL5* positive non-expressor (B), a *KIR2DL5* positive low expressor (C), and a *KIR2DL5* positive high expressor (D); and staining on two Ugandan donors: a *KIR2DL5* positive non-expressor (E) and a *KIR2DL5* positive expressor (F). The percentage of positive cells is indicated within each gate.

data shown are APC-stained cells only). These data suggest that different KIR2DL5 alleles may be present in LSHTM and Ugandan donors.

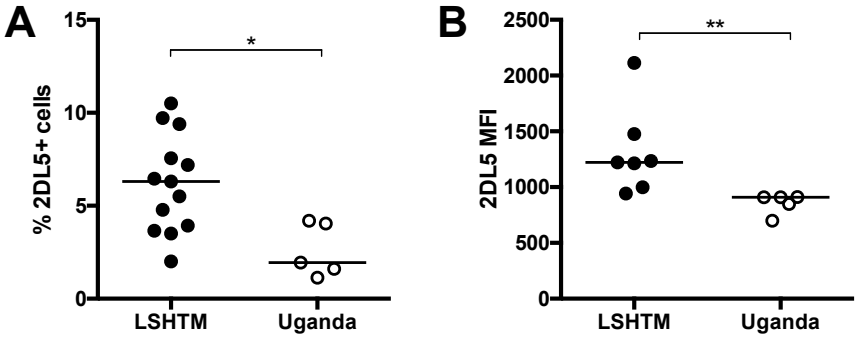

Figure 6.4: ***KIR2DL5*+ donors from LSHTM have larger populations of 2DL5+ NK cells than do *KIR2DL5*+ Ugandan donors.** Percentages of 2DL5+ NK cells are higher in donors from LSHTM (n= 13) than from Uganda (n= 5) (A). Mean fluorescence intensity (MFI) of 2DL5+ NK cells is higher in LSHTM donors (n= 7) than Ugandan donors (n= 5) (B). MFI data from 2DL5-APC stained cells shown only. Bars indicate medians, statistical analyses by Mann-Whitney t tests. * $p< 0.05$, ** $p< 0.01$.

6.3.2 KIR2DL5 presence/absence genotyping

As described in Chapter 5, both the LSHTM and Ugandan donors were genotyped for presence or absence of KIR genes including *KIR2DL5*. Due to low DNA yield from many of the Ugandan samples, a restricted genotyping panel for KIR presence/absence was run on 37 of the 53 donors looking at only *KIR2DL5*, *KIR2DL2* and *KIR3DS1* (Table 6.3). The remaining sixteen Ugandan samples and all LSHTM samples were genotyped for all seventeen KIRs (Chapter 5, Table 5.5; see also Appendix C).

Percentages of donors carrying *KIR2DL5* were similar in both groups, but *KIR3DS1* frequency was statistically significantly lower in Ugandan donors (p= 0.017, Fisher's χ^2 test), consistent with gene frequencies described elsewhere [300], whereas *KIR2DL2* frequency was slightly higher in Ugandan donors than LSHTM donors (not significant). Nine LSHTM (18.8%) and six Ugandan donors (12.0%) were positive for all of *KIR2DL5, 2DL2* and *3DS1*. One Ugandan donor (318-W) had *KIR2DL5* but neither *KIR2DL2* or *3DS1*, which is rare but has been reported [334]. As the LSHTM population has a primarily Caucasian background but is not homogenous (see Methods, Table 2.1 for donor information), these gene frequencies are consistent with the published data summarised in Table 6.1

where around half of Caucasians are *KIR2DL5*+ [85, 321, 331]. There are limited data for *KIR2DL5* frequency in African populations [300, 303], but my data are in line with previous studies suggesting that African populations have high *KIR2DL5* frequencies but tend to carry different *KIR2DL5* haplotypes from Caucasian populations. Although the frequency of *KIR2DL5*+ subjects was similar between the populations, the differing frequencies of *KIR2DL2* and *KIR3DS1* suggest that different haplotypes are present in each population. This was further investigated by ddPCR.

KIR gene	LSHTM (n=48)		Uganda (n=50)		p value
	n	%	n	%	
2DL5	32	66.7	34	68.0	1.000
2DL2	25	52.1	32	64.0	0.306
3DS1	21	43.8	10	20.0	0.017

Table 6.3: Frequency of *KIR2DL5, 2DL2* and *3DS1* in LSHTM and Ugandan donors.

6.3.3 KIR2DL5 copy number analysis

Droplet digitial PCR was used to analyse *KIR2DL5*+ samples for CNV and structural haplotype. *KIR2DL5* CNV was measured in EcoRI digested DNA by comparing CNV with a reference gene, *RPP30*, which invariably appears once per haplotype. The majority of individuals have one or two copies of *KIR2DL5* (Figure 6.5). DNA samples from donors in the UCLA KIR exchange programme previously analysed for both CNV and structural haplotype [334] (KDNA samples 0123 and 0128, copy number= 3 and 1 respectively) were used as controls in each machine run, and DNA from sample KDNA0127 was used as a reference sample (copy number= 2). DNA from donors without *KIR2DL5* did not amplify and measured copy number= 0. Machine assigned *KIR2DL5* copy numbers for each sample were made by reference to the internal reference gene *RPP30* and the KDNA0127 reference sample, an example of which can be seen in Fig. 6.5A; the sample with copy number= 3 is KDNA0123 [334], and the KDNA0127 reference and non-template control (NTC) spaces

are empty. Copy numbers could be plotted and grouped into integer copy numbers from the raw data (Fig. 6.5B).

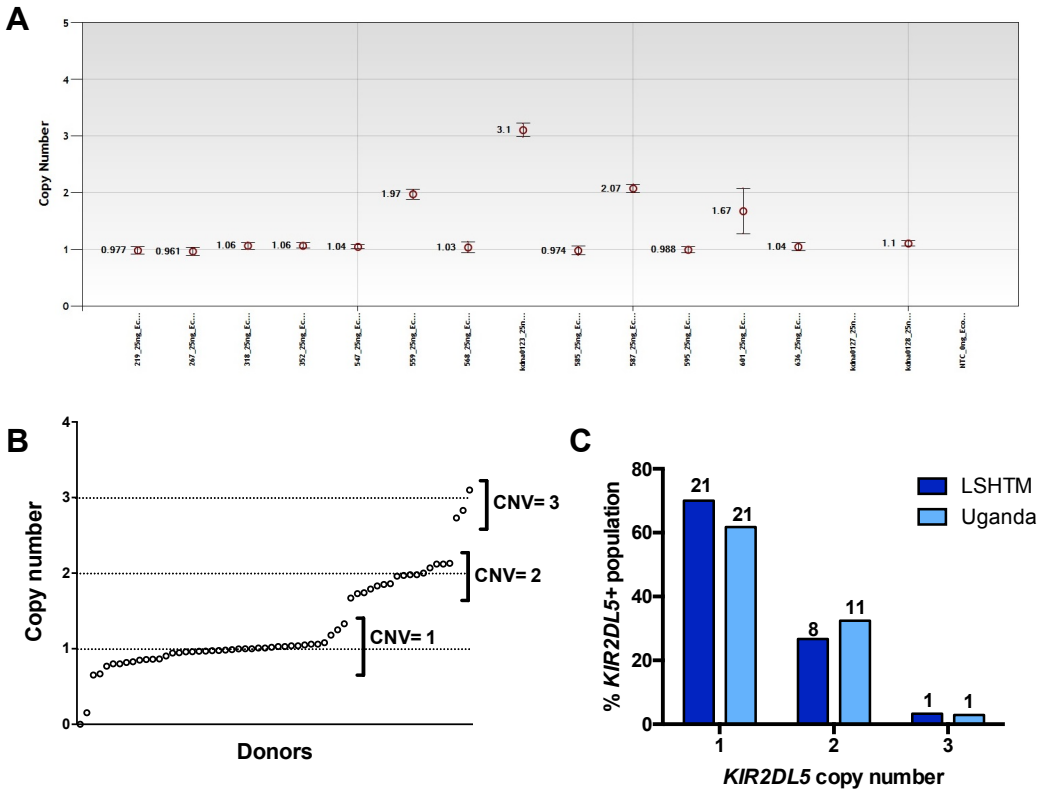

Figure 6.5: **Measuring *KIR2DL5* copy number variation using ddPCR.** CNV of *KIR2DL5* was determined as a ratio to RPP30. Copy number of each donor was assigned by the software (A), and checked manually. CNV values vary but can be assigned to an integer (0, 1, 2, 3) (B). Comparison of CNV between the LSHTM and Ugandan populations as a percentage of individuals with 1, 2 or 3 copies (C). n is indicated above each bar.

Among the LSHTM group (n= 32), 21 donors had a single copy of *2DL5*, 8 had two copies, and one had three copies. In the Ugandan group (n= 34), 21 donors had one copy of *2DL5*, 11 had two, and one had three (Fig. 6.5C). DNA quality was too low for analysis in two LSHTM donors and one Ugandan donor. There were no significant differences in *KIR2DL5* copy number frequency between the populations (Fisher's χ^2 tests).

6.3.4 KIR2DL5 structural haplotype

The location of *KIR2DL5* in the centromeric or telomeric regions of the KIR complex can be determined by linkage to *KIR2DL2* or *KIR3DS1* respectively. This analysis was carried out by ddPCR, using primers for each gene linked to a fluorescent probe in the channels FAM and HEX. Within the droplets in which the PCR reaction takes place, linked genes are more likely to be present on the same strand of DNA; therefore if *KIR2DL5* is in close proximity to either *KIR2DL2* or *KIR3DS1*, both genes in the reaction should amplify and fluoresce, creating a double positive droplet that can be detected by the plate reader. If the genes are not linked, the likelihood of both being present in the same droplet are much lower, and there will be a lower frequency of double positive droplets. Endonuclease digestion with EcoRI was used to break the linkage between genes and therefore act as a control to show that the genes are truly linked, rather than being independently captured within the same droplets.

ddPCR was carried out for all 64 donors who were *KIR2DL5+* by presence/absence genotyping to test for linkage to *KIR2DL2*, *KIR3DS1* or both based on which gene(s) prior genotyping had indicated were present (Figure 6.6). If the genotyping was unclear, linkage to both genes was tested. Sample plots from the QuantaSoft analysis software, similar to flow cytometry quadrants, show the number of double positive events (orange dots, circled) indicating linkage after DNA digestion by EcoRI (Fig. 6.6A) or without EcoRI digestion (Fig. 6.6B). Single positive events are shown in blue and green, and indicate droplets where only one PCR target has been amplified (i.e. *2DL5+2DL2-* and *2DL5-2DL2+* droplets). Linkage between *KIR2DL2* and *KIR2DL5* is clearly abrogated after digestion (Fig. 6.6C). As DNA can be sheared during extraction or handling, thus manually breaking the linkage between genes, some *KIR2DL2-2DL5* and *KIR2DL5-3DS1* linkage values were low despite a high likelihood that *KIR2DL5* was associated with *KIR2DL2/3DS1* (based on carriage of the other gene and expression data), but if linkage values are reduced by EcoRI digestion, low values are likely to be valid even if DNA quality is poor. This was clear for some donors (568, 219, 091, Fig. 6.6C) who had uncut DNA raw linkage values near the

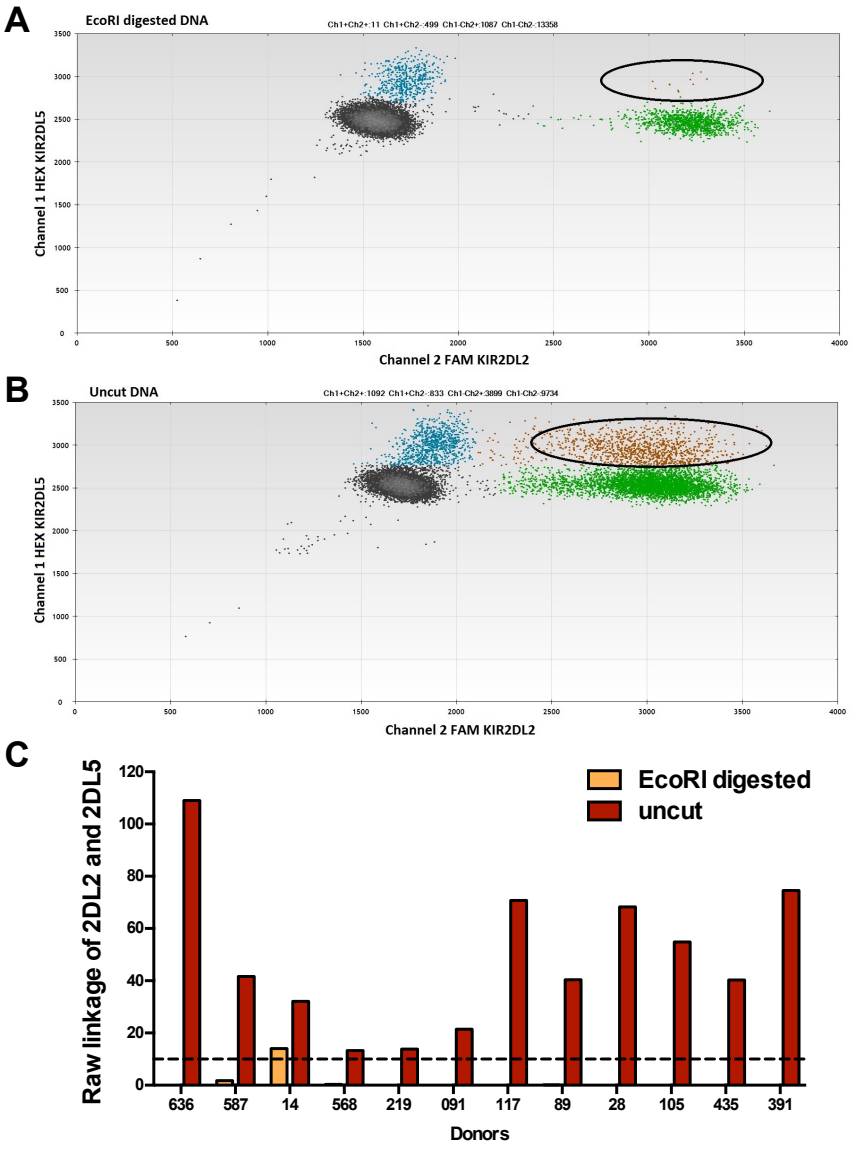

Figure 6.6: **Characterising *KIR2DL5* linkage using ddPCR analysis.** Digital droplet PCR was used to analyse linkage between *KIR2DL5* (HEX channel) and *KIR2DL2* (FAM channel). Plots of double positive (orange), single positive *KIR2DL5* (blue) and *KIR2DL2* (green), and double negative (grey) events after PCR amplification with EcoRI digested DNA (A) and uncut DNA (B) for one donor. Comparison of the linkage scores between *2DL2* and *2DL5* for digested (orange bars) and undigested DNA (red bars) for thirteen donors (C). The dotted line indicates an arbitrary cutoff value of 10, below which DNA was judged to be unlinked.

arbitrary cut off (10, indicated by the dotted line), but who had linkage scores of 0 after EcoRI digestion. DNA from donor 14 was not fully digested by EcoRI, and therefore some linkage was still detected. *KIR2DL5-3DS1* linkage analysis was carried out in the same way (not shown).

Structural haplotype analysis allowed assignment of *KIR2DL5* to the centromeric (C+) or telomeric (T+) regions. In donors with *KIR2DL5* CNV ≥ 2, it was also possible to determine whether *KIR2DL5* was present in either or both regions based on the ratio of *KIR2DL2* or *KIR3DS1* to *KIR2DL5* (Figure 6.7) in addition to the known copy number data of *KIR2DL5*. Ratios of *KIR2DL2/3DS1* to *KIR2DL5* were automatically generated by the QuantaSoft software. For example, a donor with one copy of *KIR2DL5* and a 3DS1:2DL5 ratio of 1 also has one copy of *KIR3DS1* (Fig. 6.7A, donor 352, T+), and similarly a donor with two copies of *KIR2DL5* and 3DS1:2DL5= 1 has two copies of *KIR3DS1* (donor 559, T+ T+). Conversely, a donor with a ratio of 0.5 has one copy of 3DS1 and two copies of 2DL5, and is likely to also have *KIR2DL2-2DL5* linkage (donor 587, C+ T+). Two donors each with one copy of *KIR2DL2* and *KIR3DS1* and two copies of *KIR2DL5* had 2DL2:2DL5 and 3DS1:2DL5 ratios of 0.5 (Fig. 6.7B), which indicates carriage of one *KIR2DL5* on both the centromeric and telomeric regions (C+ T+). One LSHTM donor (594) had three copies of *KIR2DL5* and one copy of both *KIR2DL2* and *KIR3DS1*, with linkage to both genes, and it was therefore not possible to be sure where the third copy of *KIR2DL5* was located. This donor has been noted as C+ T+ C/T, and may represent a haplotype with a duplication of *KIR2DL5* at one of the loci.

Analysis of structural haplotype by ddPCR showed that all but one of the donors expressing surface 2DL5 by FACS analysis had at least one telomeric *KIR2DL5* linked to *KIR3DS1*, consistent with the idea that *KIR2DL5A* alleles are expressed and *KIR2DL5B* alleles are not. In both populations combined (n= 56), four donors had two copies of *KIR2DL5* and one copy of *KIR2DL2* but did not carry *KIR3DS1*. Of these four, one donor expressed 2DL5. It is therefore possible that these donors have duplicated centromeric copies of *KIR2DL5*, or one centromeric copy and a telomeric copy that has become unlinked from *KIR3DS1*. It is not possible to definitively assign the location of the second gene to the

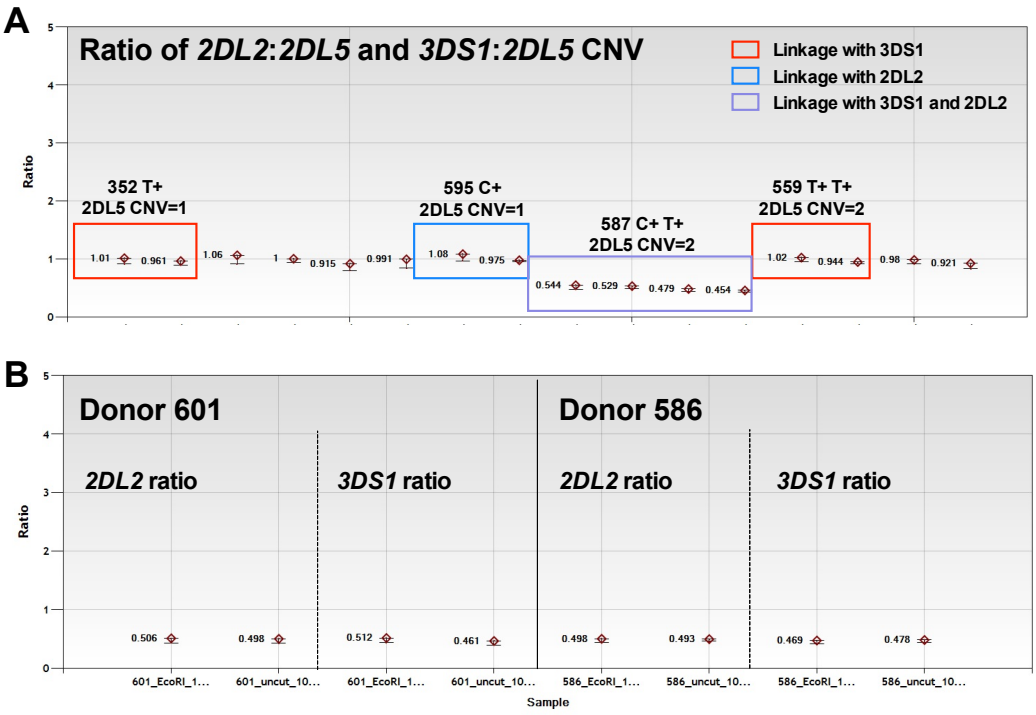

Figure 6.7: **Determining *KIR2DL2* and *3DS1* CNV as a ratio of *KIR2DL5*.** From the droplet digital PCR analysis for structural haplotype, it was possible to determine the ratio of *KIR2DL2* and *KIR3DS1* to *KIR2DL5*. Sample plots show ratios of 2DL2 (blue boxes) or 3DS1 (red boxes) to 2DL5 after ddPCR amplification for different LSHTM donors with copy numbers of 2DL5 indicated (A). The purple box indicates that both 2DL2 and 3DS1 linkage was tested in donor 587. Two donors with two copies of *KIR2DL5* and linkage to both *KIR2DL2* and *3DS1* have ratios of c. 0.5 (B).

telomeric region in the absence of *KIR3DS1* with this assay, and haplotype sequencing would be required to determine the location of the gene or whether the *KIR2DL5* allele is one of the rare expressed centromeric alleles found in African populations [303].

6.3.5 Comparing haplotype and expression between populations

From these experiments, it is possible to compare the LSHTM and Ugandan populations by carriage of *KIR2DL5*, 2DL5 expression within each group, and the frequency of *KIR2DL5A* and *KIR2DL5B* and structural haplotype within *KIR2DL5*+ individuals within each group

(Figure 6.8). The percentage of donors with *KIR2DL5* in the LSHTM and Ugandan populations is similar, but the number of individuals expressing 2DL5 on the NK cell surface is significantly lower among the Ugandan donors (p= 0.014, Fisher's χ^2 test) (Fig. 6.8A). Structural haplotyping data allowed determination of *KIR2DL5A* and *KIR2DL5B* frequencies based on linkage to *KIR3DS1* and *KIR2DL2* respectively, and showed that *KIR2DL5A* was significantly less common in Ugandan donors than in LSHTM donors (p= 0.010), but *KIR2DL5B* was present at similar frequencies (p= 0.284) (Fig. 6.8B), which is consistent with previously published studies (Table 6.1). Combining *KIR2DL5* copy number analysis and structural haplotyping therefore indicated how many donors in each group had one or more centromeric or telomeric copies of *2DL5*, grouped as C+, C+C+, T+, T+T+, C+T+, or 'other' (which includes donors with CNV= 3 and possible *KIR2DL5* duplications) (Fig. 6.8C). Ugandans with 2 copies of *KIR2DL5* were more likely to be C+C+ than C+T+ or T+T+ compared to LSHTM donors (p= 0.041, comparing n C+C+ with combined C+T+ or T+T+ donors); in this sample, no Ugandans had two copies of telomeric *KIR2DL5*. Full results of ddPCR analysis and assigned CNV and structural haplotype are shown in Appendix C.

Expression of KIR2DL5 was clearly linked to the telomeric haplotype. In both populations, donors with only C+ or C+C+ haplotypes did not express 2DL5 on the NK cell surface. One donor in the 'other' category expressed 2DL5 in the absence of a clear telomeric *KIR2DL5* gene, suggesting a rare expressed *KIR2DL5B* allele or a *KIR2DL5A* allele unlinked from *KIR3DS1*. The 2DL5 FACS antibody UP-R1 is thought to be specific for the product of *KIR2DL5A*001* only (and not *KIR2DL5A*005*), but as expressed *KIR2DL5B* alleles are so rare it is possible that UP-R1 may detect other 2DL5 alleles as well. The percentage of 2DL5+ NK cells in a donor does not appear to correlate with either total *KIR2DL5* copy number or with *KIR2DL5* T+ copy number, in contrast to the 'gene dosing' effect seen with other KIR genes where increased copy number leads to greater expression within the NK population.

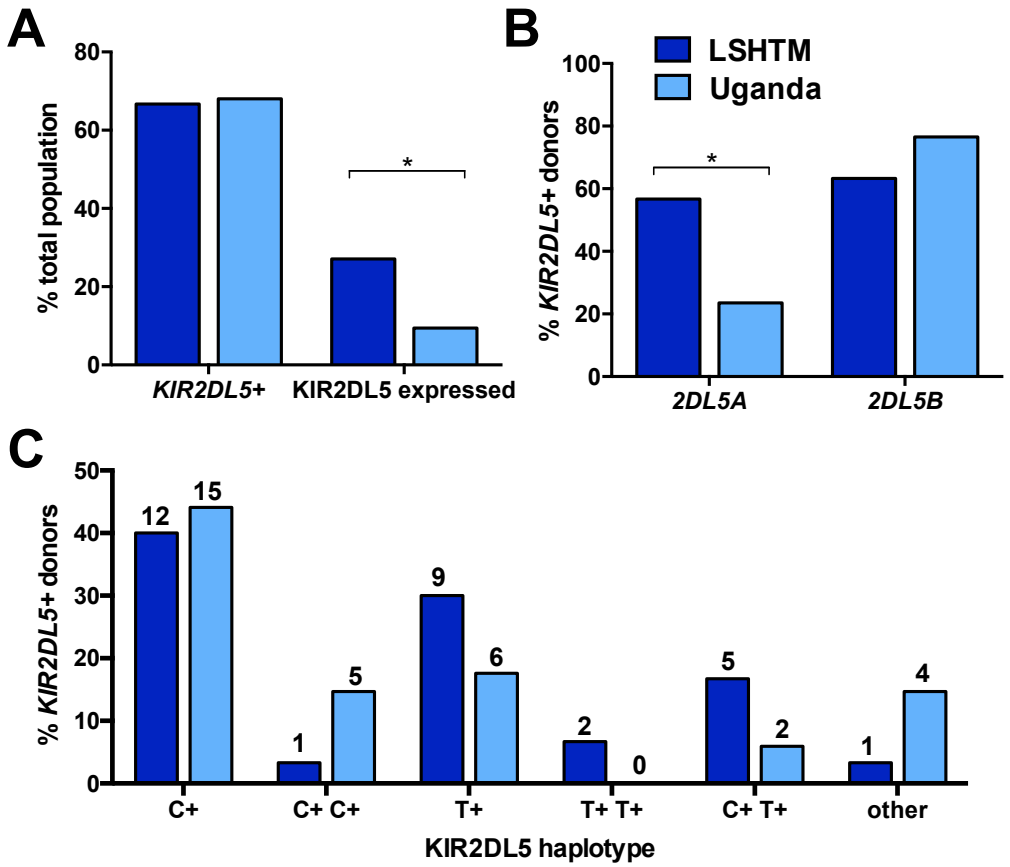

Figure 6.8: **KIR2DL5 genotype and surface expression differs between populations.** Comparison of LSHTM (dark blue) and Ugandan (light blue) populations. Percentage of the total population who are *KIR2DL5*+ and percentage that express 2DL5 on the NK cell surface (A). Percentage of *KIR2DL5*+ donors carrying *KIR2DL5A* or *KIR2DL5B* (B), and haplotype breakdowns by number of *KIR2DL5* copies and centromeric/telomeric location (C+, C+C+, T+, T+T+, C+ T+, other). n is indicated above bars. Statistical analyses by Fisher's χ^2 tests. * $p < 0.05$.

6.3.6 KIR2DL5 expression affects NK cell responses to iRBCs

The role of KIR2DL5 is unknown, and no ligands for 2DL5 have yet been identified. However, as preliminary data (Chapter 5) suggested that 2DL5 and iRBCs might interact, I analysed NK cell responses to iRBCs by whether donors were positive or negative for *KIR2DL5* and whether or not they expressed 2DL5 at the cell surface.

Two assays were used to assess NK cell function, both of which have been described in previous chapters. To measure IFN-γ and CD107a, PBMCs were incubated with schizont-stage iRBCs with or without 0.75ng/ml IL-15 for 18 hours and stained for functional markers (see Chapter 4). To measure conjugate formation, PBMCs were incubated with schizont-stage GFP+ iRBCs for 2 hours before staining for phenotypic markers including 2DL5 and measuring the percentage of CD3- CD56+ GFP+ events (i.e. a CD56+ NK cell attached to a GFP+ iRBC) (see Chapter 5). Donors were divided by carriage of *KIR2DL5* (Figure 6.9A-C) and by expression of 2DL5 on the NK cell surface (Fig. 6.9D-F).

There was a slight trend towards increased IFN-γ and CD107a responses in donors with *KIR2DL5* (Fig. 6.9A, B), but this was not statistically significant (Mann-Whitney t tests). These data are consistent with Figure 5.11, Chapter 5, and are likely to indicate a difference in KIR gene AA and Bx haplotype between donors as other B haplotype KIR genes will be present in the *2DL5+* donors, rather than the presence of *KIR2DL5* itself. There were no differences in the percentage of NK-iRBC conjugates formed based on *KIR2DL5* carriage (Fig. 6.9C). Conversely, 2DL5 expression appeared to slightly decrease both IFN-γ and CD107a responses (Fig. 6.9D, E), though the differences between expressors and non-expressors were also not statistically significant. However, donors expressing surface 2DL5 formed significantly fewer NK-iRBC conjugates than donors without 2DL5 expression (p= 0.023, Mann-Whitney t test). This suggests that 2DL5 signalling may inhibit the ability of NK cells to form conjugates and potentially to respond to malaria parasites.

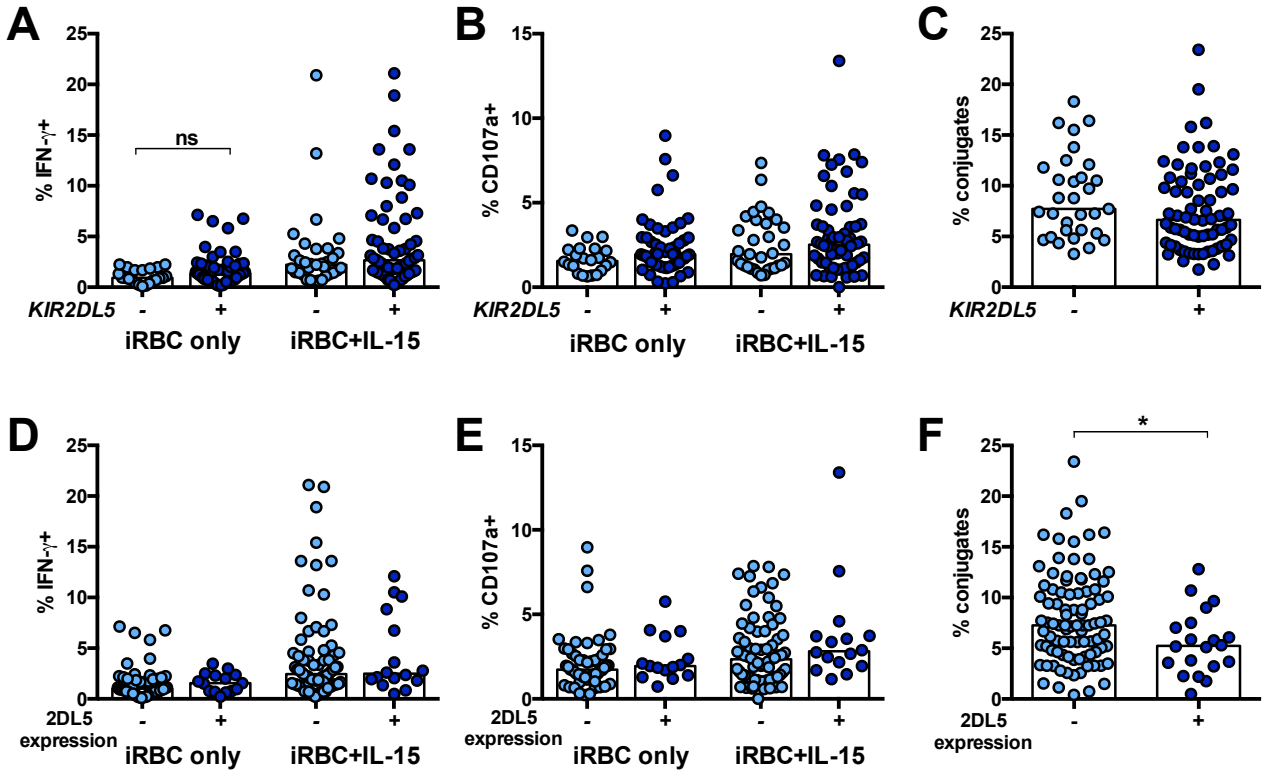

Figure 6.9: **KIR2DL5 genotype and expression correlates with NK cell IFN-γ production and conjugate formation.** Functional responses of NK cells (IFN-γ and CD107a responses to iRBCs or iRBCs+IL-15 after 18 hours, NK-iRBC conjugate formation after 2 hours) were divided into groups of *KIR2DL5* negative (n= 33) and positive donors (n= 64) (A-C), and into 2DL5 expressors (n= 16) and non-expressors (non-expressors includes both *KIR2DL5* negative and positive individuals, n= 78) (D-F). Statistical analyses by Mann-Whitney tests, bars indicate medians. * $p< 0.05$, ** $p< 0.01$, *** $p< 0.001$, **** $p< 0.0001$.

6.3.6.1 Blocking surface KIR2DL5 expression

As surface expression of KIR2Dl5 on NK cells was associated with reduced conjugate formation with iRBCs, I tested whether blocking KIR2DL5 on the NK cell surface affected conjugate formation. PBMCs and iRBCs were incubated for 2 hours with an excess of unconjugated α-KIR2DL5 antibody (UP-R1 clone). Preliminary experiments attempted to titrate the concentration of unconjugated antibody to block KIR2DL5 expression, but were unsuccessful, and so an excess of antibody was used (at a dilution of 1:5). The manufacturer's recommended concentration for FACS staining is a dilution of 1:11, although the concentrations used in our lab after titration is 1/20. A dilution of 1:5 was therefore considered to be sufficient excess antibody. In addition, the α-2DL5 antibody is prepared in sodium azide, so higher concentrations of antibody would have been detrimental to the cells in culture (see Appendix B for antibody data sheet). Six replicates of PBMCs from four *KIR2DL5*+ donors, three of whom were KIR2DL5 expressors, were incubated with uRBCs or iRBCs for two hours and then stained for KIR2DL5 and conjugate formation (CD56+ GFP+ events) measured by FACS (Figure 6.10).

Blocking 2DL5 with unconjugated UP-R1 Ab was partially successful. Gating for NK cells expressing 2DL5 with or without blocking, 2DL5 MFI, and NK-iRBC conjugate formation are shown in Fig. 6.10A. The total percentage of 2DL5+ NK cells was only slightly reduced after blocking (Fig. 6.10B) in two donors, but the mean fluorescence intensity (MFI) of 2DL5 was slightly but significantly reduced in all three donors expressing 2DL5 (donors 2-4), indicating that each cell expressed less 2DL5 after blocking (Fig. 6.10C). Comparing NK-iRBC conjugate formation with or without unconjugated 2DL5 showed a small but significant decrease in conjugate formation after blocking (p= 0.031, Wilcoxon test), which could suggest that KIR2DL5 plays a role in conjugate formation. However, as the blocking antibody did not bind all the 2DL5 on the NK cell surface, this should be interpreted with caution and repeated with higher concentrations of blocking antibody. Conjugate formation may also have been inhibited by non-specific blocking of binding sites by the antibody, as an isotype control was not used in the unblocked conditions.

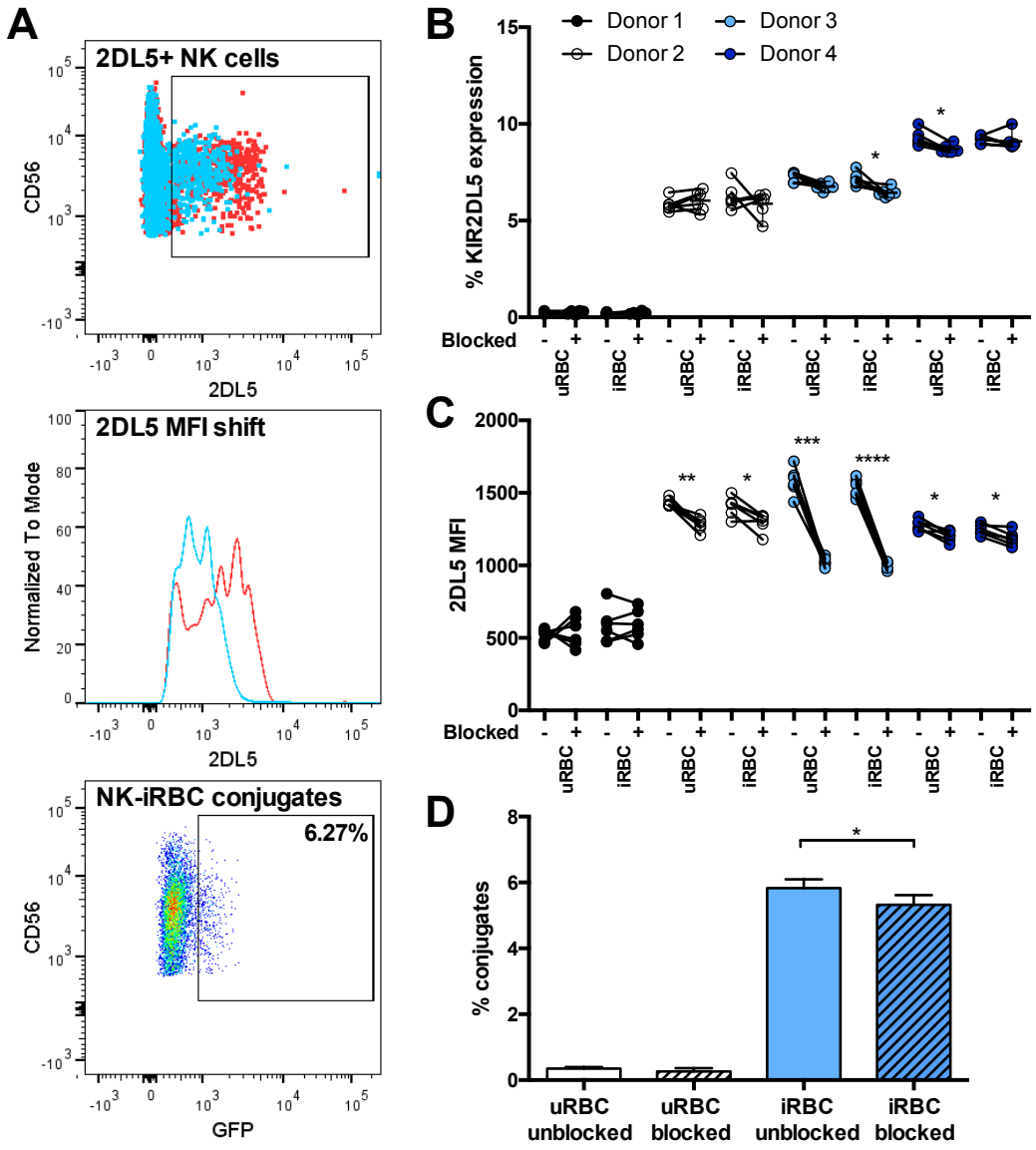

Figure 6.10: **Blocking surface KIR2DL5 genotype affects conjugate formation.** PBMCs were incubated with GFP-iRBCs in the presence or absence of unconjugated α-2DL5 antibody, then stained for FACS (n= 4). FACS plots show changes in 2DL5+ NK cells and 2DL5 mean fluoresence intensity in the absence (red dots/line) and presence (blue dots/line) of α-2DL5 Ab for donor 3, and sample gating for NK-iRBC conjugate formation without α-2DL5 Ab (A). Percentage of NK cells per donor expressing 2DL5 after incubation with uRBCs or iRBCs without (−) and with (+) α-2DL5 (B), and the change in MFI (C). Change in the percentage of NK-RBC conjugates after incubation with uRBCs or iRBCs, with or without α-2DL5 blocking Ab (D). * $p<$ 0.05, ** $p<$ 0.01, *** $p<$ 0.001, **** $p<$ 0.0001.

Overall, looking at the analysis of IFN-γ and conjugate formation against KIR2DL5 expression, the possibility that KIR2DL5 expression reduces the average number of conjugates formed suggests that KIR2DL5 is inhibiting NK cell function, which would be consistent with its hypothesised role as an inhibitory KIR, but further experiments are needed to confirm or refute this hypothesis.

6.3.7 KIR2DL5 expression may vary after incubation with iRBCs

Preliminary data indicated that KIR2DL5 surface expression was increased on NK cells from some LSHTM donors after a short (2 hour) incubation with iRBCs, raising the question of how this might occur within a short time frame. One possibility was that KIR2DL5 could be stored intracellularly and subsequently externalised during NK cell stimulation. To investigate whether there might be an intracellular store of KIR2DL5, PBMCs from both LSHTM (n= 27) and Ugandan donors (n= 53) were incubated with uRBCs or iRBCs for 2 hours and then surface stained with α-CD56, α-CD3 and α-2DL5-APC and fixed as normal, and then stained again with α-2DL5-PE in an attempted 'intracellular' stain. Whether the antibody was capable of binding to 2DL5 within the cell was unclear. As has been established, the UP-R1 antibody is selective, and intracellular 2DL5 might have a different conformation to surface expressed 2DL5. It is also possible that the second α-2DL5-PE stain could bind surface rather than internal 2DL5, although α-2DL5-APC should stably bind all available sites and any unbound 2DL5 epitopes on the cell surface will be destroyed by fixation.

Representative FACS plots of extracellular and intracellular staining from four different donors indicated that 2DL5 expression increases after incubation with iRBCs (Figure 6.11). NK cells from a *KIR2DL5* negative donor, 515F, did not express either surface or intracellular 2DL5 in response to uRBCs or iRBCs (Fig. 6.11A). However, all *KIR2DL5*+ donors showed an increase in intracellular 2DL5 expression after incubation with iRBCs (Fig. 6.11B-D). This was the case even if the donor carried *KIR2DL5B* (318F), which was not expressed on the NK cell surface; a copy of *KIR2DL5A* that was also not expressed on the

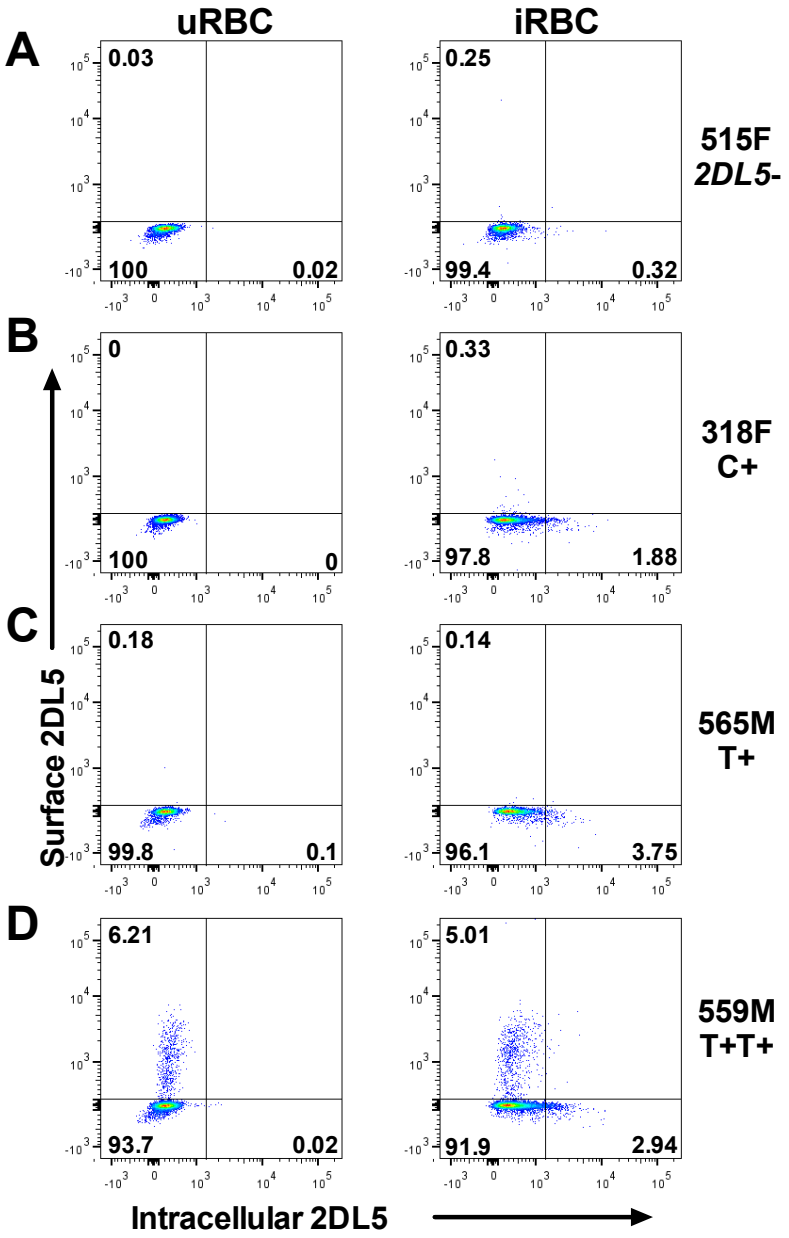

Figure 6.11: **Intracellular staining for KIR2DL5 increases after incubation with iRBCs.** FACS plots of PBMCs incubated for 2 hours with uRBCs and iRBCs and stained with surface antibodies for CD56, CD3 and KIR2DL5-APC (y-axis) before fixation and a second 'intracellular' stain with KIR2DL5-PE (x- axis). Plots show NK cells after incubation with uRBCs (left) and iRBCs (right) from donors without *KIR2DL5*, 515F (A), centromeric *KIR2DL5B*, 318F (B), telomeric *KIR2DL5A* without surface expression, 565M (C), and telomeric *KIR2DL5A* with surface expression, 559M (D).

NK cell surface (565M); or an expressed copy of *KIR2DL5A* (559M). In donor 559M (Fig. 6.11D), the percentage of NK cells expressing 2DL5 is consistent regardless of incubation with uRBCs or iRBCs, but intracellular 2DL5 staining is clearly increased.

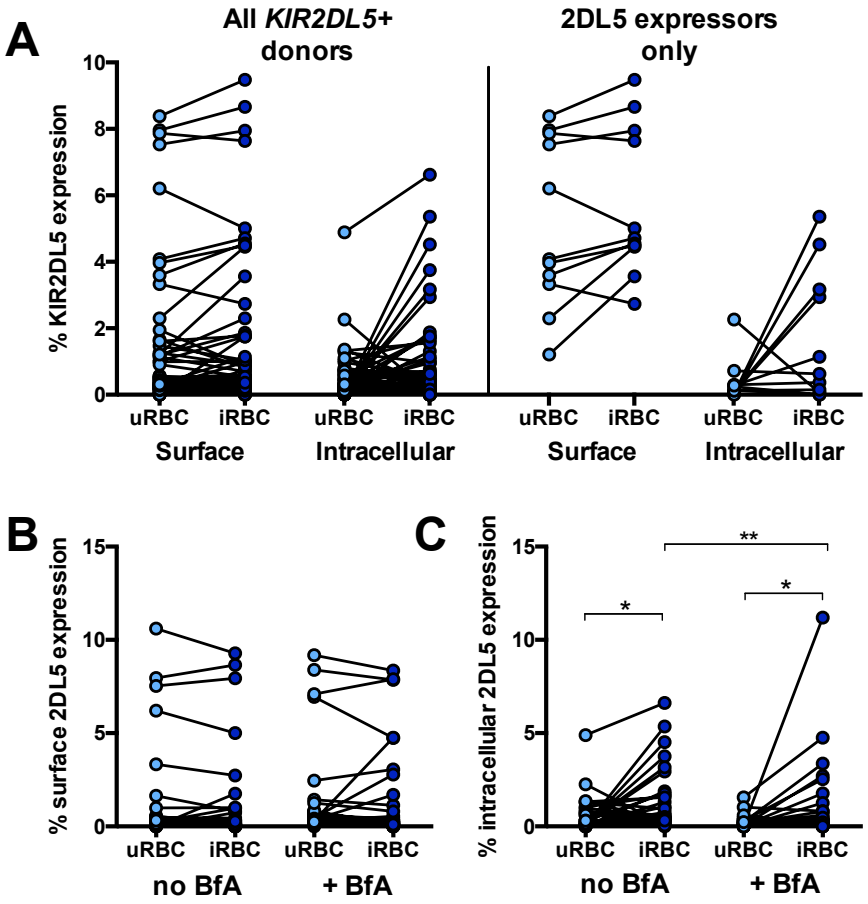

Figure 6.12: **Intracellular 2DL5 expression changes after incubation with iRBCs.** PBMCs from *KIR2DL5*+ donors from both LSHTM and Uganda were incubated with uRBCs and iRBCs and stained with surface antibodies for CD56, CD3 and α-2DL5-APC before fixation and a second 'intracellular' stain with α-2DL5-PE. Change in surface expression and intracellular expression of 2DL5 after incubation with uRBC or iRBC in all *KIR2DL5*+ donors (n= 65) or 2DL5 expressors only (n= 11) (A). Change in surface (B) or intracellular expression (C) of 2DL5 after addition of brefeldin A to culture (n= 31). * $p< 0.05$, ** $p< 0.01$.

The overall expression of surface or intracellular 2DL5 on NK cells from *KIR2DL5*+ donors from both LSHTM and Uganda was summarised as follows (Figure 6.12). Surface 2DL5

expression did not significantly differ after incubation with uRBCs or iRBCs either in the *KIR2DL5+* population as a whole (n= 65) or in donors who constitutively expressed surface 2DL5 (n= 11) (Fig. 6.12A). However, intracellular 2DL5 expression increased after incubation with iRBCs compared to uRBCs both in the total *KIR2DL5+* population and in constitutive surface 2DL5 expressors (n= 11), although this did not reach statistical significance (p= 0.24, Wilcoxon signed rank test).

Brefeldin A (BfA) blocks protein transport from the endoplasmic reticulum (ER) to the Golgi apparatus, and is used in my 18 hour functional assays to prevent release of IFN-γ from the NK cell. To test whether 2DL5 was being transported from within the cell, PBMCs from LSHTM donors (n= 31) were incubated with uRBCs or iRBCs with or without 10µl BfA for 2 hours. Adding BfA had no effect on 2DL5 surface expression (Fig. 6.12B). However, in these donors, intracellular 2DL5 expression was upregulated in response to iRBCs compared to uRBCs, both in the presence and absence of BfA (without BfA, p= 0.040; with BfA, p= 0.011) (Fig. 6.12C). There was also a statistically significant decrease in intracellular 2DL5 after incubation with either uRBCs or iRBCs when BfA was added to culture. This suggests that 2DL5 may be produced or stored in the ER and is prevented from transportation out of the ER by BfA, and that it may be specifically produced or released in response to iRBCs. Whether 2DL5 is transported to the NK cell surface is unclear, and may occur at time points after the two hours tested here.

6.3.8 Are iRBCs a ligand for KIR2DL5?

A major question arising from these results is whether iRBCs are a potential ligand for 2DL5, especially as there is a possible association between conjugate formation and KIR2DL5 expression. Cells from a reporter T cell line constitutively expressing 2DL5 on the cell surface were incubated with iRBCs to test whether a 2DL5 ligand was present on the iRBC (as described earlier in this chapter in Methods). The reporter cells are designed to express GFP if a ligand is present. Reporter cells were incubated with medium, uRBCs, 3D7A iRBCs and the positive M2 control for 18 hours in quadruplicate repeats.

To validate the reporter cell line, spare reporter cells were separately incubated in triplicate with medium, uRBCs and iRBCs and stained with α-2DL5 and α-glycophorin A to test the level of 2DL5 expression over time and whether reporter-iRBC conjugates could be detected. Conjugate formation was not detectable, but 2DL5 expression on the reporter cell line was affected by culture conditions (Figure 6.13). FACS plots showed that while the percentage of 2DL5+ cells was consistent throughout the incubation (Fig. 6.13A), the MFI of 2DL5 expression decreased after incubation with uRBCs and iRBCs (Fig. 6.13B, C). There were insufficient repeats to analyse these results statistically, and it is not clear whether iRBCs induced greater downregulation of MFI than uRBCs.

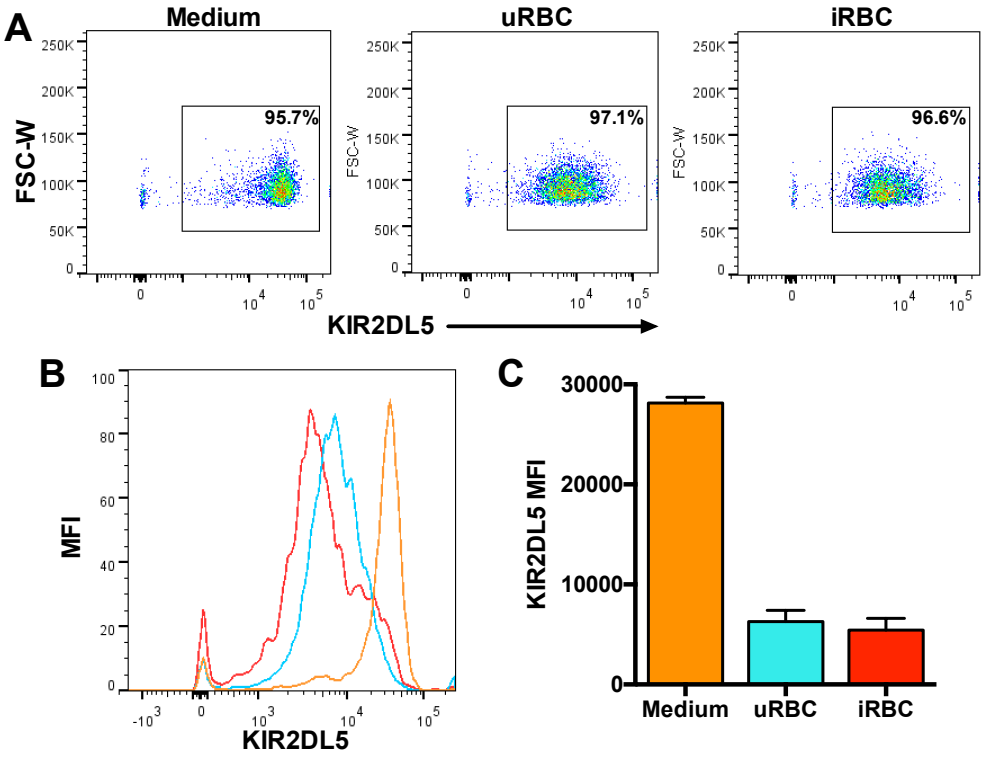

Figure 6.13: **MFI of KIR2DL5 expression on a KIR2DL5 reporter cell line decreases after incubation with iRBCs.** The reporter cell line was incubated for 18 hours with medium, uRBCs or iRBCs in triplicate and stained with α-2DL5-APC and α-glycophorin A. Representative FACS plots from each condition (A). KIR2DL5 MFI was plotted on an overlaid histogram with medium (orange), uRBC (blue) and iRBC (red) (B). MFI values were plotted on a bar graph in the same colours to illustrate the decrease in MFI (C).

However, after incubation with uRBCs or iRBCs, the reporter cells did not upregulate GFP expression, suggesting that RBCs are not functional ligands for 2DL5 (Figure 6.14). M2 represents the positive control, compared to which there is clearly no change in GFP expression in response to the other culture conditions.

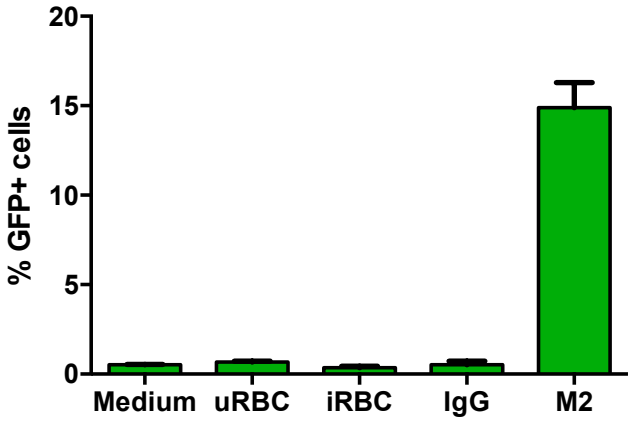

Figure 6.14: **iRBCs do not activate a KIR2DL5 reporter cell line.** A KIR2DL5+ reporter cell line was incubated with medium, uRBCs, iRBCs, IgG control or M2 positive control for 18 hours and any GFP expression measured by FACS. Columns and error bars represent the mean and range of four repeats per condition.

6.3.9 KIR2DL5 expression was upregulated by iRBCs in two donors

The final puzzle regarding KIR2DL5 expression in the presence of iRBCs arose during two different experiments on two different donors, from LSHTM (106F) and Uganda (407). During the 2 hour phenotyping assay, PBMCs were incubated with medium, uRBCs or iRBCs and stained with an antibody panel containing 2DL5 (Tables 5.1 and 5.2, Chapter 5). 2DL5 expression was not detectable on the NK cell surface after incubation with medium or uRBCs, but increased to 48.2% and 26.4% respectively after incubation with iRBCs. Figure 6.15 shows the full FACS gating for each donor.

The entire KIR genotype of donor 106F is 3DL3-2DS2-2DL2-2DL5B-2DS3-2DP1-2DL1-3DP1-2DL4-3DL1-2DS4-3DL2. Donor 407 was not fully genotyped due to insufficient

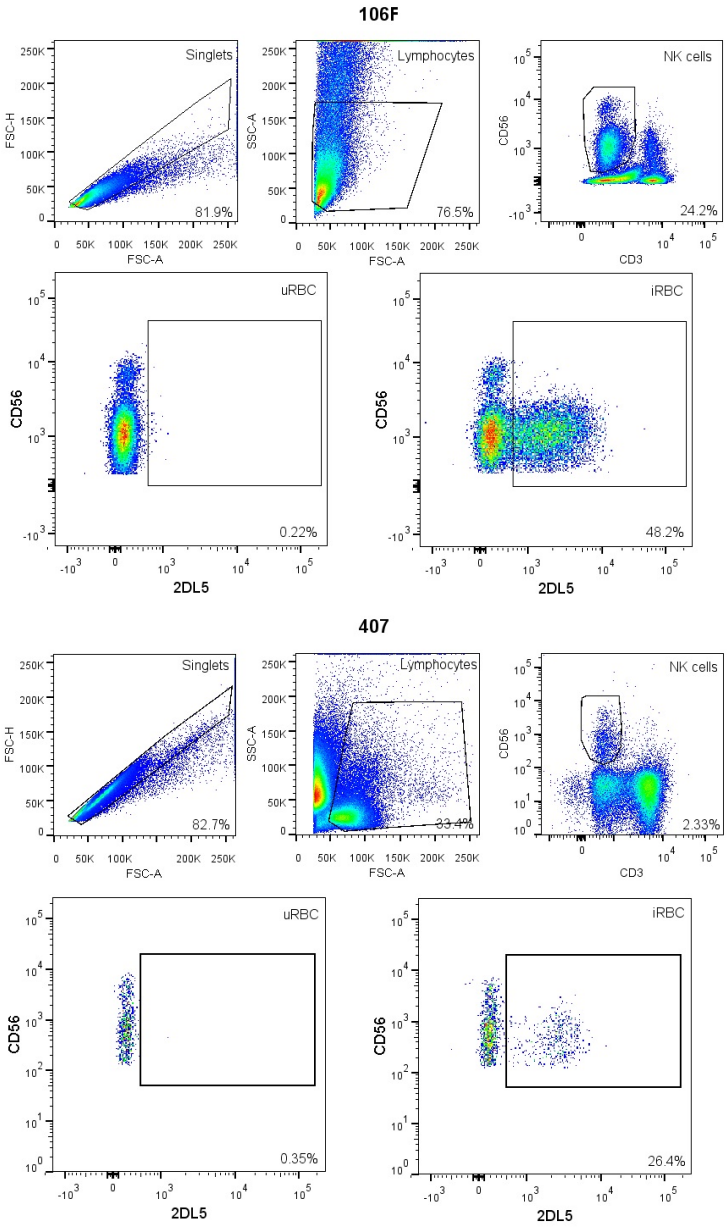

Figure 6.15: **Donors 106F and 407 appear to upregulate KIR2DL5 expression after incubation with iRBCs.** FACS plots showing gating for singlets, lymphocytes, NK cells, and 2DL5 expression after a 2 hour incubation with uRBCs or iRBCs. Both donors had large populations of CD56 dim 2DL5+ NK cells after incubation with iRBCs, but not with uRBCs.

DNA, and appeared to be negative for all of *KIR2DL5, 2DL2* and *3DS1*. So far I have not been able to find a clear explanation for these two apparent upregulations. Although human error is always possible, both wells were just one of many being stained with the same antibody panel, and both were located in the middle of a plate. The experiments took place a year apart, and used different antibodies. Cells from the first donor were stained with α-2DL5-PE and cells from the second with α-2DL5-APC, both from Miltenyi Biotec. The 2DL5 positive population was also confined to the CD56 dim cells, which is consistent with KIR expression generally. However, there are two arguments against a iRBC-specific upregulation: firstly, donor 407 appears to be *KIR2DL5* negative according to repeated presence/absence genotyping and ddPCR. There is currently no opportunity to obtain more cells or DNA from this donor, so this cannot be verified independently. One possibility is that this donor has a rare *KIR2DL5* allele that is not detected by the primers used for the PCRs, or it is also possible that the DNA is simply of insufficient quality for accurate genotyping. This donor was also apparently negative for both *KIR2DL2* and *KIR3DS1*. Secondly, I have been unable to replicate this upregulation in donor 106F from LSHTM, who has one centromeric *KIR2DL5B* and in other experiments has not expressed surface 2DL5, which increases the likelihood that this is an artefact. However, this is still potentially interesting, and one hypothesis might be that the UP-R1 antibody is not as specific as previously thought, and could bind other KIRs or other receptors under the right conditions. Alternatively, these donors might be upregulating a new receptor which is rare enough that cross-reactivity with KIR2DL5 has not been previously seen.

6.4 Discussion

6.4.1 Differences in KIR2DL5 expression between populations

Consistent with published data, different frequencies of KIR genes were found in African and Caucasian populations. Analysis of *KIR2DL5*, *2DL2* and *3DS1* by droplet digital PCR provided both copy number analysis and information about the structural haplotypes of these three genes on the KIR regions at a relatively low cost, and has been an opportunity to further validate the methods described by Roberts et al [334]. Although the majority of donors had genotypes consistent with previously published studies, with one copy of *KIR2DL5* linked to one copy of *KIR2DL2* or *KIR3DS1*, there were several Ugandan donors who had possible *KIR2DL5* duplications, and one donor who appeared to express a centromeric allele of *KIR2DL5*. It would therefore be of interest to allele type these donors for more information using sequence-specific oligonucleotide probes capable of determining which alleles of *KIR2DL5* are present [87, 344], both in donors from the LSHTM group, who are likely to be more homogenous, and from the Ugandan group, who are likely to show more genetic variability [303].

2DL5 expression on the NK cell surface has been described in only a small number of studies [87, 99, 321, 328], partially due to limitations in the techniques of detecting KIR transcription and expression. Previous work has focused mainly on mRNA transcription, which does not directly translate into cell surface expression, but the only available α-2DL5 antibody, UP-R1, is thought to only recognise the most common *KIR2DL5A* allele, *001. However, from the data described here, it is of significant interest to have surface expression data from two different populations. These data suggest that in addition to a lower frequency of telomeric and expressed *KIR2DL5* genes in Ugandan donors, 2DL5 expressors within this population have a lower percentage of 2DL5+ NK cells and express fewer 2DL5 molecules on the NK cell surface. As variation in the promoter regions of KIRs is high but is still not fully understood, this may suggest that the frequency of different KIR promoters may also vary on a population or geographic level, in addition to KIR

allelic diversity. Although the mechanisms by which promoters regulate KIR expression are still unclear (reviewed in [99]), it would be of interest to either sequence the promoter regions of *KIR2DL5* in individuals from both groups of donors to determine whether known mutations or promoter variants are present, or to measure promoter activity by reporter cell lines [321, 345].

Having more copies of *KIR2DL5* increased the likelihood of carrying an expressed telomeric allele of *KIR2DL5*, but having multiple T+ alleles did not appear to affect the percentage of 2DL5+ NK cells. There was therefore no observed 'gene dosing' effect, as has been seen with KIR3DS1 and 2DL3 [89, 293], where increased copy number correlates with increased expression of KIRs on the NK cell surface, although this may be due to the small number of donors expressing 2DL5 in this study.

6.4.2 Can a non-expressed gene be protective against disease?

The lower frequency of telomeric *KIR2DL5* in the Ugandan population is consistent with observations by Du et al (2008) [303] and Olaniyan et al (2014) [300], where African populations tended to have a greater variety of 2DL5 haplotypes and alleles but were more likely to have non-expressed centromeric alleles (as determined by mRNA expression). More interesting is the work by Olaniyan et al [300] linking carriage of centromeric B haplotypes with protection against severe malaria. In that paper, carriage of *KIR2DL5* in centromeric B motifs was significantly more common in individuals with asymptomatic malaria than in malaria cases, and the authors suggest that this KIR profile could be protective against symptomatic malaria.

The data shown here indicate that although *KIR2DL5* carriage does not significantly affect the functional responses of NK cells to iRBCs, expression of 2DL5 on the NK cell surface was associated with a decreased ability to form NK-iRBC conjugates. Although it is still unclear whether NK-iRBC conjugates lead to functional outcomes such as the death of the iRBC (described in Chapter 5), if conjugate formation is an indicator of NK cell function this suggests that 2DL5 expression has an inhibitory effect on NK cells.

If these data do therefore show that 2DL5 is an inhibitory receptor, it is still unclear whether 2DL5 is producing a direct inhibitory signal for the NK cell after binding iRBCs, or whether 2DL5 is involved in licencing the NK cell prior to iRBC exposure to restrict cytotoxic or cytokine producing functional responses. Data from the 2DL5 reporter cell line suggest that iRBCs do not bind 2DL5 in a manner that induces signal transduction, but as NK cell interactions with iRBCs are thought to require formation of the immune synapse and stabilisation via adhesion molecules such as ICAM-1 [43, 200, 290], these reporter cells may not be a good model for 2DL5-iRBC interactions. However, there are other indirect mechanisms by which 2DL5 might block conjugate formation if iRBCs are not a ligand for 2DL5 itself; it is also possible that RBCs themselves might be a ligand for 2DL5 but do not induce signalling (and therefore did not induce GFP upregulation in the reporter cell line), as both uRBCs and iRBCs downregulated 2DL5 expression.

Although the sample sizes in this study are too small to investigate differences in the size of 2DL5+ NK cell subsets, one logical question arising from the decreased formation of NK-iRBC conjugates in 2DL5 expressors is whether individuals with higher proportions of 2DL5+ subsets (e.g. 10% of NK cells) form fewer conjugates than individuals with smaller 2DL5+ subsets (e.g. 3% 2DL5+ NK cells). Additionally, as Ugandan donors in this study appeared to have smaller populations of 2DL5+ NK cells than LSHTM donors, it is possible that even expressed alleles in African populations have less active promoters, thus limiting the inhibitory effect of expressed 2DL5 on the NK cell population as a whole.

In further work on this subject, it would be important to determine whether other activating KIRs, in particular 2DS3 and 2DS5, are expressed and potentially activated after incubation with malaria iRBCs. FACS antibodies are not available for either of these receptors, but measuring mRNA levels might indicate whether these genes are expressed alongside 2DL5 or whether *KIR2DL5* promoter variation affects expression of *KIR2DS3/5* as well. However, KIR coexpression on the cell surface would likely require FACS analysis, which will not be possible until antibodies are developed for a greater range of activating KIRs.

There are few studies looking specifically at *KIR2DL5* or *KIR2DS3/5* and associations with malaria [302, 346]. Whether malaria has affected the evolution of KIR genes is not clear, but I would suggest that this seems plausible, considering the extent to which malaria has exerted selective pressure in other aspects of human genetics. Both existing literature and unpublished preliminary data from our group suggest that centromeric B haplotypes are more frequent in other African countries including the Gambia, and that surface 2DL5 expression is uncommon [102, 304, 347]. However, other genes associated with *KIR2DL5* have been associated with important biological functions that might be greater determinants for selection of certain haplotypes in different populations. Studies on the effects of KIRs on reproductive success have suggested that centromeric *KIR2DS5* may be beneficial in preventing pre-eclampsia in African populations, whereas telomeric B haplotypes prevent pre-eclampsia in Europeans [95]. As *KIR2DL5* is frequently linked to *KIR2DS5*, *KIR2DL5* could be an incidental 'hitch-hiker' during selection for a functional *KIR2DS5* gene. This explanation alone is unlikely to account for all *KIR2DL5* genes, as the most common associations of centromeric *KIR2DL5* are with *KIR2DS3* and telomeric *KIR2DL5* with *KIR2DS5* [99, 306], but other haplotypes have been observed with the reverse associations depending on the allele of *KIR2DL5* and *KIR2DS3/5* [90] and so a similar scenario may yet account for the apparent selection of certain haplotypes, for which carriage of *KIR2DL5* is just a proxy for another functional receptor.

However, the available data are too sparse to assume that 2DL5 has no independent function and is merely a bystander gene carried along in the haplotype, especially as it is found at resonably high frequencies in most populations and is not always linked to the same set of genes. Additionally, it has been suggested that as centromeric *KIR2DL5* is effectively inactivated by promoter variation rather than by a mutation in the gene itself [87, 292], it may have had or may still have relevant functions under specific circumstances. Despite this, these hypotheses still beg the question of how an apparently non-expressed gene might have a beneficial effect during infection with malaria or any other disease. Carriage of centromeric *KIR2DL5* appears to be more beneficial than not having *KIR2DL5* [300], but it is unclear if this is merely a byproduct of heterozygosity, where other B haplotype genes

are responsible for any immunological advantage, or whether an apparently unexpressed gene can still exert selective pressure in a population.

6.4.3 Does KIR2DL5 expression change in response to different stimuli?

Although the populations of KIR+ NK cells can change over time, this is predominantly linked to NK cell maturation, involving loss of NKG2A and acquisition of CD57 over time [294]. Infection with HCMV has been shown to drive expansions of NKG2C+ NK cells that coexpress inhibitory KIR molecules [14, 307]. However, short term expression patterns of KIRs are thought to be stable on the NK cell surface, and therefore the possibility that 2DL5 expression may change after a short incubation with iRBCs raises many questions about the role of this KIR in detecting and responding to iRBCs. If 2DL5 expression is upregulated, the mechanism by which this might occur is not clear. Transcription of *KIR2DL5* to produce new 2DL5 protein is theoreticaly possible within a two hour time frame, but it may be more likely that NK cells contain an intracellular store of 2DL5 protein or mRNA ready for transcription, which is upregulated under certain conditions, such as during incubation with iRBCs.

Although the change in intracellular 2DL5 after incubation with uRBCs and iRBCs was not statistically significant when considering the combined group of LSHTM and Ugandan donors, there appeared to be a significant increase in intracellular 2DL5 in response to iRBCs when considering only LSHTM donors. Whether this represents a meaningful difference between the groups of donors or is due to experimental differences between the conditions is not clear (for example, cells from Ugandan donors were frozen before use whereas cells from LSHTM donors were freshly collected on the day of the experiment). However, significantly more work is required to clarify this, beginning with a time course over several hours to clarify whether 2DL5 expression continues to change with continued incubation with iRBCs, and with analysis of mRNA transcripts at each of these time points to confirm whether expression of 2DL5 is actually changing and whether it can truly be

measured within the cell using a FACS antibody. A larger number of donors both with and without 2DL5 surface expression would also allow better investigation of whether the proportion of NK cells with increasing intracellular 2DL5 depends on donor genotype, the location of *KIR2DL5* genes in the centromeric or telomeric regions, or another factor such as copy number or promoter type.

The levels of 2DL5 surface expression seen in NK cells from donors 106F and 407 after coculture with iRBCs are currently inexplicable. These responses were unexpected, and have not been successfully repeated; however, they are too similar to dismiss as a mistake without further investigation. As the upregulation was seen only after incubation with iRBCs and appeared when using two different batches of antibody on different fluorophores, it is unlikely that these populations are due to compensation errors or shifts in fluorescence. However, repeated presence/absence genotyping and ddPCR testing indicated that donor 407 was negative for 2DL5, which suggests either that this donor carries a *KIR2DL5* variant not detected by the existing PCR primers, or that this donor is upregulating an inducible non-2DL5 molecule which crossreactively binds the UP-R1 antibody. As this donor is from Uganda, the possibility that this donor carries a new *KIR2DL5* allele cannot be completely dismissed due to the high number of novel alleles found in African populations [303], but it may be more likely that UP-R1 is cross-reactive to some other molecule. Private correspondence with the group that made the UP-R1 antibody suggested that cross-reactivity was unlikely, as the antibody does not detect proteins from the *KIR2DL5A*005* allele, but I feel this possibility cannot be ruled out. However, if these donors are an example of upregulation of *KIR2DL5* transcription specifically in response to iRBCs, it is possible that this indicates a role for constitutively non-expressed *KIR2DL5B* alleles. Donor 106F carries a single copy of centromeric *KIR2DL5B, 2DL2*, and *2DS3*, and is negative for *KIR2DL5A, 3DS1* and *2DS5*. Donor 407 was apparently negative for *KIR2DL5, 2DL2* and *3DS1*, as previously mentioned.

There are two arguments in favour of a 'genuine' upregulation of 2DL5 expression: firstly, if the epigenetically silenced *KIR2DL5B* gene carried by donor 106F (and potentially 407) is being transcribed after demethylation of its promoter region, very high levels of 2DL5+ NK

cells (over the normal 10%) would be consistent with data from experiments that measured KIR expression after *in vitro* demethylation of silenced promoters [87]. Secondly, the 2DL5 population is also CD56 dim, which is consistent with normal expression patterns of both 2DL5 and other KIRs. Expression of apparently non-expressed genes has also been seen with other KIRs at NK cell precursor stages [335], and so it may be incorrect to assume that the centromeric *KIR2DL5B* alleles are never expressed, and it should only be said that they are not expressed constitutively. Further work to determine this should both determine the alleles of these donors and attempt to replicate these observations both after incubation with iRBCs or other stimuli. The possibility that the UP-R1 antibody may also be cross-reactive should also be explored, possibly by testing a large number of donors of known *KIR2DL5* genotype (including donors who are *KIR2DL5*-) or by predicting other possible binding sites on similar molecules (including the other KIR molecules, which show high levels of cross-reactivity amongst themselves).

6.4.4 iRBCs as a KIR2DL5 ligand

One of the primary questions arising from these experiments is whether iRBCs can interact with NK cells via the KIR2DL5 receptor. Although there does appear to be a link between 2DL5 expression and reduced formation of NK-iRBC conjugates, as well as an increase in intracellular 2DL5 expression after incubation with iRBCs, the balance of evidence suggests that iRBCs are unlikely to directly interact with 2DL5. Although blocking 2DL5 sites on the NK cell surface lead to a reduction of conjugate formation after two hours, this experiment would need to be repeated and to include an antibody isotype control before firmer conclusions could be drawn from those data. This mechanism by which iRBCs interact with NK cells, and lead to both NK cell activation and possibly 2DL5 upregulation, is therefore still unknown. One possibility is that heparan sulfate, which was recently shown to be a ligand for 2DL4 [78] and shares some structural similarities with 2DL5 [76], might also be a ligand for 2DL5. Whether this is the case or not, the possibility that a 2DL5 ligand could be a relatively common molecule that only appears under certain

conditions might be one reason why a ligand has not yet been identified even though 2DL5 is common in all populations. The fact that expression is not that rare - it is restricted to a minority of NK cells, but in a Caucasian population around 25% of the total population expressed it (13/52 donors from LSHTM) - suggests that 2DL5 may be generally expressed unless there is a good reason not to do so, such as environmental pressures which drive selection of non-expressed alleles and KIR haplotypes.

If malaria parasites do cause an increase in 2DL5 expression - which in turn inhibits NK cell activation - the reasons for this may vary. It is possible that this is a protective host mechanism to limit uncontrolled pathology on an NK cell subset that may also be expressing many activating receptors. The biological relevance or benefit of conjugate formation and IFN-γ production *in vivo* are still not known. Conversely, induction of KIR2DL5 could be induced by the malaria parasite to inhibit NK cell responses and prevent parasite killing, which would be potentially consistent with the study by Olaniyan et al suggesting that unexpressed *KIR2DL5* alleles are protective [300], and perhaps suggest that NK-iRBC responses are mediated by another KIR such as *KIR2DS3/5*. If inhibition of NK cells by iRBCs as a result of expressing 2DL5 were detrimental to humans, whether via direct 2DL5 signalling or otherwise, human populations regularly exposed to malaria might reduce 2DL5 in order to avoid NK cell inhibition, which would be a possible explanation for why the non-expressed alleles are much more common in African populations compared to Caucasian populations.

6.4.5 Conclusions

The possible role for KIR2DL5 in NK-iRBC interactions has raised more questions than this study is currently capable of answering. The most pressing of these questions are firstly, if 2DL5 is being upregulated in response to iRBCs, from where is it coming? Secondly, is it possible that the *KIR2DL5B* genes thought to be non-functional could play a role in this interaction, via some form of iRBC-driven demethylation of the 2DL5 promoter sites? Thirdly, what are the outcomes of 2DL5 upregulation, both on the level of NK cell function

and for the course of malaria infection overall? It would be interesting to determine whether any 2DL5 upregulation is stable in the long term, as expanded populations of 2DL5+ NK cells have not been observed in donors from areas where malaria is highly endemic. In conclusion, these data indicate an intriguing potential role for KIR2DL5 as a mediator of NK cell responses to malaria parasites and suggest that 2DL5 expression patterns in different populations may be driven by environmental pressures.

7 | Discussion

7.1 Overview of results

In this thesis, I have made four main findings.

Firstly, jointly with Carolyn Nielsen, I have proposed a model for early NK cell activation where IL-18 synergises with either IL-15 or IL-2 during the primary or secondary immune response to drive IFN-γ and degranulation responses.

Secondly, I have compared NK cell functional responses to *P. falciparum*-infected RBCs and NK cell surface phenotypes of LSHTM and Ugandan donors, and shown that NK cells from malaria naive LSHTM donors are primed rather than activated by IL-15, and respond strongly to malaria parasites and cytokine stimulation; on the other hand, NK cells from malaria exposed Ugandan donors show very low levels of cytokine production in response to iRBCs, but strongly upregulate CD25 after activation by IL-15, which is likely to indicate increased responsiveness to IL-2. Additionally, NK cells from Ugandan donors produce only low levels of IFN-γ in the absence of IL-15, which appears to be affected by differences within NK cell subsets rather than by differing proportions of CD57- and CD57+ NK cells between the groups of donors. Ugandan children had comparable proportions of mature and differentiated NK cells to adults living in the UK, which is likely to be due to environmental factors and early HCMV infection.

Thirdly, a comparison of KIR and NKG2C genotype and phenotype indicated that KIR expression is acquired with increasing NK cell maturation in both groups of donors, but that the KIR2DL1+ NK cell subset may be selectively expanded alongside NKG2C in

Ugandan individuals. Additionally, NKG2C genotype has a significant effect on NK cell phenotype and the size of the NKG2C+, CD57+, and NKG2C+ CD57+ NK cell subsets, and may affect the speed of NK cell maturation in different age groups. However, NKG2C genotype itself had no effect on functional NK cell responses. This work also characterises expression levels of KIR receptors on the NK cell surface in a predominantly Caucasian and an east African group of individuals, on which there are limited published data.

Lastly, my fourth finding is that KIR2DL5 may play a role in NK-iRBC conjugate formation, and that carriage of a non-expressed *KIR2DL5* gene may be beneficial during malaria infection. *KIR2DL5* was found at comparable frequencies in LSHTM and Ugandan donors but showed significant differences in expression based on allelic differences between the two populations. Staining for surface expression of KIR2DL5 also indicated a possible change in its expression after a short incubation with iRBCs.

One overarching conclusion of this work is that heterogeneity in NK cell responses is closely linked to cytokine receptor and KIR expression, which are in turn heavily influenced by NK cell maturation status. I have tried to explore differences in NK cell function by examining activating and inhibitory receptor expression on NK cells from two groups of donors with very different backgrounds, and found that donors with lower IFN-γ and CD25 responses had greater proportions of more mature NKG2C+ KIR+ NK cell subsets. However, most significantly, my work suggests a possible role for *KIR2DL5* during infection with malaria and suggests a reason for the decreased expression frequency of this gene in African populations. Additionally, it raises the possibility that *KIR2DL5B*, generally thought to be non-functional, may be expressed under certain circumstances.

7.2 NK cells from Ugandan donors show 'memory-like' responses but are unlikely to be malaria-specific

Previously published data from our lab and my own experiments indicate that malaria naive individuals from LSHTM have heterogenous responses to iRBCs *in vitro*, which I

found could be enhanced with low concentrations of IL-15. In these donors, IL-15 drove low levels of CD25 upregulation but enhanced IFN-γ responses only in the presence of iRBCs, indicating a 'priming' role for this cytokine consistent with a threshold for NK cell activation. Once past this threshold, NK cells become capable of functional responses (here defined as IFN-γ, CD25 or CD107a upregulation). However, in Ugandan donors, the same low concentration of IL-15 drove strong upregulation of both CD25 and IFN-γ, independent of iRBC stimulation, whereas stimulation with iRBCs induced only a small increase in IFN-γ production. Background CD25 and CD107a expression was also higher on NK cells from Ugandan donors compared to LSHTM donors. Taken together, these data indicate that NK cells from malaria exposed individuals show markers of preactivation, and thus are more ready to respond to stimulation with IL-15.

Although the cause of this preactivation is not clear, donors from Uganda are likely to have been exposed to malaria on multiple occasions and are very likely to be HCMV seropositive, in addition to other possible common infections [11, 287]. Repeated exposure to antigen through malaria reinfection or chronic HCMV stimulates proinflammatory cytokine production by accessory cells, providing multiple opportunities to preactivate NK cells. Cytokine-induced preactivation of NK cells is thought to last for at least six to twelve weeks [16], which, in a population with low levels of circulating infections like LSHTM, is sufficient time for immune responses to return to baseline levels after infection. However, if cells are restimulated within this period of preactivation, enhanced NK cell responses have been observed [16, 211]. I therefore hypothesise that NK cells from Ugandan individuals are preactivated through frequent antigen exposure as shown by high 'resting' CD25 expression, whereas NK cells from LSHTM donors are not.

When comparing NK cell responses to iRBCs (with or without IL-15) from both groups of donors, I found that Ugandan donors did not show enhanced IFN-γ responses whereas malaria naive LSHTM donors did. Ugandan donors in fact had lower IFN-γ production after stimulation with iRBCs alone, despite my initial prediction that individuals with repeated exposure to malaria would have higher IFN-γ responses. However, as NK cell responses to malaria are partially dependent on signalling of IL-12 and IL-18 [26, 42], and

cells from Ugandan donors were less responsive to stimulation with high concentrations of these cytokines (such as HCC) than LSHTM donors, decreased responses to iRBCs may be due to a decreased response to IL-12 and IL-18. In the absence of data on NK cell responses to primary malaria infection in Ugandan donors, it is difficult to determine whether NK cells show memory responses to malaria. However, as there are differences between these groups of donors other than exposure to malaria, their responses to iRBCs *in vitro* are not directly comparable. It is possible that baseline responses to iRBCs of Ugandan individuals are lower than those of LSHTM individuals, and therefore that the responses observed here represent a higher secondary response to malaria compared to their own primary responses, but longitudinal studies following Ugandan children from soon after birth would be required to answer this question.

As HCMV seropositive individuals have been observed to make lower NK cell IFN-γ and CD25 responses to vaccines and to stimulation with IL-12 and IL-18 [17], this may be one reason for an overall reduced response to iRBCs or cytokine stimulation in Ugandan compared to LSHTM donors. Although HCMV positive individuals have expanded CD57+ NKG2C+ NK cell subsets, contributing to an overall decrease in cytokine production, Nielsen et al also found that NK cell responses were also lower *within* NK cell subsets and that CD57- NK cells from HCMV+ individuals made less IFN-γ than CD57- NK cells from HCMV- individuals. These data are consistent with my observations here, as IFN-γ and CD25 responses from all CD57 subsets from Ugandan donors were lower than the corresponding responses in LSHTM donors.

It is also possible that, due to repeated infections, immune regulatory responses are preventing overproduction of IFN-γ to avoid immunopathology. As described in the introduction to Chapter 4, IFN-γ and other proinflammatory cytokines are associated with protection against malaria (reviewed in [258]) but anti-inflammatory cytokines including IL-10 are important for regulating inflammation. Antigen-specific regulatory T cells are thought to be generated alongside effector T cells during infection, and are important for preventing immune pathology (reviewed in [225]); during a secondary infection, they may compete with NK cells (and other T cells) for IL-2 and produce IL-10, thus reducing inflammatory

responses including the production of IFN-γ (reviewed in [263]).

It is also interesting that donors aged 5-11 years had higher IFN-γ and CD25 responses than either the under five year olds or the adults. The low IFN-γ responses in the under five year olds is somewhat surprising, as these donors had the highest proportions of CD57- NK cells and should therefore have responded strongly to cytokines and iRBCs, but these donors may lack malaria-specific T cells producing IL-2. There were no differences in the functional responses of CD57- NK cells between age groups. On the other hand, in areas of moderate to high transmission, children up to approximately 10 years of age are still prone to uncomplicated clinical malaria, and it is only after this age that asymptomatic clinical immunity develops (reviewed in [129]). Therefore this 5-11 year old group may represent individuals capable of making strong early IFN-γ responses to iRBCs, but who do not yet have the ability to regulate these responses to avoid clinical malaria. Conversely, adult donors may have lower NK cell responses as they have developed a wide repertoire of malaria-specific antibodies and do not require strong inflammatory responses to clear infection, or else because they have acquired regulatory immune mechanisms (e.g. regulatory T cells) that reduce inflammatory responses. Adult donors also have higher proportions of CD57+ NK cells, which make less IFN-γ than CD57- NK cells [17].

I therefore propose the following model for NK cell responses in my malaria naive and malaria exposed donors (Figure 7.1). Resting immature NK cells express low surface levels of the cytokine receptors IL-15Rβγ, IL-12R, and IL-18R, with little to no CD25. Upon exposure to malaria, iRBCs stimulate DCs and macrophages via PRRs to produce IL-15, IL-12 and IL-18. DCs transpresent IL-15-IL-15Rα to NK cells, upregulating IL-18Rα expression on the NK cell surface and thus priming them for activation by IL-18. IL-18 then upregulates IL-12Rβ and CD25, which then drives IFN-γ production (Fig. 7.1A). NK cells may also interact directly with iRBCs via an unknown receptor-ligand combination. After the resolution of infection, for a period of time NK cells enter a preactivated post-infection state, where they express increased levels of resting CD25 (Fig. 7.1B). If NK cells are not further stimulated, after six to twelve weeks they return to their original resting state. However, within this twelve week time frame, further stimulation by cytokines, such

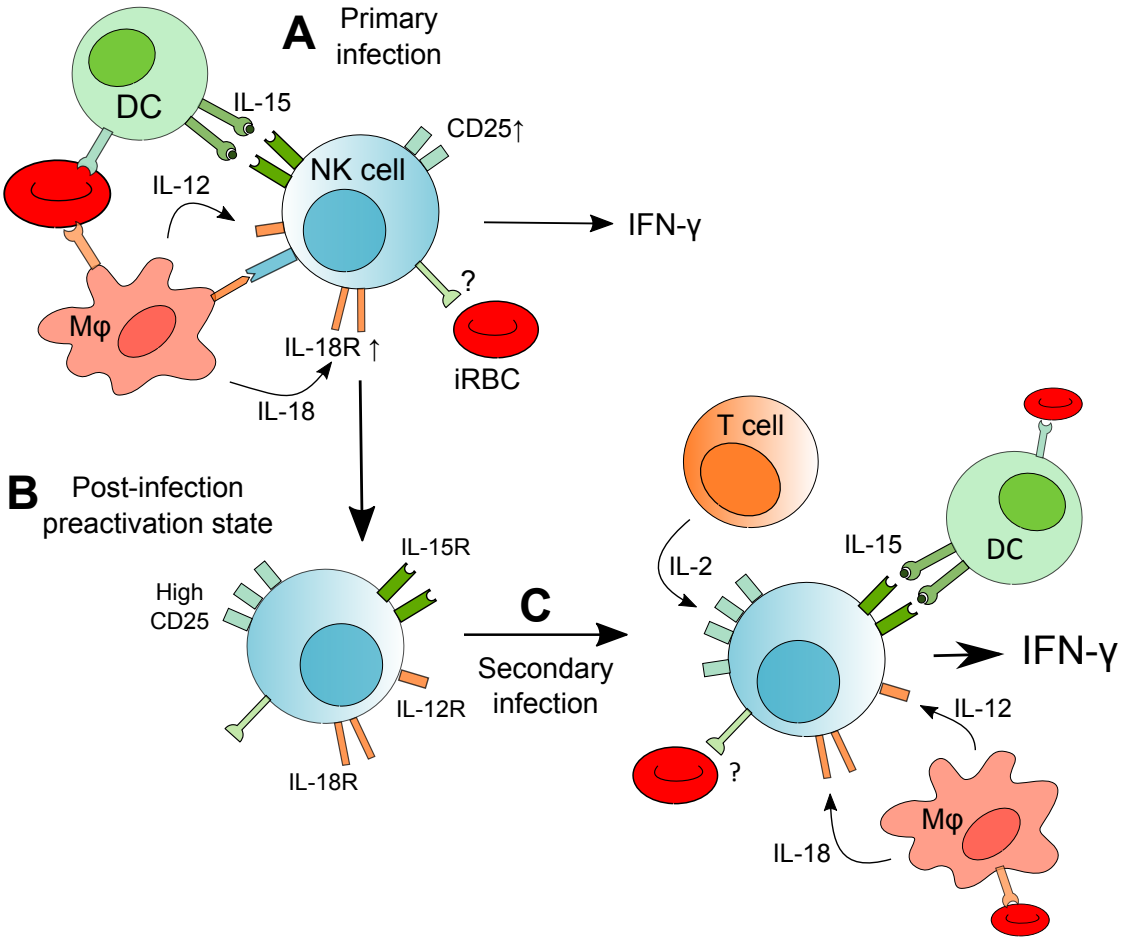

Figure 7.1: **Prior infection induces NK cell preactivation characterised by high resting CD25 expression and enhanced responsiveness to iRBC.** During a primary infection with malaria, DCs and macrophages are activated by iRBCs to produce IL-15, IL-12 and IL-18. IL-15 primes NK cells by upregulating expression of CD25 and IL-18Rα, thus lowering the threshold of activation and the minimum concentration of these cytokines required. IL-18 further drives CD25 upregulation and IL-12Rβ expression and combines with IL-12 to drive IFN-γ production. NK cells may also interact with iRBCs directly (A). After resolution of the infection, NK cells return to a resting but preactivated state and continue to express high levels of CD25 and possibly other cytokine receptors (B). If restimulation occurs within a short period of time (up to three months), NK cells may be capable of responding more strongly to cytokine stimulation by IL-15, and enhanced expression permits activation by T cell-derived IL-2 and production of IFN-γ (C). Whether NK cells produce more IFN-γ during secondary responses compared to primary responses is unclear.

as during reinfection, induces greater NK cell responses to lower levels of stimuli. Upon secondary infection with malaria, DCs and macrophages produce IL-15, IL-12 and IL-18; in addition, antigen-specific T cells generated during the primary infection produce IL-2, which signals via upregulated CD25 (Fig. 7.1C). NK cells may respond more strongly to restimulation by cytokines [16], and may also make higher levels of IFN-γ to a combination of IL-2, IL-12 and IL-18 compared to IL-15, IL-12 and IL-18 [38]. Further experiments are required to determine whether preactivated NK cells from malaria naive donors do in fact respond more strongly to iRBCs.

In theory, within this model, NK cell responses from LSHTM donors represent the first 'primary infection' pathway and responses from Ugandan donors represent activation via 'secondary infection'. In practice however, cells from Ugandan donors responded less strongly than predicted, sugesting that exogenous processes (e.g. regulatory immune mechanisms) may affect these responses. It is possible that accessory cells that become activated after infection with HCMV or another pathogen will produce the same cytokines (IL-15, IL-12 and IL-18) and therefore preactivate NK cells in the same way as malaria; however, upon activation with a different pathogen, antigen-specific T cells may be lacking and thus would not produce IL-2 and help to stimulate IFN-γ from NK cells. Although IL-2 had little effect on responses of LSHTM donors and did not enhance NK cell responses to iRBCs, the expression of the IL-2 receptor on NK cells from Ugandan donors suggests they would respond favourably to this cytokine. The role of IL-2 during secondary activation is supported by previous studies on 'recall' responses of NK cells indicating that T cells are required for secondary NK cell responses [37, 272, 348].

In addition to adding exogenous IL-2, it would be of interest in future to look at other phenotypically-defined populations of NK cells in order to determine whether they have different functional capacities. One such subset would be NKG2C+ CD57- NK cells (A. Darboe, unpublished; [16, 349]), which are thought to have increased expression of activating receptors such as NKG2C while still expressing high levels of cytokine receptors and proliferation markers. These cells may also be 'licensed' by expression of inhibitory KIR receptors, and so may have greater functional capacities for both cytokine production

and cytotoxic responses [7]. Although both the LSHTM and Ugandan donors had similar proportions of CD57- and CD57+ NK cells, the differences in functional responses strongly indicate that these NK cell populations are not the same in these two groups of donors, and that CD57 expression is a marker of maturity but not necessarily of functional capacity. Additionally, as HCMV has such an influential role in driving NK cell expansions and maturation, it is difficult determine whether changes in NK cell responses are due to previous infections with malaria or due to other environmental stimuli, and future work may require better matched donor populations for comparison of malaria-specific NK cell responses.

7.3 NK cell phenotype and KIR expression determines functionality

My next hypothesis is therefore that CD57 expression is not a direct determinant of NK cell function. CD57- NK cells showed the greatest upregulation of IFN-γ and CD107a after stimulation in both groups of donors, but the proportion of responding CD57- NK cells from Ugandan donors was lower than the proportion of responding CD57- NK cells from LSHTM donors. This therefore suggests that other markers than CD57 determine NK cell functional capacity.

KIR expression on the NK cell surface differed between the LSHTM and Ugandan populations, although the frequency of gene carriage was similar in both groups. Ugandan donors had higher proportions of KIR2DL1+ NK cells in both the CD57- and CD57+ NK cell subsets, but LSHTM donors had higher proportions of 2DL3+ and 2DS4+ NK cells. This expression pattern of 2DS4 is interesting because the number of donors expressing 2DS4 was actually higher in the Ugandan group than the LSHTM group, where carriage of the non-expressed *KIR2DS4* allele was common (consistent with other Caucasian populations [103]). A smaller proportion of LSHTM donors therefore expressed high levels of 2DS4 (30-50% NK cells), whereas most Ugandans expressed 2DS4 but on a smaller percentage of

NK cells (10-30% NK cells). These differences in KIR expression did not appear to be age-dependent, as percentages of NK cells expressing at least one KIR were similar in all age groups in Ugandan donors (Ugandan adults had higher overall KIR expression due to their higher proportions of CD57+ NK cells, but within each CD57 population KIR expression was similar). As expansions of NKG2C+ and CD57+ NK cells were observed in Ugandan donors, especially in individuals with a NKG2C+/+ genotype, and similar expansions of 2DL1+ NK cells were also seen in these donors, I hypothesise that the increased 2DL1 expression may be linked to HCMV infection. It is still unclear whether the expression of KIRs on NK cells is stochastic and simply involves NK cells transcribing KIR genes until a sufficient balance of inhibitory and activating receptors is expressed [114], or whether HLA genotype and interactions of KIRs with self-HLA ligands drives the expression of particular KIR receptors [84]. If infections such as HCMV drive expansions of 2DL1+ NK cells in Ugandan donors (rather than other inhibitory KIRs), this may suggest that 2DL1 specifically plays a role in controlling HCMV. This may also depend on the HLA genotype of the individual, so that 2DL1 is only expanded in people carrying HLA-C2 (the ligand for 2DL1), but not in individuals with only HLA-C1 (the ligand for 2DL2 and 2DL3).

Previous studies have observed expansions of KIR+ NK cell subsets in HCMV seropositive donors and suggested that expression of certain KIRs may be linked to or compensate for NKG2C expression [11, 323]. NKG2C, an activating receptor, is thought to detect upregulated HLA-E expression on HCMV-infected cells, and it has been suggested that the concomitant expression of an inhibitory KIR (either 2DL1 or 2DL3 [323]) balances the increased expression of activating receptors. Individuals lacking NKG2C may be less effective at controlling HCMV infections at a young age [11], but may expand subsets of NK cells with activating KIRs, such as 2DS1 [315] and 2DS4 [13] to compensate.

I therefore propose the following model for expansions of mature NK cells and the patterns of receptor expression in response to infection (Figure 7.2). NK cells express a balance of inhibitory and activating surface receptors that allow them to distinguish between normal and infected cells. Less mature NK cells (CD56 bright and CD56 dim CD57-) express inhibitory NKG2A, which binds HLA-E, and a variety of activating receptors including

NCRs, such as NKp30 and NKp46, and receptors for IL-12 and IL-18 (Fig. 7.2A). Subsets of NK cells expressing different combinations of receptors take part in immune responses to different pathogens, such as during malaria infection (Fig. 7.2B), where NK cells respond to IL-12 and IL-18 as well as potentially interacting with iRBCs via an unknown receptor. HCMV infection induces expression of NKG2C on the NK cell surface, allowing detection of HLA-E molecules expressing HCMV peptides. Inhibitory KIR2DL1 is expressed in tandem with NKG2C, thus balancing the activating and inhibitory receptor expression and creating expanded populations of CD57+ NKG2C+ KIR2DL1+ NK cells capable of controlling HCMV infection (Fig. 7.2C). However, in individuals lacking *NKG2C*, HCMV drives expansions of NK cells with alternative activating receptors, such as KIR2DS4 (Fig. 7.2D).

My data are therefore consistent with a model of expanded 2DL1 expression on NKG2C+ CD57+ NK cells, although I did not observe HCMV-driven expansion of other KIRs. *NKG2C* +/− donors had slightly higher percentages of 2DS4+ NK cells than +/+ donors, and with a larger sample size this may have reached statistical significance, which could indicate a possible alternative expansion of activating KIR+ NK cells. The frequency of the *NKG2C* deletion was slightly higher in Ugandan donors than in UK donors, consistent with data from other African countries [11, 313], and I suggest that the increased proportion of individuals expressing KIR2DS4 may be linked to this deletion. As these are both activating receptors with links to HCMV control [13], there may be an advantage in carrying an expressed form of *KIR2DS4* in case an individual also carries the *NKG2C* deletion, thus maintaining an ability to expand activating NK cell subsets during HCMV infection. Increased 2DS4 expression on both CD57- and CD57+ NK cells from LSHTM donors might also be one factor differentiating the functional responses of CD57- NK cells between the two groups; the increase in 2DL1 expression on CD57- NK cells in Ugandan donors may correspondingly reduce the capacity for cytokine production in these cells. Clearly more work is needed to investigate whether expression of these KIRs correlates with functional outcomes.

Understanding the mechanisms controlling expansions of NK cells with particular pheno-

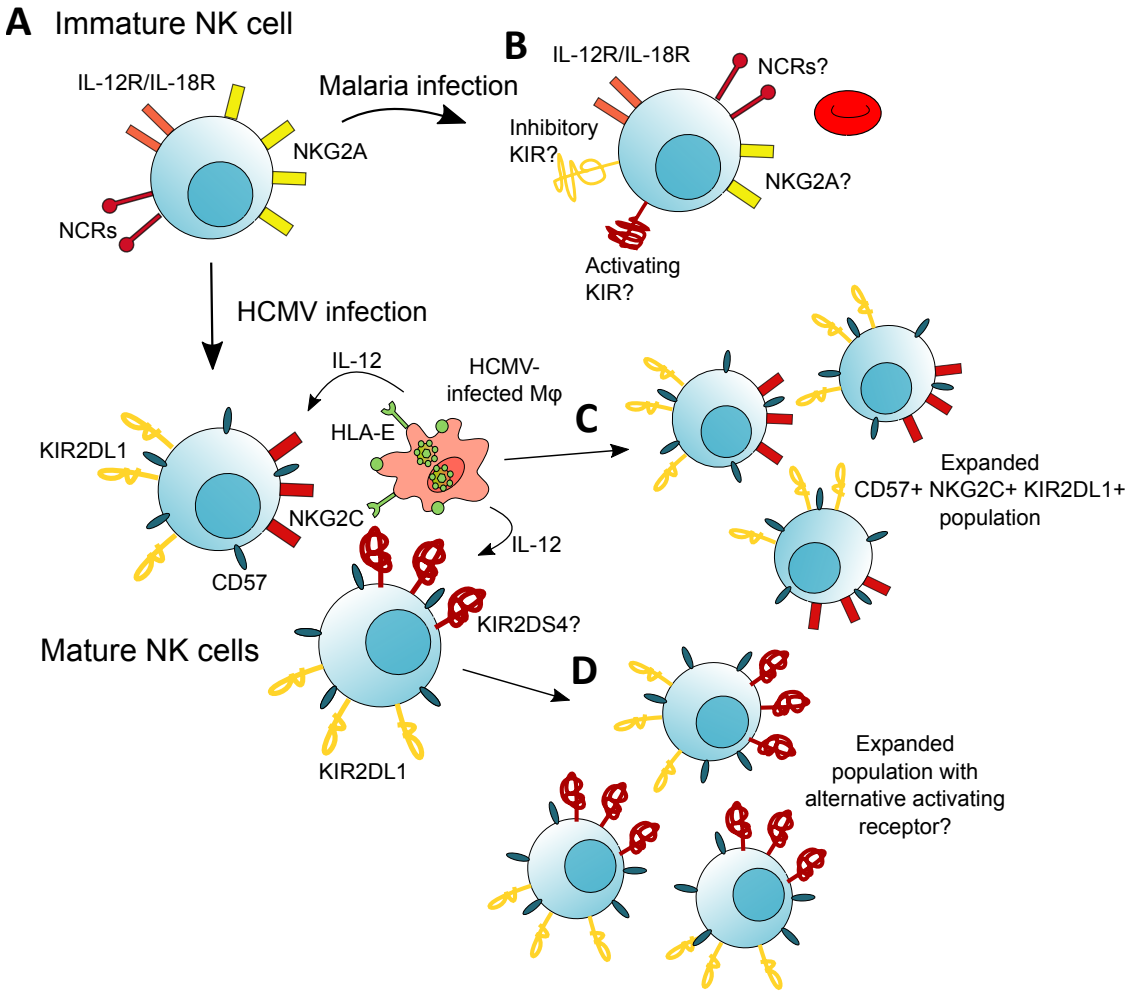

Figure 7.2: **Different subsets of NK cells respond to different infections.** NK cells express a balance of activating (red) and inhibitory (yellow) receptors that control activation. Immature NK cells express the inhibitory receptor NKG2A, cytokine receptors, and other activating receptors such as NCRs (e.g. NKp46 and NKp30) (A). During malaria infection, cytokine-driven NK cell responses are important for IFN-g production and parasite clearance. Other involved activating and inhibitory receptors are not known, but may include NCRs or KIRs (B). During HCMV infection, NK cells upregulate NKG2C and inhibitory KIR expression (e.g. KIR2DL1) and downregulate NKG2A. NK cells control HCMV via CD57+ NKG2C+ KIR2DL1+ expanded NK cell subsets (C), thought to be mediated by HLA-E-NKG2C interactions and monocyte-derived IL-12. In NKG2C-/- individuals, an alternative activating receptor may take the place of NKG2C in these expanded subsets, such as KIR2DS4 (D).

types, and controlling KIR expression on the NK cell population generally, is of particular importance if these subsets are functionally relevant to controlling disease. If NK cell licensing by KIR and self-MHC interaction is sufficient for NK cell-mediated immunity against most diseases, it may not matter which KIR+ subsets predominate in an individual as long as enough cells are licensed; however, if one receptor provides an advantage in controlling a particular infection, there may be a benefit in expanding a particular NK cell subset.

KIR2DL1+, 2DL2+, or 2DL3+ NK cells make up the majority of inhibitory KIR+ NK cells. Expression levels are thought to be modulated by self-HLA-C ligands via KIR-MHC licensing, thus linking expression of the relevant HLA ligand with expression of its KIR receptor on NK cells [84]. I have not yet analysed HLA genotype for donors in my study, but this model would suggest that most of my Ugandan donors are HLA-C2+, which would license 2DL1+ NK cells and potentially enhance expansions of these cells. Whether this is the case needs to be further analysed by HLA typing donors and correlating NK cell subset expansions with HLA expression, but a high frequency of HLA-C1/C2 and C2/C2 individuals was observed in a Ugandan population by Nakimuli et al [95].

It is also unclear whether licensed and unlicensed cells are equally capable of cytokine production during infection, which may depend on the conditions of activation. Although cytotoxic responses are thought to be enhanced by licensing, it is not clear whether cytokine production is affected. As this is thought to be the primary role of NK cells in malaria infection, the possible contribution of an expanded and licensed NK cell population in malaria exposed individuals is of particular relevance to this work. Although there is some evidence that licensed NK cells are better cytokine producers *in vitro* [111], there appears to be a clear role for unlicensed NK cells during viral infection, indicating that they are at least as capable of IFN-γ production as licensed NK cells [119, 350]; additionally, CD56 bright and CD57- NK cells usually express low levels of KIRs and are thereforelikely to be unlicensed, but are also the main producers of IFN-γ [4, 5, 11]. An important question is therefore whether CD57- NK cells, as major producers of IFN-γ, are licensed. My data showed KIR expression (predominantly 2DL1, 2DL3 and 2DS4, whose ligands are HLA-C2,

HLA-C1, and both HLA-C1 and -C2 respectively) on approximately 20-30% of CD57- NK cells in both LSHTM and Ugandan donors. This may indicate that some of these cells are licensed, but unlike CD57+ NK cells they still express receptors for IL-12 and IL-18 and are therefore capable of responding to cytokine stimulation from accessory cells.

Future work would therefore begin by HLA genotyping donors to determine what role HLA-C plays in driving expansions of 2DL1+ NK cells both in HCMV-uninfected and -infected individuals, and then focus on phenotypically defining NK cells for combinations of NK cell receptors and correlating these subsets with cytokine production and cytotoxic responses.

7.4 KIR2DL5 expression affects NK cell responses to iRBCs and may be under selective pressure by malaria

My third hypothesis is that the expression of KIR2DL5 affects NK cell responses to malaria parasites, and furthermore that there may have been selection for non-expressed and/or low-expressing alleles of 2DL5, such as *KIR2DL5B*, in malaria-endemic areas. Different frequencies of *KIR2DL5A* and *KIR2DL5B* in human populations have been described in several studies, and *KIR2DL5B* appears to be widely carried in African and south Asian populations, whereas *KIR2DL5A* is common in Caucasian and east Asian groups. There is therefore geographic overlap between areas of malaria transmission and areas of higher *KIR2DL5B* carriage. My data on (predominantly Caucasian) donors from LSHTM and African donors from Uganda support these findings, and genotyping and flow cytometry analysis allows a comparison of both genotype and phenotype between these groups of donors. In addition to a lower frequency of 2DL5 expressors among Ugandan donors, the size of the 2DL5+ NK cell population and the amount of 2DL5 on each cell (MFI) was significantly lower compared to the 2DL5+ NK populations of donors from LSHTM. This suggests that even if *KIR2DL5* is expressed in Ugandan donors, there may be some selection for alleles controlled by less active promoters, thus limiting 2DL5 expression.

An important finding from my work is the significant decrease in NK-iRBC conjugate formation in individuals expressing 2DL5. The role (if any) of NK-iRBC conjugates in malaria infection is still unclear, but my data indicate that cells from nearly all donors were capable of forming these conjugates. NK cells expressing KIRs made fewer conjugates, which may relate to inhibitory effects of these KIRs on NK cell function, although these results were not consistent between groups of donors and require further investigation. There were no other statistically significant differences in NK cell responses to iRBCs between individuals expressing or not expressing 2DL5, although it was interesting that donors with *KIR2DL5* carriage (both centromeric and telomeric) had slightly higher (though not statistically significant) IFN-γ and CD107a responses than those without. Conversely, this effect disappeared or even reversed when considering 2DL5 surface expression. The increased IFN-γ and CD107a in those carrying *KIR2DL5* is likely to relate to the increased NK cell responses of people with B KIR haplotypes rather than carriage of *KIR2DL5* itself, and so the decrease in functional responses in 2DL5 expressors may indicate the true effect of this receptor.

The other major result of these experiments is the apparent increase in 2DL5 expression after a short incubation with iRBCs *in vitro*. If 2DL5 expression changes as a result of exposure to iRBCs, and yet is less common in malaria-endemic countries, I propose the following model for the role of 2DL5 in malaria (Figure 7.3): NK cells interact with iRBCs via an activating receptor and possibly via 2DL5. 2DL5 signalling causes a net inhibitory effect on the cell, thus reducing activation and NK-iRBC conjugate formation (Fig. 7.3A). In individuals without surface 2DL5 expression (either *KIR2DL5*- or non-expressing *KIR2DL5B* carriers), there is no inhibition by 2DL5 and a net activating signal is received, allowing conjugate formation (Fig. 7.3B). However, if malaria parasites are capable of inducing upregulation of 2DL5, possibly by driving transcription of *KIR2DL5* (Fig. 7.3C), this could act as an immune evasion technique to reduce NK cell activation (Fig. 7.3D).

Other KIRs closely linked to *KIR2DL5* include *KIR2DS5*, which has been linked to prevention of pre-eclampsia during pregnancy [95], and it is possible that the benefit of this

or other KIRs outweighs the possible detrimental effect of 2DL5 during malaria infection. However, carriage of this centromeric locus containing *KIR2DL5, 2DS3* and *2DS5* was suggested to be protective against severe malaria infection [300], and individuals carrying these genes were more likely to be asymptomatic or to only suffer from uncomplicated malaria. Olaniyan et al did not consider expression of any of these genes, and so the role of 'unexpressed' 2DL5 is not clear. Additionally, the fact that *KIR2DL5B* genes are transcriptionally silenced by promoter methylation, rather than by loss-of-function gene mutations or stop codons [87] is interesting. It is possible that this gene is heavily methylated to block transcription, and the passage of time will introduce mutations and inactivate the gene itself as well as the promoter region. However, if there is an advantage in demethylating the promoter region *in vivo* and transcribing functional 2DL5, this could be one reason for preserving the intact coding gene and therefore it is possible that 2DL5 expression may also be beneficial in some circumstances.

All of these observations require further validation and investigation before firm conclusions about the role of this KIR in malaria infection can be drawn. Analysis of 2DL5 expression in a larger number of donors from different genetic backgrounds, and assessing 2DL5 upregulation in NK cells after contact with iRBCs, would clarify whether this effect is replicable. Likewise, the effect of 2DL5 expression on conjugate formation or other NK cell responses may become clearer in a larger group of subjects. Measurement of KIR mRNA levels in cells after incubation with iRBCs would also confirm or dispell the observations from flow cytometry, as tools for directly measuring KIRs on the cell surface are still being optimised. Additionally, further analysis of other KIRs linked to 2DL5, especially 2DS5 and 2DS3 could be informative with regards to NK cell function and KIR expression patterns. As most KIRs appear to be independently transcribed, it would be very interesting to understand the expression patterns of these two KIRs in particular, as they have not been looked at to my knowledge. The recent release of an FACS antibody for 2DS5 might provide more information regarding 2DS5 expression patterns, and whether 2DL5 is the mediator of the observations I have described here or a proxy for another receptor. However, if 2DL5 expression does change during exposure to malaria parasites,

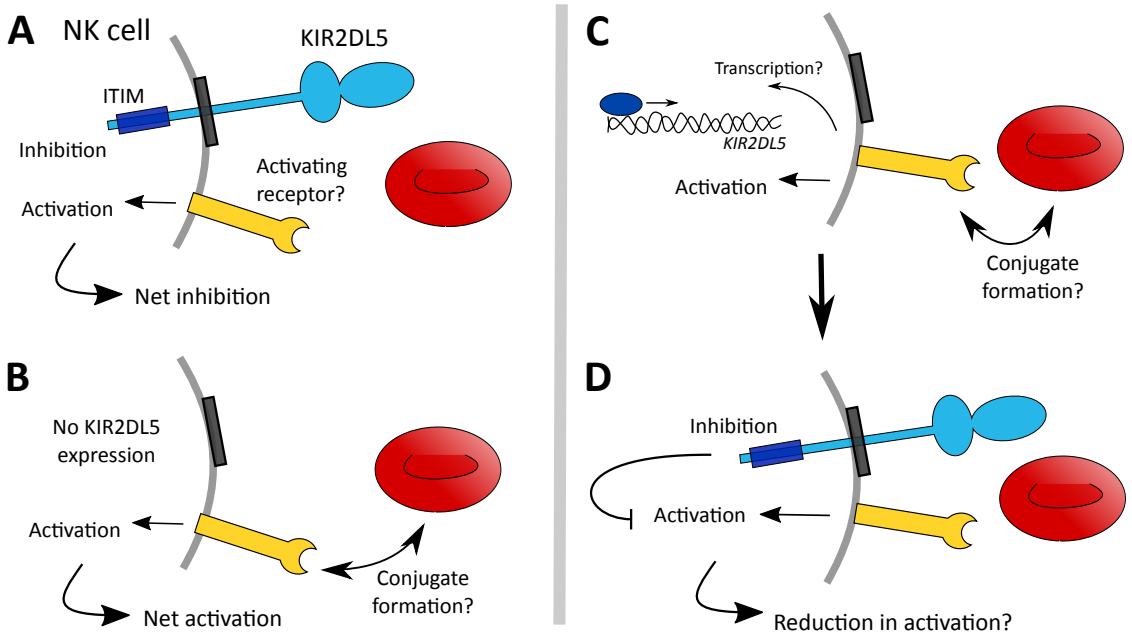

Figure 7.3: **KIR2DL5 expression may inhibit NK cell responses to iRBCs.** During malaria infection, NK cells interact with iRBCs, hypothesised to be mediated by activating receptors and to lead to NK-iRBC conjugate formation and potentially killing of iRBCs. Expression of the inhibitory receptor KIR2DL5 may induce inhibitory signalling during this interaction and lead to inhibition of the NK cell (A). However, in individuals without KIR2DL5 expression (via non-carriage of the gene or non-expression of KIR2DL5B), NK cells are not inhibited and can form conjugates and may kill iRBCs (B), and so lack of expressed KIR2DL5 may be beneficial in areas of high malaria endemnicity. However, it is possible that iRBCs can induce upregulation of KIR2DL5 expression, potentially by demethylating *KIR2DL5B* promoter regions and promoting transcription (C), leading to KIR2DL5 expression and inhibition of NK cell responses as an immune evasion response (D).

or does affect NK cell responses to iRBCs, identification of the ligand for 2DL5 would be a priority. Characterisation of 2DL5 surface expression in other African populations would also be informative, including whether HCMV drives expansions of 2DL5+ NK cells and whether 2DL5 is coexpressed with increasing CD57.

The potential role of malaria as a selective pressure on KIR haplotype would be particularly interesting to explore further, potentially by looking at 2DL5 gene carriage and expression in other populations with a recent history of endemic malaria, including in Europe. There

is some *KIR2DL5* frequency data available for Italian populations [351], but *KIR2DL5* genotype and expression data in multiple European, African and South American populations might indicate whether *KIR2DL5* has ever been under selective pressure. It might also be of interest to consider the role of NK cells on other species of malaria that are widespread in other countries, such as *P. vivax* across Asia, or *P. ovale* and *P. knowlesi* in southeast Asia; *KIR2DL5A* is widespread in these areas [303], and so it, or another KIR, could play a different role in these other malaria infections. Long-term *in vitro* culture of *P. knowlesi* is becoming possible, and so investigating NK cell responses to this parasite species might be more feasible in the near future.

7.5 Conclusions

In conclusion, the work described in this thesis indicates the level of complexity involved in defining and understanding NK cell responses, especially in response to malaria. The recent studies indicating a role for NK cells in adaptive immune responses highlight both the plasticity and variability in NK cell subsets, and understanding the effect of NK cell phenotype and receptor expression on NK cell function reinforces the model of NK cells as 'tuneable' and capable of a multitude of responses to different pathogens. The role of NK cells in malaria is both complex and heterogeneic, but the capacity to analyse the highly polymorphic KIR receptors controlling NK cell activity may allow better understanding of how NK cells can both directly interact with infected red blood cells and how indirect NK cell responses are mediated by interactions with other immune cells.

A | Publications

frontiers in Immunology

ORIGINAL RESEARCH
published: 22 March 2016
doi: 10.3389/fimmu.2016.00101

Synergy between Common γ Chain Family Cytokines and IL-18 Potentiates Innate and Adaptive Pathways of NK Cell Activation

*Carolyn M. Nielsen†, Asia-Sophia Wolf†, Martin R. Goodier and Eleanor M. Riley**

Department of Immunology and Infection, Faculty of Infectious and Tropical Diseases, London School of Hygiene and Tropical Medicine, London, UK

Studies to develop cell-based therapies for cancer and other diseases have consistently shown that purified human natural killer (NK) cells secrete cytokines and kill target cells after *in vitro* culture with high concentrations of cytokines. However, these assays poorly reflect the conditions that are likely to prevail *in vivo* in the early stages of an infection and have been carried out in a wide variety of experimental systems, which has led to contradictions within the literature. We have conducted a detailed kinetic and dose–response analysis of human NK cell responses to low concentrations of IL-12, IL-15, IL-18, IL-21, and IFN-α, alone and in combination, and their potential to synergize with IL-2. We find that very low concentrations of both innate and adaptive common γ chain cytokines synergize with equally low concentrations of IL-18 to drive rapid and potent NK cell CD25 and IFN-γ expression; IL-18 and IL-2 reciprocally sustain CD25 and IL-18Rα expression in a positive feedback loop; and IL-18 synergizes with FcγRIII (CD16) signaling to augment antibody-dependent cellular cytotoxicity. These data indicate that NK cells can be rapidly activated by very low doses of innate cytokines and that the common γ chain cytokines have overlapping but distinct functions in combination with IL-18. Importantly, synergy between multiple signaling pathways leading to rapid NK cell activation at very low cytokine concentrations has been overlooked in prior studies focusing on single cytokines or simple combinations. Moreover, although the precise common γ chain cytokines available during primary and secondary infections may differ, their synergy with both IL-18 and antigen–antibody immune complexes underscores their contribution to NK cell activation during innate and adaptive responses. IL-18 signaling potentiates NK cell effector function during innate and adaptive immune responses by synergy with IL-2, IL-15, and IL-21 and immune complexes.

Keywords: CD25, antibody, IL-2, IL-15, synergy

OPEN ACCESS

Edited by:
Angela Santoni, University Sapienza of Rome, Italy

Reviewed by:
Subramaniam Malarkannan, Medical College of Wisconsin, USA
Francesco Colucci, University of Cambridge, UK

***Correspondence:**
Eleanor M. Riley
eleanor.riley@lshtm.ac.uk

†Carolyn M. Nielsen and Asia-Sophia Wolf contributed equally to this study.

Specialty section:
This article was submitted to NK Cell Biology, a section of the journal Frontiers in Immunology

Received: *11 December 2015*
Accepted: *07 March 2016*
Published: *22 March 2016*

Citation:
Nielsen CM, Wolf AS, Goodier MR and Riley EM (2016) Synergy between Common γ Chain Family Cytokines and IL-18 Potentiates Innate and Adaptive Pathways of NK Cell Activation. Front. Immunol. 7:101. doi: 10.3389/fimmu.2016.00101

INTRODUCTION

Natural killer (NK) cells are classically regarded as innate lymphocytes that, by cytotoxicity and cytokine production, are among the earliest responders to damaged, transformed, or infected host cells. In the context of infection, they may directly lyse infected cells that no longer express self MHC Class I, mediate antibody-dependent cellular cytotoxicity (ADCC) of opsonized cells, or

secrete pro-inflammatory cytokines, such as IFN-γ, to activate phagocytes. During primary infection in a naive host, NK cells are activated by cytokines and contact-dependent signals from antigen-presenting cells [reviewed in Ref. (1)]; during secondary infection in a primed host, these innate signals are augmented by IL-2 from antigen-specific T helper cells (2–6) and by IgG immune complexes cross-linking FcRγIII (CD16) on the NK cell surface (7).

The precise cocktails of innate cytokines that most efficiently activate NK cells in response to any given pathogen, and how these cytokines synergize with adaptive responses, such as IL-2 and antibody to optimize the initial response to infection, are poorly described. Although numerous studies have reported NK cell activation by specific cytokines, they have tended to use very high concentrations of individual cytokines or combinations of cytokines, at a single concentration, to activate isolated populations of NK cells over rather long periods of time. For example, Aste-Amezaga et al. (8) demonstrated synergy between 1 ng/ml IL-12 and 100 IU/ml IL-2 for IFN-γ secretion from purified, B cell lymphoma-activated NK cells; Fehniger et al. (9) found that IL-12, IL-15, or IL-18 alone did not induce IFN-γ but that IFN-γ was produced by positively selected human NK cells after 24 h stimulation with 10 U/ml (approximately 2 ng/ml) IL-12 in combination with either 100 ng/ml IL-18 or 100 ng/ml IL-15; Son et al. (10) observed proliferation, CD25 upregulation, IFN-γ production, and cytotoxic activity in purified NK cells cultured for three days with 6 IU/ml IL-2 plus 1000 ng/ml IL-18; Trotta et al. (11) observed IFN-γ secretion from positively selected NK cells after 24 h stimulation with 10 ng/ml IL-12 plus either 100 ng/ml IL-18 or 10 μg/ml anti-CD16; and Leong et al. (12) described upregulation of CD25 (and subsequent enhanced responsiveness to IL-2) among purified NK cells cultured for 16 h with 50 ng/ml IL-18 plus either 100 ng/ml IL-15 or 10 ng/ml IL-12.

Although these studies, and others (13–16), produce a consistent picture of purified NK cells being able to proliferate and respond functionally to high concentrations of cytokines over periods of 16–72 h and are valuable in the context of developing NK cell-based therapies for cancer and other diseases, they provide little insight into the very early contribution that NK cells may make during infection. Indeed, there are no published studies that have systematically evaluated the kinetics, dose–response, and synergistic interactions leading to rapid and potent NK cell responses under conditions that mimic events early in primary infection. Similarly, there are limited data on the interaction between innate cytokines and components of the adaptive immune response to predict how NK cells might respond during secondary and subsequent infections.

In this study, we have conducted a detailed dose–response analysis of human NK cell CD25 and IFN-γ responses to IL-12, IL-15, IL-18, IL-21, and IFN-α at 6 and 18 h, and looked for synergy between low concentrations of these cytokines and IL-2. We have also investigated the capacity of IL-18 to synergize with FcRγIII (CD16) signaling to drive degranulation (CD107a) responses, in addition to CD25 and IFN-γ upregulation. Importantly, our assays have been carried out on unselected NK cells within peripheral blood mononuclear cells, in order to avoid inadvertent activation of NK cells during the purification process and in order to better reflect the cellular environment in which early responses to infection take place *in vivo*. Our data reveal potent and rapid activation of NK cells at cytokine concentrations that are orders of magnitude lower (and thus more physiologically relevant) than previously described. We also observe synergy between members of the common γ chain (γ_c) cytokine family, which includes IL-15, IL-2, and to a lesser extent IL-21, and IL-18, at exceedingly low concentrations; synergy between IL-18 and FcRγIII signaling in initiation of ADCC reactions; and synergistic, reciprocal upregulation of IL-18 receptor (IL-18Rα) and the high affinity IL-2 receptor (CD25) by IL-18 and IL-2 in an effective positive feedback loop.

In summary, these data indicate that NK cells can be very rapidly activated by exceedingly low doses of innate cytokines, such as might be found within minutes or hours at the site of infection, and can be further potentiated by adaptive immune responses (T cell IL-2 and antigen–antibody immune complexes) that are expected to occur upon re-infection.

MATERIALS AND METHODS

Study Subjects

Volunteers were recruited from among staff and students at the London School of Hygiene and Tropical Medicine. All subjects gave written consent under a protocol for recruitment of blood donors approved by the LSHTM ethics committee (reference # 5520) to provide ≤50 ml venous blood.

PBMC Preparation and Culture

PBMCs were isolated from heparinized venous blood on a Ficoll–Hypaque gradient and cryopreserved in liquid nitrogen. Before use, PBMCs were thawed into complete medium [RPMI 1640, supplemented with 100 U/ml penicillin/streptomycin and 20 mM L-glutamine (Life Technologies) and pooled 10% human AB plasma], washed, and rested for a minimum of 30 min before use.

PBMCs (2×10^5/well) were cultured for 6 or 18 h in 5% CO_2 at 37°C at in 96-well *U*-bottom plates (Nunc) in complete medium with or without varying concentrations and combinations of recombinant human IL-2, IL-12, IL-15, IFN-α, IL-21 (all from PeproTech), IL-18 (R&D Biosystems), or inactivated influenza virus H3N2 (1 μg/ml, NIBSC). GolgiStop (containing Monensin, 1/1500 concentration, BD Biosciences) and GolgiPlug (containing brefeldin A, 1/1000 final concentration, BD Biosciences) were added after 3 and 15 h (in 6 and 18 h cultures, respectively) in experiments where intracellular IFN-γ was a read-out. Similarly, anti-CD107a antibody (A488-conjugated, BD Biosciences) was included in the medium for the entirety of cell culture when CD107a upregulation was a read-out.

For activation *via* CD16 cross-linking, 96-well flat-bottom plates (Nunc) were coated with anti-human CD16 (BD Biosciences) or an isotype-matched control antibody (mIgG1κ, BD Biosciences) overnight at 4°C. Plates were washed with sterile PBS before addition of 4×10^5 PBMC per well. Cells were

harvested after 6 or 18 h. GolgiStop, GolgiPlug, and anti-CD107a were used, as described above.

Flow Cytometry

PBMCs were stained in 96-well *U*-bottom plates, as described previously (6). Briefly, cells were stained with fluorophore-labeled antibodies to cell surface markers then fixed, permeabilized (Cytofix/Cytoperm, BD Biosciences), and stained for intracellular molecules. The following monoclonal antibodies were used: anti-CD3-V500, anti-CD57-e450, anti-CD56-PECy7, anti-CD107a-A488, anti-IFN-γ-allophycocyanin, anti-CD16-allophycocyanin-H7, anti-CD16-allophycocyanin, anti-CD25-PerCPCy5.5, anti-IL-18Rα-PE, and anti-IL-18Rα-FITC (all BD or e-Biosciences). Anti-IL-12Rβ2 (R&D Systems) was conjugated to PerCP/Cy5.5 in-house (EasyLink PerCP/Cy5.5® Abcam). Cells were acquired on an LSRII flow cytometer (BD Biosciences) using FACSDiva software. Data analysis was performed using FlowJo v10 (Tree Star). Gating strategies are detailed in figure legends, with gates set on unstimulated cells (medium alone or isotype controls, with no cytokine stimulation) and applied in a standard format.

Statistical Analyses

Statistical analysis of flow cytometry data was performed using Prism 6 (GraphPad), as specified in figure legends. Data were excluded when the gated cell subset contained fewer than 100 cells. Paired Wilcoxon signed-rank tests were used to compare responses between stimulation conditions and ANOVA tests for linear trend were used to analyze cytokine titrations. Formal tests for synergy using regression analysis with an interaction term, and linear regression adjusting for confounding factors were performed in STATA (V.14.0). All statistical tests are two-sided $^{****}p \leq 0.0001$, $^{***}p < 0.001$, $^{**}p < 0.01$, $^{*}p < 0.05$. Sample sizes are stated in figure legends.

RESULTS

Common γ Chain Family Cytokines Synergize with IL-18 to Drive CD25 Expression on NK Cells

PBMCs were stimulated with increasing concentrations of IL-2, IL-12, IL-15, IL-18, or IL-21, and NK cell surface expression of CD25 was measured after 6 or 18 h (**Figures 1A–C**). Upregulation of CD25 is of interest as a marker of NK cell activation and, more specifically, increased sensitivity to IL-2; indeed, NK cell production of IFN-γ in response to picomolar levels of IL-2 has been shown to be CD25 dependent (12). The highest cytokine concentrations tested reflect those widely used as positive controls by ourselves (5, 6, 17) and others; cytokines were then titrated to concentrations at least fivefold lower than the lowest previously described effective concentration.

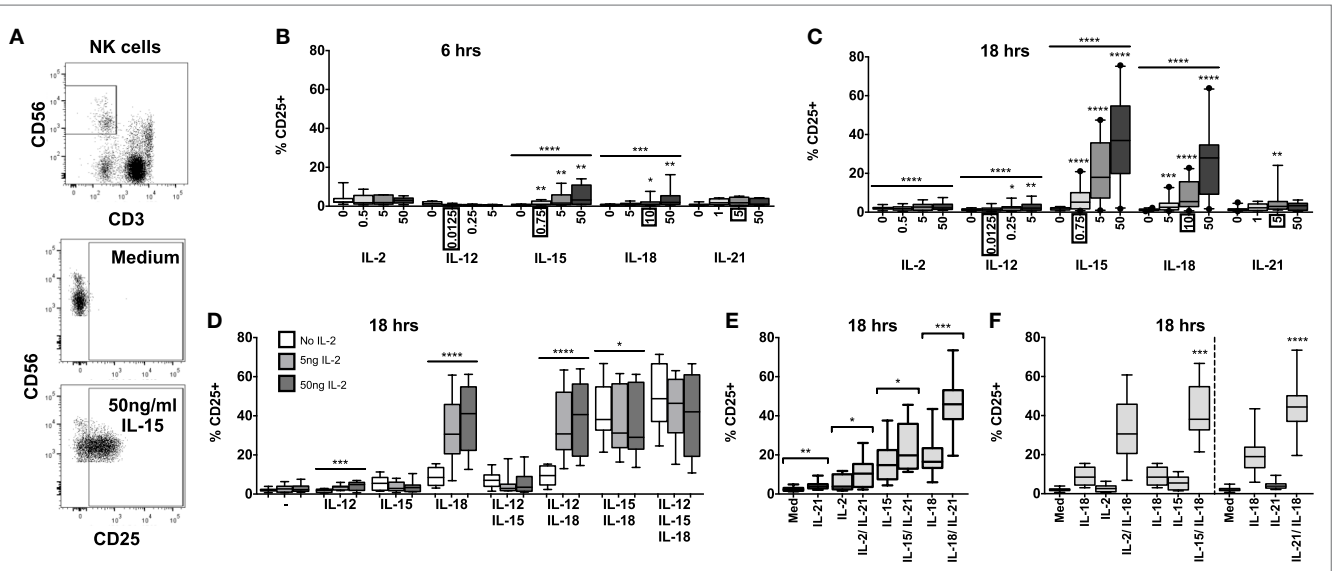

FIGURE 1 | **IL-18 and IL-15 both independently drive CD25 but interact differently with IL-2**. PBMCs were stimulated for 6 or 18 h *in vitro* and upregulation of NK cell surface expression of CD25 was measured in response to Med (medium alone), IL-2, IL-12, IL-15, IL-18, or IL-21. Representative flow cytometry plots show gating of $CD3^{-}CD56^{+}$ NK cells and surface expression of CD25 on unstimulated and IL-15-stimulated NK cells (50 ng/ml) **(A)**. CD25 expression on NK cells was measured after stimulation with Med, IL-2, IL-12, IL-15, IL-18, or IL-21 (concentrations in nanograms per milliliter as labeled) for 6 h **(B)** or 18 h **(C)** (n = 6–22, data from two to three experiments). Concentrations in boxes indicate those used in following graphs. CD25 expression on NK cells was also measured after stimulation with a titration of IL-2 (0, 5, and 50 ng/ml) in combination with IL-12 (12.5 pg/ml), IL-15 (0.75 ng/ml), and/or IL-18 (10 ng/ml) for 18 h **(D)** (n = 7–8, data from two experiments). CD25 expression on NK cells was also measured following stimulation with 5 ng/ml IL-21 in combination with 5 ng/ml IL-2, 0.75 ng/ml IL-15, or 10 ng/ml IL-18 after 18 h **(E)** (n = 8, data from one experiment). CD25 expression after stimulation for 18 h with a combination of IL-18 (10 ng/ml) and γ_c cytokines was summarized to facilitate comparison between IL-2 (5 ng/ml), IL-15 [0.75 ng/ml; both from **(D)**], and IL-21 [5 ng/ml; from **(E)**] **(F)** (n = 7–8, data from one to two experiments). Box plots show the 5th to 95th percentile range. Data were analyzed using paired Wilcoxon signed-rank tests [**(B,C,F)** no lines; lowest concentration compared to Med, **(E)** capped lines; IL-2/IL-18 and IL-15/IL-18 compared to IL-18 alone, **(F)**] or ANOVA tests for linear trend for trend analysis across increasing cytokine concentrations including Med [**(B–D)**, uncapped lines]. $^{****}p < 0.0001$, $^{***}p < 0.001$, $^{**}p < 0.01$, $^{*}p < 0.05$.

IL-15 and IL-18 each, independently, drive CD25 expression in a dose- and time-dependent manner. Significant CD25 expression could be detected within 6 h among cells cultured with cytokine concentrations as low as 0.75 ng/ml IL-15 and 10 ng/ml IL-18 (**Figure 1B**) but CD25 expression was markedly higher after 18 h for both cytokines and evident at the lowest cytokine concentrations tested (0.75 ng/ml IL-15 and 5 ng/ml IL-18) (**Figure 1C**). For IL-15, this is 6-fold lower than the previously described minimal concentration (14, 16) for upregulation of CD25, and 10- to 1000-fold lower than previously used concentrations of IL-18 (12, 15). Incubation of PBMC with IL-2, IL-12, and IL-21 induced minimal, albeit statistically significant, expression of CD25 on NK cells at 18 h, but not at 6 h.

To investigate potential synergies between cytokines in driving CD25 expression on NK cells, PBMCs were stimulated with combinations of IL-12, IL-15, and IL-18, with or without varying concentrations of IL-2, to model early NK cell activation in response to primary pathogen infection (innate cytokines only, no IL-2) and secondary infection (innate cytokines plus IL-2 from memory $CD4^+$ T cells). We selected the lowest concentrations of IL-12 and IL-15 that had been tested singly (12.5 pg/ml and 0.75 ng/ml, respectively) and, for consistency with our own previously published work (5, 6, 17), we used the middle concentration of IL-18 (10 ng/ml). The middle concentration of IL-21 (5 ng/ml), an adaptive γ_c cytokine, was selected to permit later comparisons with IL-2.

Consistent with the data presented in **Figure 1B**, CD25 expression was very low after 6 h, and there was no significant evidence of synergism between cytokines (data not shown). However, after 18 h, the data clearly showed synergy between IL-18 and IL-2 in driving NK cell CD25 expression (trend analysis $p < 0.0001$ for IL-18 in combination with increasing concentrations of IL-2) with 5 ng/ml IL-2 in combination with 10 ng/ml IL-18 giving CD25 expression levels equivalent to those seen with 50 ng/ml IL-18 alone (**Figures 1C,D**). Although adding IL-12 to a cocktail of IL-2 plus IL-18 did not further enhance CD25 expression, including a low concentration of IL-12 (0.0125 ng/ml) in the cultures did permit detection of a modest IL-2 dose response (**Figure 1D**) and much higher, though less physiological, concentrations of IL-12 (1–10 ng/ml) do synergize with IL-18 to drive CD25 expression (Figure S1 in Supplementary Material) (12, 18). There was also strong evidence that IL-15 synergizes with IL-18 to enhance NK cell CD25 expression (**Figure 1F**, test for interaction IL-15 and IL-18, $p = 0.009$).

By contrast, IL-15-driven CD25 upregulation was partially inhibited by IL-2: there was a trend for the proportion of NK cells expressing CD25 to decrease with increasing concentrations of IL-2 in all cytokine combinations that included IL-15, with a statistically significant impact observed in NK cells stimulated with IL-15 plus IL-18 (median without IL-2 = 38.1% vs. median with high concentration IL-2 = 29.0%; linear test for trend, $p = 0.04$; **Figure 1D**).

In a separate set of experiments, we also tested IL-21 and IFN-α for their ability to synergize with IL-2, IL-15, and IL-18 to drive CD25 expression on NK cells. There was no evidence that IFN-α alone induced CD25 expression nor did it enhance CD25 expression in combination with other cytokines (Figure S2 in Supplementary Material). However, IL-21 in combination with IL-2, IL-15, or, in particular, IL-18 significantly enhanced CD25 expression compared to these cytokines alone (**Figure 1E**). Indeed, there was clear evidence of synergy between IL-21 and IL-18 driving CD25 expression (**Figure 1F**, test for interaction IL-21 and IL-18, $p < 0.0001$).

In summary, these data indicate that at least three different cytokines that signal *via* the common γ chain (CD132) can individually synergize with the IL-18 pathway leading to rapid upregulation of CD25 expression on NK cells, and at much lower cytokine concentrations than previously appreciated (**Figure 1F**). As IL-15 and IL-18 are produced primarily by dendritic cells, monocytes, and macrophages, and as IL-2 and IL-21 are primarily T cell-derived, these combinations of cytokines allow for very early NK cell activation – when cytokine concentrations are still extremely low – *via* both innate and adaptive immune pathways. Moreover, there is evidence of homeostatic regulation of NK cell activation *via* γ_c cytokines, as illustrated by inhibition of IL-15-driven CD25 upregulation by IL-2.

Common γ Chain Cytokines Synergize with IL-18 to Drive Rapid and Extensive IFN-γ Production by NK Cells

Upregulation of CD25 primes NK cells for enhanced subsequent responses to IL-2 (12) but is not, in itself, a read-out of NK cell effector function. We have therefore characterized the effect of combining low concentrations of different cytokines on IFN-γ production, assessed by intracellular staining after incubation of PBMC with increasing concentrations of individual cytokines or cytokine combinations (**Figure 2**).

Increasing concentrations of IL-2, IL-12, IL-15, or IL-18 (but not IL-21) each, individually, induced significant IFN-γ production by NK cells at 18 h, although the proportions of IFN-γ^+ cells rarely exceeded 10% even at the highest cytokine concentrations (**Figure 2B**). However, combining IL-18 (at a concentration of 10 ng/ml), with as little as 5 ng/ml IL-2 (which alone did not drive IFN-γ) not only induced IFN-γ in much higher proportions of NK cells (>20%) but did so within 6 h of incubation (**Figure 2C**). Although this interaction appears additive at 6 h (test for interaction, $p = 0.22$) by 18 h the interaction is highly synergistic (test for interaction, $p = 0.006$), possibly as a result of IL-18 induced upregulation of the high affinity IL-2R.

In contrast to what we observed for CD25 expression, there was no evidence of antagonism or competition between γ_c cytokines in their induction of NK cell IFN-γ. On the contrary, there was evidence of additive or synergistic interactions between γ_c cytokines with increasing concentrations of IL-2 modestly but significantly enhancing NK cell IFN-γ responses to IL-15 + IL-18 (**Figures 2C,D**). Low concentrations of IL-15 (**Figures 2C,D**) and IL-21 (**Figure 2E**) also enhanced IL-18-induced NK cell IFN-γ production, but to a lesser extent than IL-2 (**Figures 2C,D,F**). Although IL-15 plus IL-18 has previously been shown to enhance NK cell IFN-γ, as measured by ELISA, the effects described here were apparent at an IL-15

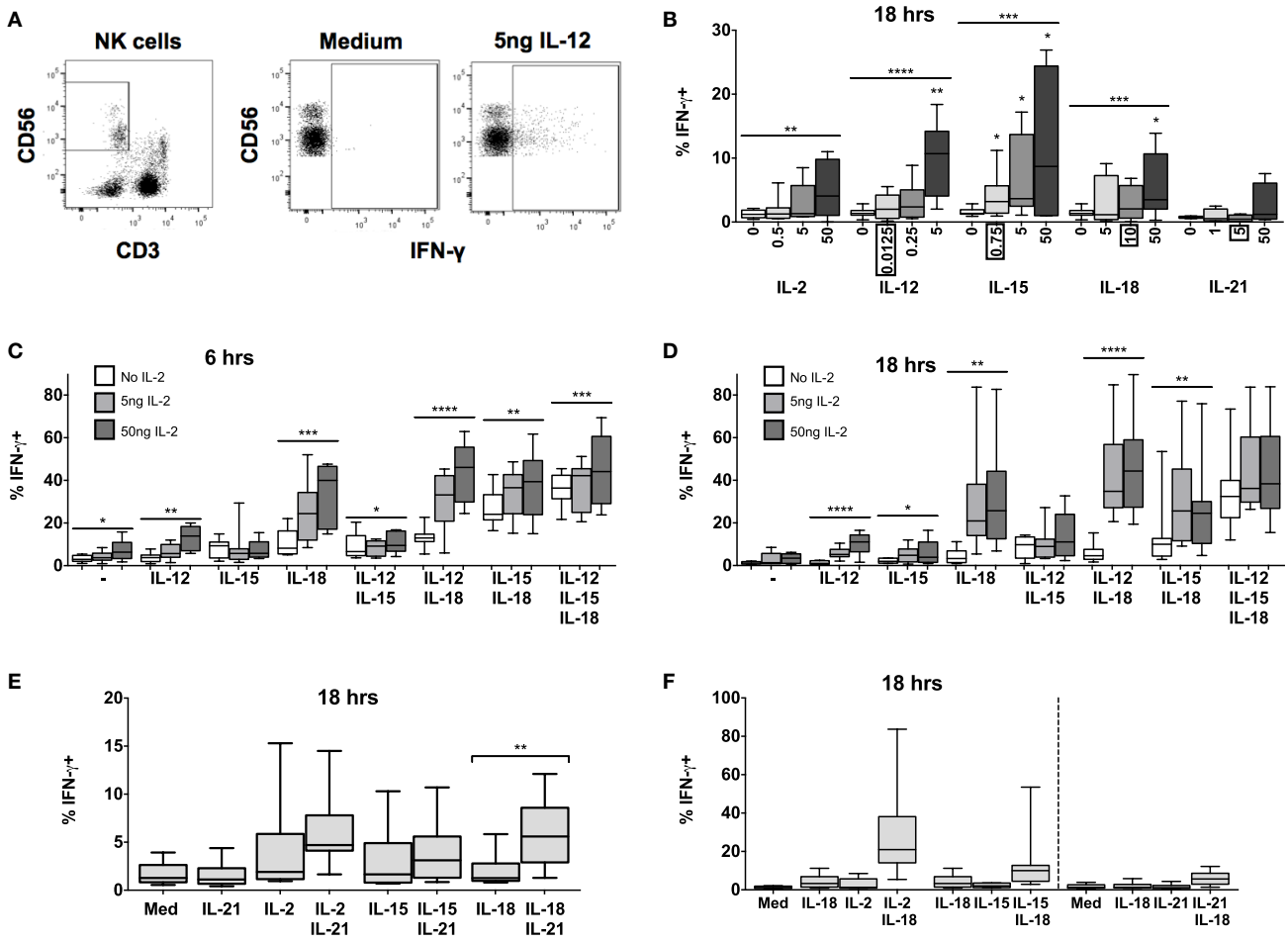

FIGURE 2 | IL-15 and IL-18 can synergize to drive IFN-γ in absence of IL-12 or IL-2. PBMCs were stimulated for 6 or 18 h *in vitro* and production of intracellular IFN-γ by NK cells was measured in response to Med (medium alone), IL-2, IL-12, IL-15, IL-18, or IL-21. Representative flow cytometry plots show gating of $CD3^-CD56^+$ NK cells and percentage of $CD56^+$ cells that are positive for intracellular IFN-γ on unstimulated and IL-12-stimulated NK cells (5 ng/ml) **(A)**. IFN-γ production by NK cells was measured after stimulation with Med, IL-2, IL-12, IL-15, IL-18, or IL-21 (concentrations in nanograms per milliliter as labeled) for 18 h **(B)** (n = 4–9, data from one to three experiments). Concentrations in boxes indicate those used in following graphs. IFN-γ production by NK cells was also measured after stimulation with a titration of IL-2 (0, 5, and 50 ng/ml) in combination with IL-12 (12.5 pg/ml), IL-15 (0.75 ng/ml), and/or IL-18 (10 ng/ml) for 6 h **(C)** or 18 h **(D)** (n = 7–8, data from two experiments). IFN-γ production by NK cells was also measured following stimulation with 5 ng/ml IL-21 in combination with 5 ng/ml IL-2, 0.75 ng/ml IL-15, or 10 ng/ml IL-18 after 18 h **(E)** (n = 8, data from one experiment). IFN-γ expression after stimulation for 18 h with a combination of IL-18 (10 ng/ml) and γ_c cytokines was re-plotted to facilitate comparison between IL-2 (5 ng/ml), IL-15 [0.75 ng/ml; both from **(D)**], and IL-21 [5 ng/ml; from **(E)**] for 18 h **(F)** (n = 7–8, data from one to two experiments). Box plots show the 5th to 95th percentile range. Data were analyzed using paired Wilcoxon signed-rank tests [**(B)**: no lines; lowest concentration compared to Med; **(E)** capped lines] or ANOVA tests for linear trend for trend analysis across increasing cytokine concentrations including Med [**(B–D)**, uncapped lines]. $^{****}p < 0.0001$, $^{***}p < 0.001$, $^{**}p < 0.01$, $^{*}p < 0.05$. $n \geq 8$, other than for IL-21 titration **(B)** where $n = 4$.

concentration (0.75 ng/ml) markedly lower than previously described (5 ng/ml) (14).

Again, as for CD25 expression, we found no evidence of a role for IFN-α in NK cell IFN-γ production (Figure S2 in Supplementary Material); this is in contrast to published data (19). Low concentrations of IL-12 (0.0125 ng/ml) – alone or in combination with IL-2 or IL-21 – had minimal effects on IFN-γ production (**Figures 2C–E**), but did enhance IFN-γ production in combination with IL-15 and IL-18 at later time points. High concentrations of IL-12 (≥1 ng/ml) synergized strongly with IL-18 to drive both IFN-γ and CD25, although we suggest that these do not reflect physiological conditions (Figure S1 in Supplementary Material) (9, 11, 12, 15, 20). Overall, however, as little as 5 ng/ml IL-2 in combination with low concentrations of IL-18 (10 ng/ml) and IL-12 (12.5 pg/ml) was the optimal combination for NK cell IFN-γ induction at 18 h.

In summary, therefore, γ_c cytokines (IL-2, IL-15, and IL-21) in combination with IL-18 induce very rapid and extensive IFN-γ production by NK cells (**Figure 2F**). Although IL-2 seems to be the most potent of these, at least at the cytokine concentrations tested, the ability of IL-15 to augment IFN-γ production offers a route for rapid, innate activation of NK cells prior to the differentiation of IL-2 secreting T cells. Of interest, given the very large body of work describing IFN-γ induction by combinations of IL-12 and IL-18, γ_c

cytokines synergize with IL-18 at extremely low concentrations. It is possible therefore that, *in vivo*, IL-12 may contribute to NK cell IFN-γ production when γ_c cytokines are lacking, such as during primary exposure (when IL-2 from antigen-specific T cells may be limiting) or later in infection when IL-15 signaling is reduced by changes in receptor expression (21, 22).

IL-18 Signaling Sustains IL-18Rα Expression on NK Cells

As IL-18 alone is able to induce both CD25 and IFN-γ expression within 6 h (**Figures 1B** and **2C**), we hypothesized that maintaining the capacity for IL-18 signaling might be required for optimal NK cell activation. Thus, the sustained or enhanced expression of the IL-18R may contribute to the synergy between IL-18 and γ_c cytokines. To determine whether, and if so which, cytokines regulate IL-18R expression, NK cell surface expression of IL-18Rα [CD218a, the receptor component required for signaling (23)] was measured after 6 or 18 h of PBMC culture with IL-2, IL-12, IL-15, IL-18, IL-21, or IFN-α, alone and in combination (**Figure 3**; Figure S2 in Supplementary Material). It was immediately obvious that resting levels of IL-18Rα expression are extremely variable between donors with the proportion of resting NK cells expressing the receptor varying from approximately 20% to >80% (**Figures 3B,C**). Polymorphisms affecting DNA methylation within the promoter region of *IL18R1*, the gene encoding IL-18Rα, and subsequent transcription of the gene have been reported and may in part explain this variation (24, 25) and we have previously observed lower levels of IL-18Rα expression in human cytomegalovirus (HCMV)-infected individuals than in HCMV-uninfected individuals (6). Despite this inter-individual variation, resting levels of IL-18Rα expression are very high in comparison to resting levels of the high affinity IL-2R (as defined by expression of the IL-2Rα chain, CD25; see **Figures 1B,C**) and fully functional IL-12R (as defined by expression of IL-12R-β2; see Figure S2 in Supplementary Material) and may explain the very rapid (within 6 h) NK cell response to exogenous IL-18 (**Figures 1B** and **2C**). Indeed, we observed a weak but statistically significant correlation between resting levels of NK cell IL-18Rα expression and upregulation of CD25 following IL-18 stimulation [$n = 18$, 50 ng/ml IL-18, linear regression (adjusting for use of PE- and FITC-conjugated anti-IL-18Rα) $R^2 = 0.241$, $p = 0.046$].

Contrary to previously published data indicating that IFN-α (13) and IL-12 (9, 11, 13, 20) can individually induce IL-18R mRNA (9, 13), IL-18Rα protein expression (11), or IL-18R expression (20) in human NK cells, and that IL-12/STAT4 signaling induces IL-18Rα expression in mice (26, 27), we found no increase in surface expression of IL-18Rα in response to increasing concentrations of either IFN-α (Figure S2 in Supplementary Material) or IL-12 (**Figure 3B**) with or without IL-2 (**Figure 3C**). There are several likely explanations for this discrepancy. For example, in previous studies, exogenous IL-2 was routinely added to NK cell cultures and IFN-α was used at much higher concentrations (13); NK cells were stimulated with very high concentrations of IL-12 (9, 11); IL-18R mRNA was assessed rather than IL-18R protein (9, 13); NK cells were purified by positive selection which may, in itself, contribute to subsequent activation (9, 11); or components of the IL-18R other than IL-18Rα were measured (9, 13, 20). Nevertheless, our data suggest that at physiological concentrations, IL-2, IL-12, and IFN-α have little, if any, effect on IL-18Rα expression. We also observed no effect of IL-21 on IL-18Rα expression (Figure S2 in Supplementary Material).

By contrast, we found clear evidence of concentration-dependent upregulation of NK cell IL-18Rα expression in response to IL-15 alone and IL-18 alone (**Figures 3B,C**). Ten nanograms per milliliter of IL-18 were sufficient to upregulate IL-18Rα within 6 h (**Figure 3B**) ($p = 0.0010$) and this effect was sustained at 18 h (**Figure 3C**) ($p = 0.0003$). IL-15 had no effect on IL-18Rα expression at 6 h, but as little as 0.75 ng/ml IL-15 was sufficient to upregulate IL-18Rα expression by 18 h (**Figures 3B,C**) ($p = 0.019$). Overall, IL-15 and IL-18 each increased the proportion of NK cells expressing IL-18Rα by approximately 15% (median percentage of IL-18Rα$^+$ NK cells: 50.1% medium only; 64.6% with 50 ng IL-18; 66.8% with 50 ng IL-15). The ability of IL-18 to rapidly augment expression of its own receptor is suggestive of a positive feedback loop, allowing for enhanced IL-18 signaling, continued synergism with other signaling pathways and efficient induction of NK cell effector functions in the first few hours of infection.

We next considered whether other cytokines might synergize with IL-18 to further enhance IL-18Rα expression. Increasing concentrations of IL-2, either alone or in combination with IL-12 or IL-15 had no significant effect on IL-18Rα expression at either 6 h (not shown) or 18 h (**Figure 3D**). However, IL-2 modestly but significantly enhanced the effects of IL-18 in a dose-dependent manner, and there was an additive effect of combining IL-15 and IL-18 in the absence of IL-2 (**Figure 3D**). Addition of other cytokines to the IL-18 + IL-2 cocktail did not further enhance IL-18Rα expression. Although at the low cytokine concentrations used in these experiments (0.0125 ng/ml IL-12, 10 ng/ml IL-18) we saw no additive or synergistic effect of adding IL-12 to IL-18, at much higher concentrations (5 ng/ml IL-12 and 50 ng/ml IL-18) we did observe a significant ($p < 0.0001$) additive effect of these two cytokines increasing IL-18Rα expression (data not shown). These data support our contention that IL-18 is the key cytokine in initiating and sustaining NK cell responses under physiologically relevant conditions such as very early infection, and that NK cell responses that can be induced with very high (non-physiological) cytokine concentrations *in vitro* may not be relevant *in vivo*.

In summary, therefore, low concentrations of IL-18 rapidly and significantly upregulate the IL-18Rα subunit and this effect is augmented by low concentrations of IL-15 and (more substantially) by IL-2. Given that IL-18 alone is sufficient to induce expression of the high affinity IL-2R (**Figures 1B,C**), it seems that IL-18 and IL-2 synergistically and reciprocally upregulate their own and each other's receptors in a potent positive feedback loop. The minimal role of low concentrations of IL-12 in this process may explain the limited synergies of exogenous IL-12 in the early NK cell IFN-γ response (**Figure 2**).

For completeness, we also examined expression of IL-12Rβ2 in response to single cytokines or cytokine

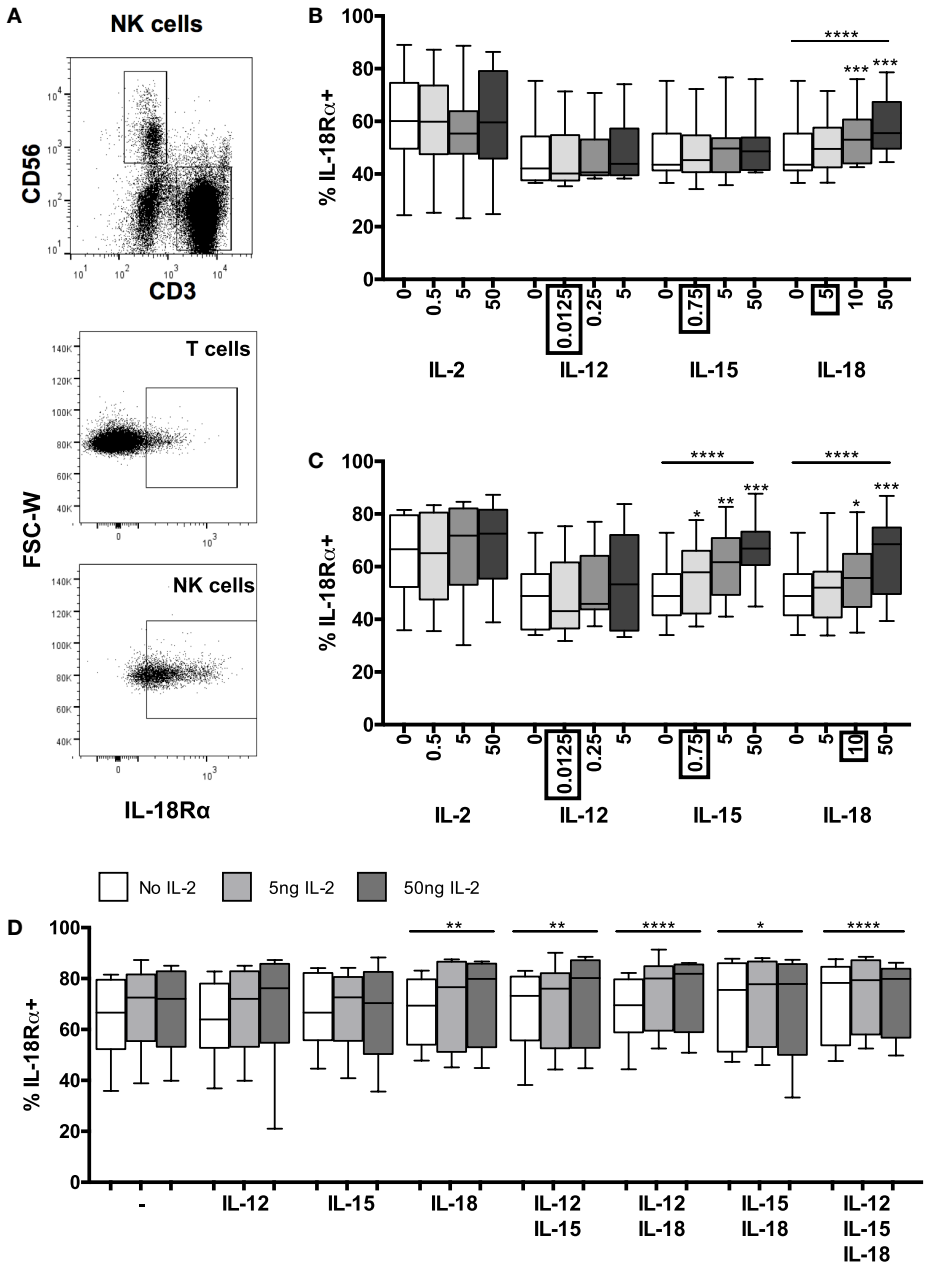

FIGURE 3 | Positive feedback from IL-18 induces IL-18R. PBMCs were stimulated for 6 or 18 h *in vitro* and changes in NK cell surface expression of IL-18Rα was measured in response to Med (medium alone), IL-2, IL-12, IL-15, IL-18, or IL-21. Representative flow cytometry plots show gating of $CD3^+$ T cells, $CD3^-CD56^+$ NK cells, and surface expression of IL-18Rα on unstimulated T cells and NK cells for IL-18Rα-FITC [N.B. as used in **(D)**; IL-18Rα-PE used in **(B,C)**] **(A)**. IL-18Rα expression on NK cells was measured after stimulation with Med, IL-2, IL-12, IL-15, IL-18, or IL-21 (concentrations per milliliter as labeled) for 6 **(B)** or 18 h **(C)** (n = 7–11 data from one to two experiments). Concentrations in boxes indicate those used in following graphs. IL-18Rα expression on NK cells was also measured after stimulation with a titration of IL-2 (0, 5, and 50 ng/ml) in combination with IL-12 (12.5 pg/ml), IL-15 (0.75 ng/ml), and/or IL-18 (10 ng/ml) after 18 h **(D)** (n = 8, data from two experiments). Box plots show the 5th to 95th percentile range. Data were analyzed using paired Wilcoxon signed-rank tests [**(B–D)** no lines; compared to Med] or ANOVA tests for linear trend for trend analysis across increasing cytokine concentrations including Med [**(B–D)**, uncapped lines]. $^{****}p < 0.0001$, $^{***}p < 0.001$, $^{**}p < 0.01$, $^{*}p < 0.05$.

combinations (Figure S3 in Supplementary Material). The proportion of NK cells expressing IL-12Rβ2 was transiently (seen at 6 h but not at 18 h) and very modestly enhanced by 10–50 ng/ml IL-18 and, in a slightly more sustained fashion, by 50 ng/ml IL-15, but the biological relevance of such small effects is unclear. There was no effect of exogenous cytokines on IL-12Rβ2 expression at the level of individual cells (as measured by MFI).

IL-18 Synergizes with FcγRIII (CD16) Signaling to Augment NK Cell-Mediated Antibody-Dependent Cellular Cytotoxicity

After vaccination, or upon secondary infection, circulating antigen–antibody complexes binding to FcγRIII (CD16) on NK cells can mediate killing of infected cells *via* ADCC. As our data suggest that IL-18, in concert with γ_c cytokines, enhances adaptive and innate pathways of NK cell activation, we wanted to test whether ADCC could be augmented by very low levels of NK cell activating cytokines, as would be present at the site of infection (**Figure 4**).

We found that IL-18, but not IL-12, IL-15, or IL-21, induced rapid (within 6 h) and sustained (persists at 18 h), concentration-dependent downregulation of CD16 expression at the NK cell surface such that cells substantially lost CD16 expression within 6 h in the presence of 10 ng/ml IL-18 (**Figures 4A,B**; Figure S2 in Supplementary Material). We have previously observed that cross-linking of CD16 with plate-bound anti-CD16 antibody leads to loss of CD16 from the NK cell surface (Goodier, unpublished data), and this is consistent with previous reports of CD16 downregulation following CD16 ligation (28). Here, we observe that the inherent capacity of IL-18 to reduce CD16 expression synergizes with the effects of CD16 cross-linking such that after 6 and 18 h, residual CD16 expression is lower when NK cells are cultured with 10 ng/ml IL-18 plus plate-bound anti-CD16 than when they are cultured with either anti-CD16 or IL-18 alone (**Figure 4C**). Taken together with data indicating that downregulation of CD16 on $CD56^{dim}$ NK cells in response to either CD16 cross-linking or to very high concentrations of IL-12 (10 ng/ml) plus IL-18 (100 ng/ml) can be blocked with a specific inhibitor specific of the metalloprotease ADAM-17 (28), these data raise the interesting hypothesis that the IL-18 and the CD16 signaling pathways may converge to induce metalloprotease-mediated cleavage of CD16 from the cell surface. We could not find any evidence that CD16 cross-linking affects expression of IL-18Rα (data not shown).

Using cross-linking of cell surface CD16 with plate-bound anti-CD16 antibody as a model of ADCC (28), we next determined the effects of low concentrations of IL-18 on NK cell cytotoxicity [assessed using the CD107a degranulation assay (29, 30)] as well as on CD25 and IFN-γ responses. Despite the very rapid downregulation of CD16 by IL-18 and CD16 cross-linking (**Figures 4B,C**), we observed that as little as 10 ng/ml IL-18 markedly and very rapidly (within 6 h) augmented NK cell degranulation and IFN-γ production in the presence of anti-CD16 antibody (**Figures 4D,E**). Furthermore, IL-18 synergized with anti-CD16 to enhance CD25 expression at 18 h (**Figure 4F**; test for interaction, $p = 0.005$). These data demonstrate that IL-18 can substantially enhance NK cell ADCC responses and also support the idea that IL-18- and anti-CD16-driven downregulation of CD16 expression is a consequence of activation of signaling pathways downstream of CD16.

To validate this apparent interaction between IL-18 and CD16, PBMCs were incubated for 18 h with or without whole, inactivated H3N2 influenza virus in the presence of plasma that had previously been shown to contain anti-H3N2 IgG and to mediate ADCC [(6); Goodier et al., submitted]. NK cell degranulation, CD25, and IFN-γ responses to H3N2 immune complexes were compared in the presence or absence of exogenous IL-18 (**Figure 5**). As reported above, IL-18 alone induced modest increases in CD107a, CD25, and IFN-γ expression. Furthermore, as previously reported for H1N1 virus (6), incubation of NK cells with H3N2 virus and plasma containing anti-H3N2 antibodies induced significant degranulation (CD107a expression) (**Figure 5A**), upregulation of CD25 (**Figure 5B**), and production of IFN-γ (**Figure 5C**). However, as little as 5 ng/ml IL-18 in combination with H3N2 and anti-H3N2 was sufficient to markedly augment CD107a, CD25, and IFN-γ expression; the effects of the combination of IL-18 plus H3N2/anti-H3N2 were additive for CD107a expression, but synergistic for CD25 and IFN-γ (**Figures 5A–C**, tests for interaction, 5 ng/ml IL-18 and H3N2 for CD107a $p = 0.269$; CD25 $p = 0.002$; and IFN-γ $p = 0.038$).

In summary, therefore, IL-18 synergizes with CD16-mediated signals to augment NK cell ADCC activity and indicates that IL-18 may play an important role in driving NK cell cytotoxicity and cytokine production.

DISCUSSION

The capacity of NK cells to be activated, within minutes or hours, by very low concentrations of innate cytokines is integral to their role as early responders during infection. Although pathogens may, ultimately, be cleared by components of the adaptive immune system, NK cells and other innate leukocytes are critical for initial containment of infection and orchestration of the subsequent adaptive response (31).

The role of exogenous cytokines in driving NK cell responses has been studied extensively in different contexts, including infection and cancer immunotherapy. However, these *in vitro* experiments have, almost exclusively, been carried out with purified NK cells stimulated with very high concentrations of cytokines that do not reflect the *in vivo* response, may over-ride natural homeostatic mechanisms that regulate the extent and duration of NK cell activation, and ignore interactions with other immune cells and with components of the adaptive immune system. Importantly, few studies have evaluated combinations of more than two cytokines and none have carefully titrated cytokine concentrations within these combinations. Thus, although we have abundant information about which cytokines and other signals can, under certain conditions, activate NK cells, we have a much less clear picture of which signals and which combinations of signals most efficiently activate NK cells in physiologically relevant conditions.

In an attempt to conduct a more physiologically relevant analysis of NK cell–cytokine interactions, we have conducted a systematic analysis of the roles of different cytokines and cytokine combinations in NK cell activation and their interaction with adaptive immune responses. We have demonstrated that NK cells can respond, within hours, to concentrations of cytokines that are orders of magnitude lower than previously appreciated and that NK cells can integrate signals, synergistically, from multiple cytokine receptors and FcγRIII, enabling them to respond

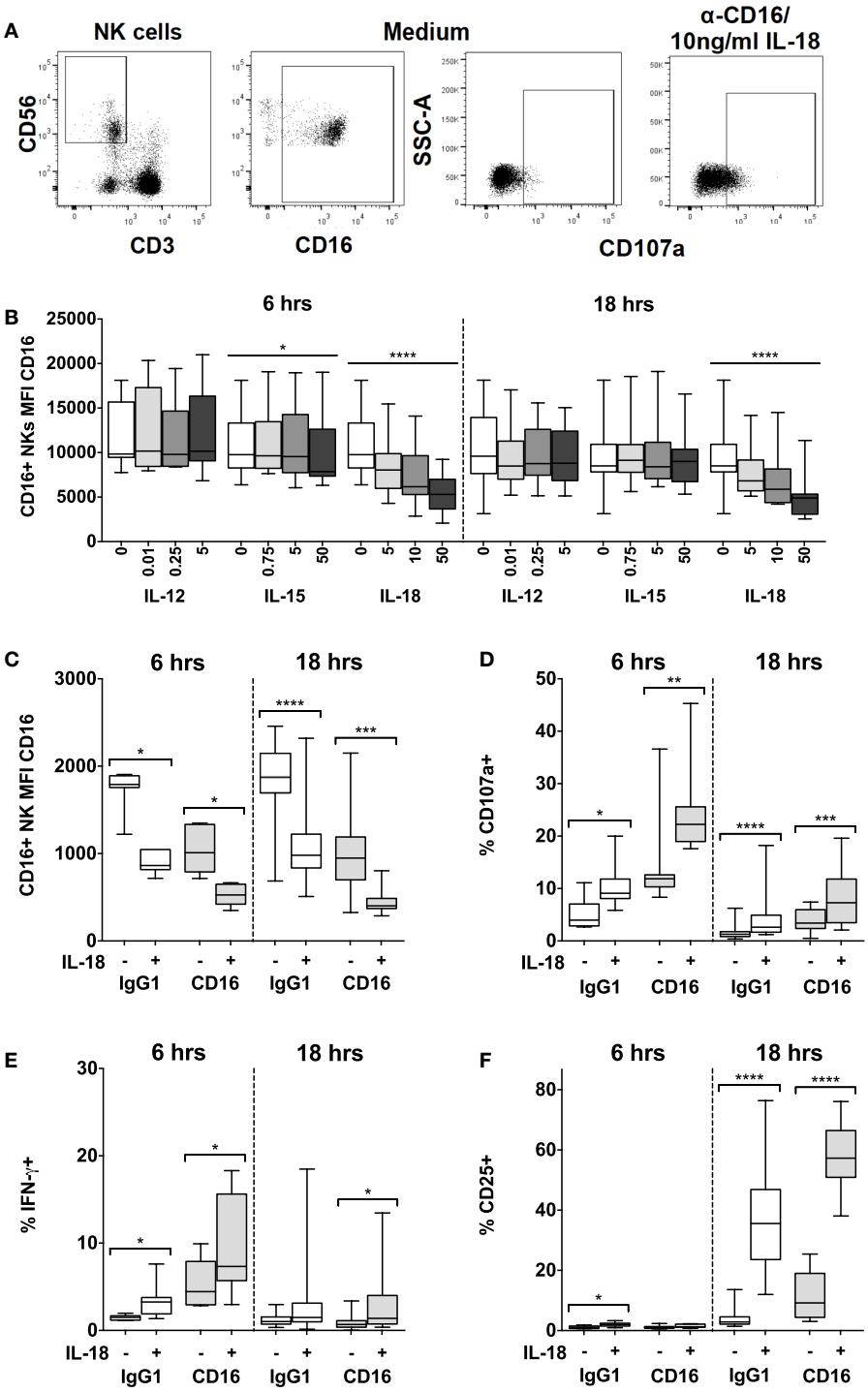

FIGURE 4 | **IL-18 enhances responses to CD16 cross-linking, while simultaneously driving CD16 downregulation**. PBMCs were stimulated for 6 or 18 h *in vitro* and changes in CD16 mean fluorescence intensity (MFI) of $CD16^+$ NK cells were measured in response to Med (medium alone), IL-12, IL-15, or IL-18. Representative flow cytometry plots show gating of $CD3^-CD56^+$ NK cells, and surface expression of CD107a or CD16 on unstimulated cells, or CD107a on NK cells activated with CD16 cross-linking and 10 ng/ml IL-18 **(A)**. CD16 MFI on $CD56^{dim}CD16^+$ NK cells was measured after stimulation with Med, IL-12, IL-15, or IL-18 (concentrations in nanograms per milliliter as labeled) for 6 or 18 h **(B)** (n = 9–13, data from two to three experiments). For the cross-linking assays (as described in the Section "Materials and Methods"), PBMCs were stimulated for 6 or 18 h *in vitro* with Med (medium alone), α-CD16 or its IgG1 isotype control, with (+) or without (–) 10 ng/ml IL-18. CD16 MFI of $CD56^{dim}CD16^+$ NK cells was measured after 6 or 18 h **(C)** (n = 7–16, data from one to two experiments). Surface expression of CD107a **(D)**, intracellular IFN-γ **(E)**, and CD25 **(F)** was measured on NK cells after 6 or 18 h (n = 7–16, data from one to two experiments). Box plots show the 5th to 95th percentile range. Data were analyzed using paired Wilcoxon signed-rank tests [**(C–F)** capped lines] or ANOVA tests for linear trend for trend analysis across increasing cytokine concentrations including Med [**(B)** uncapped lines]. $^{****}p < 0.0001$, $^{***}p < 0.001$, $^{**}p < 0.01$, $^{*}p < 0.05$.

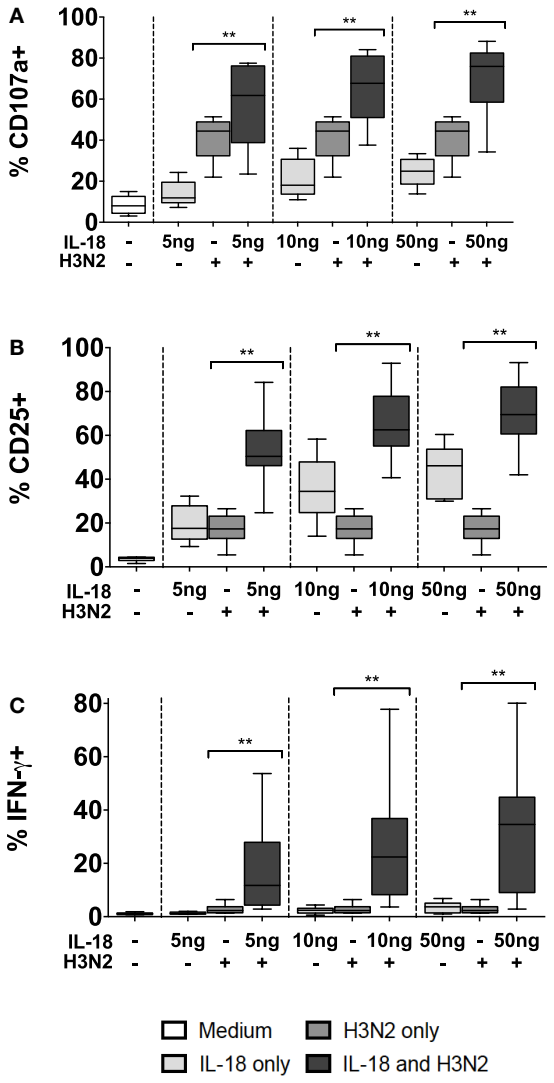

FIGURE 5 | Antibody and IL-18 synergism in response to H3N2. PBMCs were stimulated for 18 h *in vitro* Med (medium alone), 5, 10, and 50 ng/ml IL-18 with or without 1 μg/ml inactivated influenza virus H3N2. Responses were measured as the percentage of NK cells expressing surface CD107a **(A)**, surface CD25 **(B)**, or intracellular IFN-γ **(C)** (n = 7–8, data from one experiment). Box plots show the 5th to 95th percentile range. Data were analyzed with paired Wilcoxon signed-rank tests. ****$p < 0.0001$, ***$p < 0.001$, **$p < 0.01$, *$p < 0.05$.

quickly and effectively to extremely low concentrations of pro-inflammatory stimuli.

Our study differs from published work not only in the very low concentrations of stimuli used, and the use of multiple cytokines in combination, but also in that we have analyzed NK cell responses within whole PBMCs (containing other lymphocyte populations as well as monocytes, macrophages, and dendritic cells) rather than using purified NK cells. Although the use of purified NK cells removes extraneous signals and allows the effects of precisely controlled cytokine concentrations to be evaluated, this approach negates the potential role of secondary cytokine responses and cell–cell contact-mediated signals, which may potentiate the effect of the test stimulus (1). We fully accept that, in our assays, exogenous cytokines might induce other cells in the PBMC population to express accessory molecules or produce cytokines that augment NK cell responses, and indeed this may explain the rather limited contribution of exogenous IL-12 in our assays, but we argue that this better reflects the *in vivo* situation and the true potential of NK cells. Both tissue-resident NK cells and circulating NK cells that infiltrate inflamed sites will receive co-stimulatory signals from myeloid and lymphoid cells present at the site of infection, and this interplay between different components of the immune system is crucial to rapid containment of infection.

Removing accessory cells from culture abrogates many important cell–cell signals; for example, contact between NK cells and DCs is required for optimal presentation of IL-15 *via* IL-15-IL-15Rα complexes, reducing the minimally effective IL-15 concentration from the nanomolar to picomolar range (32, 33). Similarly, interactions between NK cells and macrophages mediated, for example, by NKG2D and ICAM–LFA-1, are required for NK cell activation in numerous infection models [(34, 35) and reviewed in Ref. (1, 36)]. In the absence of these co-stimulatory signals, responses of isolated NK cells to rather high concentrations of exogenous cytokines represent only a very incomplete picture of their true potential. Moreover, NK cell isolation may, in itself, introduce artifacts. Negative selection with agonistic anti-CD3 antibodies risks leaving behind a residue of highly activated, cytokine-producing T cells that may confound analysis of responses to other cytokines, and positive selection of NK cells requires cross-linking of surface receptors that may positively or negatively affect the subsequent NK cell response. On balance therefore, we suggest that the experiments reported here better reflect physiological conditions during early infection and provide novel insights into NK cell activation in this context. Although circulating NK cells are the only easily accessible population in humans, experiments using tissue-resident NK cells, such as lung-resident NK cells in the context of influenza infection, would also be of interest.

Our data point to IL-18 as the key component of the initial inflammatory response that "primes" NK cells to respond to other cytokines and to FcγRIII/CD16-mediated signals. In accordance with published data (12), we show that 50 ng/ml IL-18 is sufficient to induce CD25 expression on >40% of NK cells within 18 h; however, we extend these data to reveal significant upregulation of CD25 within 6 h at IL-18 concentrations as low as 10 ng/ml. Rapid IL-18-induced upregulation of CD25 explains the synergistic interaction we observed between IL-18 and IL-2; this has been reported previously but only at IL-18 concentrations that are 100-fold (10) higher than the concentration used here. Moreover, our data extend these findings to demonstrate that synergism between IL-18 and IL-2 enhances IFN-γ production (irrespective of the presence of IL-12 or IL-15) and we confirmed the importance of IL-18 in enhancing ADCC responses to influenza virus *via* naturally occurring anti-H3N2 antibodies in normal human plasma. Taken together, these data place IL-18 at the interface of innate and adaptive activation of NK cells.

Our data reveal that γ_c cytokines are key partners of IL-18 in this process. IL-2, IL-15, and IL-21 all signal *via* the common γ chain, CD132, while receptors for IL-2 and IL-15 also share the β subunit, CD122 [(21, 37) and reviewed in Ref. (38)]. Although IL-2 and IL-15 are often considered functionally interchangeable as a consequence of their shared STAT5 signaling pathway [reviewed in Ref. (38)], we find that resting NK cells are much more sensitive to IL-15 than to IL-2. This likely reflects the very low levels of expression of the high affinity IL-2Rα (CD25) on resting NK cells; once CD25 is upregulated, IL-2 is not only an extremely potent inducer of NK cell IFN-γ production but also further upregulates its own receptor in an autocrine, positive feedback loop. Importantly, however, although IL-15 and IL-18 both individually and synergistically upregulate CD25 expression, and IL-18 subsequently synergizes with IL-2 to increase IFN-γ production, there is no such synergy between IL-15 and IL-2. Rather, adding IL-2 to any cytokine cocktail-containing IL-15 reduces CD25 expression and has little if any beneficial effect on IFN-γ production. This is consistent with evidence that IL-2 reduces transcription of *IL15RA* (22), thereby limiting further signaling by IL-15, and may represent an important homeostatic mechanism to constrain innately driven NK cell responses once an effective adaptive immune response is underway.

Sequential activation through shared receptor components, initially by an innate cytokine (IL-15) and thence by an adaptive cytokine (IL-2), would provide a mechanism of NK cell activation that is both efficient and self-limiting, and indeed there is evidence suggesting that sequential activation of human NK cells with IL-15 and then with IL-2 potentiates STAT5 expression (12, 21). Moreover, downregulation of IL-15Rα expression by IL-2 (22) may reduce competition between IL-15Rα and IL-2Rα for the β and γ chains, facilitating formation of

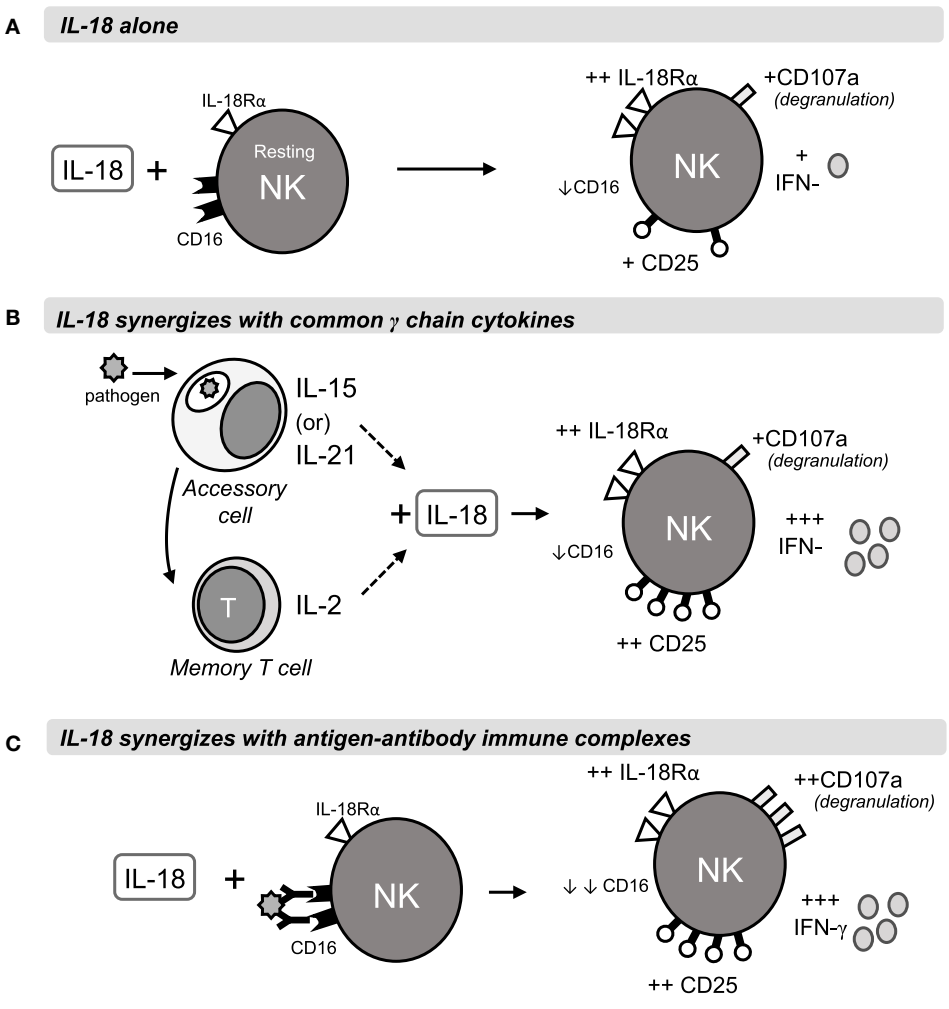

FIGURE 6 | Rapid IL-18 driven activation of NK cells. The schematic shows a proposed model of NK cell activation by IL-18 and its synergies with γ_c cytokines or antigen-antibody immune complexes during primary or secondary immune responses. Within 6 h of stimulation, IL-18 drives IL-18R upregulation and modest increases in CD25, IFN-γ and degranulation, as well as downregulation of FcγRIII (CD16) **(A)**. In combination with IL-15 or IL-21 from accessory cells, or with T cell-derived IL-2, IL-18 drives much stronger CD25 and IFN-γ responses, measurable at 6 h and peaking at 18 h **(B)**. Antigen-antibody complexes cross-link CD16 and synergise with IL-18 to drive ADCC and IFN-γ production after 6 and 18 h **(C)**.

high affinity IL-2R and thus potentiating IL-2 signaling. Competition between IL-2 and IL-15 may extend to the shared STAT5 pathway and may explain the lack of competition with IL-21 that, although sharing the common γ chain receptor, signals *via* STAT3 (38).

We show that IL-18 also synergizes with IgG/CD16, with as little as 10 ng/ml IL-18 enhancing NK cell degranulation and IFN-γ production within 6 h. IL-18 has previously been reported to enhance IFN-γ production and ADCC following CD16 ligation, albeit only at a 10-fold higher IL-18 concentration than employed here (39). The discrepancy between these two studies may be explained by the much longer (overnight) incubation times used by Srivastava et al. (39) as we found that IL-18/anti-CD16-induced responses were well past their peak after 18 h, possibly because of the very rapid downregulation of CD16 expression by IL-18 that we also observed. Although downregulation of CD16 by IL-18 has been observed previously (15, 39), it was reported only at high IL-18 concentration (100 ng/ml or 1 μg/ml) after periods of 1–5 days and the effect was not fully quantified. The speed with which CD16 is downregulated, the very low concentrations of IL-18 required to induce it, and the synergy with CD16 cross-linking have not previously been appreciated and may, again, represent a homeostatic control mechanism to prevent excessive NK cell cytolytic activity and associated tissue damage.

Taken together, our data lead us to propose the following model of early NK cell activation (**Figure 6**). At the start of a primary infection, the initial colonizing pathogens induce release of constitutively expressed IL-15, activation of constitutively expressed IL-18 precursor, and secretion of bioactive IL-18, and transcription and translation of *IL15* and *IL18* by dendritic cells and macrophages [reviewed in Ref. (40–42)]. The synergistic interaction of IL-15 and IL-18 rapidly induces NK cells to produce IFN-γ (within 6 h); this response may be further augmented by IL-12 and is sustained (for at least 18 h) by a positive feedback loop in which IL-18 sustains expression of IL-18Rα. At the same time, induced expression of CD25 allows formation of the high affinity IL-2R, priming the NK cells to take part in T cell-mediated adaptive immune responses. Later in infection, or during re-infection, after the differentiation of antigen-specific T helper cells and production of antibodies, IL-18 synergizes with IL-2 and with antibody-antigen complexes to enhance ADCC and IFN-γ production. The immediate availability of IgG antibodies allows ADCC reactions to occur within 5 h (28), and subsequent rapid downregulation of FcγRIII/CD16 by IL-18 and/or CD16 cross-linking brings the reaction to a close, thereby preventing immune pathology. As IL-2 signaling commences, downregulation of IL-15Rα and/or competition for β and γ chain receptor components inhibits further IL-15 signaling. IL-2Rα expression is now sustained by IL-18 and IL-2, further enhancing NK cell sensitivity to IL-2 and, in synergy with IL-12, maximizing IFN-γ production (12).

In summary, therefore, we have shown that IL-18 synergizes with components of both the innate (IL-15, IL-12) and the adaptive immune response (IL-2, antibody) to very rapidly induce antimicrobial NK cell responses (IFN-γ and ADCC). The extremely low concentrations of cytokines that are required for this process, and the speed with which it happens, identify IL-18 as a key "first responder" at the intersection of innate and adaptive immune responses to infection.

AUTHOR CONTRIBUTIONS

CN and A-SW designed and carried out the experiments and analysis. MG and ER advised on experimental design and analysis. CN, A-SW, and ER wrote the paper.

ACKNOWLEDGMENTS

We would like to thank the blood donors, Carolynne Stanley for subject recruitment and blood collection, Jason Mooney for help with figure design, Christian Bottomley for guidance with statistical analyses, and Elizabeth King for assistance with flow cytometry.

FUNDING

This work was jointly supported by the UK Medical Research Council and UK Department for International Development under the MRC/DFID Concordat agreement (G1000808). CN was supported by an MRC PhD Studentship in Vaccine Research (MR/J003999/1), and A-SW was supported by the Thorpe Legacy Studentship (LSHTM).

SUPPLEMENTARY MATERIAL

The Supplementary Material for this article can be found online at http://journal.frontiersin.org/article/10.3389/fimmu.2016.00101

REFERENCES

1. Newman KC, Riley EM. Whatever turns you on: accessory-cell-dependent activation of NK cells by pathogens. *Nat Rev Immunol* (2007) **7**:279–91. doi:10.1038/nri2057
2. He XS, Draghi M, Mahmood K, Holmes TH, Kemble GW, Dekker CL, et al. T cell-dependent production of IFN-gamma by NK cells in response to influenza A virus. *J Clin Invest* (2004) **114**:1812–9. doi:10.1172/JCI22797
3. Long BR, Michaelsson J, Loo CP, Ballan WM, Vu BA, Hecht FM, et al. Elevated frequency of gamma interferon-producing NK cells in healthy adults vaccinated against influenza virus. *Clin Vaccine Immunol* (2008) **15**:120–30. doi:10.1128/CVI.00357-07
4. Horowitz A, Behrens RH, Okell L, Fooks AR, Riley EM. NK cells as effectors of acquired immune responses: effector CD4+ T cell-dependent activation of NK cells following vaccination. *J Immunol* (2010) **185**:2808–18. doi:10.4049/jimmunol.1000844
5. White MJ, Nielsen CM, McGregor RH, Riley EH, Goodier MR. Differential activation of CD57-defined natural killer cell subsets during recall responses to vaccine antigens. *Immunology* (2014) **142**:140–50. doi:10.1111/imm.12239
6. Nielsen CM, White MJ, Bottomley C, Lusa C, Rodriguez-Galan A, Turner SE, et al. Impaired NK cell responses to pertussis and H1N1 influenza vaccine antigens in human cytomegalovirus-infected individuals. *J Immunol* (2015) **194**:4657–67. doi:10.4049/jimmunol.1403080

7. Leibson PJ. Signal transduction during natural killer cell activation: inside the mind of a killer. *Immunity* (1997) **6**:655–61. doi:10.1016/S1074-7613(00)80441-0
8. Aste-Amezaga M, D'Andrea A, Kubin M, Trinchieri G. Cooperation of natural killer cell stimulatory factor/interleukin-12 with other stimuli in the induction of cytokines and cytotoxic cell-associated molecules in human T and NK cells. *Cell Immunol* (1994) **156**:480–92. doi:10.1006/cimm.1994.1192
9. Fehniger TA, Shah MH, Turner MJ, VanDeusen JB, Whitman SP, Cooper MA, et al. Differential cytokine and chemokine gene expression by human NK cells following activation with IL-18 or IL-15 in combination with IL-12: implications for the innate immune response. *J Immunol* (1999) **162**:4511–20.
10. Son YI, Dallal RM, Mailliard RB, Egawa S, Jonak ZL, Lotze MT. Interleukin-18 (IL-18) synergizes with IL-2 to enhance cytotoxicity, interferon-gamma production, and expansion of natural killer cells. *Cancer Res* (2001) **61**:884–8.
11. Trotta R, Chen L, Ciarlariello D, Josyula S, Mao C, Costinean S, et al. miR-155 regulates IFN-gamma production in natural killer cells. *Blood* (2012) **119**:3478–85. doi:10.1182/blood-2011-12-398099
12. Leong JW, Chase JM, Romee R, Schneider SE, Sullivan RP, Cooper MA, et al. Preactivation with IL-12, IL-15, and IL-18 induces CD25 and a functional high-affinity IL-2 receptor on human cytokine-induced memory-like natural killer cells. *Biol Blood Marrow Transplant* (2014) **20**:463–73. doi:10.1016/j.bbmt.2014.01.006
13. Sareneva T, Julkunen I, Matikainen S. IFN-alpha and IL-12 induce IL-18 receptor gene expression in human NK and T cells. *J Immunol* (2000) **165**:1933–8. doi:10.4049/jimmunol.165.4.1933
14. Strengell M, Sareneva T, Foster D, Julkunen I, Matikainen S. IL-21 up-regulates the expression of genes associated with innate immunity and Th1 response. *J Immunol* (2002) **169**:3600–5. doi:10.4049/jimmunol.169.7.3600
15. Mailliard RB, Alber SM, Shen H, Watkins SC, Kirkwood JM, Herberman RB, et al. IL-18-induced CD83+CCR7+ NK helper cells. *J Exp Med* (2005) **202**:941–53. doi:10.1084/jem.20050128
16. Longhi LN, da Silva RM, Fornazim MC, Spago MC, de Oliveira RT, Nowill AE, et al. Phenotypic and functional characterization of NK cells in human immune response against the dimorphic fungus *Paracoccidioides brasiliensis*. *J Immunol* (2012) **189**:935–45. doi:10.4049/jimmunol.1102563
17. Goodier MR, White MJ, Darboe A, Nielsen CM, Goncalves A, Bottomley C, et al. Rapid natural killer cell differentiation in a population with near universal human cytomegalovirus infection is attenuated by NKG2C deletions. *Blood* (2014) **124**(14):2213–22. doi:10.1182/blood-2014-05-576124
18. Mirjacic Martinovic K, Babovic N, Dzodic R, Jurisic V, Matkovic S, Konjevic G. Favorable in vitro effects of combined IL-12 and IL-18 treatment on NK cell cytotoxicity and CD25 receptor expression in metastatic melanoma patients. *J Transl Med* (2015) **13**:120. doi:10.1186/s12967-015-0479-z
19. Wu CY, Gadina M, Wang K, O'Shea J, Seder RA. Cytokine regulation of IL-12 receptor beta2 expression: differential effects on human T and NK cells. *Eur J Immunol* (2000) **30**:1364–74. doi:10.1002/(SICI)1521-4141(200005)30:5<1364::AID-IMMU1364>3.0.CO;2-U
20. Kunikata T, Torigoe K, Ushio S, Okura T, Ushio C, Yamauchi H, et al. Constitutive and induced IL-18 receptor expression by various peripheral blood cell subsets as determined by anti-hIL-18R monoclonal antibody. *Cell Immunol* (1998) **189**:135–43. doi:10.1006/cimm.1998.1376
21. Pillet AH, Bugault F, Theze J, Chakrabarti LA, Rose T. A programmed switch from IL-15- to IL-2-dependent activation in human NK cells. *J Immunol* (2009) **182**:6267–77. doi:10.4049/jimmunol.0801933
22. Pillet AH, Theze J, Rose T. Interleukin (IL)-2 and IL-15 have different effects on human natural killer lymphocytes. *Hum Immunol* (2011) **72**:1013–7. doi:10.1016/j.humimm.2011.07.311
23. Hoshino K, Tsutsui H, Kawai T, Takeda K, Nakanishi K, Takeda Y, et al. Cutting edge: generation of IL-18 receptor-deficient mice: evidence for IL-1 receptor-related protein as an essential IL-18 binding receptor. *J Immunol* (1999) **162**:5041–4.
24. Barreiro LB, Tailleux L, Pai AA, Gicquel B, Marioni JC, Gilad Y. Deciphering the genetic architecture of variation in the immune response to *Mycobacterium tuberculosis* infection. *Proc Natl Acad Sci U S A* (2012) **109**:1204–9. doi:10.1073/pnas.1115761109
25. Zhang J, Zheng L, Zhu D, An H, Yang Y, Liang Y, et al. Polymorphisms in the interleukin 18 receptor 1 gene and tuberculosis susceptibility among Chinese. *PLoS One* (2014) **9**:e110734. doi:10.1371/journal.pone.0110734
26. Yu Q, Chang HC, Ahyi AN, Kaplan MH. Transcription factor-dependent chromatin remodeling of Il18r1 during Th1 and Th2 differentiation. *J Immunol* (2008) **181**:3346–52. doi:10.4049/jimmunol.181.5.3346
27. Wei L, Vahedi G, Sun HW, Watford WT, Takatori H, Ramos HL, et al. Discrete roles of STAT4 and STAT6 transcription factors in tuning epigenetic modifications and transcription during T helper cell differentiation. *Immunity* (2010) **32**:840–51. doi:10.1016/j.immuni.2010.06.003
28. Romee R, Foley B, Lenvik T, Wang Y, Zhang B, Ankarlo D, et al. NK cell CD16 surface expression and function is regulated by a disintegrin and metalloprotease-17 (ADAM17). *Blood* (2013) **121**:3599–608. doi:10.1182/blood-2012-04-425397
29. Aktas E, Kucuksezer UC, Bilgic S, Erten G, Deniz G. Relationship between CD107a expression and cytotoxic activity. *Cell Immunol* (2009) **254**:149–54. doi:10.1016/j.cellimm.2008.08.007
30. Al-Hubeshy ZB, Coleman A, Nelson M, Goodier MR. A rapid method for assessment of natural killer cell function after multiple receptor crosslinking. *J Immunol Methods* (2011) **366**:52–9. doi:10.1016/j.jim.2011.01.007
31. Rydyznski CE, Waggoner SN. Boosting vaccine efficacy the natural (killer) way. *Trends Immunol* (2015) **36**(9):536–46. doi:10.1016/j.it.2015.07.004
32. Dubois S, Mariner J, Waldmann TA, Tagaya Y. IL-15Ralpha recycles and presents IL-15 in trans to neighboring cells. *Immunity* (2002) **17**:537–47. doi:10.1016/S1074-7613(02)00429-6
33. Tamzalit F, Barbieux I, Plet A, Heim J, Nedellec S, Morisseau S, et al. IL-15. IL-15Ralpha complex shedding following trans-presentation is essential for the survival of IL-15 responding NK and T cells. *Proc Natl Acad Sci U S A* (2014) **111**:8565–70. doi:10.1073/pnas.1405514111
34. Hamerman JA, Aderem A. Functional transitions in macrophages during in vivo infection with *Mycobacterium bovis* bacillus Calmette-Guerin. *J Immunol* (2001) **167**:2227–33. doi:10.4049/jimmunol.167.4.2227
35. Klezovich-Benard M, Corre JP, Jusforgues-Saklani H, Fiole D, Burjek N, Tournier JN, et al. Mechanisms of NK cell-macrophage *Bacillus anthracis* crosstalk: a balance between stimulation by spores and differential disruption by toxins. *PLoS Pathog* (2012) **8**:e1002481. doi:10.1371/journal.ppat.1002481
36. Michel T, Hentges F, Zimmer J. Consequences of the crosstalk between monocytes/macrophages and natural killer cells. *Front Immunol* (2012) **3**:403. doi:10.3389/fimmu.2012.00403
37. Grabstein KH, Eisenman J, Shanebeck K, Rauch C, Srinivasan S, Fung V, et al. Cloning of a T cell growth factor that interacts with the beta chain of the interleukin-2 receptor. *Science* (1994) **264**:965–8. doi:10.1126/science.8178155
38. Rochman Y, Spolski R, Leonard WJ. New insights into the regulation of T cells by gamma(c) family cytokines. *Nat Rev Immunol* (2009) **9**:480–90. doi:10.1038/nri2580
39. Srivastava S, Pelloso D, Feng H, Voiles L, Lewis D, Haskova Z, et al. Effects of interleukin-18 on natural killer cells: costimulation of activation through Fc receptors for immunoglobulin. *Cancer Immunol Immunother* (2013) **62**:1073–82. doi:10.1007/s00262-013-1403-0
40. Novick D, Kim S, Kaplanski G, Dinarello CA. Interleukin-18, more than a Th1 cytokine. *Semin Immunol* (2013) **25**:439–48. doi:10.1016/j.smim.2013.10.014
41. Perera PY, Lichy JH, Waldmann TA, Perera LP. The role of interleukin-15 in inflammation and immune responses to infection: implications for its therapeutic use. *Microbes Infect* (2012) **14**:247–61. doi:10.1016/j.micinf.2011.10.006
42. van de Veerdonk FL, Netea MG, Dinarello CA, Joosten LA. Inflammasome activation and IL-1beta and IL-18 processing during infection. *Trends Immunol* (2011) **32**:110–6. doi:10.1016/j.it.2011.01.003

Conflict of Interest Statement: The authors declare that the research was conducted in the absence of any commercial or financial relationships that could be construed as a potential conflict of interest.

B | Supplementary methods and materials

Table B.1: Primer sequences for KIR SSP-PCR genotyping

Reaction	Gene	Name	Sequence	Final μM	Name	Sequence	Final μM	bp
1	KIR2DL1	Fa517	gttggtcagatgtcatgtttgaa	0.5	Rc621	cctgccaggtcttgcg	0.5	142
2	KIR2DL2	Fcon750d	aaaccttctctctcagccca	2.5	Rt854	gccctgcagagaacctaca	2.5	142
3	KIR2DL3	Fcon1254d	agaccctcaggaggtga	2.5	Rt1375	caggagacaactttggatca	2.5	156
4	KIR3DL1	Ft624	ccatyggtcccatgatgct	2.5	Rt697d	ccacgatgtccagggga	2.5	108
		Ftt624d	tccatcggtcccatgatgtt	2.5				109
5	KIR3DL2	Fg864d	catgaacgtaggctccg	0.5	Rc962	gaccacacgcagggcag	0.2	131
6	KIR2DS1	Fg621	tctccatcagtcgcatgag	2.5	Rcon682d	ggtcactgggagctgac	2.5	96
		Fa621b	tctccatcagtcgcatgaa	2.5				96
7	KIR2DS2	Fa546	tgcacagagaggggaagta	2.5	Rcon621d	ccctgcaaggtcttgca	2.5	110
8	KIR2DS3	Ft803d	cttgtcctgcagctcct	1.25	Ra925	gcatctgtaggttcctcct	1.25	158
9	KIR2DS4	Fat781d	ggttcaggcaggagagaat	2.5	Rca877d	ctggaatgttccgtkgatg	2.5	133/111
10	KIR2DS5	Fc551	agagaggggacgtttaacc	2.5	Rcon662d	ctgatagggggagtgagt	2.5	147
11	KIR3DS1	Fg624d	catcggttccatgatgcg	2.5	Rt697d	ccacgatgtccagggga	2.5	107
		Fg624bd	catcagttccatgatgcg	2.5				107
12	KIR2DP1	Fc567d	cgacactttgcacctcac	0.625	Rdel674d	gggagctgacaactgatg	0.625	141
13	KIR3DL3	Fg510d	aatgttggtcagatgtcag	2.5	Rta669bd	gcygacaactcatagggta	2.5	196
	KIR3DX1	Fma920d	tttctgtgggccgtgcaa	2.5	Rdel967bd	gtcactgggggcttatag	2.5	88
14	KIR2DL4	Ftgc157bd	tcaggacaagcccttctgc	2.5	Rga250bd	ggacagggaccccatctttc	2.5	131
15	KIR2DL5	Fag843d	atctatccagggaggggag	1.25	Rc953d	catagggtgagtcatggag	1.25	147
16	KIR3DP1	Fi2-89d	gtgtggtaggagccttag	1.25	Rg287d	gaaaacggtgtttcggaatac	1.25	279
		Fa-97bd	gtacgtcaccctcccatgatgta	1.25				398

Table B.2: Primer mixes for KIR SSP-PCR genotyping

Reaction	Gene	Name	mL	Name	mL	FDRA360	RDRA595	Total volume/ml	dH_2O/ml
1	KIR2DL1	Fa517	10	Rc621	10	2	2	24	176
2	KIR2DL2	Fcon750d	50	Rt854	50	2	2	104	96
3	KIR2DL3	Fcon1254d	50	Rt1375	50	2	2	104	96
4	KIR3DL1	Ft624	50	Rt697d	50	2	2	154	46
		Ftt624d	50						
5	KIR3DL2	Fg864d	10	Rc962	4	2	2	18	182
6	KIR2DS1	Fg621	50	Rcon682d	50	2	2	154	46
		Fa621b	50						
7	KIR2DS2	Fa546	50	Rcon621d	50	2	2	104	96
8	KIR2DS3	Ft803d	25	Ra925	25	2	2	54	146
9	KIR2DS4	Fat781d	50	Rca877d	50	2	2	104	96
10	KIR2DS5	Fc551	50	Rcon662d	50	2	2	104	96
11	KIR3DS1	Fg624d	50	Rt697d	50	2	2	154	46
		Fg624bd	50						
12	KIR2DP1	Fc567d	12.5	Rdel674d	12.5	2	2	29	171
13	KIR3DL3	Fg510d	50	Rta669bd	50	2	2	204	0
	KIR3DX1	Fma920d	50	Rdel967bd	50				
14	KIR2DL4	Ftgc157bd	50	Rga250bd	50	2	2	104	96
15	KIR2DL5	Fag843d	25	Rc953d	25	2	2	54	146
16	KIR3DP1	Fi2-89d	25	Rg287d	25	2 FDRA360	2 RDRA 633	79	121
		Fa-97bd	25						

Table B.3: Primer sequences for NKG2C wild-type or deletion genotyping

Gene	Primer name	Sequence	Product size/bp
WT NKG2C	pF201	AGTGTGGATCTTCAATGATA	201
	pR201	TTTAGTAATTGTGTGCATCCT	
NKG2C del	pF411	ACTCGGATTTCTATTTGATGC	411
	pR411	ACAAGTGATGTATAAGAAAAAG	

Table B.4: Primer sequences for ddPCR copy number analysis and structural haplotyping

Gene	Oligonucleotides	Primer sequence (5'-3')
KIR2DL5	Primer 1	CACTGCGTTTTCACACAGAC
	Primer 2	GGCAGGAGACAATGATCTT
	Probe	CCCTTCTCAGAGGCCCAAGACACC
KIR3DS1	Primer 1	CATCGGTTCCATGATGCG
	Primer 2	GGGAGCTGACAACTGATAGG
	Probe	AACAGAACCGTAGCATCTGTAGGTCCCT
KIR2DL2	Primer 1	GAGGTGGAGGCCCATGAAT
	Primer 2	TCGAGTTTGACCACTCGTAT
	Probe	AACATTCCAGGCCGACTTTCCTCTG
RPP30	Primer 1	AGATTTGGACCTGCGAGCG
	Primer 2	GAGCGGCTGTCTCCACAAGT
	Probe	TTCTGACCTGAAGGCTCTGCGCG

Table B.5: FACS antibodies and manufacturers

Antibody	Fluorophore	Manufacturer	Cat. No.
KIR2DL1_S1	PE-Cy7	Beckman Coulter	A66899
KIR2DL2_L3_S2	PE-Cy7	Beckman Coulter	A66901
KIR2DL5	APC/PE	Miltenyi Biotec	130-096-199
KIR2DS4	PE	Beckman Coulter	A60796
KIR3DL1	Vioblue	Miltenyi Biotec	130-095-234
KIR3DL1_S1	APC	Beckman Coulter	A60795
CD3	V500	BD Horizon	541416
CD16	APC/APC-H7	BD Pharmingen	560195
CD25	PE/PerCP-Cy5.5	eBioscience	45-0259-42
CD56	APC-V770	Miltenyi Biotec	130-100-676
CD56	PE-Cy7	BD Bioscience	335826
CD57	e450	eBioscience	48-0577-42
CD107a	FITC	BD Pharmingen	555800
CD235a	PerCP-e710	eBioscience	46-9987-42
IFN-γ	APC	BD Pharmingen	554702
IFNαR	APC	Miltenyi Biotec	130-099-558
IL-15Rα	PE	eBioscience	12-7159-42
IL-18Rα	FITC/PE	eBioscience	11-7183-42
NKG2A	APC	R&D Systems	FAB1059A
NKG2C	PE	R&D Systems	FAB138P

CD158f (KIR2DL5) antibodies, human

For research use only

One test corresponds to labeling of up to 10^7 cells in a total volume of 100 µL.

Product	Content	Order no.
CD158f (KIR 2DL5)-PE	for 100 tests	130-096-199
CD158f (KIR 2DL5)-APC	for 30 tests	130-098-567
CD158f (KIR 2DL5)-APC	for 100 tests	130-098-569
CD158f (KIR 2DL5)-PE-Vio770	for 30 tests	130-105-582
CD158f (KIR 2DL5)-PE-Vio770	for 100 tests	130-105-530
CD158f (KIR 2DL5)-APC-Vio770	for 30 tests	130-105-583
CD158f (KIR 2DL5)-APC-Vio770	for 100 tests	130-105-531
CD158f (KIR 2DL5) pure	100 µg in 1 mL	130-096-200

Warnings

Reagents contain sodium azide. Under acidic conditions sodium azide yields hydrazoic acid, which is extremely toxic. Azide compounds should be diluted with running water before discarding. These precautions are recommended to avoid deposits in plumbing where explosive conditions may develop.

Technical data and background information

Antigen	CD158f
Clone	UP-R1
Isotype	mouse IgG1κ
Isotype control	Mouse IgG1 – isotype control antibodies
Alternative names of antigen	KIR2DL5A, KIR2DL5B
Molecular mass of antigen [kDa]	38
Distribution of antigen	NK cells, T cells
Product format	Antibodies are supplied in buffer containing stabilizer and 0.05% sodium azide.
Fixation	Cells should be stained prior to fixation, if formaldehyde is used as a fixative.
Storage	Store protected from light at 2–8 °C. Do not freeze.

Clone UP-R1 recognizes CD158f (KIR2DL5), a member of the killer immunoglobulin-like receptor (KIR) family which recognizes subsets of HLA alleles. Expression is found mainly on $CD56^{dim}CD16^{+}$ natural killer (NK) cells but also on a subset of $CD8^{+}$ T cells.
KIRs are monomeric receptors possessing high allelic polymorphism, with either two or three Ig-like extracellular domains.

Reagent requirements

- Buffer: Prepare a solution containing phosphate-buffered saline (PBS), pH 7.2, 0.5% bovine serum albumin (BSA), and 2 mM EDTA by diluting MACS® BSA Stock Solution (# 130-091-376) 1:20 with autoMACS® Rinsing Solution (# 130-091-222). Keep buffer cold (2−8 °C).
  Note: EDTA can be replaced by other supplements such as anticoagulant citrate dextrose formula-A (ACD-A) or citrate phosphate dextrose (CPD). Buffers or media containing Ca^{2+} or Mg^{2+} are not recommended for use.
- (Optional) FcR Blocking Reagent, human (# 130-059-901) to avoid Fc receptor–mediated antibody labeling.
- (Optional) Fluorochrome-conjugated anti-biotin antibodies, e.g., Anti-Biotin-PE (# 130-090-756) as secondary antibody reagent in combination with biotinylated antibodies.
- (Optional) Propidium Iodide Solution (# 130-093-233) for flow cytometric exclusion of dead cells without fixation.
- (Optional) Fixation and Dead Cell Discrimination Kit (# 130-091-163) for cell fixation and flow cytometric exclusion of dead cells.

Protocol for cell surface staining

- The recommended antibody dilution for labeling of cells and subsequent analysis by flow cytometry is 1:11 for up to 10^7 cells/100 µL of buffer.
- Volumes given below are for up to 10^7 nucleated cells. When working with fewer than 10^7 cells, use the same volumes as indicated. When working with higher cell numbers, scale up all reagent volumes and total volumes accordingly (e.g. for 2×10^7 nucleated cells, use twice the volume of all indicated reagent volumes and total volumes).

1. Determine cell number.
2. Centrifuge cell suspension at 300×g for 10 minutes. Aspirate supernatant completely.
3. Resuspend up to 10^7 nucleated cells per 100 µL of buffer.
4. Add 10 µL of the antibody.
5. Mix well and incubate for 10 minutes in the dark in the refrigerator (2−8 °C).
   Note: Higher temperatures and/or longer incubation times may lead to non-specific cell labeling. Working on ice requires increased incubation times.
6. Wash cells by adding 1−2 mL of buffer and centrifuge at 300×g for 10 minutes. Aspirate supernatant completely.
7. (Optional) If biotinylated antibody was used, resuspend the cell pellet in 100 µL of buffer, add 10 µL of fluorochrome-conjugated anti-biotin antibody, and continue as described in steps 5 and 6.
8. Resuspend cell pellet in a suitable amount of buffer for analysis by flow cytometry or fluorescence microscopy.

Examples of immunofluorescent staining

Human peripheral blood mononuclear cells (PBMCs) were stained with CD158f (KIR2DL5) antibodies as well as with CD56 antibodies or with the corresponding isotype control antibodies (left image) and analyzed by flow cytometry using the MACSQuant® Analyzer. Cell debris and dead cells were excluded from the analysis based on scatter signals and propidium iodide fluorescence.

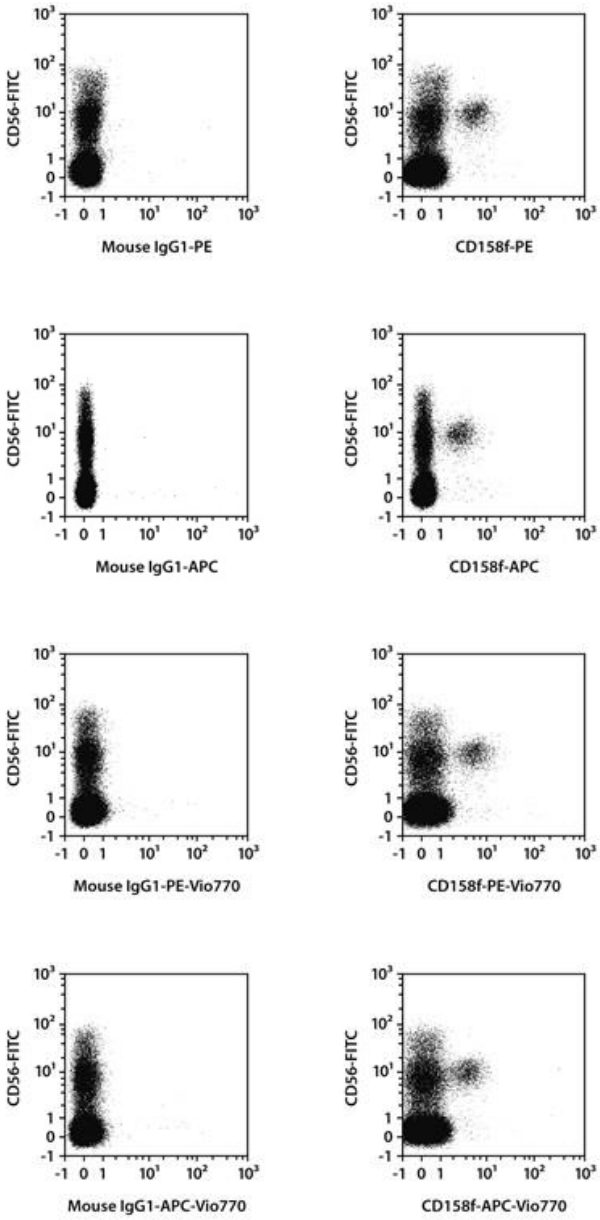

Warranty

The products sold hereunder are warranted only to be free from defects in workmanship and material at the time of delivery to the customer. Miltenyi Biotec GmbH makes no warranty or representation, either expressed or implied, with respect to the fitness of a product for a particular purpose. There are no warranties, expressed or implied, which extend beyond the technical specifications of the products. Miltenyi Biotec GmbH's liability is limited to either replacement of the products or refund of the purchase price. Miltenyi Biotec GmbH is not liable for any property damage, personal injury or economic loss caused by the product.

Miltenyi Biotec GmbH | Friedrich-Ebert-Straße 68 | 51429 Bergisch Gladbach | Germany | Phone +49 2204 8306-0 | Fax +49 2204 85197 | macs@miltenyibiotec.de | **www.miltenyibiotec.com**
Miltenyi Biotec provides products and services worldwide. Visit **www.miltenyibiotec.com/local** to find your nearest Miltenyi Biotec contact.

C | Full donor genotyping

For KIR genotyping, 1 indicates presence and 0 indicates absence of the indicated gene. For KIR2DS4, which has a common deleted variant, 1 indicates presence of the full length gene, - indicates the deletion variant, and 0 indicates complete absence of the gene (1/- indicates full/del heterozygotes). NKG2C genotype is indicated as ++ homozygous positive, +- heterozygous deletion, or - - homozygous deletion.

* Donor was *KIR2DL5+* by presence/absence genotyping, but structural haplotype and CNV were not analysed.

** Donor 407 was negative for *KIR2DL2, 2DL5* and *3DS1*, but after incubation with iRBCs strongly upregulated KIR2DL5 expression (see Chapter 6).

Table C.1: Presence/absence KIR and NKG2C genotypes of LSHTM donors

Donor	Haplotype	3DL3	2DS2	2DL2	2DL3	2DL5A	2DL5B	2DS3	2DS5	2DP1	2DL1	3DP1	2DL4	3DL1	3DS1	2DS1	2DS4	3DL2	NKG2C
014X	B	1	1	1	0	0	1	1	1	1	1	del	0	1	0	0	0	1	++
091M	B	1	1	1	0	1	1	1	1	1	1	full	1	1	1	1	1	1	n/a
106F	B	1	1	1	1	0	1	1	0	1	1	del	1	1	0	0	1/-	1	++
173F	B	1	1	1	1	1	1	0	1	1	1	full	1	1	1	1	-	1	+-
219F	B	1	1	1	1	0	1	1	0	1	1	full	1	1	0	0	-	1	++
267M	B	1	1	1	1	0	1	1	0	1	0	del	1	1	0	0	-	1	++
318F	B	1	1	1	1	0	1	1	0	1	1	del	1	1	0	0	-	1	++
339F	B	1	1	1	1	0	0	0	0	1	1	full	1	1	0	1	1/-	1	++
349F	AA	1	0	0	1	0	0	0	0	1	1	del	1	1	0	0	-	1	n/a
352F	B	1	0	0	1	1	0	0	0	1	1	del	1	1	1	1	1	1	++
377F	B	1	1	1	1	0	0	0	0	1	1	del	1	1	0	0	1	1	n/a
383M	AA	1	0	0	1	0	0	0	0	1	1	del	1	1	0	0	-	1	- -
385F	AA	1	0	0	1	0	0	0	0	1	1	full	1	1	0	0	-	1	+-
407F	B	1	1	1	1	0	0	0	0	1	1	full	1	1	0	0	1/-	1	n/a
463M	B	1	0	0	1	1	0	0	1	1	1	del	1	1	1	1	-	1	n/a
492M	B	1	0	0	1	1	0	0	0	1	1	del	1	1	1	0	-	1	++
515F	B	1	0	0	1	0	0	0	0	1	1	full	1	1	1	0	-	1	+-
521F	AA	1	0	0	1	0	0	0	0	1	1	del	1	1	0	0	1/-	1	+-
527F	AA	1	0	0	1	0	0	0	0	1	1	full	1	1	0	0	-	1	n/a
534F	B	1	0	0	1	1	0	0	1	1	1	full	1	0	1	1	0	1	++
545F	B	1	1	1	0	0	1	1	0	1	1	del	0	1	0	0	-	1	++
547M	B	1	1	1	1	0	1	1	0	1	1	del	1	1	0	0	-	1	+-
559M	B	1	0	0	1	1	0	0	0	1	1	del	0	1	1	1	-	1	+-

Continued on next page

Table C.1 – *Continued from previous page*

Donor	Haplotype	3DL3	2DS2	2DL2	2DL3	2DL5A	2DL5B	2DS3	2DS5	2DP1	2DL1	3DP1	2DL4	3DL1	3DS1	2DS1	2DS4	3DL2	NKG2C
564M	AA	1	0	0	1	0	0	0	0	1	1	del	1	1	0	0	1/-	1	++
565M	B	1	0	0	1	1	0	0	0	1	1	del	1	1	1	1	-	1	++
568F	B	1	1	1	1	0	1	1	0	1	1	del	1	1	0	0	1/-	1	++
576M	AA	1	0	0	1	0	0	0	0	1	1	del	1	1	0	0	-	1	++
580F	B	1	0	0	1	1	0	0	1	1	1	del	1	1	1	1	0	1	n/a
583F	B	1	0	0	1	1	0	0	1	1	1	del	1	1	1	1	-	1	+-
585F	B	1	0	0	1	1	0	0	1	1	1	del	1	1	1	1	-	1	++
586M	B	1	1	1	1	1	1	1	1	1	1	del	1	1	1	1	-	1	+-
587F	B	1	1	1	1	1	1	1	1	1	1	del	1	1	1	1	1	1	+-
591F	AA	1	0	0	1	0	0	0	0	1	1	full	1	1	0	0	-	1	++
594M	B	1	1	1	1	1	1	1	1	1	1	del	1	0	1	1	0	1	++
595F	B	1	1	1	1	0	1	1	0	1	1	full	1	1	0	0	-	1	++
596M	B	1	0	0	1	1	0	0	1	1	1	full	1	1	1	1	-	1	++
598F	B	1	1	1	1	*	0	1	0	1	1	full	1	1	1	1	1/-	1	n/a
601F	B	1	1	1	1	1	1	1	1	1	1	del	1	1	1	1	-	1	++
604M	AA	1	0	0	1	0	0	0	0	1	1	del	1	1	0	0	-	1	- -
607F	B	1	1	1	1	0	1	0	1	1	1	del	1	1	0	0	1/-	1	n/a
609F	B	1	1	1	1	0	1	1	0	1	1	del	1	1	0	0	1/-	1	++
615F	B	1	1	1	1	0	0	0	0	1	1	full	1	1	0	0	-	1	++
620F	AA	1	0	0	1	0	0	0	0	1	1	del	1	1	0	0	1/-	1	++
626F	B	1	1	1	1	*	0	1	1	1	1	del	1	1	1	1	-	1	+-
636F	B	1	1	1	1	0	1	1	0	1	1	full	1	1	1	0	1	1	+-
637F	AA	1	0	0	1	0	0	0	0	1	1	del	1	1	0	0	1/-	1	n/a
640F	B	1	0	0	1	1	0	0	1	1	1	del	1	1	1	1	-	1	++
641M	B	1	1	1	1	0	1	1	0	1	1	del	1	1	0	0	1	1	n/a

Table C.2: *KIR2DL5* CNV and structural haplotypes of LSHTM donors

Donor	KIR2DL5 expression	*KIR2DL5* CNV	Structural haplotype	*KIR2DL2* CNV	*KIR3DS1* CNV
014X	-	2	C+ C+	2	0
091M	+	2	C+ T+	1	1
106F	-	1	C+	1	0
173F	+	2	C+ T+	1	1
219F	-	1	C+	1	0
267M	-	1	C+	1	0
318F	-	1	C+	1	0
352F	+	1	T+	0	1
463M	+	1	T+	0	1
492M	+	1	T+	0	1
534F	-	1	T+	0	1
545F	-	1	C+	1	0
547M	-	1	C+	1	0
559M	+	2	T+ T+	0	2
565M	-	1	T+	0	1
568F	-	1	C+	1	0
580F	+	2	T+ T+	0	2
583F	-	1	T+	0	1
585F	+	1	T+	0	1
586M	+	2	C+ T+	1	1
587F	+	2	C+ T+	1	1
594M	+	3	C+ T+ C/T	1	1
595F	-	1	C+	1	0
596M	-	1	T+	0	1

Continued on next page

Table C.2 – *Continued from previous page*

Donor	KIR2DL5 expression	*KIR2DL5* CNV	Structural haplotype	*KIR2DL2* CNV	*KIR3DS1* CNV
601F	+	2	C+ T+	1	1
607F	-	1	C+	1	0
609F	-	1	C+	1	0
636F	-	1	C+	1	1
640F	+	1	T+	0	1
641F	-	1	C+	1	0

Table C.3: Presence/absence KIR genotypes of 16 Ugandan donors

Donor	Haplotype	3DL3	2DS2	2DL2	2DL3	2DL5A	2DL5B	2DS3	2DS5	2DP1	2DL1	3DP1	2DL4	3DL1	3DS1	2DS1	2DS4	3DL2
1	Bx	1	1	1	0	0	0	0	0	0	1	full+del	1	1	0	0	1	1
28	Bx	1	0	1	1	0	1	0	1	1	1	full	1	1	0	0	1	1
44	AA	1	0	0	1	0	0	0	0	1	1	full	1	1	0	0	1/-	1
89	Bx	1	1	1	1	0	1	1	0	1	1	full	1	1	0	0	1	1
104	Bx	1	1	1	1	0	1	1	0	1	1	full	1	1	0	0	1/-	1
109	AA	1	0	0	1	0	0	0	0	1	1	full	1	1	0	0	-	1
117	Bx	1	1	1	1	1	1	1	1	1	1	full	1	1	1	1	-	1
187	AA	1	0	0	1	0	0	0	0	1	1	full	1	1	0	0	-	1
190	Bx	1	1	1	1	0	0	1	0	1	1	full+del	1	1	0	0	0	1
244	Bx	1	1	1	0	0	1	0	1	0	0	full+del	1	1	0	1	0	1
318	Bx	1	0	0	1	0	1	0	1	1	1	full	1	1	0	0	0	1
329	Bx	1	0	0	1	1	0	0	1	1	1	full	1	1	1	1	-	1
338	AA	1	0	0	1	0	0	0	0	1	1	full	1	1	0	0	1	1
368	AA	1	0	0	1	0	0	0	0	1	1	full	1	1	0	0	-	1
391	Bx	1	1	1	0	0	1	0	1	1	1	full+del	1	1	0	0	-	1
435	Bx	1	0	1	1	0	1	0	1	1	1	full+del	1	1	0	0	1	1

Table C.4: *KIR2DL5* CNV, structural haplotype and NKG2C genotype of Ugandan donors

Donor	KIR2DL5 expression	*KIR2DL5* CNV	Structural haplotype	*KIR2DL2* CNV	*KIR3DS1* CNV	Putative KIR haplotype	NKG2C genotype
014	-	1	C+	+	-	B	++
028	-	1	C+	+	-	B	++
059	-	2	C+ C+	+	-	B	++
061	-	1	C+	-	-	B	+-
089	-	0		+	-	B	+-
104	-	0		-	-	AA	+-
148	-	2	C+ C+	+	-	B	++
182	-	2	C+ C+	+	-	B	+-
192	-	1	C+	+	-	B	++
203	-	2	C+ ?	+	-	B	++
249	-	0		-	+	B	++
280	-	2	C+ C+	+	+	B	+-
338	-	0		n/a	-	AA	++
349	-	0		n/a	n/a	n/a	+-
368	-	0		-	-	AA	++
371	-	0		-	-	AA	++
373	-	*		+	-	B	+-
384	-	n/a		n/a	n/a	n/a	- -
401	-	1	C+	+	-	B	+-
405	-	0		-	-	B	+-
407	**	**		-	-	AA	+-
408	-	1	C+	+	-	B	+-

Continued on next page

Table C.4 – *Continued from previous page*

Donor	KIR2DL5 expression	*KIR2DL5* CNV	Structural haplotype	*KIR2DL2* CNV	*KIR3DS1* CNV	Putative KIR haplotype	NKG2C genotype
418	-	0		-	-	AA	++
432	+	1	T+	n/a	+	B	+-
435	-	1	C+	+	-	B	+-
001W	-	0		-	-	AA	+-
011W	-	1	T+	-	+	B	++
021W	-	1	C+	+	-	B	+-
044W	-	0		-	-	AA	++
048W	-	1	T+	+	+	B	+-
083W	+	2	C+ ?	+	-	B	+-
089W	-	1	C+	+	-	B	++
104W	-	1	C+	+	-	B	++
105W	+	2	C+ T+	+	+	B	++
106W	-	1	T+	+	+	B	++
109W	-	0		-	-	AA	++
117W	+	2	C+ T+	+	+	B	++
145W	-	2	C+ C+	+	-	B	++
157W	-	0		+	-	B	+-
187W	-	0		-	-	AA	+-
190W	-	0		+	-	B	- -
229W	-	1	T+	+	+	B	++
244W	-	1	C+	+	-	B	+-
318W	-	3	?	-	-	B	+-
329W	+	1	T+	-	+	B	++

Continued on next page

Table C.4 – *Continued from previous page*

Donor	KIR2DL5 expression	*KIR2DL5* CNV	Structural haplotype	*KIR2DL2* CNV	*KIR3DS1* CNV	Putative KIR haplotype	NKG2C genotype
336W	-	0		+	-	B	++
354W	-	2	C+ ?	+	-	B	- -
373W	-	0		-	-	AA	+-
390W	-	2	C+ ?	+	-	B	+-
391W	-	1	C+	+	-	B	+-
393W	-	1	C+	+	-	B	- -
409W	-	1	C+	+	-	B	++
411W	-	1	C+	+	-	B	++

Bibliography

1. Kärre, K. How to recognize a foreign submarine. *Immunol Rev* **155,** 5–9 (1997).
2. Kim, S., Poursine-Laurent, J., Truscott, S. M., Lybarger, L., Song, Y.-J., Yang, L., French, A. R., Sunwoo, J. B., Lemieux, S., Hansen, T. H. & Yokoyama, W. M. Licensing of natural killer cells by host major histocompatibility complex class I molecules. *Nature* **436,** 709–13 (2005).
3. Parham, P. MHC class I molecules and KIRs in human history, health and survival. *Nat Rev Immunol* **5,** 201–14 (2005).
4. Lopez-Vergès, S., Milush, J. M., Pandey, S., York, V. A., Arakawa-Hoyt, J., Pircher, H., Norris, P. J., Nixon, D. F. & Lanier, L. L. CD57 defines a functionally distinct population of mature NK cells in the human CD56dimCD16+ NK cell subset. *Blood* **116,** 3865–74 (2010).
5. Nielsen, C. M., White, M. J., Goodier, M. R. & Riley, E. M. Functional Significance of CD57 Expression on Human NK Cells and Relevance to Disease. *Front Immunol* **4,** 422 (2013).
6. White, M. J., Nielsen, C. M., McGregor, R. H. C., Riley, E. H. C. & Goodier, M. R. Differential activation of CD57-defined natural killer cell subsets during recall responses to vaccine antigens. *Immunology* **142,** 140–50 (2014).
7. Björkström, N. K., Riese, P., Heuts, F., Andersson, S., Fauriat, C., Ivarsson, M. A., Björklund, A. T., Flodström-Tullberg, M., Michaëlsson, J., Rottenberg, M. E., Guzmán, C. A., Ljunggren, H.-G. & Malmberg, K.-J. Expression patterns of NKG2A, KIR, and CD57 define a process of CD56dim NK cell differentiation uncoupled from NK cell education. *Blood* **116,** 3853–64 (2010).
8. Lutz, C. T., Karapetyan, A., Al-Attar, A., Shelton, B. J., Holt, K. J., Tucker, J. H. & Presnell, S. R. Human NK cells proliferate and die in vivo more rapidly than T cells in healthy young and elderly adults. *J Immunol* **186,** 4590–8 (2011).

9. Domaica, C. I., Fuertes, M. B., Uriarte, I., Girart, M. V., Sardañons, J., Comas, D. I., Di Giovanni, D., Gaillard, M. I., Bezrodnik, L. & Zwirner, N. W. Human natural killer cell maturation defect supports in vivo CD56(bright) to CD56(dim) lineage development. *PLoS One* **7,** e51677 (2012).

10. Gayoso, I., Sanchez-Correa, B., Campos, C., Alonso, C., Pera, A., Casado, J. G., Morgado, S., Tarazona, R. & Solana, R. Immunosenescence of human natural killer cells. *J Innate Immun* **3,** 337–43 (2011).

11. Goodier, M. R., White, M. J., Darboe, A., Nielsen, C. M., Goncalves, A., Bottomley, C., Moore, S. E. & Riley, E. M. Rapid NK cell differentiation in a population with near-universal human cytomegalovirus infection is attenuated by NKG2C deletions. *Blood* **124,** 2213–22 (2014).

12. Gumá, M., Angulo, A., Vilches, C., Gómez-Lozano, N., Malats, N. & López-Botet, M. Imprint of human cytomegalovirus infection on the NK cell receptor repertoire. *Blood* **104,** 3664–71 (2004).

13. Béziat, V. *et al.* NK cell responses to cytomegalovirus infection lead to stable imprints in the human KIR repertoire and involve activating KIRs. *Blood* **121,** 2678–88 (2013).

14. Djaoud, Z., David, G., Bressollette, C., Willem, C., Rettman, P., Gagne, K., Legrand, N., Mehlal, S., Cesbron, A., Imbert-Marcille, B.-M. & Retière, C. Amplified NKG2C+ NK cells in cytomegalovirus (CMV) infection preferentially express killer cell Ig-like receptor 2DL: functional impact in controlling CMV-infected dendritic cells. *J Immunol* **191,** 2708–16 (2013).

15. Schlums, H. *et al.* Cytomegalovirus infection drives adaptive epigenetic diversification of NK cells with altered signaling and effector function. *Immunity* **42,** 443–56 (2015).

16. Goodier, M. R., Rodriguez-Galan, A., Lusa, C., Nielsen, C. M., Darboe, A., Moldoveanu, A. L., White, M. J., Behrens, R. & Riley, E. M. Influenza Vaccination Generates Cytokine-Induced Memory-like NK Cells: Impact of Human Cytomegalovirus Infection. *J Immunol* **197,** 313–25 (2016).

17. Nielsen, C. M., White, M. J., Bottomley, C., Lusa, C., Rodríguez-Galán, A., Turner, S. E. G., Goodier, M. R. & Riley, E. M. Impaired NK Cell Responses to Pertussis and H1N1 Influenza Vaccine Antigens in Human Cytomegalovirus-Infected Individuals. *J Immunol* **194,** 4657–67 (2015).

18. Artavanis-Tsakonas, K. & Riley, E. M. Innate immune response to malaria: rapid induction of IFN-gamma from human NK cells by live Plasmodium falciparum-infected erythrocytes. *J Immunol* **169,** 2956–63 (2002).

19. Aste-Amezaga, M, D'Andrea, A, Kubin, M & Trinchieri, G. Cooperation of natural killer cell stimulatory factor/interleukin-12 with other stimuli in the induction of cytokines and cytotoxic cell-associated molecules in human T and NK cells. *Cell Immunol* **156,** 480–92 (1994).

20. Lieberman, L. A. & Hunter, C. A. Regulatory pathways involved in the infection-induced production of IFN-γ by NK cells. *Microbes Infect* **4,** 1531–8 (2002).

21. Neves, P. C. C., Santos, J. R., Tubarão, L. N., Bonaldo, M. C. & Galler, R. Early IFN-γ production after YF 17D vaccine virus immunization in mice and its association with adaptive immune responses. *PLoS One* **8,** e81953 (2013).

22. Fehniger, T. A., Shah, M. H., Turner, M. J., VanDeusen, J. B., Whitman, S. P., Cooper, M. A., Suzuki, K, Wechser, M, Goodsaid, F & Caligiuri, M. A. Differential cytokine and chemokine gene expression by human NK cells following activation with IL-18 or IL-15 in combination with IL-12: implications for the innate immune response. *J Immunol* **162,** 4511–20 (1999).

23. Haeberlein, S., Sebald, H., Bogdan, C. & Schleicher, U. IL-18, but not IL-15, contributes to the IL-12-dependent induction of NK cell effector functions by Leishmania infantum in vivo. *Eur J Immunol* **40,** 1708–17 (2010).

24. Lauwerys, B. R., Garot, N, Renauld, J. C. & Houssiau, F. A. Cytokine production and killer activity of NK/T-NK cells derived with IL-2, IL-15, or the combination of IL-12 and IL-18. *J Immunol* **165,** 1847–53 (2000).

25. Lapaque, N., Walzer, T., Méresse, S., Vivier, E. & Trowsdale, J. Interactions between human NK cells and macrophages in response to Salmonella infection. *J Immunol* **182,** 4339–48 (2009).

26. Newman, K. C., Korbel, D. S., Hafalla, J. C. & Riley, E. M. Cross-talk with myeloid accessory cells regulates human natural killer cell interferon-gamma responses to malaria. *PLoS Pathog* **2,** e118 (2006).

27. Akdis, M. *et al.* Interleukins, from 1 to 37, and interferon-γ: receptors, functions, and roles in diseases. *J Allergy Clin Immunol* **127,** 701–21.e1–70 (2011).

28. Altare, F *et al.* Impairment of mycobacterial immunity in human interleukin-12 receptor deficiency. *Science* **280,** 1432–5 (1998).

29. Kovanen, P. E. & Leonard, W. J. Cytokines and immunodeficiency diseases: critical roles of the gamma(c)-dependent cytokines interleukins 2, 4, 7, 9, 15, and 21, and their signaling pathways. *Immunol Rev* **202,** 67–83 (2004).

30. Horowitz, A., Stegmann, K. A. & Riley, E. M. Activation of natural killer cells during microbial infections. *Front Immunol* **2,** 88 (2011).

31. McGuinness, D. H., Dehal, P. K. & Pleass, R. J. Pattern recognition molecules and innate immunity to parasites. *Trends Parasitol* **19,** 312–9 (2003).

32. Son, Y. I., Dallal, R. M., Mailliard, R. B., Egawa, S, Jonak, Z. L. & Lotze, M. T. Interleukin-18 (IL-18) synergizes with IL-2 to enhance cytotoxicity, interferon-gamma production, and expansion of natural killer cells. *Cancer Res* **61,** 884–8 (2001).

33. Trotta, R., Chen, L., Ciarlariello, D., Josyula, S., Mao, C., Costinean, S., Yu, L., Butchar, J. P., Tridandapani, S., Croce, C. M. & Caligiuri, M. A. miR-155 regulates IFN-γ production in natural killer cells. *Blood* **119,** 3478–85 (2012).

34. Ing, R. & Stevenson, M. M. Dendritic cell and NK cell reciprocal cross talk promotes gamma interferon-dependent immunity to blood-stage Plasmodium chabaudi AS infection in mice. *Infect Immun* **77,** 770–82 (2009).

35. Lucas, M., Schachterle, W., Oberle, K., Aichele, P. & Diefenbach, A. Dendritic cells prime natural killer cells by trans-presenting interleukin-15. *Immunity* **26,** 503–17 (2007).

36. Nandagopal, N., Ali, A. K., Komal, A. K. & Lee, S.-H. The Critical Role of IL-15-PI3K-mTOR Pathway in Natural Killer Cell Effector Functions. *Front Immunol* **5,** 187 (2014).

37. Horowitz, A., Newman, K. C., Evans, J. H., Korbel, D. S., Davis, D. M. & Riley, E. M. Cross-talk between T cells and NK cells generates rapid effector responses to Plasmodium falciparum-infected erythrocytes. *J Immunol* **184,** 6043–52 (2010).

38. Nielsen, C. M., Wolf, A.-S., Goodier, M. R. & Riley, E. M. Synergy between Common γ Chain Family Cytokines and IL-18 Potentiates Innate and Adaptive Pathways of NK Cell Activation. *Front Immunol* **7,** 101 (2016).

39. Pillet, A.-H., Bugault, F., Thèze, J., Chakrabarti, L. A. & Rose, T. A programmed switch from IL-15- to IL-2-dependent activation in human NK cells. *J Immunol* **182,** 6267–77 (2009).

40. Pillet, A.-H., Thèze, J. & Rose, T. Interleukin (IL)-2 and IL-15 have different effects on human natural killer lymphocytes. *Hum Immunol* **72,** 1013–7 (2011).

41. Rochman, Y., Spolski, R. & Leonard, W. J. New insights into the regulation of T cells by gamma(c) family cytokines. *Nat Rev Immunol* **9,** 480–90 (2009).

42. Baratin, M., Roetynck, S., Lépolard, C., Falk, C., Sawadogo, S., Uematsu, S., Akira, S., Ryffel, B., Tiraby, J.-G., Alexopoulou, L., Kirschning, C. J., Gysin, J., Vivier, E. & Ugolini, S. Natural killer cell and macrophage cooperation in MyD88-dependent innate responses to Plasmodium falciparum. *Proc Natl Acad Sci U S A* **102,** 14747–52 (2005).

43. Baratin, M., Roetynck, S., Pouvelle, B., Lemmers, C., Viebig, N. K., Johansson, S., Bierling, P., Scherf, A., Gysin, J., Vivier, E. & Ugolini, S. Dissection of the role of PfEMP1 and ICAM-1 in the sensing of Plasmodium falciparum-infected erythrocytes by natural killer cells. *PLoS One* **2,** e228 (2007).

44. Michel, T., Hentges, F. & Zimmer, J. Consequences of the crosstalk between monocytes/ macrophages and natural killer cells. *Front Immunol* **3,** 403 (2012).

45. Yoshida, A, Takahashi, H. K., Nishibori, M, Iwagaki, H, Yoshino, T, Morichika, T, Yokoyama, M, Kondo, E, Akagi, T & Tanaka, N. IL-18-induced expression of intercellular adhesion molecule-1 in human monocytes: involvement in IL-12 and IFN-gamma production in PBMC. *Cell Immunol* **210,** 106–15 (2001).

46. Yoshida, A., Kohka Takahashi, H., Iwagaki, H., Yoshino, T., Morichika, T., Yokoyama, M., Itoh, H., Mori, S., Akagi, T., Nishibori, M. & Tanaka, N. Essential role of ICAM-1/LFA-1 interaction in synergistic effect of IL-18 and IL-12 on IFN-γ production in human PBMC. *Naunyn Schmiedebergs Arch Pharmacol* **365,** 181–6 (2002).

47. Degli-Esposti, M. A. & Smyth, M. J. Close encounters of different kinds: dendritic cells and NK cells take centre stage. *Nat Rev Immunol* **5,** 112–24 (2005).

48. Anguille, S., Van Acker, H. H., Van den Bergh, J., Willemen, Y., Goossens, H., Van Tendeloo, V. F., Smits, E. L., Berneman, Z. N. & Lion, E. Interleukin-15 Dendritic Cells Harness NK Cell Cytotoxic Effector Function in a Contact- and IL-15-Dependent Manner. *PLoS One* **10,** e0123340 (2015).

49. Mortier, E., Woo, T., Advincula, R., Gozalo, S. & Ma, A. IL-15Rα chaperones IL-15 to stable dendritic cell membrane complexes that activate NK cells via trans presentation. *J Exp Med* **205,** 1213–25 (2008).

50. Orange, J. S. Formation and function of the lytic NK cell immunological synapse. *Nat Rev Immunol* **8,** 713–25 (2008).

51. Wang, S. & El-Deiry, W. S. TRAIL and apoptosis induction by TNF-family death receptors. *Oncogene* **22,** 8628–33 (2003).

52. Desmet, C. J. & Ishii, K. J. Nucleic acid sensing at the interface between innate and adaptive immunity in vaccination. *Nat Rev Immunol* **12,** 479–91 (2012).

53. Iwasaki, A. & Medzhitov, R. Toll-like receptor control of the adaptive immune responses. *Nat Immunol* **5,** 987–95 (2004).

54. Zwirner, N. W. & Domaica, C. I. Cytokine regulation of natural killer cell effector functions. *Biofactors* **36,** 274–88 (2010).

55. Hashimoto, G, Wright, P. F. & Karzon, D. T. Antibody-dependent cell-mediated cytotoxicity against influenza virus-infected cells. *J Infect Dis* **148,** 785–94 (1983).

56. Vivier, E, Morin, P, O'Brien, C, Druker, B, Schlossman, S. F. & Anderson, P. Tyrosine phosphorylation of the Fc gamma RIII(CD16): zeta complex in human natural killer cells. Induction by antibody-dependent cytotoxicity but not by natural killing. *J Immunol* **146,** 206–10 (1991).

57. Wirthmueller, U, Kurosaki, T, Murakami, M. S. & Ravetch, J. V. Signal transduction by Fc gamma RIII (CD16) is mediated through the gamma chain. *J Exp Med* **175,** 1381–90 (1992).

58. Vivier, E., Raulet, D. H., Moretta, A., Caligiuri, M. A., Zitvogel, L., Lanier, L. L., Yokoyama, W. M. & Ugolini, S. Innate or adaptive immunity? The example of natural killer cells. *Science* **331,** 44–9 (2011).

59. Srivastava, S., Pelloso, D., Feng, H., Voiles, L., Lewis, D., Haskova, Z., Whitacre, M., Trulli, S., Chen, Y.-J., Toso, J., Jonak, Z. L., Chang, H.-C. & Robertson, M. J. Effects of interleukin-18 on natural killer cells: costimulation of activation through Fc receptors for immunoglobulin. *Cancer Immunol Immunother* **62,** 1073–82 (2013).

60. Kruse, P. H., Matta, J., Ugolini, S. & Vivier, E. Natural cytotoxicity receptors and their ligands. *Immunol Cell Biol* **92,** 221–9 (2014).

61. O'Connor, G. M., Hart, O. M. & Gardiner, C. M. Putting the natural killer cell in its place. *Immunology* **117,** 1–10 (2006).

62. Lanier, L. L. NK cell recognition. *Annu Rev Immunol* **23,** 225–74 (2005).

63. Bevan, M. J. Altered self, altered world. *J Immunol* **173,** 2897–8 (2004).

64. Petersen, J. L., Morris, C. R. & Solheim, J. C. Virus evasion of MHC class I molecule presentation. *J Immunol* **171,** 4473–8 (2003).

65. Moretta, A, Bottino, C, Vitale, M, Pende, D, Cantoni, C, Mingari, M. C., Biassoni, R & Moretta, L. Activating receptors and coreceptors involved in human natural killer cell-mediated cytolysis. *Annu Rev Immunol* **19,** 197–223 (2001).

66. Koch, J., Steinle, A., Watzl, C. & Mandelboim, O. Activating natural cytotoxicity receptors of natural killer cells in cancer and infection. *Trends Immunol* **34,** 182–91 (2013).

67. Middleton, D., Curran, M. & Maxwell, L. Natural killer cells and their receptors. *Transpl Immunol* **10,** 147–64 (2002).

68. Braud, V. M., Allan, D. S., O'Callaghan, C. A., Söderström, K, D'Andrea, A, Ogg, G. S., Lazetic, S, Young, N. T., Bell, J. I., Phillips, J. H., Lanier, L. L. & McMichael, A. J. HLA-E binds to natural killer cell receptors CD94/NKG2A, B and C. *Nature* **391,** 795–9 (1998).

69. Lee, N, Llano, M, Carretero, M, Ishitani, A, Navarro, F, López-Botet, M & Geraghty, D. E. HLA-E is a major ligand for the natural killer inhibitory receptor CD94/NKG2A. *Proc Natl Acad Sci U S A* **95,** 5199–204 (1998).

70. Lee, N, Goodlett, D. R., Ishitani, A, Marquardt, H & Geraghty, D. E. HLA-E surface expression depends on binding of TAP-dependent peptides derived from certain HLA class I signal sequences. *J Immunol* **160,** 4951–60 (1998).

71. Blum, J. S., Wearsch, P. A. & Cresswell, P. Pathways of antigen processing. *Annu Rev Immunol* **31,** 443–73 (2013).

72. Kaiser, B. K., Pizarro, J. C., Kerns, J. & Strong, R. K. Structural basis for NKG2A/CD94 recognition of HLA-E. *Proc Natl Acad Sci U S A* **105,** 6696–701 (2008).

73. Tomasec, P, Braud, V. M., Rickards, C, Powell, M. B., McSharry, B. P., Gadola, S, Cerundolo, V, Borysiewicz, L. K., McMichael, A. J. & Wilkinson, G. W. Surface expression of HLA-E, an inhibitor of natural killer cells, enhanced by human cytomegalovirus gpUL40. *Science* **287,** 1031 (2000).

74. Gumá, M., Budt, M., Sáez, A., Brckalo, T., Hengel, H., Angulo, A. & López-Botet, M. Expansion of CD94/NKG2C+ NK cells in response to human cytomegalovirus-infected fibroblasts. *Blood* **107,** 3624–31 (2006).

75. Raulet, D. H., Gasser, S., Gowen, B. G., Deng, W. & Jung, H. Regulation of ligands for the NKG2D activating receptor. *Annu Rev Immunol* **31,** 413–41 (2013).

76. Rajagopalan, S. & Long, E. O. KIR2DL4 (CD158d): An activation receptor for HLA-G. *Front Immunol* **3,** 258 (2012).

77. Moffett, A. & Colucci, F. Co-evolution of NK receptors and HLA ligands in humans is driven by reproduction. *Immunol Rev* **267,** 283–97 (2015).

78. Brusilovsky, M., Cordoba, M., Rosental, B., Hershkovitz, O., Andrake, M. D., Pecherskaya, A., Einarson, M. B., Zhou, Y., Braiman, A., Campbell, K. S. & Porgador, A. Genome-wide siRNA screen reveals a new cellular partner of NK cell receptor KIR2DL4: heparan sulfate directly modulates KIR2DL4-mediated responses. *J Immunol* **191,** 5256–67 (2013).

79. Cognet, C., Farnarier, C., Gauthier, L., Frassati, C., André, P., Magérus-Chatinet, A., Anfossi, N., Rieux-Laucat, F., Vivier, E. & Schleinitz, N. Expression of the HLA-C2-specific activating killer-cell Ig-like receptor KIR2DS1 on NK and T cells. *Clin Immunol* **135,** 26–32 (2010).

80. Körner, C. & Altfeld, M. Role of KIR3DS1 in human diseases. *Front Immunol* **3,** 326 (2012).

81. Martin, M. P., Gao, X., Lee, J.-H., Nelson, G. W., Detels, R., Goedert, J. J., Buchbinder, S., Hoots, K., Vlahov, D., Trowsdale, J., Wilson, M., O'Brien, S. J. & Carrington, M. Epistatic interaction between KIR3DS1 and HLA-B delays the progression to AIDS. *Nat Genet* **31,** 429–34 (2002).

82. Parham, P. Immunogenetics of killer cell immunoglobulin-like receptors. *Mol Immunol* **42,** 459–62 (2005).

83. Parham, P. & Moffett, A. Variable NK cell receptors and their MHC class I ligands in immunity, reproduction and human evolution. *Nat Rev Immunol* **13,** 133–44 (2013).

84. Schönberg, K., Sribar, M., Enczmann, J., Fischer, J. C. & Uhrberg, M. Analyses of HLA-C-specific KIR repertoires in donors with group A and B haplotypes suggest a ligand-instructed model of NK cell receptor acquisition. *Blood* **117,** 98–107 (2011).

85. Gómez-Lozano, N., Gardiner, C. M., Parham, P. & Vilches, C. Some human KIR haplotypes contain two KIR2DL5 genes: KIR2DL5A and KIR2DL5B. *Immunogenetics* **54,** 314–9 (2002).

86. Vilches, C, Rajalingam, R, Uhrberg, M, Gardiner, C. M., Young, N. T. & Parham, P. KIR2DL5, a novel killer-cell receptor with a D0-D2 configuration of Ig-like domains. *J Immunol* **164,** 5797–804 (2000).

87. Gómez-Lozano, N., Trompeter, H.-I., de Pablo, R., Estefanía, E., Uhrberg, M. & Vilches, C. Epigenetic silencing of potentially functional KIR2DL5 alleles: Implications for the acquisition of KIR repertoires by NK cells. *Eur J Immunol* **37,** 1954–65 (2007).

88. Martin, M. P. *et al.* Innate partnership of HLA-B and KIR3DL1 subtypes against HIV-1. *Nat Genet* **39,** 733–40 (2007).

89. Pelak, K. *et al.* Copy number variation of KIR genes influences HIV-1 control. *PLoS Biol* **9,** e1001208 (2011).

90. Pyo, C.-W., Guethlein, L. A., Vu, Q., Wang, R., Abi-Rached, L., Norman, P. J., Marsh, S. G. E., Miller, J. S., Parham, P. & Geraghty, D. E. Different patterns of evolution in the centromeric and telomeric regions of group A and B haplotypes of the human killer cell Ig-like receptor locus. *PLoS One* **5,** e15115 (2010).

91. Estefanía, E, Gómez-Lozano, N, Portero, F, de Pablo, R, Solís, R, Sepúlveda, S, Vaquero, M, González, M. A., Suárez, E, Roustán, G & Vilches, C. Influence of KIR gene diversity on the course of HSV-1 infection: resistance to the disease is associated with the absence of KIR2DL2 and KIR2DS2. *Tissue Antigens* **70,** 34–41 (2007).

92. Ordóñez, D, Meenagh, A, Gómez-Lozano, N, Castaño, J, Middleton, D & Vilches, C. Duplication, mutation and recombination of the human orphan gene KIR2DS3 contribute to the diversity of KIR haplotypes. *Genes Immun* **9,** 431–7 (2008).

93. Graef, T., Moesta, A. K., Norman, P. J., Abi-Rached, L., Vago, L., Older Aguilar, A. M., Gleimer, M., Hammond, J. A., Guethlein, L. A., Bushnell, D. A., Robinson, P. J. & Parham, P. KIR2DS4 is a product of gene conversion with KIR3DL2 that introduced specificity for HLA-A*11 while diminishing avidity for HLA-C. *J Exp Med* **206,** 2557–72 (2009).

94. Merino, A. M., Dugast, A.-S., Wilson, C. M., Goepfert, P. A., Alter, G., Kaslow, R. A. & Tang, J. KIR2DS4 promotes HIV-1 pathogenesis: new evidence from analyses of immunogenetic data and natural killer cell function. *PLoS One* **9,** e99353 (2014).

95. Nakimuli, A. *et al.* A KIR B centromeric region present in Africans but not Europeans protects pregnant women from pre-eclampsia. *Proc Natl Acad Sci U S A* **112,** 845–50 (2015).

96. Campbell, K. S. & Purdy, A. K. Structure/function of human killer cell immunoglobulin-like receptors: lessons from polymorphisms, evolution, crystal structures and mutations. *Immunology* **132,** 315–25 (2011).

97. Belkin, D., Torkar, M., Chang, C., Barten, R., Tolaini, M., Haude, A., Allen, R., Wilson, M. J., Kioussis, D. & Trowsdale, J. Killer cell Ig-like receptor and leukocyte Ig-like receptor transgenic mice exhibit tissue- and cell-specific transgene expression. *J Immunol* **171,** 3056–63 (2003).

98. Middleton, D. & Gonzelez, F. The extensive polymorphism of KIR genes. *Immunology* **129,** 8–19 (2010).

99. Cisneros, E., Moraru, M., Gómez-Lozano, N., López-Botet, M. & Vilches, C. KIR2DL5: An Orphan Inhibitory Receptor Displaying Complex Patterns of Polymorphism and Expression. *Front Immunol* **3,** 289 (2012).

100. Vilches, C. & Parham, P. KIR: diverse, rapidly evolving receptors of innate and adaptive immunity. *Annu Rev Immunol* **20,** 217–51 (2002).

101. Jiang, W., Johnson, C., Jayaraman, J., Simecek, N., Noble, J., Moffatt, M. F., Cookson, W. O., Trowsdale, J. & Traherne, J. A. Copy number variation leads to considerable diversity for B but not A haplotypes of the human KIR genes encoding NK cell receptors. *Genome Res* **22,** 1845–54 (2012).

102. Hou, L., Chen, M., Jiang, B., Wu, D., Ng, J. & Hurley, C. K. Thirty allele-level haplotypes centered around KIR2DL5 define the diversity in an African American population. *Immunogenetics* **62,** 491–8 (2010).

103. Middleton, D., Gonzalez, A. & Gilmore, P. M. Studies on the expression of the deleted KIR2DS4*003 gene product and distribution of KIR2DS4 deleted and nondeleted versions in different populations. *Hum Immunol* **68,** 128–34 (2007).

104. Li, H., Pascal, V., Martin, M. P., Carrington, M. & Anderson, S. K. Genetic control of variegated KIR gene expression: polymorphisms of the bi-directional KIR3DL1 promoter are associated with distinct frequencies of gene expression. *PLoS Genet* **4,** e1000254 (2008).

105. Davies, G. E., Locke, S. M., Wright, P. W., Li, H, Hanson, R. J., Miller, J. S. & Anderson, S. K. Identification of bidirectional promoters in the human KIR genes. *Genes Immun* **8,** 245–53 (2007).

106. Charoudeh, H. N., Schmied, L., Gonzalez, A., Terszowski, G., Czaja, K., Schmitter, K., Infanti, L., Buser, A. & Stern, M. Quantity of HLA-C surface expression and licensing of KIR2DL+ natural killer cells. *Immunogenetics* **64,** 739–45 (2012).

107. Boyington, J. C. & Sun, P. D. A structural perspective on MHC class I recognition by killer cell immunoglobulin-like receptors. *Mol Immunol* **38,** 1007–21 (2002).

108. Penman, B. S., Moffett, A., Chazara, O., Gupta, S. & Parham, P. Reproduction, infection and killer-cell immunoglobulin-like receptor haplotype evolution. *Immunogenetics* **68,** 755–764 (2016).

109. Moesta, A. K., Norman, P. J., Yawata, M., Yawata, N., Gleimer, M. & Parham, P. Synergistic polymorphism at two positions distal to the ligand-binding site makes KIR2DL2 a stronger receptor for HLA-C than KIR2DL3. *J Immunol* **180,** 3969–79 (2008).

110. Norman, P. J. *et al.* Unusual selection on the KIR3DL1/S1 natural killer cell receptor in Africans. *Nat Genet* **39,** 1092–9 (2007).

111. Yokoyama, W. M. & Kim, S. Licensing of natural killer cells by self-major histocompatibility complex class I. *Immunol Rev* **214,** 143–54 (2006).

112. Furukawa, H, Yabe, T, Watanabe, K, Miyamoto, R, Miki, A, Akaza, T, Tadokoro, K, Tohma, S, Inoue, T, Yamamoto, K & Juji, T. Tolerance of NK and LAK activity for HLA class I-deficient targets in a TAP1-deficient patient (bare lymphocyte syndrome type I). *Hum Immunol* **60,** 32–40 (1999).

113. Höglund, P. & Brodin, P. Current perspectives of natural killer cell education by MHC class I molecules. *Nat Rev Immunol* **10,** 724–34 (2010).

114. Valiante, N. M., Uhrberg, M, Shilling, H. G., Lienert-Weidenbach, K, Arnett, K. L., D'Andrea, A, Phillips, J. H., Lanier, L. L. & Parham, P. Functionally and structurally distinct NK cell receptor repertoires in the peripheral blood of two human donors. *Immunity* **7,** 739–51 (1997).

115. Andersson, S., Fauriat, C., Malmberg, J.-A., Ljunggren, H.-G. & Malmberg, K.-J. KIR acquisition probabilities are independent of self-HLA class I ligands and increase with cellular KIR expression. *Blood* **114,** 95–104 (2009).

116. Brodin, P., Lakshmikanth, T., Johansson, S., Kärre, K. & Höglund, P. The strength of inhibitory input during education quantitatively tunes the functional responsiveness of individual natural killer cells. *Blood* **113,** 2434–41 (2009).

117. Ivarsson, M. A., Michaëlsson, J. & Fauriat, C. Activating killer cell Ig-like receptors in health and disease. *Front Immunol* **5,** 184 (2014).

118. Fauriat, C., Ivarsson, M. A., Ljunggren, H.-G., Malmberg, K.-J. & Michaëlsson, J. Education of human natural killer cells by activating killer cell immunoglobulin-like receptors. *Blood* **115,** 1166–74 (2010).

119. Orr, M. T., Murphy, W. J. & Lanier, L. L. 'Unlicensed' natural killer cells dominate the response to cytomegalovirus infection. *Nat Immunol* **11,** 321–7 (2010).

120. WHO. *Eliminating malaria* tech. rep. (World Health Organisation, 2016).

121. WHO. *World Malaria Report* tech. rep. (World Health Organisation, 2015).

122. Amaratunga, C. *et al.* Dihydroartemisinin-piperaquine resistance in Plasmodium falciparum malaria in Cambodia: a multisite prospective cohort study. *Lancet Infect Dis* **16,** 357–65 (2016).

123. Ashley, E. A. *et al.* Spread of artemisinin resistance in Plasmodium falciparum malaria. *N Engl J Med* **371,** 411–23 (2014).

124. Niaré, K., Dara, A., Sagara, I., Sissoko, M. S., Guindo, C. O., Cissé, N. H., Coulibaly, C. O., Ringwald, P., Benoit-Vical, F., Berry, A., Djimdé, A. A. & Doumbo, O. K. In Vivo Efficacy and Parasite Clearance of Artesunate + Sulfadoxine-Pyrimethamine Versus Artemether-Lumefantrine in Mali. *Am J Trop Med Hyg* **94,** 634–9 (2016).

125. Shayo, A., Buza, J. & Ishengoma, D. S. Monitoring of efficacy and safety of artemisinin-based anti-malarials for treatment of uncomplicated malaria: a review of evidence of implementation of anti-malarial therapeutic efficacy trials in Tanzania. *Malar J* **14,** 135 (2015).

126. Millar, S. B. & Cox-Singh, J. Human infections with Plasmodium knowlesi - zoonotic malaria. *Clin Microbiol Infect* **21,** 640–8 (2015).

127. Centres for Disease Control. *Malaria biology* 2016. <`http://www.cdc.gov/malaria/about/biology/`>.

128. Idro, R., Marsh, K., John, C. C. & Newton, C. R. J. Cerebral malaria: mechanisms of brain injury and strategies for improved neurocognitive outcome. *Pediatr Res* **68,** 267–74 (2010).

129. Marsh, K & Kinyanjui, S. Immune effector mechanisms in malaria. *Parasite Immunol* **28,** 51–60 (2006).

130. Carneiro, I., Roca-Feltrer, A., Griffin, J. T., Smith, L., Tanner, M., Schellenberg, J. A., Greenwood, B. & Schellenberg, D. Age-patterns of malaria vary with severity, transmission intensity and seasonality in sub-Saharan Africa: a systematic review and pooled analysis. *PLoS One* **5,** e8988 (2010).

131. Reyburn, H., Mbatia, R., Drakeley, C., Bruce, J., Carneiro, I., Olomi, R., Cox, J., Nkya, W. M. M. M., Lemnge, M., Greenwood, B. M. & Riley, E. M. Association of transmission intensity and age with clinical manifestations and case fatality of severe Plasmodium falciparum malaria. *JAMA* **293,** 1461–70 (2005).

132. Griffin, J. T., Ferguson, N. M. & Ghani, A. C. Estimates of the changing age-burden of Plasmodium falciparum malaria disease in sub-Saharan Africa. *Nat Commun* **5,** 3136 (2014).

133. Griffin, J. T., Hollingsworth, T. D., Reyburn, H., Drakeley, C. J., Riley, E. M. & Ghani, A. C. Gradual acquisition of immunity to severe malaria with increasing exposure. *Proc Biol Sci* **282,** 20142657 (2015).

134. Sondo, P., Derra, K., Diallo Nakanabo, S., Tarnagda, Z., Kazienga, A., Zampa, O., Valéa, I., Sorgho, H., Owusu-Dabo, E., Ouédraogo, J.-B., Guiguemdé, T. R. & Tinto, H. Artesunate-Amodiaquine and Artemether-Lumefantrine Therapies and Selection of Pfcrt and Pfmdr1 Alleles in Nanoro, Burkina Faso. *PLoS One* **11,** e0151565 (2016).

135. Boussaroque, A., Fall, B., Madamet, M., Wade, K. A., Fall, M., Nakoulima, A., Fall, K. B., Dionne, P., Benoit, N., Diatta, B., Diemé, Y., Wade, B. & Pradines, B. Prevalence of anti-malarial resistance genes in Dakar, Senegal from 2013 to 2014. *Malar J* **15,** 347 (2016).

136. Pelleau, S., Moss, E. L., Dhingra, S. K., Volney, B., Casteras, J., Gabryszewski, S. J., Volkman, S. K., Wirth, D. F., Legrand, E., Fidock, D. A., Neafsey, D. E. & Musset, L. Adaptive evolution of malaria parasites in French Guiana: Reversal of chloroquine resistance by acquisition of a mutation in pfcrt. *Proc Natl Acad Sci U S A* **112,** 11672–7 (2015).

137. Mbengue, A. *et al.* A molecular mechanism of artemisinin resistance in Plasmodium falciparum malaria. *Nature* **520,** 683–7 (2015).

138. Tilley, L., Straimer, J., Gnädig, N. F., Ralph, S. A. & Fidock, D. A. Artemisinin Action and Resistance in Plasmodium falciparum. *Trends Parasitol* **32,** 682–96 (2016).

139. Boussaroque, A., Fall, B., Madamet, M., Camara, C., Benoit, N., Fall, M., Nakoulima, A., Dionne, P., Fall, K. B., Diatta, B., Diémé, Y., Wade, B. & Pradines, B. Emergence

of Mutations in the K13 Propeller Gene of Plasmodium falciparum Isolates from Dakar, Senegal, in 2013-2014. *Antimicrob Agents Chemother* **60,** 624–7 (2015).

140. Su, Z & Stevenson, M. M. Central role of endogenous gamma interferon in protective immunity against blood-stage Plasmodium chabaudi AS infection. *Infect Immun* **68,** 4399–406 (2000).

141. Stevenson, M. M. & Riley, E. M. Innate immunity to malaria. *Nat Rev Immunol* **4,** 169–80 (2004).

142. Chen, Q. *et al.* Human natural killer cells control Plasmodium falciparum infection by eliminating infected red blood cells. *Proc Natl Acad Sci U S A* **111,** 1479–84 (2014).

143. Mota, M. M., Brown, K. N., Holder, A. A. & Jarra, W. Acute Plasmodium chabaudi chabaudi malaria infection induces antibodies which bind to the surfaces of parasitized erythrocytes and promote their phagocytosis by macrophages in vitro. *Infect Immun* **66,** 4080–6 (1998).

144. Fritsche, G, Larcher, C, Schennach, H & Weiss, G. Regulatory interactions between iron and nitric oxide metabolism for immune defense against Plasmodium falciparum infection. *J Infect Dis* **183,** 1388–94 (2001).

145. Fowkes, F. J. I., Boeuf, P. & Beeson, J. G. Immunity to malaria in an era of declining malaria transmission. *Parasitology* **143,** 139–53 (2016).

146. McGregor, I. A. The passive transfer of human malarial immunity. *Am J Trop Med Hyg* **13,** Suppl. 237–9 (1964).

147. Dutta, S., Haynes, J. D., Barbosa, A., Ware, L. A., Snavely, J. D., Moch, J. K., Thomas, A. W. & Lanar, D. E. Mode of action of invasion-inhibitory antibodies directed against apical membrane antigen 1 of Plasmodium falciparum. *Infect Immun* **73,** 2116–22 (2005).

148. Boyle, M. J., Reiling, L., Feng, G., Langer, C., Osier, F. H., Aspeling-Jones, H., Cheng, Y. S., Stubbs, J., Tetteh, K. K. A., Conway, D. J., McCarthy, J. S., Muller, I., Marsh, K., Anders, R. F. & Beeson, J. G. Human antibodies fix complement to inhibit Plasmodium falciparum invasion of erythrocytes and are associated with protection against malaria. *Immunity* **42,** 580–90 (2015).

149. Joos, C., Marrama, L., Polson, H. E. J., Corre, S., Diatta, A.-M., Diouf, B., Trape, J.-F., Tall, A., Longacre, S. & Perraut, R. Clinical protection from falciparum malaria correlates with neutrophil respiratory bursts induced by merozoites opsonized with human serum antibodies. *PLoS One* **5,** e9871 (2010).

150. Kapelski, S., Klockenbring, T., Fischer, R., Barth, S. & Fendel, R. Assessment of the neutrophilic antibody-dependent respiratory burst (ADRB) response to Plasmodium falciparum. *J Leukoc Biol* **96,** 1131–42 (2014).

151. Osier, F. H., Feng, G., Boyle, M. J., Langer, C., Zhou, J., Richards, J. S., McCallum, F. J., Reiling, L., Jaworowski, A., Anders, R. F., Marsh, K. & Beeson, J. G. Opsonic phagocytosis of Plasmodium falciparum merozoites: mechanism in human immunity and a correlate of protection against malaria. *BMC Med* **12,** 108 (2014).

152. Chan, J.-A., Fowkes, F. J. I. & Beeson, J. G. Surface antigens of Plasmodium falciparum-infected erythrocytes as immune targets and malaria vaccine candidates. *Cell Mol Life Sci* **71,** 3633–57 (2014).

153. Nogaro, S. I., Hafalla, J. C., Walther, B., Remarque, E. J., Tetteh, K. K. A., Conway, D. J., Riley, E. M. & Walther, M. The breadth, but not the magnitude, of circulating memory B cell responses to P. falciparum increases with age/exposure in an area of low transmission. *PLoS One* **6,** e25582 (2011).

154. Osier, F. H. A. *et al.* Breadth and magnitude of antibody responses to multiple Plasmodium falciparum merozoite antigens are associated with protection from clinical malaria. *Infect Immun* **76,** 2240–8 (2008).

155. Offeddu, V., Thathy, V., Marsh, K. & Matuschewski, K. Naturally acquired immune responses against Plasmodium falciparum sporozoites and liver infection. *Int J Parasitol* **42,** 535–48 (2012).

156. Murphy, K. M. & Stockinger, B. Effector T cell plasticity: flexibility in the face of changing circumstances. *Nat Immunol* **11,** 674–80 (2010).

157. Grau, G. E., Heremans, H, Piguet, P. F., Pointaire, P, Lambert, P. H., Billiau, A & Vassalli, P. Monoclonal antibody against interferon gamma can prevent experimental cerebral malaria and its associated overproduction of tumor necrosis factor. *Proc Natl Acad Sci U S A* **86,** 5572–4 (1989).

158. Senaldi, G, Shaklee, C. L., Guo, J, Martin, L, Boone, T, Mak, T. W. & Ulich, T. R. Protection against the mortality associated with disease models mediated by TNF and IFN-γ in mice lacking IFN regulatory factor-1. *J Immunol* **163,** 6820–6 (1999).

159. Villegas-Mendez, A., Greig, R., Shaw, T. N., de Souza, J. B., Gwyer Findlay, E., Stumhofer, J. S., Hafalla, J. C. R., Blount, D. G., Hunter, C. A., Riley, E. M. & Couper, K. N. IFN-γ-producing CD4+ T cells promote experimental cerebral malaria by modulating CD8+ T cell accumulation within the brain. *J Immunol* **189,** 968–79 (2012).

160. Boeuf, P. S., Loizon, S., Awandare, G. A., Tetteh, J. K. A., Addae, M. M., Adjei, G. O., Goka, B., Kurtzhals, J. A. L., Puijalon, O., Hviid, L., Akanmori, B. D. & Behr, C. Insights into deregulated TNF and IL-10 production in malaria: implications for understanding severe malarial anaemia. *Malar J* **11,** 253 (2012).

161. Van der Heyde, H. C., Pepper, B, Batchelder, J, Cigel, F & Weidanz, W. P. The time course of selected malarial infections in cytokine-deficient mice. *Exp Parasitol* **85,** 206–13 (1997).

162. Li, C., Sanni, L. A., Omer, F., Riley, E. & Langhorne, J. Pathology of Plasmodium chabaudi chabaudi infection and mortality in interleukin-10-deficient mice are ameliorated by anti-tumor necrosis factor alpha and exacerbated by anti-transforming growth factor beta antibodies. *Infect Immun* **71,** 4850–6 (2003).

163. Oakley, M. S., Sahu, B. R., Lotspeich-Cole, L., Solanki, N. R., Majam, V., Pham, P. T., Banerjee, R., Kozakai, Y., Derrick, S. C., Kumar, S. & Morris, S. L. The transcription factor T-bet regulates parasitemia and promotes pathogenesis during Plasmodium berghei ANKA murine malaria. *J Immunol* **191,** 4699–708 (2013).

164. Freitas do Rosário, A. P., Lamb, T., Spence, P., Stephens, R., Lang, A., Roers, A., Muller, W., O'Garra, A. & Langhorne, J. IL-27 promotes IL-10 production by effector Th1 CD4+ T cells: a critical mechanism for protection from severe immunopathology during malaria infection. *J Immunol* **188,** 1178–90 (2012).

165. Couper, K. N., Blount, D. G., Wilson, M. S., Hafalla, J. C., Belkaid, Y., Kamanaka, M., Flavell, R. A., de Souza, J. B. & Riley, E. M. IL-10 from CD4 CD25 Foxp3 CD127 adaptive regulatory T cells modulates parasite clearance and pathology during malaria infection. *PLoS Pathog* **4,** e1000004 (2008).

166. Walther, M., Jeffries, D., Finney, O. C., Njie, M., Ebonyi, A., Deininger, S., Lawrence, E., Ngwa-Amambua, A., Jayasooriya, S., Cheeseman, I. H., Gomez-Escobar, N., Okebe, J., Conway, D. J. & Riley, E. M. Distinct roles for FOXP3 and FOXP3 CD4 T cells in regulating cellular immunity to uncomplicated and severe Plasmodium falciparum malaria. *PLoS Pathog* **5,** e1000364 (2009).

167. O'Garra, A. & Vieira, P. T(H)1 cells control themselves by producing interleukin-10. *Nat Rev Immunol* **7,** 425–8 (2007).

168. Jagannathan, P., Eccles-James, I., Bowen, K., Nankya, F., Auma, A., Wamala, S., Ebusu, C., Muhindo, M. K., Arinaitwe, E., Briggs, J., Greenhouse, B., Tappero, J. W., Kamya, M. R., Dorsey, G. & Feeney, M. E. IFNγ/IL-10 co-producing cells dominate the CD4 response to malaria in highly exposed children. *PLoS Pathog* **10,** e1003864 (2014).

169. Hansen, D. S. & Schofield, L. Natural regulatory T cells in malaria: host or parasite allies? *PLoS Pathog* **6,** e1000771 (2010).

170. Perez-Mazliah, D. & Langhorne, J. CD4 T-cell subsets in malaria: TH1/TH2 revisited. *Front Immunol* **5,** 671 (2014).

171. Crotty, S. Follicular helper CD4 T cells (TFH). *Annu Rev Immunol* **29,** 621–63 (2011).

172. Reinhardt, R. L., Liang, H.-E. & Locksley, R. M. Cytokine-secreting follicular T cells shape the antibody repertoire. *Nat Immunol* **10,** 385–93 (2009).

173. Walther, M. *et al.* Upregulation of TGF-β, FOXP3, and CD4+CD25+ regulatory T cells correlates with more rapid parasite growth in human malaria infection. *Immunity* **23,** 287–96 (2005).

174. Torcia, M. G. *et al.* Functional deficit of T regulatory cells in Fulani, an ethnic group with low susceptibility to Plasmodium falciparum malaria. *Proc Natl Acad Sci U S A* **105,** 646–51 (2008).

175. Trimnell, A., Takagi, A., Gupta, M., Richie, T. L., Kappe, S. H. & Wang, R. Genetically attenuated parasite vaccines induce contact-dependent CD8+ T cell killing of Plasmodium yoelii liver stage-infected hepatocytes. *J Immunol* **183,** 5870–8 (2009).

176. Weiss, W. R. & Jiang, C. G. Protective CD8+ T lymphocytes in primates immunized with malaria sporozoites. *PLoS One* **7,** e31247 (2012).

177. Jobe, O., Lumsden, J., Mueller, A.-K., Williams, J., Silva-Rivera, H., Kappe, S. H. I., Schwenk, R. J., Matuschewski, K. & Krzych, U. Genetically attenuated Plasmodium berghei liver stages induce sterile protracted protection that is mediated by major histocompatibility complex Class I-dependent interferon-gamma-producing CD8+ T cells. *J Infect Dis* **196,** 599–607 (2007).

178. Chakravarty, S., Baldeviano, G. C., Overstreet, M. G. & Zavala, F. Effector CD8+ T lymphocytes against liver stages of Plasmodium yoelii do not require gamma interferon for antiparasite activity. *Infect Immun* **76,** 3628–31 (2008).

179. Ewer, K. J. *et al.* Protective CD8+ T-cell immunity to human malaria induced by chimpanzee adenovirus-MVA immunisation. *Nat Commun* **4,** 2836 (2013).

180. Hafalla, J. C. R., Bauza, K., Friesen, J., Gonzalez-Aseguinolaza, G., Hill, A. V. S. & Matuschewski, K. Identification of targets of CD8+ T cell responses to malaria liver stages by genome-wide epitope profiling. *PLoS Pathog* **9,** e1003303 (2013).

181. Carvalho, L. H., Sano, G.-I., Hafalla, J. C. R., Morrot, A., Curotto de Lafaille, M. A. & Zavala, F. IL-4-secreting CD4+ T-cells are crucial to the development of CD8+ T-cell responses against malaria liver stages. *Nat Med* **8,** 166–70 (2002).

182. Corradin, G. & Levitskaya, J. Priming of CD8+ T Cell Responses to Liver Stage Malaria Parasite Antigens. *Front Immunol* **5,** 527 (2014).

183. Artavanis-Tsakonas, K., Eleme, K., McQueen, K. L., Cheng, N. W., Parham, P., Davis, D. M. & Riley, E. M. Activation of a subset of human NK cells upon contact with Plasmodium falciparum-infected erythrocytes. *J Immunol* **171,** 5396–405 (2003).

184. Mohan, K, Moulin, P & Stevenson, M. M. Natural killer cell cytokine production, not cytotoxicity, contributes to resistance against blood-stage Plasmodium chabaudi AS infection. *J Immunol* **159,** 4990–8 (1997).

185. Couper, K. N., Blount, D. G., Hafalla, J. C. R., van Rooijen, N., de Souza, J. B. & Riley, E. M. Macrophage-mediated but gamma interferon-independent innate immune responses control the primary wave of Plasmodium yoelii parasitemia. *Infect Immun* **75,** 5806–18 (2007).

186. Borges da Silva, H., Fonseca, R., Cassado, A. D. A., Machado de Salles, É., de Menezes, M. N., Langhorne, J., Perez, K. R., Cuccovia, I. M., Ryffel, B., Barreto, V. M., Marinho, C. R. F., Boscardin, S. B., Álvarez, J. M., D'Império-Lima, M. R. & Tadokoro, C. E. In vivo approaches reveal a key role for DCs in CD4+ T cell activation and parasite clearance during the acute phase of experimental blood-stage malaria. *PLoS Pathog* **11,** e1004598 (2015).

187. Hoffman, S. L. *et al.* Protection of humans against malaria by immunization with radiation-attenuated Plasmodium falciparum sporozoites. *J Infect Dis* **185,** 1155–64 (2002).

188. Roestenberg, M. *et al.* Protection against a malaria challenge by sporozoite inoculation. *N Engl J Med* **361,** 468–77 (2009).

189. RTS,S Clinical Trials Partnership. Efficacy and safety of RTS,S/AS01 malaria vaccine with or without a booster dose in infants and children in Africa: final results of a phase 3, individually randomised, controlled trial. *Lancet* **386,** 31–45 (2015).

190. Ewer, K. J., Sierra-Davidson, K., Salman, A. M., Illingworth, J. J., Draper, S. J., Biswas, S. & Hill, A. V. S. Progress with viral vectored malaria vaccines: A multi-stage approach involving "unnatural immunity". *Vaccine* **33,** 7444–51 (2015).

191. Penny, M. A. *et al.* Public health impact and cost-effectiveness of the RTS,S/AS01 malaria vaccine: a systematic comparison of predictions from four mathematical models. *Lancet* **387,** 367–75 (2016).

192. Penny, M. A., Pemberton-Ross, P. & Smith, T. A. The time-course of protection of the RTS,S vaccine against malaria infections and clinical disease. *Malar J* **14,** 437 (2015).

193. Longley, R. J., Hill, A. V. S. & Spencer, A. J. Malaria vaccines: identifying Plasmodium falciparum liver-stage targets. *Front Microbiol* **6,** 965 (2015).

194. Ogwang, C. *et al.* Prime-boost vaccination with chimpanzee adenovirus and modified vaccinia Ankara encoding TRAP provides partial protection against Plasmodium falciparum infection in Kenyan adults. *Sci Transl Med* **7,** 286re5 (2015).

195. Ouattara, A., Barry, A. E., Dutta, S., Remarque, E. J., Beeson, J. G. & Plowe, C. V. Designing malaria vaccines to circumvent antigen variability. *Vaccine* **33,** 7506–12 (2015).

196. Ogutu, B. R. *et al.* Blood stage malaria vaccine eliciting high antigen-specific antibody concentrations confers no protection to young children in Western Kenya. *PLoS One* **4,** e4708 (2009).

197. Drew, D. R. & Beeson, J. G. PfRH5 as a candidate vaccine for Plasmodium falciparum malaria. *Trends Parasitol* **31,** 87–8 (2015).

198. Genton, B., Betuela, I., Felger, I., Al-Yaman, F., Anders, R. F., Saul, A., Rare, L., Baisor, M., Lorry, K., Brown, G. V., Pye, D., Irving, D. O., Smith, T. A., Beck, H.-P. & Alpers, M. P. A recombinant blood-stage malaria vaccine reduces Plasmodium falciparum density and exerts selective pressure on parasite populations in a phase 1-2b trial in Papua New Guinea. *J Infect Dis* **185,** 820–7 (2002).

199. Doolan, D. L. & Hoffman, S. L. IL-12 and NK cells are required for antigen-specific adaptive immunity against malaria initiated by CD8+ T cells in the Plasmodium yoelii model. *J Immunol* **163,** 884–92 (1999).

200. Korbel, D. S., Newman, K. C., Almeida, C. R., Davis, D. M. & Riley, E. M. Heterogeneous human NK cell responses to Plasmodium falciparum-infected erythrocytes. *J Immunol* **175,** 7466–73 (2005).

201. Dodoo, D, Omer, F. M., Todd, J, Akanmori, B. D., Koram, K. A. & Riley, E. M. Absolute levels and ratios of proinflammatory and anti-inflammatory cytokine production in vitro predict clinical immunity to Plasmodium falciparum malaria. *J Infect Dis* **185,** 971–9 (2002).

202. Korbel, D. S., Norman, P. J., Newman, K. C., Horowitz, A., Gendzekhadze, K., Parham, P. & Riley, E. M. Killer Ig-like receptor (KIR) genotype predicts the capacity of human KIR-positive CD56dim NK cells to respond to pathogen-associated signals. *J Immunol* **182,** 6426–34 (2009).

203. Talman, A. M., Blagborough, A. M. & Sinden, R. E. A Plasmodium falciparum strain expressing GFP throughout the parasite's life-cycle. *PLoS One* **5,** e9156 (2010).

204. Lambros, C & Vanderberg, J. P. Synchronization of Plasmodium falciparum erythrocytic stages in culture. *J Parasitol* **65,** 418–20 (1979).

205. Roberts, C. H. *3.01 KIR Typing 2* Protocol (chrissyhroberts@yahoo.co.uk, 2009).

206. Vilches, C, Castaño, J, Gómez-Lozano, N & Estefanía, E. Facilitation of KIR genotyping by a PCR-SSP method that amplifies short DNA fragments. *Tissue Antigens* **70,** 415–22 (2007).

207. Roberts, C. H. & Butcher, R. *SOP 7.03 Droplet Digital PCR* (chrissyhroberts@yahoo.co.uk, 2014).

208. For Biotechnology Information, N. C. *IL2RG interleukin 2 receptor subunit gamma Homo sapiens (human)* <`http://www.ncbi.nlm.nih.gov/gene/3561`>.

209. De Jong, J. L., Farner, N. L., Widmer, M. B., Giri, J. G. & Sondel, P. M. Interaction of IL-15 with the shared IL-2 receptor beta and gamma(c) subunits. The IL-15/beta/gamma(c) receptor-ligand complex is less stable than the IL-2/beta/gamma(c) receptor-ligand complex. *J Immunol* **156,** 1339–48 (1996).

210. Ellery, J. M. & Nicholls, P. J. Possible mechanism for the alpha subunit of the interleukin-2 receptor (CD25) to influence interleukin-2 receptor signal transduction. *Immunol Cell Biol* **80,** 351–7 (2002).

211. Leong, J. W., Chase, J. M., Romee, R., Schneider, S. E., Sullivan, R. P., Cooper, M. A. & Fehniger, T. A. Preactivation with IL-12, IL-15, and IL-18 induces CD25 and a functional high-affinity IL-2 receptor on human cytokine-induced memory-like natural killer cells. *Biol Blood Marrow Transplant* **20,** 463–73 (2014).

212. Romee, R., Foley, B., Lenvik, T., Wang, Y., Zhang, B., Ankarlo, D., Luo, X., Cooley, S., Verneris, M., Walcheck, B. & Miller, J. NK cell CD16 surface expression and function is regulated by a disintegrin and metalloprotease-17 (ADAM17). *Blood* **121,** 3599–608 (2013).

213. Wu, C. Y., Gadina, M, Wang, K, O'Shea, J & Seder, R. A. Cytokine regulation of IL-12 receptor beta2 expression: differential effects on human T and NK cells. *Eur J Immunol* **30,** 1364–74 (2000).

214. Huang, Y., Lei, Y., Zhang, H., Zhang, M. & Dayton, A. Interleukin-12 treatment down-regulates STAT4 and induces apoptosis with increasing ROS production in human natural killer cells. *J Leukoc Biol* **90,** 87–97 (2011).

215. Huang, Y., Lei, Y., Zhang, H., Hou, L., Zhang, M. & Dayton, A. I. MicroRNA regulation of STAT4 protein expression: rapid and sensitive modulation of IL-12 signaling in human natural killer cells. *Blood* **118,** 6793–802 (2011).

216. Teng, M. W. L., Bowman, E. P., McElwee, J. J., Smyth, M. J., Casanova, J.-L., Cooper, A. M. & Cua, D. J. IL-12 and IL-23 cytokines: from discovery to targeted therapies for immune-mediated inflammatory diseases. *Nat Med* **21,** 719–29 (2015).

217. Mazodier, K., Marin, V., Novick, D., Farnarier, C., Robitail, S., Schleinitz, N., Veit, V., Paul, P., Rubinstein, M., Dinarello, C. A., Harlé, J.-R. & Kaplanski, G. Severe imbalance of IL-18/IL-18BP in patients with secondary hemophagocytic syndrome. *Blood* **106,** 3483–9 (2005).

218. Okamura, H, Tsutsi, H, Komatsu, T, Yutsudo, M, Hakura, A, Tanimoto, T, Torigoe, K, Okura, T, Nukada, Y & Hattori, K. Cloning of a new cytokine that induces IFN-γ production by T cells. *Nature* **378,** 88–91 (1995).

219. Sareneva, T, Julkunen, I & Matikainen, S. IFN-α and IL-12 induce IL-18 receptor gene expression in human NK and T cells. *J Immunol* **165,** 1933–8 (2000).

220. Mailliard, R. B., Alber, S. M., Shen, H., Watkins, S. C., Kirkwood, J. M., Herberman, R. B. & Kalinski, P. IL-18-induced CD83+CCR7+ NK helper cells. *J Exp Med* **202,** 941–53 (2005).

221. Mirjačić Martinović, K., Babović, N., Džodić, R., Jurišić, V., Matković, S. & Konjević, G. Favorable in vitro effects of combined IL-12 and IL-18 treatment on NK cell cytotoxicity and CD25 receptor expression in metastatic melanoma patients. *J Transl Med* **13,** 120 (2015).

222. Novick, D., Kim, S., Kaplanski, G. & Dinarello, C. A. Interleukin-18, more than a Th1 cytokine. *Semin Immunol* **25,** 439–48 (2013).

223. Zelante, T., Fric, J., Wong, A. Y. W. & Ricciardi-Castagnoli, P. Interleukin-2 production by dendritic cells and its immuno-regulatory functions. *Front Immunol* **3,** 161 (2012).

224. Sharfe, N, Dadi, H. K., Shahar, M & Roifman, C. M. Human immune disorder arising from mutation of the alpha chain of the interleukin-2 receptor. *Proc Natl Acad Sci U S A* **94,** 3168–71 (1997).

225. Lohr, J., Knoechel, B. & Abbas, A. K. Regulatory T cells in the periphery. *Immunol Rev* **212,** 149–62 (2006).

226. Sakaguchi, S, Sakaguchi, N, Asano, M, Itoh, M & Toda, M. Immunologic self-tolerance maintained by activated T cells expressing IL-2 receptor alpha-chains (CD25). Breakdown of a single mechanism of self-tolerance causes various autoimmune diseases. *J Immunol* **155,** 1151–64 (1995).

227. Waldmann, T. A. The biology of interleukin-2 and interleukin-15: implications for cancer therapy and vaccine design. *Nat Rev Immunol* **6,** 595–601 (2006).

228. Ing, R., Gros, P. & Stevenson, M. M. Interleukin-15 enhances innate and adaptive immune responses to blood-stage malaria infection in mice. *Infect Immun* **73,** 3172–7 (2005).

229. Parra, M., Liu, X., Derrick, S. C., Yang, A., Molina-Cruz, A., Barillas-Mury, C., Zheng, H., Thao Pham, P., Sedegah, M., Belmonte, A., Litilit, D. D., Waldmann, T. A., Kumar, S., Morris, S. L. & Perera, L. P. Co-expression of Interleukin-15 Enhances the Protective Immune Responses Induced by Immunization with a Murine Malaria MVA-Based Vaccine Encoding the Circumsporozoite Protein. *PLoS One* **10,** e0141141 (2015).

230. Perera, P.-Y., Lichy, J. H., Waldmann, T. A. & Perera, L. P. The role of interleukin-15 in inflammation and immune responses to infection: implications for its therapeutic use. *Microbes Infect* **14,** 247–61 (2012).

231. Anthony, S. M., Howard, M. E., Hailemichael, Y., Overwijk, W. W. & Schluns, K. S. Soluble interleukin-15 complexes are generated in vivo by type I interferon dependent and independent pathways. *PLoS One* **10,** e0120274 (2015).

232. Huntington, N. D. The unconventional expression of IL-15 and its role in NK cell homeostasis. *Immunol Cell Biol* **92,** 210–3 (2014).

233. Mortier, E., Advincula, R., Kim, L., Chmura, S., Barrera, J., Reizis, B., Malynn, B. A. & Ma, A. Macrophage- and dendritic-cell-derived interleukin-15 receptor alpha supports homeostasis of distinct CD8+ T cell subsets. *Immunity* **31,** 811–22 (2009).

234. Dubois, S., Mariner, J., Waldmann, T. A. & Tagaya, Y. IL-15Rα recycles and presents IL-15 In trans to neighboring cells. *Immunity* **17,** 537–47 (2002).

235. Castillo, E. F. & Schluns, K. S. Regulating the immune system via IL-15 transpresentation. *Cytokine* **59,** 479–90 (2012).

236. Neely, G. G., Epelman, S., Ma, L. L., Colarusso, P., Howlett, C. J., Amankwah, E. K., McIntyre, A. C., Robbins, S. M. & Mody, C. H. Monocyte surface-bound IL-15 can function as an activating receptor and participate in reverse signaling. *J Immunol* **172,** 4225–34 (2004).

237. Rubinstein, M. P., Kovar, M., Purton, J. F., Cho, J.-H., Boyman, O., Surh, C. D. & Sprent, J. Converting IL-15 to a superagonist by binding to soluble IL-15Rα. *Proc Natl Acad Sci U S A* **103,** 9166–71 (2006).

238. Kunikata, T, Torigoe, K, Ushio, S, Okura, T, Ushio, C, Yamauchi, H, Ikeda, M, Ikegami, H & Kurimoto, M. Constitutive and induced IL-18 receptor expression by various peripheral blood cell subsets as determined by anti-hIL-18R monoclonal antibody. *Cell Immunol* **189,** 135–43 (1998).

239. Strengell, M., Sareneva, T., Foster, D., Julkunen, I. & Matikainen, S. IL-21 up-regulates the expression of genes associated with innate immunity and Th1 response. *J Immunol* **169,** 3600–5 (2002).

240. Wendt, K., Wilk, E., Buyny, S., Schmidt, R. E. & Jacobs, R. Interleukin-21 differentially affects human natural killer cell subsets. *Immunology* **122,** 486–95 (2007).

241. Jeffe, F., Stegmann, K. A., Broelsch, F., Manns, M. P., Cornberg, M. & Wedemeyer, H. Adenosine and IFN-α synergistically increase IFN-γ production of human NK cells. *J Leukoc Biol* **85,** 452–61 (2009).

242. Aktas, E., Kucuksezer, U. C., Bilgic, S., Erten, G. & Deniz, G. Relationship between CD107a expression and cytotoxic activity. *Cell Immunol* **254,** 149–54 (2009).

243. Al-Hubeshy, Z. B., Coleman, A, Nelson, M & Goodier, M. R. A rapid method for assessment of natural killer cell function after multiple receptor crosslinking. *J Immunol Methods* **366,** 52–9 (2011).

244. Hoshino, K, Tsutsui, H, Kawai, T, Takeda, K, Nakanishi, K, Takeda, Y & Akira, S. Cutting edge: generation of IL-18 receptor-deficient mice: evidence for IL-1 receptor-related protein as an essential IL-18 binding receptor. *J Immunol* **162,** 5041–4 (1999).

245. Barreiro, L. B., Tailleux, L., Pai, A. A., Gicquel, B., Marioni, J. C. & Gilad, Y. Deciphering the genetic architecture of variation in the immune response to Mycobacterium tuberculosis infection. *Proc Natl Acad Sci U S A* **109,** 1204–9 (2012).

246. Zhang, J., Zheng, L., Zhu, D., An, H., Yang, Y., Liang, Y., Zhao, W., Ding, W. & Wu, X. Polymorphisms in the interleukin 18 receptor 1 gene and tuberculosis susceptibility among Chinese. *PLoS One* **9,** e110734 (2014).

247. Wei, L., Vahedi, G., Sun, H.-W., Watford, W. T., Takatori, H., Ramos, H. L., Takahashi, H., Liang, J., Gutierrez-Cruz, G., Zang, C., Peng, W., O'Shea, J. J. & Kanno, Y. Discrete roles of STAT4 and STAT6 transcription factors in tuning epigenetic modifications and transcription during T helper cell differentiation. *Immunity* **32,** 840–51 (2010).

248. Yu, Q., Chang, H.-C., Ahyi, A.-N. N. & Kaplan, M. H. Transcription factor-dependent chromatin remodeling of Il18r1 during Th1 and Th2 differentiation. *J Immunol* **181,** 3346–52 (2008).

249. Xue, H.-H., Kovanen, P. E., Pise-Masison, C. A., Berg, M., Radovich, M. F., Brady, J. N. & Leonard, W. J. IL-2 negatively regulates IL-7 receptor alpha chain expression in activated T lymphocytes. *Proc Natl Acad Sci U S A* **99,** 13759–64 (2002).

250. Klezovich-Bénard, M., Corre, J.-P., Jusforgues-Saklani, H., Fiole, D., Burjek, N., Tournier, J.-N. & Goossens, P. L. Mechanisms of NK cell-macrophage Bacillus anthracis crosstalk: a balance between stimulation by spores and differential disruption by toxins. *PLoS Pathog* **8,** e1002481 (2012).

251. Tamzalit, F., Barbieux, I., Plet, A., Heim, J., Nedellec, S., Morisseau, S., Jacques, Y. & Mortier, E. IL-15.IL-15Rα complex shedding following trans-presentation is essential for the survival of IL-15 responding NK and T cells. *Proc Natl Acad Sci U S A* **111,** 8565–70 (2014).

252. Hamerman, J. A. & Aderem, A. Functional transitions in macrophages during in vivo infection with Mycobacterium bovis bacillus Calmette-Guérin. *J Immunol* **167,** 2227–33 (2001).

253. Newman, K. C. & Riley, E. M. Whatever turns you on: accessory-cell-dependent activation of NK cells by pathogens. *Nat Rev Immunol* **7,** 279–91 (2007).

254. Van de Veerdonk, F. L., Netea, M. G., Dinarello, C. A. & Joosten, L. A. B. Inflammasome activation and IL-1β and IL-18 processing during infection. *Trends Immunol* **32,** 110–6 (2011).

255. De Souza, J. B., Williamson, K. H., Otani, T & Playfair, J. H. Early gamma interferon responses in lethal and nonlethal murine blood-stage malaria. *Infect Immun* **65,** 1593–8 (1997).

256. Li, C, Corraliza, I & Langhorne, J. A defect in interleukin-10 leads to enhanced malarial disease in Plasmodium chabaudi chabaudi infection in mice. *Infect Immun* **67,** 4435–42 (1999).

257. Lepenies, B., Gaworski, I., Tartz, S., Langhorne, J., Fleischer, B. & Jacobs, T. CTLA-4 blockade differentially influences the outcome of non-lethal and lethal Plasmodium yoelii infections. *Microbes Infect* **9,** 687–94 (2007).

258. McCall, M. B. B. & Sauerwein, R. W. Interferon gamma - central mediator of protective immune responses against the pre-erythrocytic and blood stage of malaria. *J Leukoc Biol* **88,** 1131–43 (2010).

259. Luty, A. J., Lell, B, Schmidt-Ott, R, Lehman, L. G., Luckner, D, Greve, B, Matousek, P, Herbich, K, Schmid, D, Migot-Nabias, F, Deloron, P, Nussenzweig, R. S. & Kremsner, P. G. Interferon-gamma responses are associated with resistance to reinfection with Plasmodium falciparum in young African children. *J Infect Dis* **179,** 980–8 (1999).

260. Roestenberg, M., Teirlinck, A. C., McCall, M. B. B., Teelen, K., Makamdop, K. N., Wiersma, J., Arens, T., Beckers, P., van Gemert, G., van de Vegte-Bolmer, M., van der Ven, A. J. A. M., Luty, A. J. F., Hermsen, C. C. & Sauerwein, R. W. Long-term protection against malaria after experimental sporozoite inoculation: an open-label follow-up study. *Lancet* **377,** 1770–6 (2011).

261. Bejon, P. *et al.* Early gamma interferon and interleukin-2 responses to vaccination predict the late resting memory in malaria-naive and malaria-exposed individuals. *Infect Immun* **74,** 6331–8 (2006).

262. Rhee, M. S., Akanmori, B. D., Waterfall, M & Riley, E. M. Changes in cytokine production associated with acquired immunity to Plasmodium falciparum malaria. *Clin Exp Immunol* **126,** 503–10 (2001).

263. Finney, O. C., Riley, E. M. & Walther, M. Regulatory T cells in malaria - friend or foe? *Trends Immunol* **31,** 63–70 (2010).

264. Depinay, N., Franetich, J. F., Grüner, A. C., Mauduit, M., Chavatte, J.-M., Luty, A. J. F., van Gemert, G.-J., Sauerwein, R. W., Siksik, J.-M., Hannoun, L., Mazier, D., Snounou, G. & Rénia, L. Inhibitory effect of TNF-α on malaria pre-erythrocytic stage development: influence of host hepatocyte/parasite combinations. *PLoS One* **6,** e17464 (2011).

265. Doolan, D. L. & Hoffman, S. L. The complexity of protective immunity against liver-stage malaria. *J Immunol* **165,** 1453–62 (2000).

266. Mellouk, S, Green, S. J., Nacy, C. A. & Hoffman, S. L. IFN-γ inhibits development of Plasmodium berghei exoerythrocytic stages in hepatocytes by an L-arginine-dependent effector mechanism. *J Immunol* **146,** 3971–6 (1991).

267. Stevenson, M. M., Tam, M. F., Wolf, S. F. & Sher, A. IL-12-induced protection against blood-stage Plasmodium chabaudi AS requires IFN-gamma and TNF-alpha and occurs via a nitric oxide-dependent mechanism. *J Immunol* **155,** 2545–56 (1995).

268. Gowda, N. M., Wu, X., Kumar, S., Febbraio, M. & Gowda, D. C. CD36 contributes to malaria parasite-induced pro-inflammatory cytokine production and NK and T cell activation by dendritic cells. *PLoS One* **8,** e77604 (2013).

269. Ojo-Amaize, E. A., Salimonu, L. S., Williams, A. I., Akinwolere, O. A., Shabo, R, Alm, G. V. & Wigzell, H. Positive correlation between degree of parasitemia, interferon titers, and natural killer cell activity in Plasmodium falciparum-infected children. *J Immunol* **127,** 2296–300 (1981).

270. Ojo-Amaize, E. A., Vilcek, J, Cochrane, A. H. & Nussenzweig, R. S. Plasmodium berghei sporozoites are mitogenic for murine T cells, induce interferon, and activate natural killer cells. *J Immunol* **133,** 1005–9 (1984).

271. Agudelo, O., Bueno, J., Villa, A. & Maestre, A. High IFN-gamma and TNF production by peripheral NK cells of Colombian patients with different clinical presentation of Plasmodium falciparum. *Malar J* **11,** 38 (2012).

272. McCall, M. B. B., Roestenberg, M., Ploemen, I., Teirlinck, A., Hopman, J., de Mast, Q., Dolo, A., Doumbo, O. K., Luty, A., van der Ven, A. J. A. M., Hermsen, C. C. & Sauerwein, R. W. Memory-like IFN-γ response by NK cells following malaria infection reveals the crucial role of T cells in NK cell activation by P. falciparum. *Eur J Immunol* **40,** 3472–7 (2010).

273. Hermsen, C. C., Konijnenberg, Y, Mulder, L, Loé, C, van Deuren, M, van der Meer, J. W. M., van Mierlo, G. J., Eling, W. M. C., Hack, C. E. & Sauerwein, R. W. Circulating concentrations of soluble granzyme A and B increase during natural and experimental Plasmodium falciparum infections. *Clin Exp Immunol* **132,** 467–72 (2003).

274. Mavoungou, E., Held, J., Mewono, L. & Kremsner, P. G. A Duffy binding-like domain is involved in the NKp30-mediated recognition of Plasmodium falciparum-parasitized erythrocytes by natural killer cells. *J Infect Dis* **195,** 1521–31 (2007).

275. Böttger, E., Multhoff, G., Kun, J. F. J. & Esen, M. Plasmodium falciparum-infected erythrocytes induce granzyme B by NK cells through expression of host-Hsp70. *PLoS One* **7,** e33774 (2012).

276. Orago, A. S. & Facer, C. A. Cytotoxicity of human natural killer (NK) cell subsets for Plasmodium falciparum erythrocytic schizonts: stimulation by cytokines and inhibition by neomycin. *Clin Exp Immunol* **86,** 22–9 (1991).

277. Cerwenka, A. & Lanier, L. L. Natural killer cell memory in infection, inflammation and cancer. *Nat Rev Immunol* **16,** 112–23 (2016).

278. Teirlinck, A. C., McCall, M. B. B., Roestenberg, M., Scholzen, A., Woestenenk, R., de Mast, Q., van der Ven, A. J. A. M., Hermsen, C. C., Luty, A. J. F. & Sauerwein, R. W. Longevity and composition of cellular immune responses following experimental Plasmodium falciparum malaria infection in humans. *PLoS Pathog* **7,** e1002389 (2011).

279. Tang, F., Sally, B., Ciszewski, C., Abadie, V., Curran, S. A., Groh, V., Fitzgerald, O., Winchester, R. J. & Jabri, B. Interleukin 15 primes natural killer cells to kill via NKG2D and cPLA2 and this pathway is active in psoriatic arthritis. *PLoS One* **8,** e76292 (2013).

280. Longhi, L. N. A., da Silva, R. M., Fornazim, M. C., Spago, M. C., de Oliveira, R. T. D., Nowill, A. E., Blotta, M. H. S. L. & Mamoni, R. L. Phenotypic and functional characterization of NK cells in human immune response against the dimorphic fungus Paracoccidioides brasiliensis. *J Immunol* **189,** 935–45 (2012).

281. Finton, K. A. & Strong, R. K. Structural insights into activation of antiviral NK cell responses. *Immunol Rev* **250,** 239–57 (2012).

282. Owen, R. E., Sinclair, E., Emu, B., Heitman, J. W., Hirschkorn, D. F., Epling, C. L., Tan, Q. X., Custer, B., Harris, J. M., Jacobson, M. A., McCune, J. M., Martin, J. N., Hecht, F. M., Deeks, S. G. & Norris, P. J. Loss of T cell responses following long-term cryopreservation. *J Immunol Methods* **326,** 93–115 (2007).

283. Posevitz-Fejfár, A., Posevitz, V., Gross, C. C., Bhatia, U., Kurth, F., Schütte, V., Bar-Or, A., Meuth, S. G. & Wiendl, H. Effects of blood transportation on human peripheral mononuclear cell yield, phenotype and function: implications for immune cell biobanking. *PLoS One* **9,** e115920 (2014).

284. Struik, S. S., Omer, F. M., Artavanis-Tsakonas, K. & Riley, E. M. Uninfected erythrocytes inhibit Plasmodium falciparum-induced cellular immune responses in whole-blood assays. *Blood* **103,** 3084–92 (2004).

285. Vyse, A. J., Hesketh, L. M. & Pebody, R. G. The burden of infection with cytomegalovirus in England and Wales: how many women are infected in pregnancy? *Epidemiol Infect* **137,** 526–33 (2009).

286. Alter, G., Malenfant, J. M. & Altfeld, M. CD107a as a functional marker for the identification of natural killer cell activity. *J Immunol Methods* **294,** 15–22 (2004).

287. Brantsæter, A. B., Johannessen, A., Holberg-Petersen, M., Sandvik, L., Naman, E., Kivuyo, S. L., Rollag, H., Bruun, J. N. & Kvale, D. Cytomegalovirus viremia in dried blood spots is associated with an increased risk of death in HIV-infected patients: a cohort study from rural Tanzania. *Int J Infect Dis* **16,** e879–85 (2012).

288. Lee, S. A., Sinclair, E., Hatano, H., Hsue, P. Y., Epling, L., Hecht, F. M., Bangsberg, D. R., Martin, J. N., McCune, J. M., Deeks, S. G. & Hunt, P. W. Impact of HIV on CD8+ T cell CD57 expression is distinct from that of CMV and aging. *PLoS One* **9,** e89444 (2014).

289. Rudd, C. E., Taylor, A. & Schneider, H. CD28 and CTLA-4 coreceptor expression and signal transduction. *Immunol Rev* **229,** 12–26 (2009).

290. Dustin, M. L. & Long, E. O. Cytotoxic immunological synapses. *Immunol Rev* **235,** 24–34 (2010).

291. Griffiths, G. M., Tsun, A. & Stinchcombe, J. C. The immunological synapse: a focal point for endocytosis and exocytosis. *J Cell Biol* **189,** 399–406 (2010).

292. Vilches, C, Gardiner, C. M. & Parham, P. Gene structure and promoter variation of expressed and nonexpressed variants of the KIR2DL5 gene. *J Immunol* **165,** 6416–21 (2000).

293. Béziat, V., Traherne, J. A., Liu, L. L., Jayaraman, J., Enqvist, M., Larsson, S., Trowsdale, J. & Malmberg, K.-J. Influence of KIR gene copy number on natural killer cell education. *Blood* **121,** 4703–7 (2013).

294. Yawata, M., Yawata, N., Draghi, M., Partheniou, F., Little, A.-M. & Parham, P. MHC class I-specific inhibitory receptors and their ligands structure diverse human NK-cell repertoires toward a balance of missing self-response. *Blood* **112,** 2369–80 (2008).

295. Anfossi, N., André, P., Guia, S., Falk, C. S., Roetynck, S., Stewart, C. A., Breso, V., Frassati, C., Reviron, D., Middleton, D., Romagné, F., Ugolini, S. & Vivier, E. Human NK cell education by inhibitory receptors for MHC class I. *Immunity* **25,** 331–42 (2006).

296. Chan, H.-W., Miller, J. S., Moore, M. B. & Lutz, C. T. Epigenetic control of highly homologous killer Ig-like receptor gene alleles. *J Immunol* **175,** 5966–74 (2005).

297. Yawata, M., Yawata, N., Draghi, M., Little, A.-M., Partheniou, F. & Parham, P. Roles for HLA and KIR polymorphisms in natural killer cell repertoire selection and modulation of effector function. *J Exp Med* **203,** 633–45 (2006).

298. Trompeter, H.-I., Gómez-Lozano, N., Santourlidis, S., Eisermann, B., Wernet, P., Vilches, C. & Uhrberg, M. Three structurally and functionally divergent kinds of promoters regulate expression of clonally distributed killer cell Ig-like receptors (KIR), of KIR2DL4, and of KIR3DL3. *J Immunol* **174,** 4135–43 (2005).

299. Fernandez, N. C., Treiner, E., Vance, R. E., Jamieson, A. M., Lemieux, S. & Raulet, D. H. A subset of natural killer cells achieves self-tolerance without expressing inhibitory receptors specific for self-MHC molecules. *Blood* **105,** 4416–23 (2005).

300. Olaniyan, S. A., Amodu, O. K., Yindom, L.-M., Conway, D. J., Aka, P., Bakare, A. A. & Omotade, O. O. Killer-cell immunoglobulin-like receptors and falciparum malaria in southwest Nigeria. *Hum Immunol* **75,** 816–21 (2014).

301. Yindom, L.-M., Forbes, R, Aka, P, Janha, O, Jeffries, D, Jallow, M, Conway, D. J. & Walther, M. Killer-cell immunoglobulin-like receptors and malaria caused by Plasmodium falciparum in The Gambia. *Tissue Antigens* **79,** 104–13 (2012).

302. Hirayasu, K., Ohashi, J., Kashiwase, K., Hananantachai, H., Naka, I., Ogawa, A., Takanashi, M., Satake, M., Nakajima, K., Parham, P., Arase, H., Tokunaga, K., Patarapotikul, J. & Yabe, T. Significant association of KIR2DL3-HLA-C1 combination with cerebral malaria and implications for co-evolution of KIR and HLA. *PLoS Pathog* **8,** e1002565 (2012).

303. Du, Z, Sharma, S. K., Spellman, S, Reed, E. F. & Rajalingam, R. KIR2DL5 alleles mark certain combination of activating KIR genes. *Genes Immun* **9,** 470–80 (2008).

304. Nakimuli, A., Chazara, O., Farrell, L., Hiby, S. E., Tukwasibwe, S., Knee, O., Jayaraman, J., Traherne, J. A., Elliott, A. M., Kaleebu, P., Mirembe, F. & Moffett, A. Killer cell immunoglobulin-like receptor (KIR) genes and their HLA-C ligands in a Ugandan population. *Immunogenetics* **65,** 765–75 (2013).

305. Norman, P. J., Carrington, C. V. F., Byng, M, Maxwell, L. D., Curran, M. D., Stephens, H. A. F., Chandanayingyong, D, Verity, D. H., Hameed, K, Ramdath, D. D. & Vaughan, R. W. Natural killer cell immunoglobulin-like receptor (KIR) locus profiles in African and South Asian populations. *Genes Immun* **3,** 86–95 (2002).

306. Vendelbosch, S, de Boer, M, van Leeuwen, K, Pourfarzad, F, Geissler, J, van den Berg, T. K. & Kuijpers, T. W. Novel insights in the genomic organization and hotspots of recombination in the human KIR locus through analysis of intergenic regions. *Genes Immun* **16,** 103–11 (2015).

307. Grzywacz, B., Kataria, N., Sikora, M., Oostendorp, R. A., Dzierzak, E. A., Blazar, B. R., Miller, J. S. & Verneris, M. R. Coordinated acquisition of inhibitory and activating receptors and functional properties by developing human natural killer cells. *Blood* **108,** 3824–33 (2006).

308. Arnon, T. I. *et al.* Inhibition of the NKp30 activating receptor by pp65 of human cytomegalovirus. *Nat Immunol* **6,** 515–23 (2005).

309. Wang, E. C. Y., McSharry, B., Retiere, C., Tomasec, P., Williams, S., Borysiewicz, L. K., Braud, V. M. & Wilkinson, G. W. G. UL40-mediated NK evasion during productive infection with human cytomegalovirus. *Proc Natl Acad Sci U S A* **99,** 7570–5 (2002).

310. Dokun, A. O., Kim, S, Smith, H. R., Kang, H. S., Chu, D. T. & Yokoyama, W. M. Specific and nonspecific NK cell activation during virus infection. *Nat Immunol* **2,** 951–6 (2001).

311. Marcus, A. & Raulet, D. H. Evidence for natural killer cell memory. *Curr Biol* **23,** R817–20 (2013).

312. Miyashita, R., Tsuchiya, N., Hikami, K., Kuroki, K., Fukazawa, T., Bijl, M., Kallenberg, C. G. M., Hashimoto, H., Yabe, T. & Tokunaga, K. Molecular genetic analyses of human NKG2C (KLRC2) gene deletion. *Int Immunol* **16,** 163–8 (2004).

313. Goncalves, A. *et al.* Differential frequency of NKG2C/KLRC2 deletion in distinct African populations and susceptibility to Trachoma: a new method for imputation of KLRC2 genotypes from SNP genotyping data. *Hum Genet* (2016).

314. Noyola, D. E., Fortuny, C., Muntasell, A., Noguera-Julian, A., Muñoz-Almagro, C., Alarcón, A., Juncosa, T., Moraru, M., Vilches, C. & López-Botet, M. Influence of congenital human cytomegalovirus infection and the NKG2C genotype on NK-cell subset distribution in children. *Eur J Immunol* **42,** 3256–66 (2012).

315. Della Chiesa, M., Falco, M., Bertaina, A., Muccio, L., Alicata, C., Frassoni, F., Locatelli, F., Moretta, L. & Moretta, A. Human cytomegalovirus infection promotes rapid maturation of NK cells expressing activating killer Ig-like receptor in patients transplanted with NKG2C-/- umbilical cord blood. *J Immunol* **192,** 1471–9 (2014).

316. Maier, A. G., Cooke, B. M., Cowman, A. F. & Tilley, L. Malaria parasite proteins that remodel the host erythrocyte. *Nat Rev Microbiol* **7,** 341–54 (2009).

317. *UCLA KIR Exchange* <`http://www.hla.ucla.edu/cellDna.htm`>.

318. *Report of the 33rd UCLA International KIR Exchange* (2014). <`http://www.hla.ucla.edu/pdf/KIR_summary/KIR33.pdf`>.

319. Middleton, D, Meenagh, A & Gourraud, P. A. KIR haplotype content at the allele level in 77 Northern Irish families. *Immunogenetics* **59,** 145–58 (2007).

320. González-Galarza, F. F., Takeshita, L. Y. C., Santos, E. J. M., Kempson, F., Maia, M. H. T., da Silva, A. L. S., Teles e Silva, A. L., Ghattaoraya, G. S., Alfirevic, A., Jones, A. R. & Middleton, D. Allele frequency net 2015 update: new features for HLA epitopes, KIR and disease and HLA adverse drug reaction associations. *Nucleic Acids Res* **43,** D784–8 (2015).

321. Mulrooney, T. J., Hou, L., Steiner, N. K., Chen, M., Belle, I., Ng, J. & Hurley, C. K. Promoter variants of KIR2DL5 add to diversity and may impact gene expression. *Immunogenetics* **60,** 287–94 (2008).

322. Gardiner, C. M., Guethlein, L. A., Shilling, H. G., Pando, M, Carr, W. H., Rajalingam, R, Vilches, C & Parham, P. Different NK cell surface phenotypes defined by the DX9 antibody are due to KIR3DL1 gene polymorphism. *J Immunol* **166,** 2992–3001 (2001).

323. Charoudeh, H. N., Terszowski, G., Czaja, K., Gonzalez, A., Schmitter, K. & Stern, M. Modulation of the natural killer cell KIR repertoire by cytomegalovirus infection. *Eur J Immunol* **43,** 480–7 (2013).

324. Chrul, S., Polakowska, E., Szadkowska, A. & Bodalski, J. Influence of interleukin IL-2 and IL-12 + IL-18 on surface expression of immunoglobulin-like receptors KIR2DL1, KIR2DL2, and KIR3DL2 in natural killer cells. *Mediators Inflamm* **4,** 46957 (2006).

325. Gagne, K., Willem, C., Legrand, N., Djaoud, Z., David, G., Rettman, P., Bressollette-Bodin, C., Senitzer, D., Esbelin, J., Cesbron-Gautier, A., Schneider, T. & Retière, C. Both the nature of KIR3DL1 alleles and the KIR3DL1/S1 allele combination affect the KIR3DL1 NK cell repertoire in the French population. *Eur J Immunol* **43,** 1085–98 (2013).

326. Marangon, A. V., Visentainer, J. E. L., Guelsin, G. A. S., Clementino, S. L., Rudnick, C. C. C., de Melo, F. C., Braga, M. A. & Sell, A. M. Investigation of deletion of 22pb in KIR2DS4 gene in a population of southern Brazil. *J Clin Lab Anal* **28,** 440–5 (2014).

327. Sivori, S., Carlomagno, S., Falco, M., Romeo, E., Moretta, L. & Moretta, A. Natural killer cells expressing the KIR2DS1-activating receptor efficiently kill T cell blasts and dendritic cells: implications in haploidentical HSCT. *Blood* **117,** 4284–92 (2011).

328. Estefanía, E., Flores, R., Gómez-Lozano, N., Aguilar, H., López-Botet, M. & Vilches, C. Human KIR2DL5 is an inhibitory receptor expressed on the surface of NK and T lymphocyte subsets. *J Immunol* **178,** 4402–10 (2007).

329. Santin, I, Castellanos-Rubio, A, Perez de Nanclares, G, Vitoria, J. C., Castaño, L & Bilbao, J. R. Association of KIR2DL5B gene with celiac disease supports the susceptibility locus on 19q13.4. *Genes Immun* **8,** 171–6 (2007).

330. Kimoto, Y. *et al.* Association of killer cell immunoglobulin-like receptor 2DL5 with systemic lupus erythematosus and accompanying infections. *Rheumatology (Oxford)* **49,** 1346–53 (2010).

331. García-León, J. A., Pinto-Medel, M. J., García-Trujillo, L., López-Gómez, C., Oliver-Martos, B., Prat-Arrojo, I., Marín-Bañasco, C., Suardíaz-García, M., Maldonado-Sanchez, R., Fernández-Fernández, O. & Leyva-Fernández, L. Killer cell immunoglobulin-like receptor genes in Spanish multiple sclerosis patients. *Mol Immunol* **48,** 1896–902 (2011).

332. Martin, M. P., Bashirova, A., Traherne, J., Trowsdale, J. & Carrington, M. Cutting edge: expansion of the KIR locus by unequal crossing over. *J Immunol* **171,** 2192–5 (2003).

333. Norman, P. J. *et al.* Meiotic recombination generates rich diversity in NK cell receptor genes, alleles, and haplotypes. *Genome Res* **19,** 757–69 (2009).

334. Roberts, C. H., Jiang, W., Jayaraman, J., Trowsdale, J., Holland, M. J. & Traherne, J. A. Killer-cell Immunoglobulin-like Receptor gene linkage and copy number variation analysis by droplet digital PCR. *Genome Med* **6,** 20 (2014).

335. Gómez-Lozano, N., Estefanía, E., Williams, F., Halfpenny, I., Middleton, D., Solís, R. & Vilches, C. The silent KIR3DP1 gene (CD158c) is transcribed and might encode a secreted receptor in a minority of humans, in whom the KIR3DP1, KIR2DL4 and KIR3DL1/KIR3DS1 genes are duplicated. *Eur J Immunol* **35,** 16–24 (2005).

336. Santourlidis, S., Trompeter, H.-I., Weinhold, S., Eisermann, B., Meyer, K. L., Wernet, P. & Uhrberg, M. Crucial role of DNA methylation in determination of clonally distributed killer cell Ig-like receptor expression patterns in NK cells. *J Immunol* **169,** 4253–61 (2002).

337. Cichocki, F., Miller, J. S. & Anderson, S. K. Killer immunoglobulin-like receptor transcriptional regulation: a fascinating dance of multiple promoters. *J Innate Immun* **3,** 242–8 (2011).

338. Yusa, S.-i., Catina, T. L. & Campbell, K. S. KIR2DL5 can inhibit human NK cell activation via recruitment of Src homology region 2-containing protein tyrosine phosphatase-2 (SHP-2). *J Immunol* **172,** 7385–92 (2004).

339. Zhi-ming, L., Yu-lian, J., Zhao-lei, F., Chun-xiao, W., Zhen-fang, D., Bing-chang, Z. & Yue-ran, Z. Polymorphisms of killer cell immunoglobulin-like receptor gene: possible association with susceptibility to or clearance of hepatitis B virus infection in Chinese Han population. *Croat Med J* **48,** 800–6 (2007).

340. Taniguchi, M. & Kawabata, M. KIR3DL1/S1 genotypes and KIR2DS4 allelic variants in the AB KIR genotypes are associated with Plasmodium-positive individuals in malaria infection. *Immunogenetics* **61,** 717–30 (2009).

341. BioRad. *Droplet Digital PCR Technology* <`http://www.bio-rad.com/en-uk/applications-technologies/droplet-digital-pcr-ddpcr-technology`> (2016).

342. Arase, H., Mocarski, E. S., Campbell, A. E., Hill, A. B. & Lanier, L. L. Direct recognition of cytomegalovirus by activating and inhibitory NK cell receptors. *Science* **296,** 1323–6 (2002).

343. Baía, D., Pou, J., Jones, D., Mandelboim, O., Trowsdale, J., Muntasell, A. & López-Botet, M. Interaction of the LILRB1 inhibitory receptor with HLA class Ia dimers. *Eur J Immunol* (2016).

344. Guinan, K. J., Cunningham, R. T., Meenagh, A, Gonzalez, A, Dring, M. M., McGuinness, B. W., Middleton, D & Gardiner, C. M. Signatures of natural selection and coevolution between killer cell immunoglobulin-like receptors (KIR) and HLA class I genes. *Genes Immun* **11,** 467–78 (2010).

345. Van Bergen, J., Stewart, C. A., van den Elsen, P. J. & Trowsdale, J. Structural and functional differences between the promoters of independently expressed killer cell Ig-like receptors. *Eur J Immunol* **35,** 2191–9 (2005).

346. Takeshita, L. Y. C., Gonzalez-Galarza, F. F., dos Santos, E. J. M., Maia, M. H. T., Rahman, M. M., Zain, S. M. S., Middleton, D. & Jones, A. R. A database for curating the associations between killer cell immunoglobulin-like receptors and diseases in worldwide populations. *Database (Oxford)* (2013).

347. Roberts, C. H., Molina, S., Makalo, P., Joof, H., Harding-Esch, E. M., Burr, S. E., Mabey, D. C. W., Bailey, R. L., Burton, M. J. & Holland, M. J. Conjunctival scarring in trachoma is associated with the HLA-C ligand of KIR and is exacerbated by heterozygosity at KIR2DL2/KIR2DL3. *PLoS Negl Trop Dis* **8,** e2744 (2014).

348. He, X.-S., Draghi, M., Mahmood, K., Holmes, T. H., Kemble, G. W., Dekker, C. L., Arvin, A. M., Parham, P. & Greenberg, H. B. T cell-dependent production of IFN-gamma by NK cells in response to influenza A virus. *J Clin Invest* **114,** 1812–9 (2004).

349. Romee, R., Schneider, S. E., Leong, J. W., Chase, J. M., Keppel, C. R., Sullivan, R. P., Cooper, M. A. & Fehniger, T. A. Cytokine activation induces human memory-like NK cells. *Blood* **120,** 4751–60 (2012).

350. Marquardt, N., Ivarsson, M. A., Blom, K., Gonzalez, V. D., Braun, M., Falconer, K., Gustafsson, R., Fogdell-Hahn, A., Sandberg, J. K. & Michaëlsson, J. The Human NK Cell Response to Yellow Fever Virus 17D Is Primarily Governed by NK Cell Differentiation Independently of NK Cell Education. *J Immunol* **195,** 3262–72 (2015).

351. Bontadini, A *et al.* Distribution of killer cell immunoglobulin-like receptors genes in the Italian Caucasian population. *J Transl Med* **4,** 44 (2006).